



Cheripelli, Bharath kumar (2020) *Acute ischaemic stroke-multimodal imaging and stroke outcomes*. MD thesis.

<http://theses.gla.ac.uk/81736/>

Copyright and moral rights for this work are retained by the author

A copy can be downloaded for personal non-commercial research or study, without prior permission or charge

This work cannot be reproduced or quoted extensively from without first obtaining permission in writing from the author

The content must not be changed in any way or sold commercially in any format or medium without the formal permission of the author

When referring to this work, full bibliographic details including the author, title, awarding institution and date of the thesis must be given

Enlighten: Theses

<https://theses.gla.ac.uk/>
research-enlighten@glasgow.ac.uk

Acute Ischaemic Stroke- Multi modal Imaging and Stroke outcomes

Dr Bharathkumar Cheripelli
MBBS, MRCP, CCT (Neurology)

A thesis which fulfils the requirements of the University of
Glasgow for the degree of Doctorate of Medicine

Institute of Neuroscience and Psychology
University of Glasgow
October 2019

Abstract

Introduction

Acute stroke Imaging plays a crucial role in understanding the cerebral tissue states and multimodal imaging with perfusion, collaterals and vessel occlusion provides more information on tissue dynamics in individual patient which can be useful for tailored treatments and prognosis. Perfusion parameters and their validation are important in achieving clinical practicality. A novel tissue parameter, Capillary transit time heterogeneity has been suggested to identify micro vascular flow patterns. The clinical utility of this is not yet established.

Stroke outcome is dependant not only on the imaging parameters but also on patient demographics, co morbidities and probably on complex socio-economic and other unidentified patient factors.

Methods

Using a database of single centre multi modal imaging I derived perfusion metrics in commercial software (Mlstar). I conducted a few different analyses on: penumbra relationship with time, collaterals; haemorrhage, oedema relationship with recanalisation; Safety in Stroke Thrombolysis (SITS) registry Stroke outcomes; Deriving a new perfusion parameter called 'Capillary transit time heterogeneity (CTTH)' and comparing the values in different tissue compartments.

Results

In a cross-sectional sample imaged within 6h, neither the proportions of penumbral tissue nor "target mismatch" varied by time from onset. A trend for reducing penumbra proportion only among those with poor collaterals may have pathophysiological and therapeutic importance.

Among patients treated with IV thrombolysis, 24h recanalisation was not independently associated with significant early (24h) vasogenic oedema or significant haemorrhage, although incidence of HI/HI2 ICH was higher. Large ischaemic core was associated with both significant brain oedema and poor outcome. There was no interaction of recanalisation and large core lesions for any imaging outcomes. Early major clinical improvement as a marker of probable early reperfusion was associated with lower incidence of both significant haemorrhage and oedema.

In SITS registry study, poorer 90 day outcomes after IV thrombolysis occurred frequently at a hospital (Southern General Hospital) that accepted secondary transfer patients compared to a hospital in the same city (Western Infirmary Glasgow) that did not routinely take such patients.

Capillary transit time heterogeneity (CTTH) voxel wise maps were derived successfully using “vascular model” in Brain Lab, Arhus, Denmark. The CTTH values are closely related with MTT. There is no significant difference of CTTH between Core, penumbra.

Conclusion

Multimodal imaging can provide us with valuable information on understanding ischemic brain tissue, predict patient outcomes in stroke. Patient imaging and clinical outcomes depend on recanalisation, and patient factors. A novel perfusion parameter, CTTH has been successfully derived and its utility and validity is yet to be evaluated.

Table of Contents

Chapter 0 Table of Contents

Abstract.....	2
Table of Contents	4
List of Tables.....	7
Table of Figures	8
Publications and Presentations	10
Acknowledgement.....	13
Contribution to the thesis work and Stroke Research activity during fellowship ..	14
Author's declaration	15
Definitions/Abbreviations.....	16
Chapter 1 Introduction	19
1.1 Acute Ischaemic stroke (overview)	19
1.2 Pathophysiology	21
1.2.1 Cellular pathology of ischaemic stroke	22
1.2.2 Cerebral haemodynamics in response to ischaemia	22
1.3 Types of Cerebral oedema	24
1.4 Haemorrhagic Transformation (HT) in Ischaemic stroke	25
1.5 Evidence from animal studies	26
1.5.1 Multimodal imaging of tissue outcomes in focal ischaemia animal models	27
1.5.2 Evidence for irreversible (Core) and reversible (Penumbra) ischaemia and evolution over time	28
1.5.3 Tissue Thresholds.....	30
1.6 Human Positron Emission Tomography (PET) studies	34
1.7 Acute stroke imaging in Humans.....	35
1.7.1 Non-contrast CT (NCCT).....	35
1.8 Perfusion Imaging	36
1.8.1 CT perfusion (CTP)	37
1.8.2 Post acquisition CT perfusion processing.....	39
1.9 Role of capillaries in haemodynamic regulation	49
1.10 Magnetic Resonance Imaging (MRI)	53
1.10.1 MRI for penumbra identification	54
1.10.2 NCCT vs. MRI.....	56
1.11 Non-core-non-penumbra Infarction:	57
1.12 Intravenous thrombolysis (IVT):	57
1.13 Using imaging for treatment selection	60

1.14	Intra arterial therapy (IAT).....	61
1.15	Cerebral angiogram.....	62
1.16	Cerebral Collateral circulation	63
Chapter 2	Study Population and Methods	65
2.1	Study population	65
2.2	Imaging.....	67
2.2.1	Imaging acquisition	67
2.2.2	Imaging processing and analysis	68
2.3	Collateral grading:	76
2.4	Recanalisation	78
2.5	Haemorrhage classification	78
2.6	Oedema classification	79
2.7	Modified Rankin Scale	80
Chapter 3	Methods for Capillary Transit Time Heterogeneity (CTTH) work in Chapters 6, 7.....	82
3.1	Introduction	82
3.2	Detailed steps.....	83
3.3	Study population of CTTH work.....	99
Chapter 4	Does the Penumbra Shrink over Time? Penumbra volume and collaterals in the first 6 hours after acute ischemic stroke	101
4.1	Introduction	101
4.2	Methods.....	102
4.2.1	Study Population	102
4.2.2	Imaging acquisition	103
4.2.3	Imaging processing and analysis	103
4.2.4	Penumbra definition	103
4.2.5	Collateral scores.....	104
4.2.6	Target mismatch	104
4.2.7	Statistical analysis	104
4.3	Results	104
4.4	Discussion.....	111
4.5	Conclusions.....	114
Chapter 5	Interaction of Recanalisation, Intracerebral Haemorrhage and Cerebral Oedema after Intravenous thrombolysis.....	115
5.1	Introduction	115
5.2	Methods.....	116
5.2.1	Study population	116
5.2.2	Image acquisition.....	117
5.2.3	Image analysis	117
5.2.4	Core, penumbra definition.....	118

5.2.5	Collateral grading	118
5.2.6	Haemorrhage, oedema classification	118
5.3	Results	119
5.4	Discussion.....	132
5.5	Conclusions.....	135
Chapter 6	Explore Capillary transit time heterogeneity (CTTH) within different components of the tissue - core, penumbra, ‘non-core-non-penumbra’ infarct, normal brain	136
6.1	Introduction.....	136
6.2	Methods.....	138
6.3	Results	139
6.4	Discussion.....	148
6.5	Conclusions.....	150
Chapter 7	What are the clinical characteristics of subjects with ‘non-core-non-penumbra’ infarction?	151
7.1	Introduction.....	151
7.2	Methods.....	152
7.3	Results	152
7.4	Discussion.....	155
7.5	Conclusions.....	157
Chapter 8	Is secondary transfer for stroke thrombolysis optimal? - Comparing outcomes between two hospitals with different model of care and with the rest of UK	158
8.1	Introduction.....	158
8.2	Methods.....	159
8.3	Results:	162
8.3.1	Regression analysis.....	169
8.3.2	Survival analysis	173
8.3.3	Propensity score matching of SGH with UK subjects	176
8.4	Discussion.....	180
8.5	Conclusions.....	183
Chapter 9	: Summary of chapters: Exploration of Perfusion Imaging; Applicability of Capillary transit time heterogeneity (CTTH) in perfusion Imaging; Stroke outcomes in different Care settings.....	184
9.1	Introduction.....	184
9.2	Imaging factors	184
9.3	Stroke care model and/ or Organisational factors:	186
	Bibliography.....	188

List of Tables

Table 2-1 Test set inter-rater agreement in continuous variables	68
Table 2-2 Study scans Inter-rater agreement in continuous variables	69
Table 2-3 TIMI scale.....	78
Table 2-4 Brain swelling classification (adapted from IST-3 trial).....	80
Table 2-5 Modified Rankin scale	80
Table 4-1 Baseline characteristics of study population (n=144)	106
Table 4-2 Univariate linear regression for predictors of penumbra proportion ...	109
Table 4-3 Multivariate regression for predictors of penumbra proportion	110
Table 5-1 Recanalisation rates grouped by occlusion site lin comparison with Interventioanl Management of Stroke (IMS-3) study	119
Table 5-2 Baseline characteristics of study population (n=123)	120
Table 5-3 Regression for association of large core and recanalisation, and their interaction for imaging and clinical outcomes	128
Table 5-4 Comparison of early improvers vs. non-early improvers.....	130
Table 6-1 Baseline charactersitics of subjects included for final anlysis (n=132).	140
Table 6-2 The perfusion parameters in different tissue zones (core, penumbra, 'non-core-non-penumbra' infarction and normal contralateral brain)	144
Table 7-1 Volumes of Salvaged Penumbra, Infarction and 'non-core-non-penumbra' infarction	153
Table 7-2 Clinical, Imaging characteristics of the subjects with NC/NP =< 2.3 ml vs. >2.3 ml.....	154
Table 8-1 Baseline characteristics of study population	163
Table 8-2 Un-adjusted improtant clinical outcomes in different hospital groups.	168
Table 8-3 Univariate regression for poor 90 day modified Rankin score (mRS3-6) in all study population.....	169
Table 8-4 Multivariate regression for poor 90 day modified Rankin score (mRS3-6)	170
Table 8-5 Univariate regression for death at 90 days in all study population	171
Table 8-6 Multivariate regression for death at 90days	172
Table 8-7 Cox's regression analysis for death at 90 days.....	174
Table 8-8 Univariate regression for poor outcome at 90 days (mRS>2) in SGH, UK post matched groups.....	177
Table 8-9 Multivariate regression for poor outcomes at 90 days (mRS>2) in SGH, UK post matched group.....	178
Table 8-10 Univariate regression for death at 90 days in SGH, UK post matched groups	179
Table 8-11 Multivariate regression for death at 90 days in SGH, UK post matched groups	180

Table of Figures

Figure 1-1 Arterial occlusion site and extent of Cerebral infarction.....	21
Figure 1-2 Changes in Cerebral variables with cerebral perfusion pressure reduction	24
Figure 1-3 Biochemical imaging of "core" and "penumbra"	28
Figure 1-4 Hypoperfused brain compartments in MCA territory ischaemic stroke.	29
Figure 1-5 Dynamic penumbra	30
Figure 1-6 Dynamic ischaemic thresholds during permanent vascular occlusion...	31
Figure 1-7 CBF thresholds for Ischaemia in awake monkey.....	32
Figure 1-8 CBF thresholds for preservation of function and morphology of brain tissue changes with time.....	33
Figure 1-9 Fick's principle.	40
Figure 1-10 Maximum slope method.....	41
Figure 1-11 Impulse Residue function.....	43
Figure 1-12 Residue function.	44
Figure 1-13 The tracer kinetics	45
Figure 1-14 Delay metrics.....	45
Figure 1-15 "Vascular model" a schematic representation.....	48
Figure 1-16 Residue function modelled from a family of gamma variate functions.	48
Figure 1-17 Roles of CBF, CTTH, Oxygen tension in brain oxygenation.....	50
Figure 1-18 Model overview with single capillary (top) and multiple capillaries (bottom)	51
Figure 1-19 Effects of capillary flow heterogeneity on oxygen extraction.....	52
Figure 1-20 Effect of time delay on intravenous thrombolysis outcomes	58
Figure 2-1 Flow chart of MASIS study subjects included in thesis	65
Figure 2-2 Flow chart of POSH study population included in thesis.....	66
Figure 2-3 Flow chart of ATTEST study subjects	67
Figure 2-4 CTP maps	71
Figure 2-5 CTP maps thresholding	72
Figure 2-6 CTP maps with bone, CSF masking	72
Figure 2-7 CTP maps with thresholding for CBV	73
Figure 2-8 CTP, CT coregistration step 1	74
Figure 2-9 CTP, CT Coregistration- step 2.....	75
Figure 2-10 CTP, CT Coregistration- step 3	75
Figure 2-11 Reformatting of images after coregistration	76
Figure 2-12 ROIs for core, penumbra.....	76
Figure 2-13 CTP angiography for collateral grading	77
Figure 2-14 ECASS II classification of ICH.....	79
Figure 3-1 Motion correction of CTP images	84
Figure 3-2 AIF, VOF selection	85
Figure 3-3 AIF and VOF curves	86
Figure 3-4 Concentration tissue curves	87
Figure 3-5 Vasculature removal from CTP.....	87
Figure 3-6 Histogram of distribution of vascular thresholds.....	88
Figure 3-7 Examples of CTP images after vasculature removal.....	88
Figure 3-8 ROI drawing of TTP mask	89
Figure 3-9 TTP masks after ROIs chosen in a subject.....	90

Figure 3-10 CT Infarction ROI	91
Figure 3-11 Coregistration of Follow up CT and acute CTP.....	91
Figure 3-12 An Illustration of good coregistration of both manual and automated methods.....	92
Figure 3-13 An Illustration of manual coregistration better than automated method	92
Figure 3-14 An Illustration of automated coregistration better than manual method	93
Figure 3-15 Non bolus voxels	94
Figure 3-16 Non bolus mask.....	94
Figure 3-17 Non bolus voxels (light blue) in White matter	95
Figure 3-18 Scattered CBV voxels.....	95
Figure 3-19 Final masks derived after the previous steps	96
Figure 3-20 Final masks after fusion of MTT, FU Infarction	96
Figure 3-21 An example of standard SVD map	97
Figure 3-22 An example of vascular model map.....	97
Figure 3-23 Mirroring of TTP, FU Infarct masks	98
Figure 3-24 Core, penumbra and FU Infarction masks.....	98
Figure 3-25 An example of non-core-non-penumbra Infarct mask.	99
Figure 3-26 Flow chart of study population for CTTH work	100
Figure 4-1 Study population CONSORT diagram	105
Figure 4-2 Core, penumbra volumes in relation to collaterals and time	108
Figure 4-3 Penumbra volume in relation with collaterals and time	109
Figure 4-4 Penumbra in relation with time in proximal occlusion (ICA or M1) group	110
Figure 4-5 Collaterals and time relation with penumbra in proximal (ICA or M1) occlusion.....	111
Figure 5-1 Types of haemorrhage in occluded vs. recanalised small or large core groups	126
Figure 5-2 Types of oedema in occluded vs. recanalised small or large core groups	126
Figure 5-3 Type of haemorrhage in early improvers vs. non early improvers	131
Figure 5-4 Types of oedema in early improvers vs. non early improvers.....	131
Figure 5-5 90 day modified Rankin scales in early improvers vs. non early improvers	132
Figure 6-1 Example of maps derived in vascular model.....	141
Figure 6-2 An example of SVD maps.....	142
Figure 6-3 An example of ROIs for core, penumbra and FU Infarct	143
Figure 6-4 Box plot of median CTTH in different tissue zones	145
Figure 6-5 Box plot of median MTT in different tissue zones	146
Figure 6-6 Box plot of median CBV in different tissue zones.....	146
Figure 6-7 Box plot of median CBF in different tissue zones	147
Figure 8-1 Study population CONSORT diagram	162
Figure 8-2 90 day modified Rankin scales in different hospitals.....	169
Figure 8-3 Log rank test comparing hospitals (Log-Rank $p < 0.01$).....	173
Figure 8-4 Cox's proportion Hazard function.....	174
Figure 8-5 Causes of death in the hospitals.....	175
Figure 8-6 Propensity score distribution before matching (SGH, ----- UK).....	176
Figure 8-7 Propensity score distribution after matching (SGH, ----- UK).....	176

Publications and Presentations

Papers

- What is the relationship among penumbra volume, collaterals and time since onset in the first 6h after acute ischemic stroke? *Cheripelli BC, Huang X, McVerry F, Muir KW, Int J Stroke. 2016 Apr; 11(3):338-46*
- Interaction of Recanalisation, Intracerebral Haemorrhage and Cerebral Oedema after Intravenous thrombolysis in acute stroke. *Cheripelli BC, Huang X, MacIsaac R, Muir KW, Stroke.2016 Jul ;47(7):1761-7.*
- Alteplase versus tenecteplase for thrombolysis after ischaemic stroke (ATTEST): a phase 2, randomised, open-label, blinded endpoint study. *Huang X.; Cheripelli BK, Lloyd SM, Kalladka D, Moreton FC, Siddiqui A, Ford I, Muir KW, Lancet Neurol. 2015 Apr;14 (4):368-376*
- Intravenous Thrombolysis for Acute Stroke: Current Standards and Future Directions. *Ramani L, Huang X, Cheripelli B, Muir KW, Curr Treat Options Cardiovasc Med. 2015 Apr;17(4):373.*
- Coagulation and Fibrinolytic activity of tenecteplase and alteplase in acute ischaemic stroke. *Huang X, Moreton FC, Kalladka D, Cheripelli BC, MacIsaac R, Tait RC, Muir KW, Stroke. 2015;46(12):3543-6*
- MRI-Guided Thrombolysis for Stroke with Unknown Time of Onset. *Thomalla G, Simonsen CZ, Boutitie F, Andersen G, Berthezene Y, Cheng B, Cheripelli B, Cho TH, Fazekas F, Fiehler J, Ford I, Galinovic I, Gellissen S, Golsari A, Gregori J, Günther M, Guibernau J, Häusler KG, Hennerici M, Kemmling A, Marstrand J, Modrau B, Neeb L, Perez de la Ossa N, Puig J, Ringleb P, Roy P, Scheel E, Schonewille W, Serena J, Sunaert S, Villringer K, Wouters A, Thijs V, Ebinger M, Endres M, Fiebach JB, Lemmens R, Muir KW, Nighoghossian N, Pedraza S, Gerloff C; WAKE-UP Investigators. N Engl J Med. 2018 Aug 16;379(7):611-622.*

- Tenecteplase in ischemic stroke offers improved recanalisation: Analysis of 2 trials. *Bivard A, Huang X, Levi CR, Spratt N, Campbell BCV, Cheripelli BK, Kalladka D, Moreton FC, Ford I, Bladin CF, Davis SM, Donnan GA, Muir KW, Parsons MW. Neurology. 2017 Jul 4;89(1):62-67.*
- Impact of Computed Tomography Perfusion imaging on the Response to Tenecteplase in Ischemic Stroke: Analysis of two Randomized Controlled Trials. *Bivard A, Huang X, McElduff P, Levi CR, Campbell BC, Cheripelli BK, Kalladka D, Moreton FC, Ford I, Bladin CF, Davis SM, Donnan GA, Muir KW, Parsons MW. Circulation. 2017 Jan 31;135(5):440-448.*
- How many stroke patients might be eligible for mechanical thrombectomy? *Tawil SE, Cheripelli B, Huang X, Moreton F, Kalladka D, MacDougal NJ, McVerry F, Muir KW. Eur Stroke J. 2016 Dec;1(4):264-271.*
- Differences in wake-up and unknown onset stroke examined in a stroke registry. *Reid JM, Dai D, Cheripelli B, Christian C, Reidy Y, Gubitz GJ, Phillips SJ. Int J Stroke. 2015 Apr;10(3):331-5.*
- Comparing mismatch strategies for patients being considered for ischemic stroke tenecteplase trial. *Bivarad A, Huang X, Levi CR, Campbell BC, Cheripelli B, Chen C, Kalladka D, Moreton FC, Ford I, Davis SM, Donnan GA, Muir KW, Parsons MW. Int J stroke. 2019 Nov 4.*

Abstract Presentations

- Haemorrhage and oedema patterns and relation to the recanalization status after IV-thrombolysis in acute ischaemic stroke. *Cheripelli B, Huang X, Muir KW. Institute of Neuroscience and psychology. International Journal of stroke 2015; 10 (Suppl.2) 306.*

- “Does the penumbra shrink over time? Penumbra volumes and collaterals in the first 6 hours after acute ischemic stroke”. *Cheripelli B, Huang X, Muir KW. International Journal of Stroke 2015; 10(Suppl.2):306.*
- Alteplase-tenecteplase trial evaluation for stroke thrombolysis (ATTEST) pilot phase. *Huang X, Cheripelli BK, Kalladka D, Moreton FC, McConnachie A, Siddiqui A, Muir KW. Cerebrovas Dis 2014;37(suppl 1):179*
- Analysis of coagulation and fibrinolytic activity of tenecteplase and alteplase in acute ischaemic stroke. *Huang X, Moreton FC, Kalladka D, Cheripelli BK, Siddiqui A, Muir KW., Int J Stroke. 2014;Vol 9(suppl. 4):5*
- Pooled analysis of Scottish and Australian Randomised trials of Tenecteplase versus Alteplase in stroke. *Bivard A, Huang X, Muir KW, Levi C, Kalladka D, Moreton FC, Cheripelli BK, Spratt NJ, Campbell B, Parsons M, Int J Stroke. 2015; Vol 10(suppl. 2):18*
- How many stroke patients can benefit from mechanical thrombectomy? *El-Tawil S, Huang X, Cheripelli B, Moreton FC, MacDougal N, McVerry F, Muir KW, International Journal of Stroke 2015; 10 (Suppl.5):53-54.*
- Stability of SWI acute ischemic signs during transient hyperoxia in stroke. *Dani K, Moreton FC, Santosh C, Brennan D, Huang X, Cheripelli B, Kalladka D, El-Tawil S, Muir KW, International Journal of Stroke 2015; 10 (Suppl.2):308.*
- CT predictors of malignant cerebral infarction. *McAughtrie R, Cheripelli BK, Moreton FC. Journal of Neurology, Neurosurgery & Psychiatry 2016;87:e1.*

Acknowledgement

I would like to express my gratitude to many people who offered guidance and support throughout my time in research at University of Glasgow.

Professor Keith Muir is my supervisor whom I am ever grateful for kindness and patience. He is undoubtedly a genius with clinical and research acumen second to none. He is most approachable person on Earth and would reply to mails quicker than you could ever expect. He was there to support when I was struggling with multitude of research questions and complex stuff that I would have never understood on my own. I am ever so grateful to him.

The Research fellows that I worked with were humble and I learnt many things from them. Dr Xuya Huang was instrumental in teaching me the perfusion imaging software. Dr Dheeraj Kalladka, Dr Fiona Moreton, Dr Salwa El-Tawil recruited patients and imaging data from these subjects formed a major part of my thesis. Dr Niall MacDougall, Dr Fergal McVerry recruited patients to studies that I used for thesis work. Sally Baird, Wilma Smith, Angela Welsh and Nicola Day, the stroke research nurses who kept me right in patient recruitment and following research policies. Ian Anderson, the project manager for WAKE-UP trial in the UK assisted with the study conduct and visited the UK sites with me.

I thank Stroke consultants Dr Tracy Baird, Dr George Duncan, Dr Phil Birschel, Dr Fozia Nazir, Dr Amy Conley and Dr Johann Selvaraja who have given me insight into clinical experience in managing stroke patients.

I would also like to thank Dr Rachael MacIsaac in helping to understand the statistics, Professor Kennedy Lees who kindly provided the SITS registry data. I would like to thank WAKEUP trial team in Germany.

I am thankful to Dr Andrew Demchuk, Professor Michael Hill from the University of Calgary who adjudicated the ICH classification.

I am indebted to the brilliant brains in Brain lab, Arhus University, Denmark. Prof Leif Østergaard, Kim Mouridsen, Irene Mikkelsen, Lars Riisgaard Ribe and Jesper Frandsen were instrumental in conducting the Capillary transit time work.

I am grateful to my wife Lismy, my children Aaron and Alaina for abundance of love. I love my parents without whom I do not exist.

Contribution to the thesis work and Stroke Research activity during fellowship

I spent three years as a Research fellow at Southern General Hospital (now called Queen Elizabeth University Hospital) during 2012-2016. Along with other Research fellows, Dr Dheeraj Kalladka, Dr Fiona Moreton, Dr Xuya Huang and Dr Salwa El-Tawil, I recruited subjects to various Stroke trials. The trials included the CTX stem cell in stroke (PISCES-II), Alteplase versus Tenecteplase in stroke thrombolysis (ATTEST phase II), Clinical relevance of micro bleeds in stroke (CROMIS), Restart or stop antithrombotic Randomised trial (RESTART), Desmoteplase stroke trial (DIAS-4), Thrombolysis of wakeup and unknown onset stroke using MRI (WAKE-UP), Platelet transfusion in ICH (PATCH) and Ultrasonography in acute ischaemic stroke (CLOT BUST-ER).

Under supervision of Prof. Keith Muir, I initiated the study participating sites in the UK for WAKE-UP trial. This involved visiting sites and meeting local research teams and training for the trial conduct. I responded to recruitment, monitoring queries from the sites with support from Dr Ian Anderson, study manager. I recruited patients for this study in the Queen Elizabeth University Hospital, Glasgow.

Dr Xuya Huang taught me the basic principles of CT perfusion software using Mlstar and educated me the steps in deriving the perfusion metrics. I have also learnt the reading of CT angiograms, collateral scoring, and classification of oedema, haemorrhage and recanalisation grading. This data has been used throughout the thesis.

The database for perfusion consisted of subjects recruited for Post stroke Hyperglycemia (POSH), MASIS and Alteplase versus Tenecteplase in stroke

thrombolysis (ATTEST) trials. Dr Niall MacDougall, Dr Ferghal McVerry and Dr Xuya Huang were responsible for the studies respectively. I performed all the manual steps for deriving perfusion metrics, classifying ICH, oedema classification, collateral grading, measuring infarct volume and angiography information. I also performed the statistical work for these chapters. The extensive statistical work for SITS registry was performed by me with support of Rachael MacIsaac, our statistician.

I travelled to Aarhus, Denmark for a period of 3 months to process the CT perfusion using their mat lab platform. The travel fund was granted by Scottish Imaging Network: A platform for Scientific Excellence (SINAPSE). I have performed all the manual steps described in the chapters 7-8.

Author's declaration

I declare that, except where explicit reference is made to the contribution of others, this dissertation is the result of my own work and has not been submitted for any other degree at the University of Glasgow or any other institution.

Signature _____

Printed name _____

Definitions/Abbreviations

4D	4 Dimensional
ACA	Anterior Cerebral Artery coefficient
ADC	Apparent diffusion coefficient
AF	Atrial Fibrillation
AIF	Arterial Input Function
AIS	Acute Ischaemic Stroke
ANOVA	Analysis of Variance
ASPECTS	Alberta Stroke Program Early CT Score
ATP	Adenosine Triphosphate
ATTEST	Alteplase - Tenecteplase Trial Evaluation for Stroke Thrombolysis
BBB	Blood Brain Barrier
BKCR	Bohr-Kety-Crone-Renkin
BP	Blood Pressure
CTTH	Capillary transit time heterogeneity
CBF	Cerebral Blood Flow
CBV	Cerebral Blood Volume
CI	Confidence Interval
CMRglu	Cerebral Metabolic Rate of Glucose
CMRO2	Cerebral Metabolic Rate of Oxygen
COV	Coefficient of variation
CPP	Cerebral Perfusion Pressure
CSF	Cerebro-Spinal Fluid
CT	Computed Tomography
CTA	CT Angiography
CTP	CT Perfusion
CVR	Cerebrovascular Resistance
DEFUSE Evaluation	Diffusion and Perfusion Imaging Evaluation for Understanding Stroke Evaluation
DICOM	Digital Imaging and Communications in Medicine
DWI	Diffusion Weighted Imaging (MRI)
DSA	Digital Subtraction Angiography
DT	Delay Time
ECASS	European Cooperative Acute Stroke Study EIC (Early Ischaemic changes)
EPITHET	Echoplanar Imaging Thrombolytic Evaluation Trial
ESCAPE	Endovascular Treatment for small Core and Anterior Circulation Proximal Occlusion with Emphasis on Minimising Computed Tomography to Recanalisation Times
EXTEND	Extending the Time for Thrombolysis in Emergency Neurological Deficits
FLAIR	Fluid-Attenuated Inversion Recovery imaging (MRI)
FMSIO	F18-fluormisonidazole
FOV	Field of View
GRE	Gradient Echo (MRI)
HI	Haemorrhagic Infarction
HU	Hounsfield Unit
IA	Intra-arterial
ICA	Internal Carotid Artery
ICH	Intra cerebral Haemorrhage
IQR	Inter quartile Range
IST3	International Stroke Trial 3

IV	Intravenous
LACS	Lacunar stroke
LMF	Leptomeningeal collateral flow
LMA	Leptomeningeal collateral arteries
MASIS	Multicentre Acute Stroke Imaging Study
MCA	Middle Cerebral Artery
MIP	Maximum Intensity Projection
MR CLEAN	Multicenter Randomized Clinical Trial of Endovascular Treatment for Acute Ischemic Stroke in the Netherlands
MRI	Magnetic Resonance Imaging
MR RESCUE	Mechanical Retrieval and Recanalisation of Stroke Clots Using Embolectomy
mRS	modified Rankin Scale
MTT	Mean Transit Time
NCCT	Non-Contrast Computed Tomography
NCCP	Non-core-non-penumbra
NIFTI	Neuroimaging Informatics Technology Initiative
NIHSS	National Institute of Health Stroke Scale
NINDS	National Institute of Neurological Disorders and Stroke
NMDA	N-methyl-D-aspartate
NNT	Number Needed to Treat
NVD	Neurovascular dysfunction
OCSP	Oxfordshire Community Stroke Project
OEF	Oxygen Extraction Fraction
OR	Odds Ratio
oSVD	Circular Singular value decomposition
OTT	Onset-to-treatment Time
PACS	Partial anterior circulation stroke
PCA	Posterior Cerebral Artery
PDF	Probability density function
PET	Positron Emission Tomography
PH	Parenchymal Haemorrhage
POCS	Posterior circulation stroke
POSH	Post Stroke Hyperglycaemia
PRACTISE	Penumbra and Recanalisation Acute Computed Tomography in Ischaemic Stroke Evaluation
PROBE	Prospective Randomised Open Blinded End-point
PWI	Perfusion Weighted Imaging (MRI)
RAPID	Rapid Processing of Perfusion and Diffusion
RCT	Randomised Controlled Trial
REVASCAT	Randomized Trial of Revascularization with Solitaire FR Device versus Best Medical Therapy in the Treatment of Acute Stroke Due to Anterior Circulation Large Vessel Occlusion Presenting within Eight Hours of Symptom Onset
ROI	Region of Interest
rtPA	recombinant tissue Plasminogen Activator
SD	Standard Deviation
SGH	Southern General Hospital
SI	Source images
SICH	Symptomatic Intra-cerebral Haemorrhage
SITS	Safety in stroke thrombolysis
SITS-MOST	Safe Implementation of Thrombolysis in Stroke Monitoring Study
SPECT	Single Photon Emission CT
SWI	Susceptibility Weighted Imaging (MRI)

SWIFT-PRIME	Solitaire with intention for Thrombectomy as Primary Endovascular Treatment
sSVD	Standard Singular Value Decomposition
TACS	Total anterior stroke
TEMPIS	Telemedicine Pilot Project for Integrative Stroke Care
TIA	Transient Ischaemic Attack
TICI	Thrombolysis in Cerebral Infarction
TIMI	Thrombolysis in Myocardial Infarction
Tmax	Time to Maximum
TNK	Tenecteplase
TOAST	Trial of ORG 10172 in Acute Stroke Treatment
TOF	Time of Flight Imaging (MRA)
tPA	Tissue Plasminogen Activator
TTP	time to peak
UK	United Kingdom
VM	Vascular model
VOF	Venous Output Function
WAKE-UP	Efficacy and Safety of MRI-based Thrombolysis in Wake-up Stroke
WGI	Western general Infirmary

Chapter 1 Introduction

1.1 Acute Ischaemic stroke (overview)

Stroke represents a substantial socioeconomic burden globally. It is the second most common cause of mortality worldwide and the leading cause of adult disability¹. In UK prevalence is 518 per 100,000 and annual incidence is around 110 per 100,000.

Despite a decline in incidence and mortality over the past three decades, stroke continues to be a disabling disease, with one half having residual hemi paresis, one third unable to walk or requiring institutional care at six months. In the UK societal costs are estimated at £8.9 billion per year²⁻⁴. Ischemic stroke accounts for 87% of all strokes while primary intra cerebral haemorrhage accounts for 10%⁵. A Stroke registry study in 1712 ischaemic stroke patients showed prevalence of atherothrombosis (23.7%), Cardio-embolic (26.5%), small vessel disease (22.9%), cryptogenic (14.7%), two causes (4.7%) and not sufficiently studied (6.4%)⁶.

TOAST (a set of criteria originally developed for the Trial of Org 10172 in Acute stroke treatment) classification was suggested to classify ischemic stroke based on the aetiology⁷. A German stroke registry study in stroke patients using TOAST criteria showed prevalence of atherothrombosis (20.9%), cardio-embolic (25.6%) and small vessel disease (20.5%)⁸. SSS-TOAST is a modified TOAST criteria using imaging, cardiovascular, historical, laboratory information to assign the mechanism with certainty⁹. This classifies stroke aetiology as:

- Large artery atherosclerosis (evident-probable-possible)
- Cardiac embolism
- Small vessel occlusion
- Stroke of other determined aetiology

- Stroke of undetermined aetiology
- Unknown-cryptogenic embolism
- Unknown-other cryptogenic
- Unknown-incomplete evaluation
- Unclassified

The most commonly affected territory in ischemic stroke is middle cerebral artery (46.6%), followed by posterior cerebral artery (10.7%), basilar artery (8%), anterior choroidal artery (6.2%), cerebellar arteries (4.8%) and anterior cerebral artery (3.2%)⁶.

Intravenous thrombolysis within 4.5 hours has been the mainstay of treatment since publication of the National Institute of Neurological Disorders and Stroke (NINDS)¹⁰ and third European Co-operative acute stroke study (ECASS-III)¹¹ trials. Intra arterial thrombectomy (IAT) has been proven to be beneficial in selected patients with proximal large artery occlusions as an adjunct to intra venous thrombolysis^{12,13}. IAT is now considered as an adjunctive treatment to IV thrombolysis for a selected population in the UK¹⁴. Multimodal Imaging has played a crucial role in patient selection, both in research settings and in routine clinical practice. Tissue level imaging with perfusion metrics has been studied in research trials¹⁵⁻¹⁷. Large artery recanalisation does not reflect the tissue and clinical outcomes. Among many other factors, a possible explanation is the role of “microcirculation” with incomplete reperfusion at microcirculatory level^{18,19}. There is potential role of the microcirculation in acute ischemic stroke and how this may play a role in tissue fate²⁰⁻²². Of important development in this area is “capillary transit time heterogeneity”²³.

In this thesis, I looked at the 3 month stroke outcomes between UK centres (2 hospitals in Glasgow, and rest of the UK) using Safety in Stroke Thrombolysis (SITS) stroke registry. I then looked at the cross sectional variation in penumbra volumes over time (within 6 hours of stroke) and role of collaterals in this relation of penumbra with time. I also investigated the effect of recanalisation

in respect to haemorrhage and oedema occurrence after IV thrombolysis. I investigated a novel approach in deriving perfusion maps by incorporating “capillary transit time heterogeneity” using vascular model to understand and investigate the tissue states.

1.2 Pathophysiology

Ischaemic stroke is caused by a critical reduction of regional cerebral blood flow beyond a critical duration. This can be caused by atherothrombosis, cardiac or large artery embolism or small vessel occlusion. The extent of ischaemic infarction depends on the site of vessel occlusion, compensatory capacity of vascular bed (fig.1-1). Large artery occlusion with poor collateral flow can cause large Middle cerebral artery (MCA) territory infarction whereas with good collateral flow the extent of infarction can be less²⁴. Border zones can be affected with critical stenosis of large arteries, whereas, lacunar infarctions are caused by different mechanisms: embolism from the heart, carotid artery; atheroma of parent artery or perforating arterioles; intrinsic small vessel disease (lipohyalinosis or fibrinoid necrosis)²⁵.

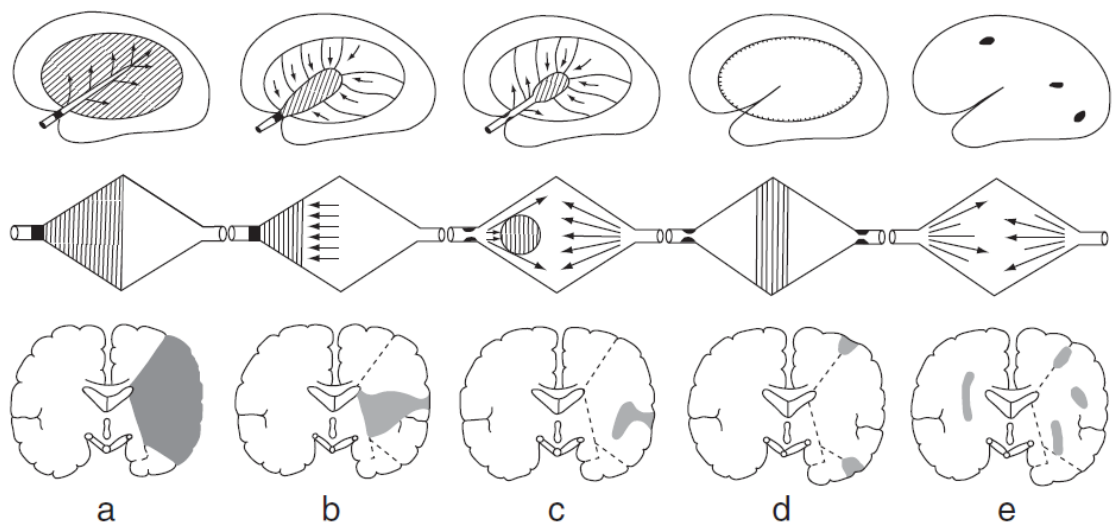


Figure 1-1 Arterial occlusion site and extent of Cerebral infarction

a. Total territorial infarct b. Core infarct c. Territorial infarct in centre of supply area, due to branch occlusion d. Border zone infarction in watershed areas e. Lacunar infarction due to small vessel disease. Reproduced with permission from Textbook of stroke medicine (p. 4), Brainin M and Heiss W-D(eds), 2010, Cambridge University press.

1.2.1 Cellular pathology of ischaemic stroke

Ischaemia is defined as reduction in cerebral blood flow causing altered cellular function. The reduction in cerebral blood flow is not uniform throughout the ischaemic territory, there is gradient of reducing blood flow from periphery to the core²⁶. A normal adult brain comprises of 130 billion neurons (21 billion in neo cortex)²⁷ comprising only 2% of body weight, but consumes approximately 20% of the body's total oxygen consumption. The brain's oxygen consumption is almost exclusively used for oxidative metabolism of glucose²⁸. Approximately 70% of metabolic demand is due to the N-K ATPase pump that maintains the ion gradient across neuronal membranes. Ischaemia causes depletion of ATP, leading to influx of calcium, sodium and efflux of potassium. Cerebral blood flow thresholds below the requirement for the ATP synthesis are established within a few minutes of ischaemia²⁹. The mechanism of death in this tissue is thought to be necrosis. The consequence of membrane depolarisation is Glutamate release³⁰. This leads to calcium influx³¹ in nearby neurons by stimulation of N-methyl-D-aspartate receptors³². This calcium influx causes "excito-toxicity" and ultimately contributes to cell death³³. Further, a cascade of oxidative³⁴, nitrate stress³², inflammation³⁵ cause "apoptosis"³⁶, and necrosis. In parallel to molecular events above, a physiological process, "Cortical spreading depressions or depolarisation" (CSD)³⁷, a sustained depolarisation spreading out from core in adjacent neuronal membranes is also identified as a stroke mechanism. CSD has been demonstrated in patients suffering from ischaemic stroke³⁸.

1.2.2 Cerebral haemodynamics in response to ischaemia

Relative Cerebral Blood Flow (rCBF) values of approximately 50ml/100gm/min is maintained for a wide range of Cerebral Perfusion Pressure (80-150 mmHg, CPP)³⁹. This is due to autoregulation mediated through changes in Cerebral Vascular Resistance (CVR). The relationship between CBF and CVR is known with an equation $rCBF = r CPP / r CVR$. r CPP represents the difference between arterial pressure forcing blood into the cerebral circulation and the venous back pressure. When CBF falls below 20ml/100gm/min impairment in function, and below 8ml/100g/min infarction develops²⁶. A three stage model of haemodynamic change is commonly accepted in response to reduction in CPP⁴⁰ (fig.1-2). In stage 0, CPP is normal, Cerebral Blood Volume (CBV), Mean Transi

Time (MTT) are not elevated, while r CBF response to vasodilatory stimulus is normal. In stage 1, vasodilation of arterioles occurs to maintain a constant rCBF when CPP falls. So, CBV, and MTT increase ($MTT = (CBV/CBF)$), but Oxygen Extraction Fraction (OEF) remains the same. In stage 2, autoregulatory capacity for compensatory vasodilatation is exceeded. Further reductions in CPP now produce decrease in CBF. While oxygen supply is diminished due to decreasing CBF, there is an increase in OEF to maintain Cerebral Metabolic Rate of Oxygen ($CMRO_2$).

If CPP continues to fall CBF will progressively decline until the increase in OEF is no longer adequate to supply the energy needs of the brain⁴¹. Clinical evidence of brain dysfunction now appears and this may be reversible if circulation is rapidly restored. In the oligoemic phase $CMRO_2$ is normal but in ischaemia $CMRO_2$ is decreased.

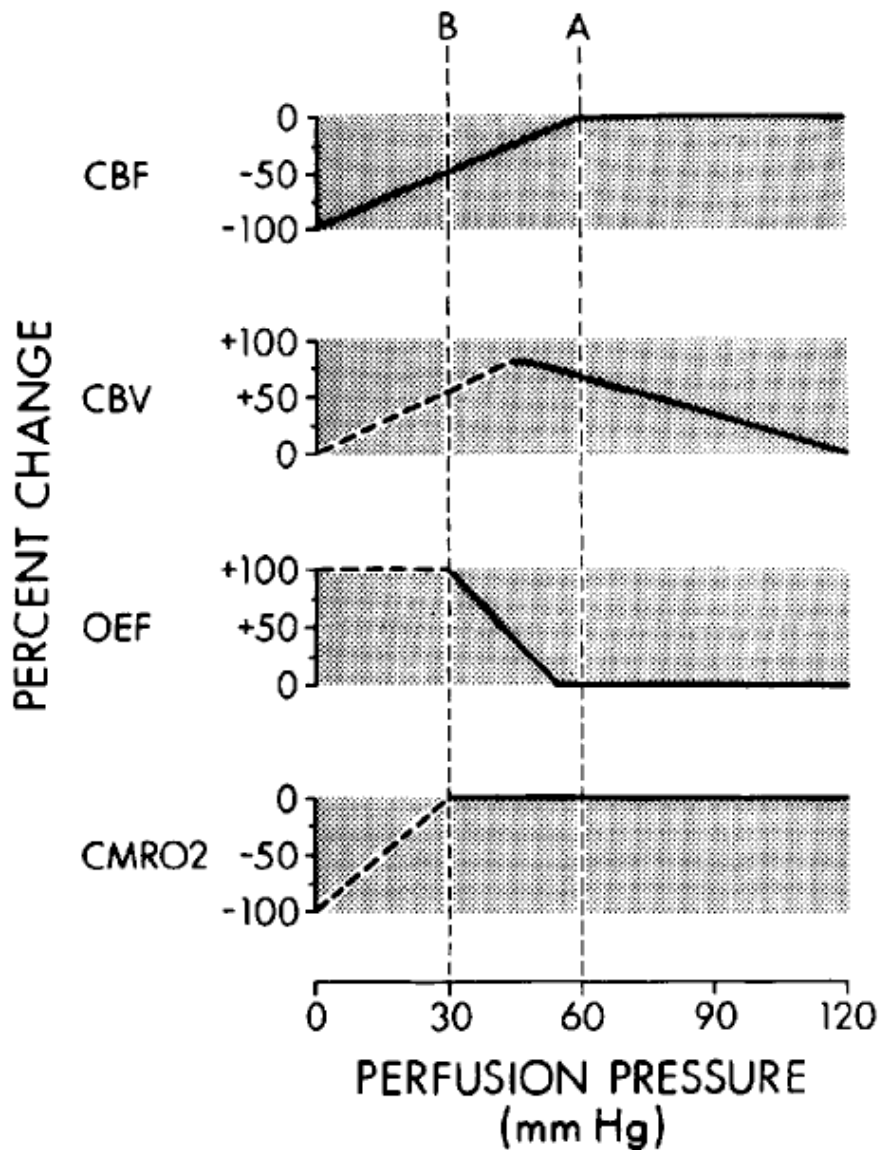


Figure 1-2 Changes in Cerebral variables with cerebral perfusion pressure reduction

Illustration of the changes in cerebral variables during a progressive decrease in cerebral perfusion pressure and progression through various stages of impaired cerebral circulation. The stages are referenced to the changes in OEF. Stage I (Perfusion pressure >60), OEF is unchanged. Stage II (perfusion pressure 30-60), OEF begins to increase. Stage III (perfusion pressure <30), OEF declines again. Solid lines show changes that are known and dashed lines, those that are postulated. Reproduced with permission from "Cerebral haemodynamics in ischaemic cerebrovascular disease", by Powers et al⁴⁰, 1991, *Ann Neurol*, 29 (3),231-240.

1.3 Types of Cerebral oedema

The initial type of oedema following cerebral ischemia is cytotoxic oedema. Cytotoxic oedema is the result of cells being unable to maintain ATP-dependent Na-K membrane pumps which are responsible for high extracellular and low intracellular Sodium (Na) concentration⁴². When energy fails, these pumps cease to operate and Sodium accumulates in the cells, drawing with it chloride (Cl⁻),

and water along an osmotic gradient. Cytotoxic oedema is blood flow threshold dependant. At flow values of approximately 30% of control, anaerobic metabolism causes increase of intra cellular osmolality and hence osmotic swelling. At levels below 20% of control, anoxic depolarisation and equilibration of ion gradients further enhance intracellular osmolality and swelling⁴³. This occurs due to osmotic gradient created by influx of Na. The movement of ions and water into cells causing cytotoxic oedema results in depletion of these constituents from extracellular space⁴⁴. In absence of blood flow, cell swelling occurs at the expense of extracellular fluid but net water content is unchanged. The shift of fluid is reflected by decrease in Apparent diffusion coefficient (ADC) of water, causing increased Diffusion-weighted (DWI) signal in MRI⁴⁵. However, if there is residual flow, the net water content increases, resulting in brain swelling, “Ionic oedema”.

In Ionic oedema, an earliest phase of endothelial dysfunction, there is transport of Sodium across the Blood Brain Barrier (BBB), generating an electrical gradient for Cl⁻ and osmotic gradient for water, replenishing Na⁺, Cl⁻, and water in the extracellular space⁴². This ionic oedema is responsible for tissue swelling and precedes vasogenic oedema by approximately 6 hours⁴⁶. With advancing cell necrosis and degradation of the vascular basal lamina, the blood brain barrier breaks down⁴⁷. After 4-6 hours serum proteins leak from the blood into brain. This initiates a vasogenic oedema that reaches its peak in 1-2 days⁴⁸, enhancing total water content. SUR1-TRMP4 an ion channel is up regulated by all cell types in the neurovascular unit after ischaemia⁴⁹. In rats, this channel blockade reduces oedema and haemorrhage⁵⁰. Molecule therapy with glyburide is effective in blocking this channel⁴⁹. This agent was studied in pilot phase II study of humans to evaluate safety and feasibility⁵¹.

1.4 Haemorrhagic Transformation (HT) in Ischaemic stroke

The disruption of BBB and impairment of the auto regulatory capacity of cerebral vasculature predisposes to blood extravasation when ischaemic tissue is reperfused⁵². The degree of this disruption appears highly on the duration of ischaemia. It is proposed that IV tPA may augment matrix metalloproteinase

(MMP) dysregulation, IV tPA may degrade the extracellular matrix integrity and increase the risk of BBB leakage, oedema and haemorrhage⁵³.

Haemorrhagic transformation (HT) is a known complication of Ischaemic stroke, especially after thrombolytic therapy⁵⁴. HT can be divided into Haemorrhagic Infarction (HI) and Parenchymal Haematoma (PH). HI is a heterogeneous hyperdensity occupying a portion of an ischaemic infarct zone on CT, whereas PH refers to a more homogeneous dense haematoma with mass effect. The subtypes are: HI1, HI2, PH1 and PH2. HI1- small petechiae, HI2- more confluent hyperdensity (no mass effect), PH1- <30% Infarct zone, PH2 >30% Infarct zone (both PH1, PH2 have homogeneous hyperdensity and mass effect)

The incidence depends on many factors, such as age, blood glucose level, thrombolytic agent used, route of administration, time window of therapy^{55,56}. There is positive correlation between Infarct area and incidence of HT⁵⁷. AF and cerebral embolism are associated with increased risk of HT⁵⁸. Hyperglycemia has a major role in post Ischemic HT.

In experimental transient MCAO model, acute hyperglycemia resulted in HT. Human trials also revealed this association⁵⁹. Poor collaterals may result in a high frequency of HT with worsened clinical neurological status⁶⁰. IV-tPA is independently associated with HT in major studies. Prognosis of HT depends on the type: PH2 is found to be significant predictor of neurological deterioration and high mortality.

1.5 Evidence from animal studies

Experimental animal models have provided us with important insights into ischemia. Different animal models exist; global⁶¹ or focal ischaemia^{62,63}. Global ischaemia is achieved by four vessel occlusion⁶¹. Focal ischaemia models can be transient where the Middle cerebral artery (MCA) occlusion with intra luminal thread placement which is reversed in 2-3 hours; or permanent, where the irreversible MCA occlusion is achieved by diathermy, surgical section or

photocoagulation. Focal ischaemia is more useful as this is translatable into human stroke; however it is not without pitfalls.

Focal ischaemia in the territory of MCA is the dominating cause of clinical stroke. This is reflected by predominantly MCA occlusion models in animal experiments. In these models, occlusion of MCA at its origin including lenticulostriate arteries- end arteries supplying basal ganglia that suffer severe reduction of blood flow, whereas cortex exhibits a gradient of blood flow with decrease from periphery to central parts⁶⁴. Trans-orbital MCA occlusion was initially applied in monkeys⁶⁵, but later experimented in cats, dogs, rabbits and rats. In this model, there is no retraction of brain; however, removal of the eye ball can cause functional disturbances, and vasospasm⁶⁶. Trans- cranial approaches were commonly used for mice since the MCA originates close to brain surface⁶⁷. Filament occlusion of MCA is most widely used technique, described by Koizumi⁶⁸. A nylon suture with acryl thickened tip is placed in the origin of MCA. This method commonly affects large part of MCA territory often resulting in oedema, therefore, usually after 1-2 hours filament is withdrawn although it may be left in produce permanent ischaemia.

1.5.1 Multimodal imaging of tissue outcomes in focal ischaemia animal models

Consecutive cryostat section of brain can be analysed using pictorial methods that can give a good regional resolution⁶⁹. Bio-luminescence methods are available to identify ATP⁷⁰, glucose⁷¹, lactate⁷². Loss of ATP on bioluminescent images is the “core” of hypoperfused tissue. “Penumbra” can be identified by mismatch between acidosis, inhibition of protein synthesis (which occurs at high flow thresholds) and ATP (i.e. core. Fig.1-3)⁷³. Other invasive methods apply fluorescence (NADH for tissue acidosis⁷⁴) or mapping gene expression⁷⁵.

Non-invasive imaging in animal studies mainly employs Positron emission tomography (PET) or Magnetic resonance Imaging (MRI). The parameters commonly used for imaging of ischaemia are cerebral blood flow (CBF), metabolic rate of oxygen (CMRO₂) and glucose consumption (CMRGl), Oxygen extraction fraction (OEF)⁷⁶ and binding of ligands such as Flumazenil which is a marker for neuronal cell bodies with benzodiazepine receptors⁷⁷. With declining

cerebral blood flow, blood OEF rises to cover oxygen needs of aerobic metabolism. At flows approximately <50% of control, oxygen consumption declines and anaerobic glycolysis begins. With further lower flow rates this also fails, energy metabolism fails and flumazenil do no longer bind to their receptors. So, ischaemic core can be delineated by reduction of oxygen, glucose consumption or by loss of flumazenil binding⁷⁷ where as ischaemic penumbra has increased glucose utilisation⁷⁸ or increased oxygen extraction⁷⁹.

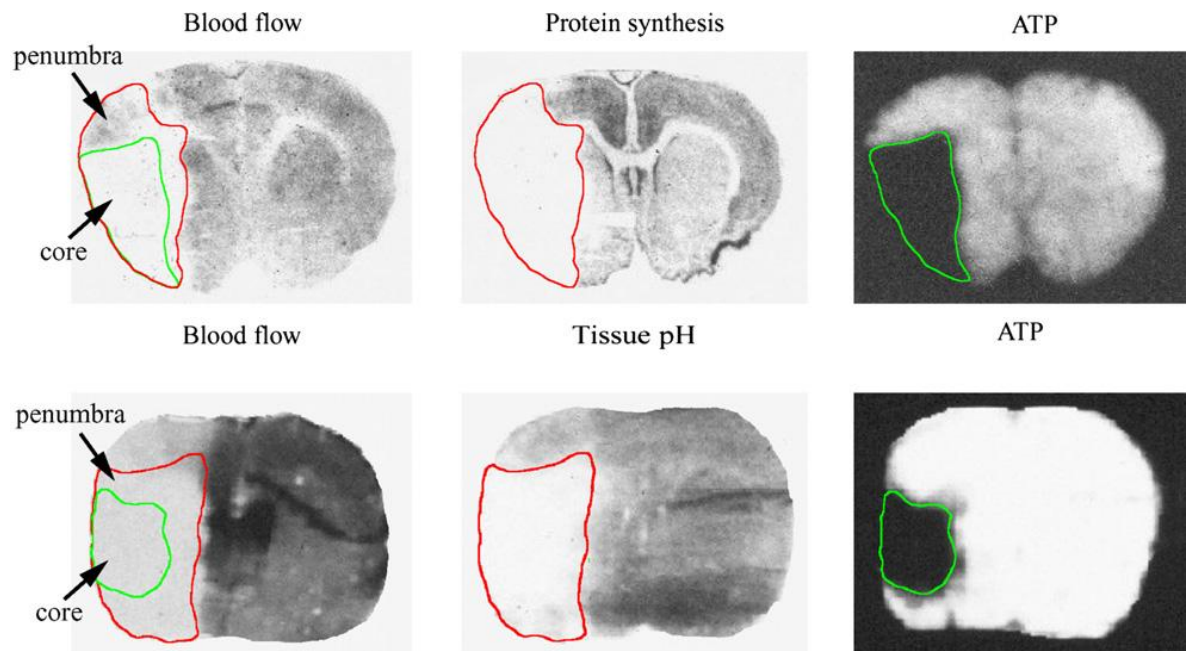


Figure 1-3 Biochemical imaging of "core" and "penumbra"

The core is identified by ATP depletion and the penumbra by the mismatch between the suppression of protein synthesis and ATP depletion (top) or by the mismatch between tissue acidosis and ATP (bottom). The mismatch areas are highlighted by projecting the outlines of the biochemical disturbances on the corresponding autoradiogram of cerebral blood flow. Reproduced with permission from "Multimodal mapping of the ischemic penumbra in animal models" in *Informa Health care* (p. 77-92), by Donnan GA et al, 2007, New York: MerceL Dekker⁷³.

1.5.2 Evidence for irreversible (Core) and reversible (Penumbra) ischaemia and evolution over time

Different energy requirements and flow thresholds exist for maintenance of membrane function, preservation of neuronal function (functional threshold) and morphological integrity²⁹. Some function of CBF reduction and its duration probably defines threshold for irreversible infarction. Symon et al, in baboons

(trans-orbital or retro-orbital approach MCA occlusion), showed the linear relationship of local blood flow reduction and degree of neurological impairment⁸⁰. The tissue that lost its electrical function but no release of potassium characterises tissue death⁸⁰. This functionally silent but viable tissue regained function if occlusion was removed. In this model, core of ischaemia was located in the basal ganglia and sylvian opercula, penumbra stretching almost entire lateral aspect of cerebral hemisphere⁸¹. The area between these two thresholds is structurally viable and was termed as penumbra (analogy to moon eclipse, since this area is between infracted and normal tissue)²⁶. Since viability of brain tissue requires maintenance of energy-dependant metabolic processes, the penumbra may be defined as region of constrained blood supply in which energy metabolism is preserved⁸².

Different brain regions have variable thresholds for ischaemic cell damage, white matter being more resilient than grey matter. The key concept is distinct compartments in hypoperfused tissue; tissue that is irreversibly damaged (core), tissue that will survive (oligaemia), and tissue that may survive (penumbra) if reperfusion occurs in time(fig. 1-4)⁸³.

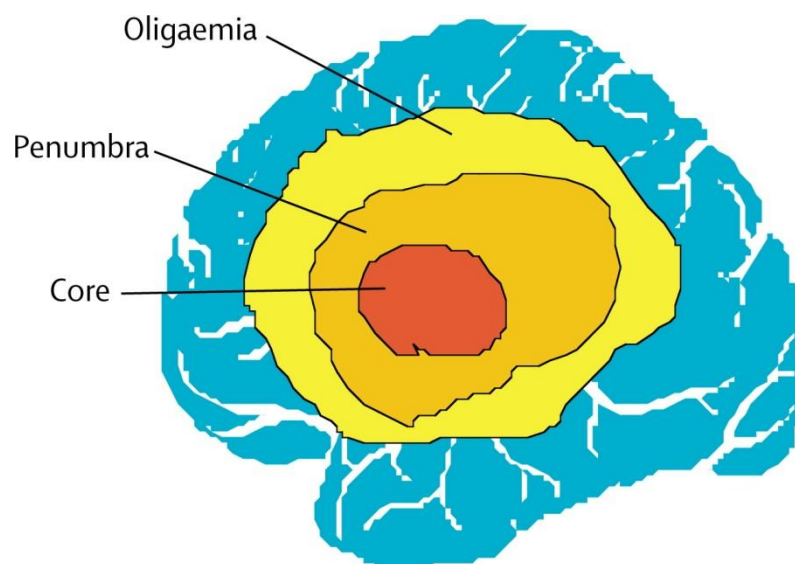


Figure 1-4 Hypoperfused brain compartments in MCA territory ischaemic stroke.
 Reproduced with permission from "Imaging of acute stroke", by Muir et al, 2006,. Lancet Neurology,5 (9),755-68⁸³

Jones et al, first reported the dynamic nature of “penumbra”⁸⁴. In their study in awake monkeys, within 3 hrs a very little penumbra survived (fig.1-5). Baron et al,⁸⁵ defined penumbra as a tissue that exists between threshold of infarction and penumbra threshold. Operationally, penumbral tissue must satisfy the criteria of being 1) functionally impaired hypoperfused tissue with undetermined fate that is at risk of infarction if not salvaged 2) contributing to clinical deficit 3) its resolution is associated with proportional recovery of neurological function. Oligoemic tissue surrounds critically ischaemic tissue where the decreased CPP is compensated by collaterals^{86,87}.

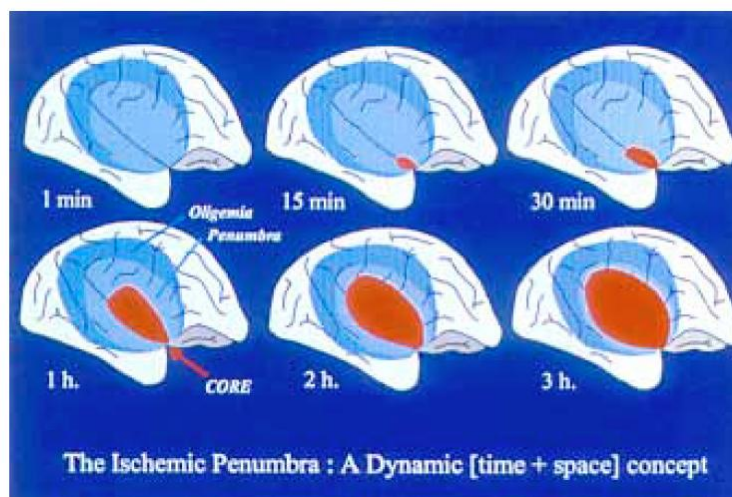


Figure 1-5 Dynamic penumbra

The time course of infarct growth at the expense of penumbra, from the situation immediately following MCA occlusion (top left) , to 3h later (bottom right). The oligoemia is not at risk of infarction. Reproduced with permission from “Mapping the ischemic penumbra with PET: Implications for acute stroke treatment”, by Baron et al⁸⁸, Idealised diagram of baboon’s brain. (using data from Jones et al⁸⁴), 1999, *Cerebrovasc Dis*,9 (4),193-201.

1.5.3 Tissue Thresholds

Biochemical and functional changes were correlated with CBF values in several studies. The normal value for CBF is 50-60 ml/100g/min in grey matter. This is 2-3 times less in white matter. Protein synthesis was completely suppressed at CBF of 35ml/100g/min⁸⁹. Glucose utilisation sharply declines below CBF of 35ml/100g/min⁹⁰. This corresponds to beginning of acidosis and accumulation of lactate⁹¹. At flow rates below 26ml/100g/min tissue acidosis becomes pronounced and ATP begins to decline. This is the threshold for energy failure⁹². Na-K ratio of brain increases at flows below 10-15ml/100g/min⁶⁶ and

extracellular ion changes occur at rates between 6 and 15 ml/100g/min^{29,93,94}. This is the threshold for anoxic depolarisation (pump failure). In animal studies, Cerebral Blood flow (CBF) values of less than 20ml/100g/min results in impaired neural function (electric failure) but temporarily intact tissue integrity, defining penumbra, and, early, irreversibly damaged tissue had CBF values of 6-10 ml/100gm/min^{26,29,95,96}.

Suppression of EEG activity occurs at rates between 15 and 23 ml/100g/min^{29,97}. In cats, neuronal firing stops at flows of 18 ml/100g/min⁹⁶. Narcotized baboons lose somato-sensory evoked potentials when CBF falls below 15ml/100g/min⁹⁸.

In contrast to biochemical and functional changes, histological changes require sometime before being visible. Studies determining the dynamic changes in CBF thresholds indicate that thresholds may change with time (fig.1-6).

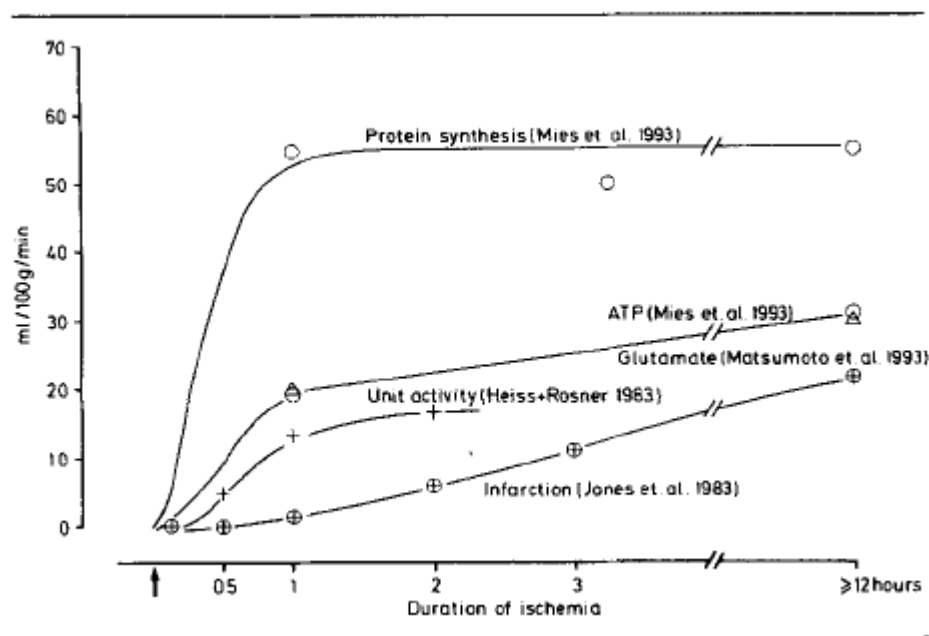


Figure 1-6 Dynamic ischaemic thresholds during permanent vascular occlusion.

CBF thresholds increase with duration of ischaemia for ATP, glutamate, unit rate but static for protein synthesis. Reproduced with permission from "Variability thresholds and the penumbra of focal ischaemia", by Hossmann K-A⁸², 1994, Ann Neurol, 36 (4),557-565.

The prototype of the penumbra definition is focal ischemia through MCA occlusion in which blood flow gradually declines from periphery to the core region. Jones et al, in awake monkeys showed that blood flow thresholds for Infarction are higher with longer duration of occlusion⁸⁴. CBF threshold for

neurological symptoms was 23 ml/100g/min. When this fell below 8ml/100g/min, neurological deficit became permanent. Moderate CBF (15ml/100g/min) was tolerated for 2-3 hours. After 2-3 hours, CBF below 10-12 ml/100g/min resulted in infarction, whereas with permanent occlusion CBF below 17ml/100g/min resulted in infarction⁸⁴ (fig.1-7).

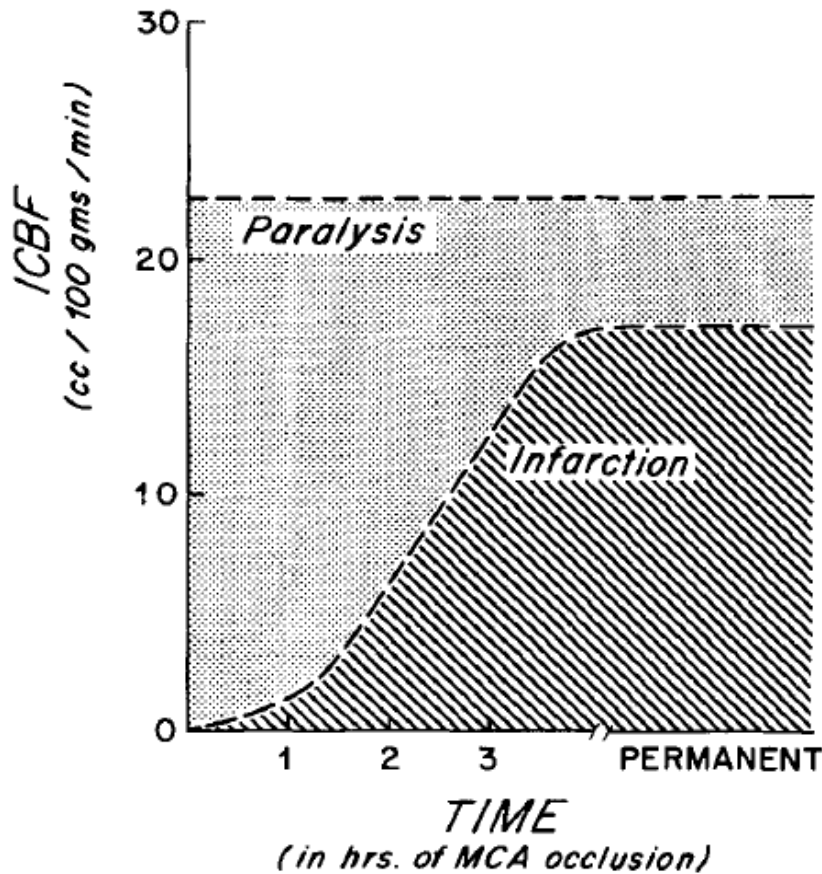


Figure 1-7 CBF thresholds for Ischaemia in awake monkey

Reproduced with permission from "Thresholds for focal cerebral ischaemia in awake monkeys, by Jones et al⁸⁴, 1981, J Neurosurg, 54 (6),773-82.

The tissue outcome is shown to depend on severity of flow reduction and duration was also reported by others^{99,100}. Using high contrast PET, serial functions were measured over 24 hours after permanent MCA occlusion in cats⁹⁹. A dynamic nature of penumbra with progressive increase in core size was found. In six cats, they showed gradual changes (at 3 time points of <1 hr, 1-4 hr, 24 hr) in metabolic parameters. CBF fell to 40% of control immediately and very gradually to 20%; whereas CMRO₂ fell to 55% and then to 20% of control gradually. Areas of increased OEF moved from the centre to periphery. The interaction of severity and duration of ischaemia in tissue outcome was studied

in cats by recording neuronal activity and blood flow¹⁰¹. Possible combinations of residual cerebral blood flow and duration of ischaemia and neuronal recovery is shown in Fig.1-8¹⁰². CBF threshold that define irreversibly damaged tissue increases with time.

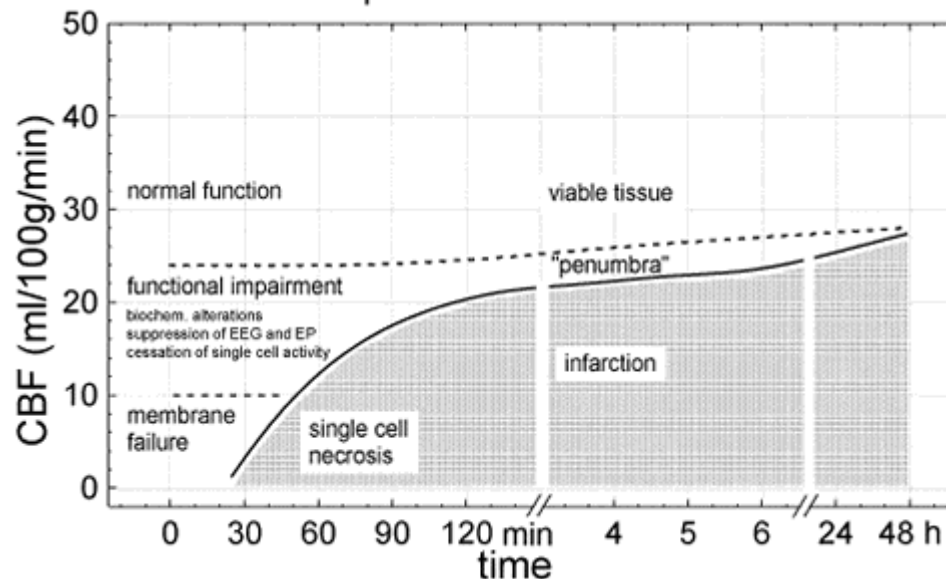


Figure 1-8 CBF thresholds for preservation of function and morphology of brain tissue changes with time

The activity of individual neurons is blocked when flow decreases below a certain threshold (dashed line) and returns when flow is raised above this threshold. The solid line separates structurally damaged from functionally impaired but morphologically intact tissue, the penumbra. Reproduced with permission from "The ischemic Penumbra: Correlates in Imaging and Implications for treatment of Ischemic stroke", by Heiss WD, 2011, *Cerebrovascular Dis*, 32 (4), 307-320¹⁰².

Tolerance to focal cerebral ischemia is clearly related to residual CBF which - must be provided by collateral circulation¹⁰³. In non-anaesthetised macaque monkeys, the extent of CBF reduction correlated well with infarct size: when CBF fell below 12ml/100g/min for 2 hours or longer, a larger infarction occurred and at higher residual CBF a smaller infarction occurred; good collaterals led to little or no infarction whereas poor collaterals produced fatal infarction⁹⁸

Volume of brain infarct after 3 hours of temporary MCA occlusion is same as after permanent ligation¹⁰⁴. Lassen et al, concluded that penumbra remains viable for only one or perhaps a few hours but not longer⁸⁶. After 2 hours of permanent MCA occlusion in rats, the ratio of restricted diffusion lesion (DWI) volume to ATP depleted lesion declines to 1.4 and after 7 hours these are congruent⁶⁹. Blood flow remains stable throughout this initial ours of ischemia

which excludes the possibility of the infarct growth due to progression of ischemia. The reason for the expansion of tissue injury into penumbra may be due to peri-infarct depression like depolarisations^{37,105}. PET studies in baboons showed that tissue with misery perfusion escaped infarction if vessel reopened within 6 hours but infarcted with permanent occlusion¹⁰⁶⁻¹¹⁰. Jones et al, study in awake monkeys, moderate to large infarction was seen in 2-3 hrs⁸⁴. Heiss et al, study in cats also showed faster (within 6-8 hrs) demise of penumbra⁹⁹.

Animal models do not translate directly to human stroke. Focal ischemic models did not have any change in hemodynamic parameters (respiration, pulse etc.) which is not the case in human stroke. Moreover, stroke in humans is heterogeneous and has associated co morbidities, which make it difficult to translate animal models to Humans. Successful translation of animal experiments should reflect human co-morbidities and variability in mechanism of stroke¹¹¹. However, this would mean increased sample size.

1.6 Human Positron Emission Tomography (PET) studies

PET introduction allowed the repeated quantitative determination of physiological variables in brain. PET with oxygen-15 tracers became the gold standard for evaluation of pathophysiological changes in early ischaemic stroke¹¹². PET studies provided the data on flow and metabolic variables predicting final infarction. Relatively preserved CMRO2 indicated maintained neuronal function in regions with severely reduced CBF “misery perfusion”. OEF is increased up to 80% in this area.

PET study using oxygen-15-steady state technique in humans showed the existence of penumbra in one third of patients imaged between 5 and 18 hours and detected penumbra as late as 16 hours in some patients⁸⁸. Another prospective study showed existence of penumbra (in 10 out of 11 patients) up to 18 hours¹¹³. They have also showed that neurological recovery was proportional to the volume of penumbra that is rescued. Using multi-tracer PET, viable tissue in the border zone of ischaemia was seen up to 48 hours¹¹⁴. In another study, all 8 eligible subjects had substantial volume of tissue with CMRO2 values above threshold for tissue viability¹¹⁵. These voxels constituted 10%-52% (mean 32%) of the final infarct volume. Read et al, using¹⁸F fluoromisonidazole to identify

hypoxic tissue found that on average 45% of total hypoxic tissue volume survived in those patients studied up to 51 hours¹¹⁶. Another study using ¹⁸F fluoromisonidazole in patients up to 48 hrs, spontaneously surviving proportion of hypoxic tissue (median 46%) was not significantly different between two time epochs (≤ 12 hrs or >12 hrs) , and also showed that survival of penumbra has a definite neurological benefit¹¹⁷. However, PET imaging although useful in understanding pathophysiology, it is not feasible in clinical practice.

1.7 Acute stroke imaging in Humans

1.7.1 Non-contrast CT (NCCT)

In the National Institute of Neurological Disorders and Stroke (NINDS) study, only NCCT was the requirement before inclusion of subjects for IV thrombolysis¹⁰. NCCT is commonly used to exclude contraindications such as haemorrhagic stroke before thrombolysis¹¹⁸. If established hypodensity or early ischemic changes in $>1/3$ MCA territory, the risk of haemorrhage with thrombolysis is greater¹¹⁹. Early ischemic changes include hypodensity because of combination of cytotoxic oedema and reduced blood volume, and loss of grey-white matter differentiation. In patients with known stroke onset time of <4.5 hours, if NCCT is normal or showing only subtle early ischemic changes, or $<1/3$ MCA territory hypodensity, IV thrombolysis is deemed safe¹²⁰.

Early ischemic changes (EIC) can give a positive diagnosis but are not really helpful in indicating the time since stroke onset in acute stage. If there is no major hypodensity, however, it is possible that onset is <4.5 hours. This is an inclusion criterion for a currently ongoing randomised, Tenecteplase in wake-up ischemic stroke trial (TWIST [clinicaltrials.gov NCT03181360](https://clinicaltrials.gov/ct2/show/study/NCT03181360)). In hyper acute stage, the Na-K channel failure in ischaemic brain tissue leads to cytotoxic oedema without any net increase of water. The Hounsfield Unit (HU) attenuation is directly proportional to the tissue water content, therefore proportional to the degree of vasogenic oedema but not cytotoxic oedema: for every 1% increase in tissue water content , X-ray attenuation decreases by 3-5%, which corresponds to a drop of 2.5 HU on NCCT images¹²¹. Early ischemic changes described on

NCCT encompass both decreased attenuation (e.g. obscuration of basal ganglia, loss of grey white differentiation) or localised tissue swelling (hemispheric sulcal effacement in the cortex)^{122,123}. These appearances represent different patho-physiological processes^{123,124}. Hypo attenuation represents an increase in tissue water content which results in reduction of tissue density. This occurs following a series of compartmental fluid shifts (intravascular>interstitial>intracellular) that ultimately result in additional water within the brain¹²⁵. Hypo attenuated regions represent irreversibly injured tissue that is destined for infarction^{126,127}. Isolated sulcal effacement results from the compensatory increase in the cerebral blood volume (CBV) that occurs in penumbral tissue¹²⁷⁻¹²⁹. Tomura et al, reported that in embolic middle cerebral artery or internal carotid artery distribution ischemic stroke patients, the earliest sign was obscuration of the lentiform nucleus due to cytotoxic oedema¹³⁰.

In European Cooperative Acute Stroke Study (ECASS; n=620), NCCT had limited sensitivity (40-70%) to detect acute ischemic changes within the first 6 hours^{131,132}. A systematic review of the literature showed the sensitivity for early ischemic signs on NCCT in subjects presenting <6hrs varied from poor to moderate¹³³. The sensitivities varied as the number of subjects in these studies are small, problems in clinician experience in detecting subtle early parenchymal changes and different definitions of early ischemic signs. Moderately good inter observer agreement (mean 82%-84%) was observed between neuro-radiologists for detection of acute hypo density within 6 hrs¹³⁴. Inter-rater agreement and sensitivity of ischemic signs on CT in <7 hrs is imperfect in other studies that compared CT with MRI¹³⁵⁻¹³⁸.

1.8 Perfusion Imaging

The goal of acute stroke therapies is to normalise perfusion to preserve maximal amount of penumbral tissue¹³⁹. In acute ischaemic stroke, patient tailored treatment approaches need information on core and penumbra. CT perfusion (CTP) is widely available and provides similar pathophysiological information as MRI¹⁴⁰.

1.8.1 CT perfusion (CTP)

Most commonly, imaging for CTP consists of 4-8 slices of brain each with 10-20mm thickness at level of basal ganglia. Approximately 7-10 sec after IV Iodinated contrast injection, series of scans acquired for about 50sec. These temporally acquired images are reconstructed and post processed using one of the several algorithms.

CTP imaging has been used to evaluate the infarct core and potentially salvageable penumbra¹⁴¹. Without early reperfusion, core can expand¹⁴²⁻¹⁴⁴, and with early reperfusion penumbra can be rescued^{145,146}, hence the need for assessing these acutely. Selection of perfusion parameters and thresholds to identify core, penumbra remain a challenge¹⁴⁷. Studies using different post processing software reported different parameters and different thresholds for accurately identifying core and penumbra^{141,148}.

Bolus tracking CTP¹⁴⁹ generates maps of Cerebral blood flow (CBF), Cerebral blood volume (CBV), Time to Peak(TTP) and Mean transit time (MTT) (fig 1-14). CBV is defined as the total volume of flowing blood in a given volume of the brain (millilitres of blood in 100g of brain); CBF is defined as the volume of blood passing through the given volume of brain per unit time (millilitres of blood in 100g of brain); MTT represent the average time for blood transiting through the given brain region (in seconds); TTP is an index of time between the beginning of blood perfusion and maximum enhancement in the given region. Depending on mathematical model, T_{max} (time to the peak of the residual function) or DT (delay time to the peak of the residual function) can be generated instead of TTP.

In CTP, thresholds for both core and penumbra have to be derived unlike in MRI. In MRI acute DWI lesion volume has been reported to be highly correlated to core¹⁵⁰. When quantitative interpretation of all CTP maps was performed and compared to final infarct volume using the Alberta Stroke Program early CT score (ASPECTS)¹²⁷, CBV maps were close predictors of outcome lesion extent in subjects with major reperfusion by 24 hrs, while MTT and CBF were predictive of the infarct extent in those who did not have major reperfusion¹⁵¹. Reduced CBV has therefore been considered a marker for infarct core, whereas prolonged MTT

with normal CBV being a marker for ischemic tissue at risk of infarction¹⁴⁰. Wintermark et al, using ROC curve analysis using follow-up MRI as a gold standard (each pixel in selected CT perfusion parameter and selected threshold is categorised (TP true positive, FP false positive, TN true negative, FN false negative against reference MR images). Wintermark group showed in case of persistent arterial occlusion, relative MTT (AUC 0.962) predicted penumbra, with an optimal threshold >145% and absolute CBV (AUC 0.927) in cases of large artery recanalisation predicted the core, with an optimal threshold <2 ml/100gm/min¹⁴¹. The software relies on central volume principle as contrast injection rates were slow. Non iterative deconvolution was applied to derive MTT map. CBV is calculated from area under the time enhancement curve. CBF is derived from central volume principle ($CBF=CBV/MTT$). In CTP, with ROC curve analysis using more stringent criteria including volumetric (mean difference between CTP lesion and 2h DW lesion volumes) and clinical validation (24 h and 90 day clinical outcomes), relative CBF threshold (rel. CBF< 40%) most accurately predicted the core (AUC 0.95) and relative delay time (r DT)>2 sec accurately predicted penumbra (AUC 0.86) in a study by Bivard et al¹⁴⁸. The commercial software MiStar (Apollo Medical Imaging Technology, Australia) used singular value decomposition with delay or dispersion correction. This methodology produced Delay time than Tmax. Relative CBF volume thresholds in hypoperfused tissue have been found to be similar to those found in Single Photon emission CT (SPECT) studies^{151 152}. MTT and TTP maps are found to be more sensitive to ischemia than CBF or CBV maps¹⁵³. It is observed that TTP lesion volumes are closely related to final infarct volume in those who do not recanalise¹⁵⁴. The penumbra not progressing to infarction was predictive of clinical recovery¹⁵⁴. Additional studies have confirmed good correlations of CBF values on CTP maps compared with PET¹⁵⁵ or Xenon CT¹⁵⁶.

There are several other parameters, either alone, or in combination in predicting the tissue states. Threshold derivation from other groups showed a product of CBF and CBV was the best predictor of core pixels for white matter¹⁵⁷. Each CT scanner manufacturer use different algorithms for deriving the parameters, which complicates the uniform interpretation, and standardisation of CTP parameters.

Marked variability across different post processing software limit any generalisation of perfusion parameter threshold maps between platforms. rMTT, a most accurate predictor of penumbra by Wintermark et al, might not be generalisable to newer, longer CTP acquisition protocols or CTP maps generated by different post processing platforms for example new “delay corrected” algorithms¹⁵⁸.

1.8.2 Post acquisition CT perfusion processing

Two commonly applied mathematical methods for CT perfusion are maximum slope and deconvolution methods. These are first pass bolus tracking techniques. Non diffusible tracer (iodinated contrast) is injected into ante cubital fossa and its concentrations repeatedly measured during its first pass through an intracranial vessel. Contrast transit through the vasculature produces a change in time attenuation. These changes can be graphed as time attenuation curves for each voxel in brain tissue. These are also called tissue concentration curves (CTC). Tissue perfusion measurements using CTP was first reported by Axel in 1980¹⁵⁹. Maximum slope model assumes no venous outflow. For this, a very high rate of contrast injection (10ml/s) is required¹⁶⁰ which cannot be achieved routinely in practice. This method yields relative rather than absolute values. Both deconvolution, non-deconvolution techniques apply Fick's principle (fig.1-9).

Fick Principle: Conservation of volume

- One pipe goes into the box (=artery)
- One pipe comes out of the box (=vein)
- Black box = tissue

$$Q(T) = CBF \cdot \int_0^T [C_{artery}(t) - C_{vein}(t)] dt$$

Note the assumptions!

- Single inflow
- Single outflow
- No delays (instantaneous bolus)
- No dispersion (one path)

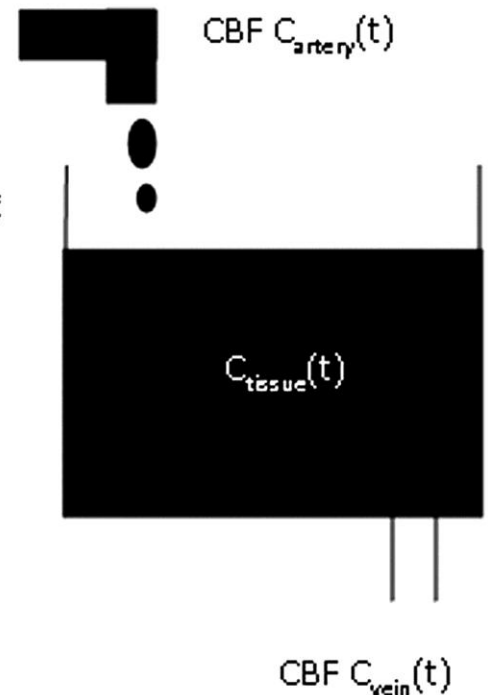


Figure 1-9 Fick's principle.

Conservation of mass to a given region of interest within the brain parenchyma. Reproduced with permission from "Theoretic basis and technical implementations of CT Perfusion in Acute Ischemic Stroke, Part1¹⁶¹: Theoretic Basis", by A.A. Konstas et al, 2009, AJNR, 30 (4), 662-668.

1.8.2.1 Maximum slope model:

As contrast enters the area being imaged, the signal intensity of the time-concentration curve, measured in HU rises linearly (fig.1-10)¹⁵⁹. The amount of accumulated contrast material $Q(t)$ is the product of CBF and the difference on arterio-venous concentration:

$$Q(t) = CBF \cdot \int_0^t [C_{artery}(t) - C_{vein}(t)] dt$$

In order to make the CBF calculation less complicated, it is assumed that the output from the capillary bed into the venous system is zero, termed the no venous outflow assumption. To satisfy this assumption, injection rates must be very rapid. Using these assumptions, the equation can be simplified as

$$Q(t) = CBF \cdot \int_0^t C_{artery}(t) dt$$

$$\int_0^T C_{\text{artery}}(t) dt$$

The equation is known as the Mullani-Gould formulation¹⁶². The rate of contrast accumulation is related to the CBF and the arterial concentration at time (t) and from the Mullani-Gould equation the peak rate of contrast accumulation will occur when arterial concentration is maximum:

$$\left[\frac{dQ(t)}{dt} \right]_{\text{max}} = \text{CBF} \cdot [C_{\text{artery}}(t)]_{\text{max}}$$

The ratio of the maximal slope of Q (t) to the maximal arterial concentration can therefore be used to measure CBF.

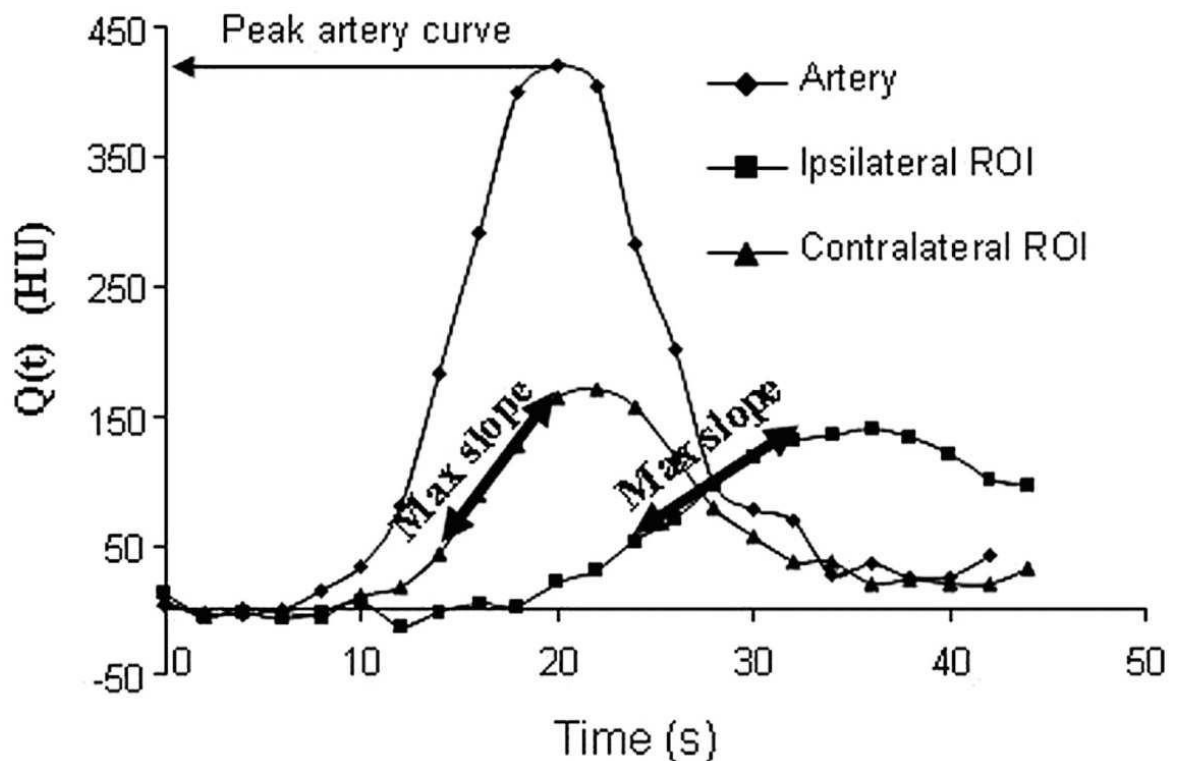


Figure 1-10 Maximum slope method.

CBF can be calculated from the ratio of maximal slope of Q (t) to the maximal arterial concentration. Different maximal slopes in different ROIS reflect different CBF values. Reproduced with permission from "Theoretic basis and technical implementations of CT perfusion in acute ischemic stroke, part 2: technical implementations", by Konostas A.A. et al, 2009. AJNR,30 (5),885-92¹⁶³

However, this equation relies upon assumptions which may influence calculation of CBF. Specifically it is assumed there is no venous flow of contrast flow before the peak arterial enhancement which in turn requires that injection rates of 10-20ml/sec are used to reduce the possibility of venous contamination¹⁶³. In clinical practice these rates are not achievable and therefore CBF calculations may be inaccurate¹⁶⁴. As rates of injection for IV contrast material are typically no more than 5ml/sec alternative methods to interpret the time - concentration curves must be considered.

1.8.2.2 Deconvolution model:

Deconvolution is a commonly applied post-processing mathematical process whereby the brain tissue contrast concentration-time curves from each pixel are 'scaled' to the tissue concentration-time curve from a feeding artery (arterial input function, AIF). This gives each pixel a residual function tissue concentration-time curve that is used to measure parameters such as CBF, T_{max} and DT. Crucial physiological information from perfusion imaging is obtained by conversion of concentration time curve (CTC) into reliable estimates of CBF, CBV and MTT. Assumption for rapid contrast injection does not hold true, therefore MTT cannot directly be obtained from normalised CTC. So, Tracer kinetic method applies that observed CTC is the convolution of AIF with a residue function, scaled by CBF (Fig.1-13).

Considering a bolus of contrast tracer material injected into a tissue voxel of interest, we can define the concentration ($C_{tissue}(t)$) of tracer in the tissue in terms of two functions: 1) Residue function, $R(t)$: a fraction of tracer is still present in the voxel of interest at time t following an ideal instantaneous unit bolus injection. $R(t)$ is unit less and is equal to 1 at $t=0$ ¹⁶⁵. 2) Arterial Input function (AIF), $C_{artery}(t)$: concentration of tracer in the feeding vessel to the voxel of interest at time t . Calculation of CBF requires measurement of the temporal shape of both the arterial input and the tissue-time-attenuation curves¹⁶⁶. The true input into the tissue voxel of interest cannot be measured directly; in practice, the AIF is estimated from a major artery, with the assumption that this represents the exact input to the tissue of interest. Any

delays or dispersion from AIF to the tissue of interest will introduce errors in quantification of CBF¹⁶⁷. The observed tissue-time-attenuation curve represents a combination the effects of the AIF and the inherent tissue properties. Thus, to fit the model, the effects of the AIF on the tissue concentration curve must be removed by using a mathematic process known as “deconvolution” to derive $R(t)$, which is dependent only on the haemodynamic properties of the voxel under consideration. $R(t)$ demonstrates an abrupt rise, a plateau of duration equal to the minimum transit time through the tissue of interest and then decay towards baseline (fig.1-11 & 1-12). The impulse residue function is the idealized tissue time attenuation curve that would result if the entire bolus of contrast material was administered instantaneously into the artery supplying given area of brain. The plateau of the impulse residue function reflects the length of time during which the contrast material is passing through the capillary network. Assuming the contrast remains within the vascular space, the shape of the impulse residue function will be as below (fig.1-11)¹⁶⁸. The venous output function serves as a reference against which the CTP parametric values are normalized and scaled. This should have least amount of partial volume averaging. CBV values are affected by the chosen venous output function.

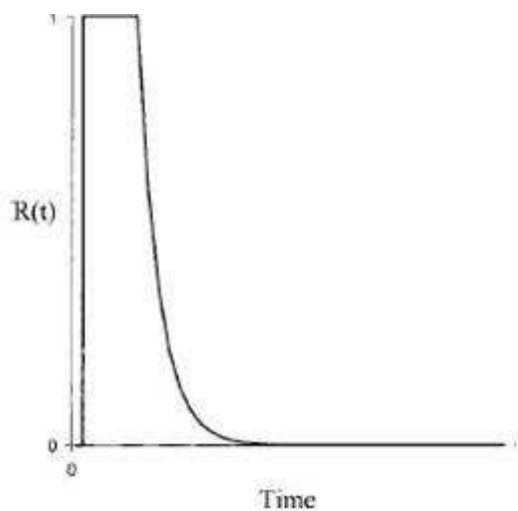


Figure 1-11 Impulse Residue function

Schematic representing the impulse residue function $R(t)$ in a vascular network where the tracer remains intravascular. Reproduced with permission from “CT perfusion scanning with deconvolution analysis: pilot study in patients with acute middle cerebral artery stroke”¹⁶⁸, by Eastwood et al, 2002, Radiology, 222 (1):227-36

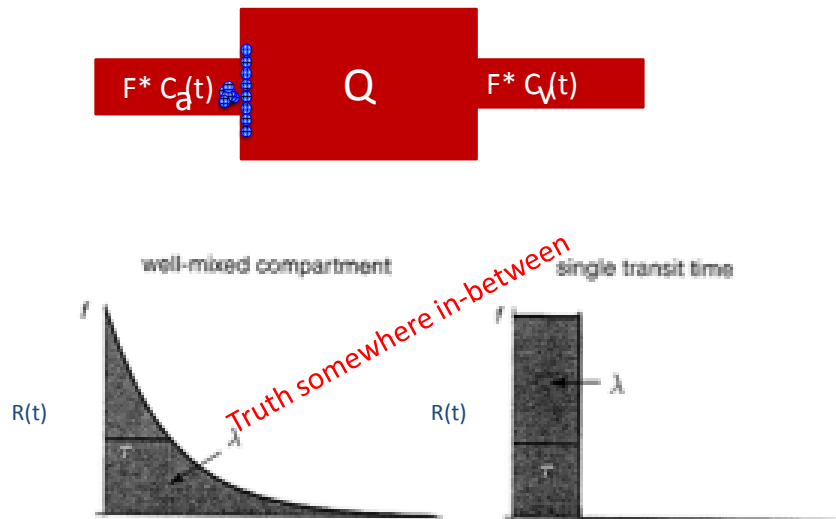


Figure 1-12 Residue function.

The residue function $R(t)$ is the fraction of tracer still retained in tissue at time t after injection. Shape of the residue function depends on the vasculature of the tissue voxel. Q is amount of contrast agent in tissue (mmol), C_a Concentration of contrast agent in the artery (mmol/l), C_v concentration of contrast agent in Vein (mmol/l) F flow (ml/min).

Use of deconvolution to derive perfusion measures does not rely on the assumption of no venous outflow, but instead considers outflow in the calculation. In deconvolution, attenuation values of an artery are integrated with time-attenuation curves of brain tissue on a voxel-by-voxel basis in mathematical operation called deconvolution (fig.1-13). $C(t) = CBF \cdot [C_a(t) * R(t)]$ $C(t)$ is the tissue attenuation curve; $C_a(t)$ is the arterial time -attenuation curve; $R(t)$ is the impulse residue function, $*$ is the convolution operator. $C(t)$ and $C_a(t)$ can each be measured and deconvolution produces $CBF \cdot R(t)$ which is plotted over time. CBF is obtained from the peak height of the curve, while CBV is the area under the curve. Once CBF , CBV are derived, MTT can be derive according to the central volume principle¹⁶⁹: $CBF = CBV / MTT$ (fig. 1-14). Other delay metrics such as T_{max} , TTP , DT can be derived similar to MTT .

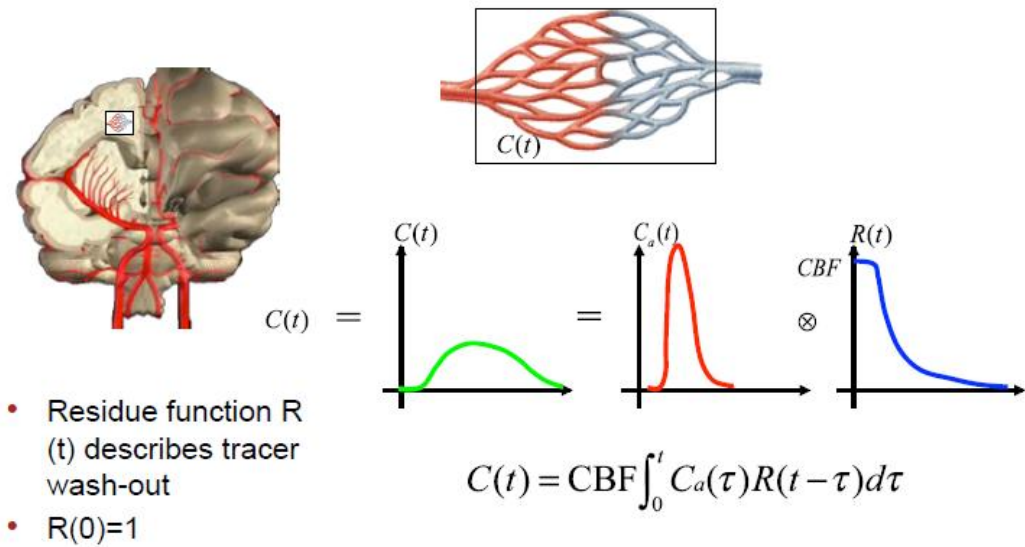


Figure 1-13 The tracer kinetics

Tissue concentration time curve in Tracer kinetic equation: observed CTC is the convolution of AIF with a residue function, scaled by CBF. C_a : Concentration of agent in the artery at time t . C_t : Concentration agent in the tissue at time t . CBF (perfusion)(ml/100g/min). $R(t)$ is residue function.

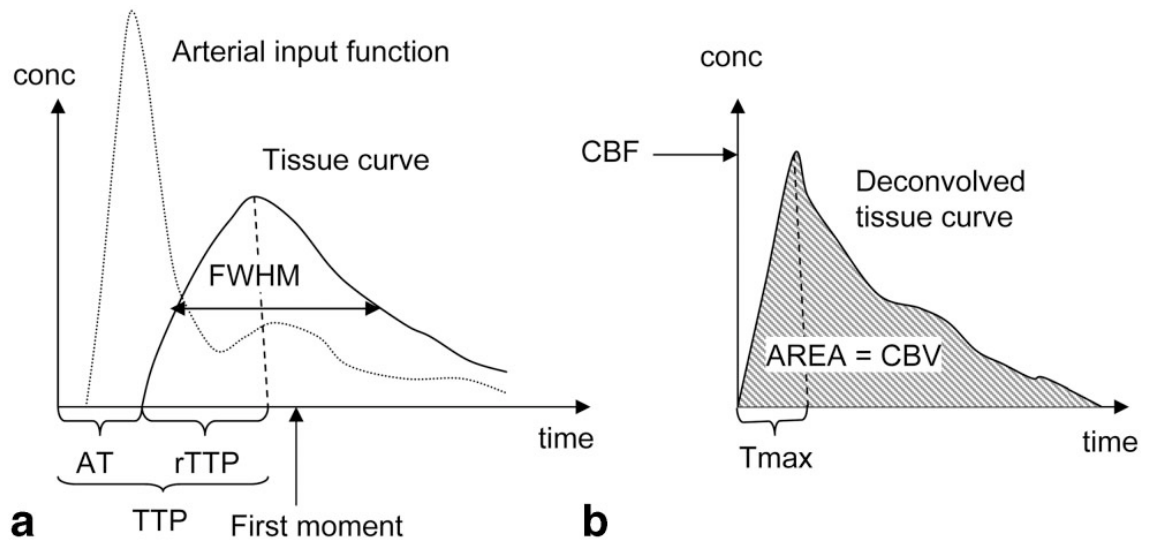


Figure 1-14 Delay metrics

a: The measured tissue concentration time curve (tissue curve) gives rise to various measures of the transit time that all depend on the local shape of the AIF. The arrival time (AT) of the bolus mainly reflects collateral circulation. The time to peak, to some extent, reflects tissue transit time (rTTP) and, if arrival delay is included, also reflects collateral circulation (TTP). The first moment (the centre of gravity) and the full width at half maximum (FWHM) of the tissue concentration time curve mainly depend on tissue MTT. b: Deconvolution of the curves in (a) removes the dependence on the arterial input curve and produces the deconvolved tissue curve. In the presence of arterial delays, the deconvolved curve is not maximal at $t=0$, but instead is maximal (the tissue impulse response function) after a certain delay (T_{max}). CBF is usually taken as the curve

height of the deconvolved curve at time T_{max} . MTT is calculated as CBV/CBF , where CBV is determined as the area under the deconvolved curve (b) or the tissue curve (a). However, calculation of CBV from the tissue curve requires laborious corrections for tracer recirculation. Reproduced with permission from "Principles of cerebral perfusion imaging by bolus tracking"¹⁷⁰, by Leif Ostegard et al, 2005, Journal of Magnetic resonance Imaging, 22(6),710-7.

Several methods to deconvolve equation and hence solve for $CBF.R(t)$ have been proposed and are divided into two main categories: Parametric (vascular model) and non-parametric methods. With parametric method a specific analytic expression for $R(t)$ is assumed. Assuming a specific shape for $R(t)$ imposes assumptions on the inherent tissue properties that cannot be known priori with sufficient precision^{166,171}.

Since non-parametric methods do not assume a shape for $R(t)$, they are commonly used. Deconvolution equation is unstable, oscillations (i.e. noise) is produced in computation of the solution for $R(t)$. There are two methods of dealing with the noise¹⁷²: 1) Fourier transformation 2) singular value decomposition (SVD). Predominant technique for estimating CBF is based on deconvolving the AIF with the CTC using Singular Value Decomposition (SVD) to estimate the $CBF.R(t)$ (called impulse response)^{166, 173}. SVD yielded the most robust results from all the deconvolution methods used to map CBF ¹⁷¹. The creation of accurate quantitative maps of CBF , CBV , MTT using deconvolution methods has been validated in a number of studies^{156,174}.

SVD algorithm by Østergaard¹⁷¹ et al is susceptible to dispersion and delay of measured AIF. In setting of major disease this may underestimate CBF , therefore overestimate MTT (i.e. penumbra) by including benign oligoemic tissue^{175,176}. Despite this, it is reported to be better in tissue state prediction¹⁷⁷. Fourier transformation makes this insensitive to delay but sensitive to noise, thus unsuitable for CBF calculation. Block circular decomposition matrix SVD (oSVD) method, a tracer -arrival timing insensitive technique was introduced by Wu et al¹⁷³. This technique basically removed the causality assumption (i.e. that the tissue of interest signal intensity cannot arrive before the AIF) built into SVD.

A new approach, "parametric (vascular) model" was suggested which assumes the physiological model of exponentially decreasing tracer kinetics¹⁷⁸. This

model, in addition the standard parameters, also provides capillary transit time heterogeneity (CTTH). The tissue residue function that denotes proportion of contrast that remains in vasculature at a given time (t) is directly related to vascular transit times $h(t)$, hence to CTTH¹⁷⁷. The shape of residue function reflects micro vascular retention of tracer and thereby distribution of capillary velocities¹⁷⁷.

Estimated residue function has oscillations. This compromises their physiological interpretation (i.e. fraction of contrast agent as a function of time, after an impulse injection, is a decreasing function of time¹⁷³ and estimation of flow heterogeneity difficult. So model free deconvolution approaches are not adequate. SVD cannot delineate between dispersion to increased transit times. Gaussian process deconvolution produces smoother estimate of the residue function¹⁷⁹. Regularisation steps of model free deconvolution approaches^{166,173}, may stabilise CBF¹⁷⁹⁻¹⁸¹, but, they are not optimised to detect salient features of the residue function. Hence, Parametric (vascular) model (fig.1-15) was suggested^{177,182}. CTTH, OEF max can be calculated in addition to macroscopic perfusion markers¹⁷⁸. Gamma variate distribution of probability density function (pdf) was used to describe the transit time distributions. Fraction of particles distributed to tube (i) is $h(i)$. By increasing number of tubes to t , $h(t)$ represent continuous pdf for transit times t (transit time distribution). The mean of this pdf is MTT and standard deviation is CTTH. In this parametric method, alpha and beta are the parameters. MTT is derived as product of alpha and beta, where as CTTH is square root of this product (fig.1-16). Modelling the dynamics of micro vasculature, a smooth monotonically decreasing residue function is derived. Bayesian system identification approach¹⁸³ based on Levenberg-Marquart type Expectation-Maximisation (EM) algorithm, was applied. A monte-carlo simulation study showed it does not underestimate high flows and unaffected by low signal to noise ratio. It is also robust to delays between AIF and CTC. Blood flow, oxygen binding to haemoglobin, capillary transit time heterogeneity can influence the oxygen delivery. Flow heterogeneity can be derived from the slope of deconvolved tissue curve along with CBF¹⁷⁷. Putative effects of increased CTTH were reported in stroke, ischemic heart disease, and dementia in a series of papers by Ostergaard¹⁸⁴⁻¹⁸⁶. Tissue with abnormal flow heterogeneity is shown to correlate with final infarct in ischaemic stroke^{21, 187}.

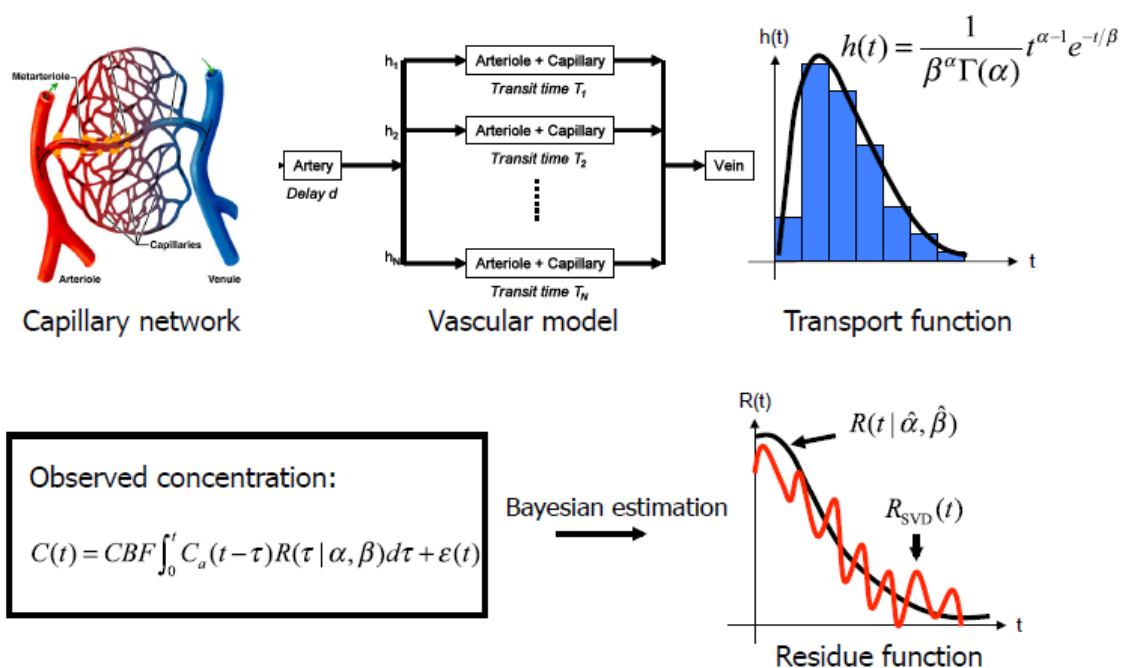


Figure 1-15 "Vascular model" a schematic representation

Blood is delivered to the tissue with a delay δ relative to the measure arterial Input function. Within the tissue, particles are distributed to a number of tubes (N), each with a different transit time T_i . The fraction of particles distributed to tube i is h_i . The h_i 's form an empirical density function for the transit times which characterises the microvasculature. This indicated by the histogram on the right hand side. By increasing the number of tubes, the histogram will converge and represent an estimate of the underlying continuous density function $h(t)$ for the transit times t . Modelling the dynamics of microvasculature a smooth monotonically decreasing residue function is derived .

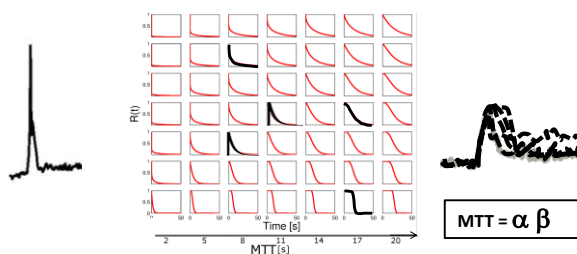


Figure 1-16 Residue function modelled from a family of gamma variate functions.

MTT is the distribution of transit time mean value ($\alpha\beta$) whereas variance ($\sqrt{\alpha\beta}$) is the CTTH. Reproduced from "Bayesian estimate of cerebral perfusion using a physiological model of microvasculature", by Kim Mouridsen et al, 2006, Neuroimage, 33(2),570-9.¹⁷⁸

1.9 Role of capillaries in haemodynamic regulation

Neurovascular coupling is an intrinsic brain microcirculation regulatory mechanism that adapts local cerebral blood flow (CBF) in accordance with underlying neuronal activity¹⁸⁸.

Normal regulation of CBF to meet metabolic demands of brain tissue is deranged in conditions predisposing to stroke such as, ageing, hypertension, and diabetes¹⁸⁹. This “neurovascular dysfunction (NVD)” is characterised by reduced response of CBF in response to neuronal activity and the mechanism is not fully understood but thought to be related to depletion of nitrous oxide (NO), as superoxide anions¹⁸⁹ from endothelium react with NO to form peroxy nitrite¹⁹⁰. Peroxy nitrite disturbs the smooth muscle contractility¹⁹¹ and inactivates tissue plasminogen activator¹⁹². This dysfunction is not restricted to blood vessels that affect CBF. This was also seen in capillary level¹⁹³. Capillary flow patterns have been speculated to affect oxygen delivery¹⁹⁴. In studies of direct microscopy in animals¹⁹⁵ and perfusion MRI in Humans^{21,23} it was found that capillaries do undergo changes in ischaemia.

Increase in Capillary transit time heterogeneity (CTTH) was shown to reduce the maximum oxygen availability (OEF max) for a given CBF and oxygen tension²³. This effect was thought to be caused by increasing proportion of erythrocytes passing too fast to effectively extract oxygen. This can affect the way CBF can support the metabolic needs, and, accordingly abnormal capillary responses can contribute to abnormal CBF responses seen in NV dysfunction and to metabolic derangements seen in penumbra, where tissue survival depends on the effective oxygen extraction¹⁹⁶.

Relationship of CBF to oxygen availability was described by Classical flow-diffusion (Bohr-Kety-Crone-Renkin (BKCR)) equation¹⁹⁷, but it assumes homogenous flow in capillaries. In a human study, it is found that any degree of heterogeneity of capillary flow will lead to reduction of tissue oxygen utilisation^{21,177}. Heterogeneity of capillary flow velocities can be caused by capillary wall disturbances or blood cell morphology and this reduces oxygen utilisation. Changes in number, diameter, and endothelial adhesion are known to affect the distribution of capillary flow across capillary bed. Low grade

inflammation and infection is shown to disturb flow patterns and result in shunting of erythrocytes through capillary bed¹⁹⁸. Also shedding of glycocalyx from endothelium in inflammation seems to affect the microcirculatory haemodynamics¹⁹⁹. Extending the classic flow diffusion equation, capillary blood mean transit time (MTT) and capillary transit time heterogeneity (CTH) together determines the maximum OEF that can be achieved for a given tissue oxygen tension. Extended BKCR equation²³ shows that oxygen availability is determined partly by MTT of erythrocytes across all capillaries and partly by heterogeneity (CTTH) of these transit times (fig.1-17). Probability density function of capillary transit times $h(t)$ is parameterised by gamma-variate function (parameters α and β). CTTH is parameterised by the standard deviation of gamma-variate capillary transit time distribution ($\sigma=\sqrt{\alpha\beta}$) (fig.1-18)²³. Vascular mean transit time μ is then determined as $\alpha\beta$ ($\mu=\alpha\beta$).

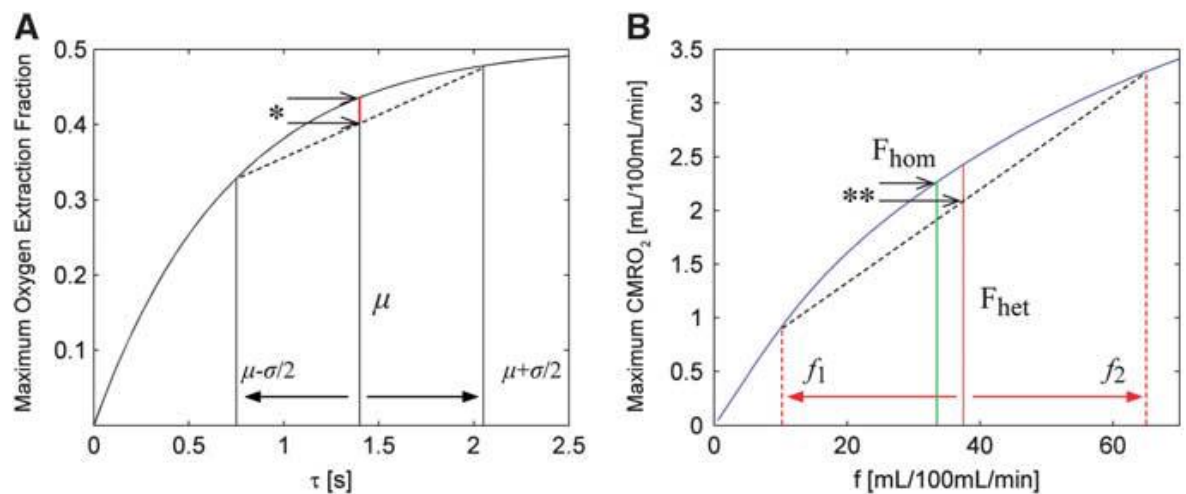


Figure 1-17 Roles of CBF, CTTH, Oxygen tension in brain oxygenation

Oxygen extraction as a function of capillary transit time. (A) The maximum attainable oxygen extraction fraction versus transit time is shown. Note that oxygen extraction becomes inefficient toward short mean transit times, $\mu=CBV'/CBF$. The same principle applies to individual transit times along separate paths in the capillary tree. However, the effect is nonlinear, and because of the concave nature of the curve, a broad capillary transit time distribution (illustrated here by two populations with transit times $\mu-\sigma/2$ and $\mu+\sigma/2$) yields considerably lower OEF max (indicated by the asterisk) for this distribution than the corresponding homogenous distribution, where all capillary transits have identical transit time μ . The same phenomenon may result in a decreased net oxygen extraction despite an increased net flow: in (B), maximum CMRO₂ is plotted versus flow using our model, and here the green line indicates the flow and associated CMRO₂max from a homogeneous population of capillaries with a net flow F_{hom} . A slightly larger flow $F_{het}>F_{hom}$, indicated by the red line is now accommodated by the same capillary bed, but divided into two populations, where one population has flow f_1 and the other f_2 , $f_1+f_2=F_{het}$. However, the net oxygen extraction in this case (intersection of the dashed diagonal line with the red vertical line) is in fact smaller than that obtained for the homogenous, lower flow case, as indicated by the double asterisk. Reproduced with permission from "The roles of cerebral blood flow, capillary transit time

heterogeneity, and oxygen tension in brain oxygenation and metabolism”, by Jespersen et al²³, 2012, J Cereb Blood Flow Metab, 32(2), 264-277.

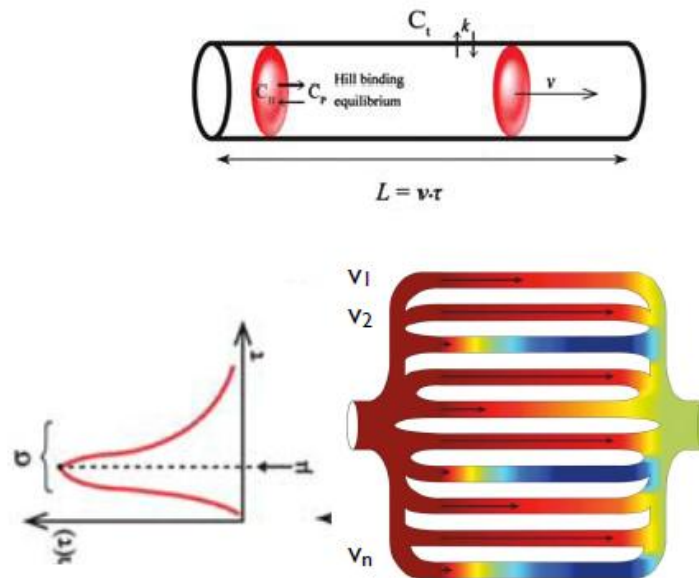


Figure 1-18 Model overview with single capillary (top) and multiple capillaries (bottom)

Single capillary model has three compartments, oxygen bound to haemoglobin, oxygen in plasma, and oxygen in tissue. Oxygen in plasma is assumed to be in equilibrium with oxygen bound to haemoglobin, their concentrations related by Hill's equation. Transfer of oxygen across the capillary membrane is modelled as first-order exchange process with the rate constant k . The capillary has length L , and blood moves with velocity v resulting in transit time $t=L/v$. The capillary bed below is then obtained as a collection of capillaries modelled as described, with different transit times t taken from the transit time distribution $h(t)$. Reproduced with permission from “The roles of cerebral blood flow, capillary transit time heterogeneity, and oxygen tension in brain oxygenation and metabolism”, by Jespersen et al, 2012, JCBFM, 32 (2), 264-77.²³

The oxygen extraction is compared between to homogenous and heterogeneous capillary flow is shown in fig.1-19.

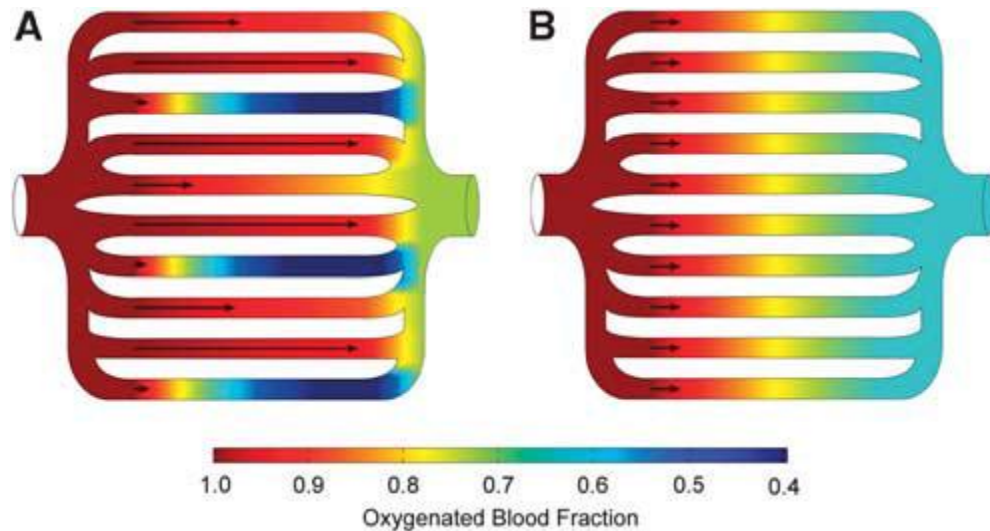


Figure 1-19 Effects of capillary flow heterogeneity on oxygen extraction

Compare the extraction of oxygen from individual capillaries according to BKCR kinetics when the same flow is distributed across the same number of capillary paths with homogenous (B) capillary flow velocities (arrows), and heterogeneous flow velocities (A), respectively. Transit times in resting, heterogeneous cases were obtained by sampling gamma distribution with parameters corresponding to recordings of mean and standard deviation of transit times in a rat²⁰⁰. Notice the heterogeneity of capillary flows, in spite of identical total blood flows and number of open capillaries. Reproduced with permission from “The roles of cerebral blood flow, capillary transit time heterogeneity, and oxygen tension in brain oxygenation and metabolism”, by Jespersen et al, 2012, *JCBFM*, 32 (2), 264-77.²³.

Oxygen extraction efficacy (OEF_{max}) always increases with increasing MTT and with decreasing CTH. During functional activation, the reduction in CTH occurs in parallel with the arteriolar dilation partly maintaining the oxygen extraction efficacy during hyperaemia. During resting phase, along some capillary paths, flow velocities are so high that little oxygen is extracted from blood. In normal brain, hyperaemia is accompanied by a reduction in CTH (homogenisation). This homogenisation decreases number of capillary paths with high flow and limited oxygen extraction, causing net oxygen availability to increase as a function of CBF.¹⁸⁵

$CMRO2_{max}$ and thereby tissue oxygen availability always increases with decreasing flow heterogeneity. Haemodynamic states above a threshold are unique that in that increases in the CBF (reductions in MTT) will lead to states of lower tissue oxygen availability. These states are referred to as malignant CTTH. The metabolic consequence of increased CBF with vasodilatation without

concomitant reductions in CTH (i.e. homogenisation) would not lead to a net increase in availability of oxygen in tissue ¹⁸⁵.

There is a need for robust estimation of CTH, MTT, OEF_{max} to test the above hypotheses further. This will inform to what extent CBF or CTH, or both contribute to oxygen availability.

1.10 Magnetic Resonance Imaging (MRI)

MRI can provide information on time-sensitive pathophysiological changes and therefore potentially act as an indicator of time since onset of ischaemia. In hyper-acute ischemic stroke Sodium-potassium channel failure causes a shift of fluid and potassium from extracellular to intracellular compartment (cytotoxic oedema) after a latency of only a few minutes²⁰¹. Cytotoxic oedema leads to narrowing of extracellular matrix and, thus, to a reduction of Brownian molecular motion in the extracellular space. This phenomenon can be measured with diffusion weighted sequence (DWI) in minutes ²⁰²⁻²⁰⁴. Cerebral oedema increases gradually with shift of water from extracellular space to intra-cellular space, and only after 4 hours, disruption of the Blood-Brain Barrier(BBB) was noted in animal studies ^{205,206}. This initial phase of cytotoxic oedema is not seen on T2 weighted fast spin echo images²⁰⁷. Conventional MRI sequences (T1, T2) show abnormalities based on vasogenic oedema which occurs only after BBB breakdown, therefore, less sensitive to identify hyper acute infarcts^{202,203}. Tissues with increased water content appear hyper intense on T2 sequence. Cerebrospinal fluid (CSF) also appears bright and, to improve delineation from pathology, an inversion pulse can be used to attenuate signal from pure water (FLAIR).

FLAIR imaging has been proposed as a “tissue clock” - a means of judging stroke onset time when this cannot be ascertained from history²⁰⁸⁻²¹⁰. The lack of FLAIR hyper intensity with positive DWI allocated ischemic lesions within 3hrs or less with a high specificity (0.93) and positive predictive value (0.94) , whereas sensitivity (0.48) and specificity (0.43) were low ²⁰⁸. In this study the sensitivities were 27% (FLAIR alone) 50% (with knowledge of DWI) ≤ 3 hrs increased to 56.7%

(FLAIR alone) 93.3% (with knowledge of DWI) after 3-6 hrs. The PRE-FLAIR study showed DWI-FLAIR mismatch (a positive DWI lesion, and no marked FLAIR hyper intensity) could identify strokes with <4.5 hrs onset with 62% sensitivity, 80% specificity and 83% positive predictive value and 54% negative predictive value²¹⁰. Using this principle of the DWI-FLAIR match as surrogate for time of stroke onset, a randomised trial of IV thrombolysis resulted in significantly better functional outcome in unknown time of onset ischemic stroke patients²¹¹.

1.10.1 MRI for penumbra identification

Reduced Apparent diffusion (ADC) of water approximately corresponds to core²¹². In acute stroke patients, the area with perfusion abnormalities is generally larger than the DWI hyper intensity area^{213,214}. It was suggested that this perfusion-diffusion mismatch may reflect ischemic penumbra^{214,215}. Lesion growth between early and late imaging time points corresponds with degree of mismatch between diffusion and perfusion^{216,217}. In Human MRI studies, successful recanalisation led to salvage of penumbra with neurological improvement²¹⁸. This assumption is disputed however²¹⁹. It was shown that ADC decline starts before energy metabolism fails. Moreover, PWI-detectable flow decreases are relevant only at flow values that interfere with adequate oxygen supply to tissue. Therefore PWI/DWI mismatch often may include normal viable tissue, therefore PWI-DWI mismatch-defined penumbra may overestimate the extent of infarction at follow up¹⁴⁶.

DWI lesion representing unique physiological parameter with echo planar imaging was studied in human stroke²²⁰. Baird et al,²²¹ suggested, penumbra can be operationally defined as mismatch between the lesion volume detected by Perfusion abnormality and DWI lesion. However, this was thought to be an oversimplification, and in some studies DWI lesion is shown to reverse with reperfusion and therefore this mismatch model may overestimate the irreversible infarcted tissue²²². This may overestimate the tissue at risk by including oligoemic tissue^{83,223}. There are uncertainties with DWI lesion physiological accuracy and what parameters to define the tissue at risk^{224,225}. Hypothesis of mismatch is correlated with penumbra is challenged by combined

PET and MRI studies showing DWI lesion contained penumbra²²⁶, and mismatch contained oligoemic tissue²²³.

Perfusion weighted Imaging (PWI) uses a bolus tracking technique after application of paramagnetic intravascular contrast agent. Maps of Time to peak (TTP) provide a robust estimate of hypo perfusion. Normalised TTP (rel.TTP) are comparable among individuals and different imaging facilities²²⁵. However, delay of tracer arrival is not necessarily accompanied by reduction in CBF (for example in chronic carotid occlusion) and renders delayed TTP values to potentially be false positive and susceptible to collateral circulation²²⁷. For better tissue identification, a deconvolution method is applied^{166,171}. T_{max} reflects the bolus delay between Arterial input function and tissue²²⁸. Hypoperfusion with T_{max} was measured in various studies^{229 230,231}. There is no consensus on which perfusion parameter best identifies hypo perfusion and predicts infarct growth. Clinical studies reported the following range of thresholds for hypo perfusion: rel. TTP: >2 to >8 s; rel.MTT: >4s to >8s; CBF: <20 to 42 ml/100gm/min; T_{max} >2 s to >8 s^{217,232-234}.

A comparative MRI and PET study showed large variability in mismatch volume depending on thresholds applied, mostly overestimating penumbra²²⁵. In an MRI validation with PET study in 26 stroke patients, penumbral flow thresholds were MTT > 5.3 s; CBF <21.7 ml/100g/min, TTP >4.2 sec, CBV <1.5ml/100g and T_{max} >5.5 s²³⁵. Quantification of PWI maps remains a major source of heterogeneity. The type of deconvolution^{171,173} and placement of AIF^{236,237} lack a standardisation definition across studies. Variability in PWI/DWI mismatch definition was used in different studies and this can influence the mismatch volumes^{225,238 239}. Adding to this, predictive power of PWI changes with time from onset and site of tissue imaged (grey matter vs. White matter), degree of reperfusion and age^{240,241}. A comparison of various perfusion software packages found substantial differences in the calculated volume of hypoperfusion for maps of MTT, CBF, and T_{max} among three tested software packages²⁴².

Schlaug and colleagues using MRI demonstrated penumbra comprises about 40% of the total ischemic territory in patients with any vessel occlusion studied within 24 hours²¹⁵. This was also reported by others^{231,243,244}. This “mismatch”

pattern is seen in 70% of patients with anterior circulation stroke scanned <6 h²¹⁴. Its resolution on reperfusion was associated with neurological recovery²⁴⁴.

Volume of mismatch depends on the definition applied and no standardisation exists²⁴⁵. It is unclear what mismatch ratio justifies therapy. Arbitrary volumetric difference in a ratio of >1.2 (DW: PWI) was used initially in studies without being evaluated²⁴⁶. Recent late thrombolysis trials (EXTEND, ECASS-IV) used hypoperfusion to core volume ratio of >1.2 to include for randomisation. In DEFUSE-2 trial, SWIFT-PRIME chose target mismatch of 1.8 whereas EXTEND-IA chose 1.2. Kakuda et al, described DWI: PWI ratio of 2.6 to predict optimal response to thrombolysis²⁴⁷. Heterogeneity arises from the definition itself,²³⁹ but also from choice of PWI and post processing²⁴⁵ software. If different mismatch definitions are applied to same patient, variability can easily result in mismatch exceeding 20%²⁴⁵. A few randomised thrombolysis studies used the mismatch concept for patient selection^{15,246,248}. A meta-analysis concluded that mismatch based delayed thrombolysis was not beneficial²⁴⁹. But the studies differed in conceptual issues and therefore mismatch concept is still a valid idea in current situation. Further randomised trials of IV alteplase were done using mismatch concept between 4.5- 9 hours^{250,251}. A recent meta-analysis of late time window thrombolysis studies (EPITHET, ECASS-4, EXTEND) was reported showing that those with salvageable tissue had better functional outcomes with IV alteplase than those given placebo. 36% patients in alteplase group and 29% in the placebo group had achieved excellent functional outcome at 3 months (adjusted OR 1.86 (1.15-2.99), p=0.011). However, the rate of symptomatic Intra cerebral haemorrhage was higher in alteplase group (5% in alteplase 1% in placebo group)²⁵².

1.10.2 NCCT vs. MRI

NCCT is more easily available and has rapid acquisition time. It is better tolerated by unwell, uncooperative patients than MRI. Some patients may not be suitable for MRI (e.g. those with pacemakers, aneurysm clips). Kucinski et al,²⁵³ showed in a cohort of 25 patients who were imaged with NCCT and MRI between 1.3-5.4 hours, ADC decrease was almost complete within 1.5 hours, whereas NCCT density was a continuous linear decrease. Sensitivity of NCCT when compared to MRI in identifying acute ischemic lesion is only 42-63% (average

time for CT 2.6 hrs, MRI 5.1 hrs)²⁵⁴. NCCT has lower sensitivity (75%) to acute ischemic changes whereas DWI had 100% sensitivity¹³⁷. In a single centre, blind comparison of CT with MRI in acute stroke referrals, relative to the final clinical diagnosis, MRI had sensitivity of 83% (181/217) and CT of 26% (56/217) for the diagnosis of any acute stroke²⁵⁵. DWI has greater inter observer and intra observer reliability than NCCT^{202,203,256,257}. Wintermark et al, showed in 42 stroke patients imaged within 3 to 9 hours, a good correlation between multimodal CT (CT, CTP, CTA) and MRI for infarct size, cortical involvement and occlusion site²⁵⁸. Ischaemic Core defined by CBV threshold closely matched DWI lesion volume and penumbral tissue plus core on CT perfusion matched the MTT lesion²⁵⁹.

1.11 Non-core-non-penumbra Infarction:

There is variability in early neurological outcomes between individuals with anterior circulation stroke. Alawneh et al, hypothesized that clinically silent tissue reflected as “non-core-non-penumbra” may succumb to infarction²⁶⁰. Voxel-wise analysis was done to map acutely silent but infarcted tissue (acute CT perfusion or MR perfusion in comparison to MRI at 1 month). Acutely silent but infarcted tissue was seen in most patients although much smaller volumes than salvaged penumbra volumes. In around 10% subjects the volume of acutely silent but infarcted tissue was substantial. In a multivariate regression model, even after correcting for the effect of salvaged penumbra, the infarction of acutely silent tissue negatively influenced the clinical course.

1.12 Intravenous thrombolysis (IVT):

Intravenous thrombolysis with alteplase, a recombinant tissue plasminogen activator is established as the standard of care for patients with acute ischaemic stroke presenting within 4.5h of symptom onset. The chances of independent survival decline steeply with time to treatment delivery, reflecting a limited tolerance of the brain to ischemia (Fig. 1-20). Standards accordingly emphasise optimization of patient pathways to minimize onset-to-treatment times.

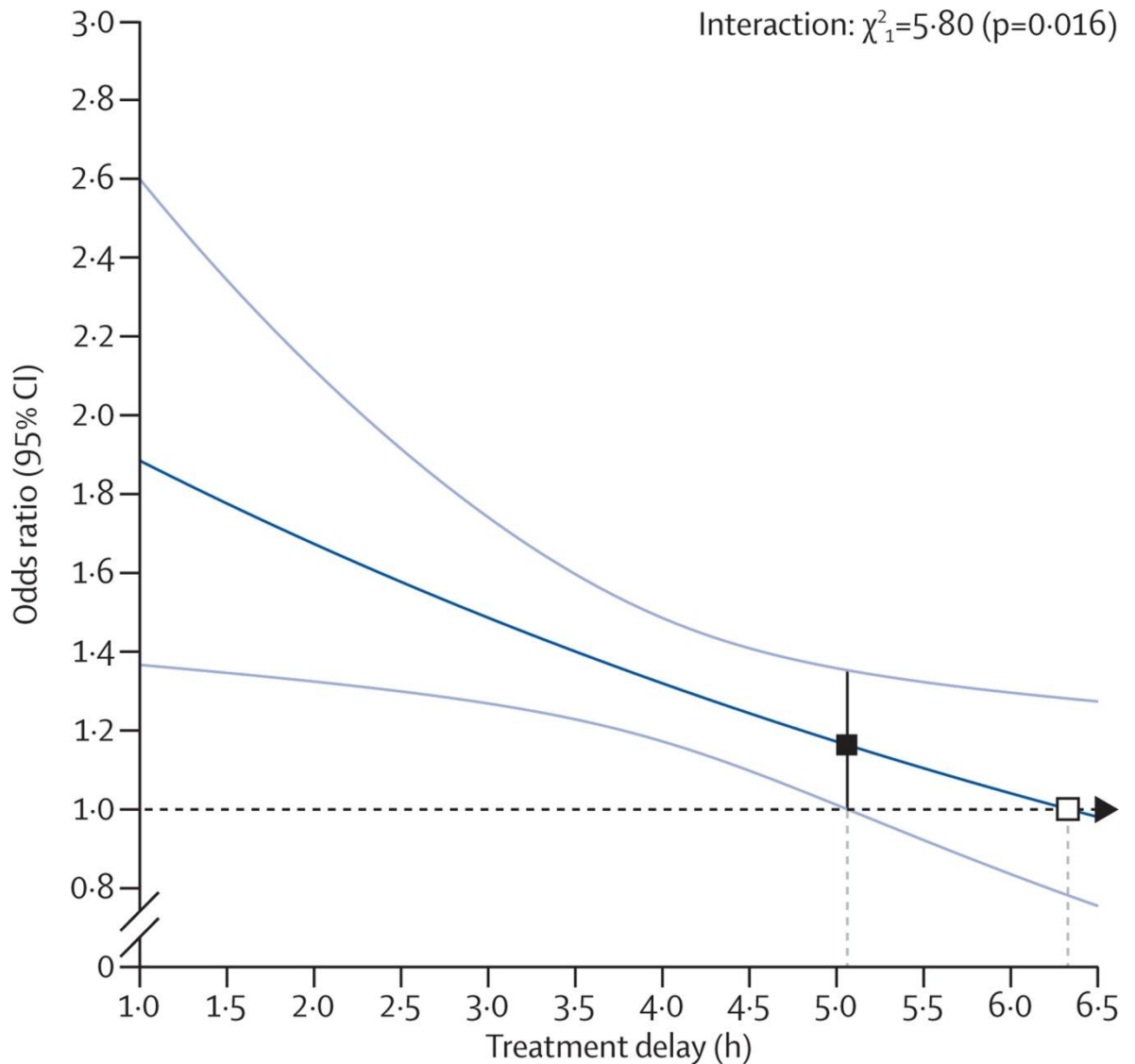


Figure 1-20 Effect of time delay on intravenous thrombolysis outcomes

Effect of timing of alteplase treatment on good stroke outcome (mRS 0–1). The solid line is the best linear fit between the log odds ratio for a good stroke outcome for patients given alteplase compared with those given control (vertical axis) and treatment delay (horizontal axis; $p_{\text{interaction}}=0.016$). Estimates are derived from a regression model in which alteplase, time to treatment, age, and stroke severity (handled in a quadratic manner) are included as main effects but the only treatment interaction included is with time to treatment. Only 198 patients (159 from IST–3) had a time from stroke onset to treatment of more than 6 h. The white box shows the point at which the estimated treatment effect crosses 1. The black box shows the point at which the lower 95% CI for the estimated treatment effect first crosses 1.0. mRS=modified Rankin Scale. Reproduced with permission from “The effect of treatment delay, age, and stroke severity on the effects of intra venous thrombolysis with alteplase for acute ischaemic stroke: a meta-analysis of individual patient data from randomised trials”, by Emberson et al, 2014, *Lancet*, 384 (9958), 1929–35²⁶¹.

In 1995, the landmark National Institutes of Neurological Disorders and Stroke (NINDS) rt-PA Stroke Trial was the first to demonstrate significant benefit of IV alteplase given within 3h of symptom onset, with a 16% absolute increase in the

proportion of patients making excellent recovery (modified Rankin Scale of 0 or 1) at 3 months. NNT was 3 for any improvement in modified Rankin scale. Rates of symptomatic intra-cerebral haemorrhage (SICH) within 36 hours of stroke onset were higher in the alteplase treatment group (6.2% vs. 0.6% in placebo group)¹⁰, using a very conservative definition of SICH. A number of other randomised controlled trials^{131,262} of IV alteplase throughout the 1990s failed individually to show benefit for treatment, but all had longer time windows for treatment initiation, and average onset to treatment (OTT) time exceeded the latest times for treatment in NINDS. The NINDS trial uniquely enforced very early treatment delivery by permitting centres to randomise a patient in the 91-180 minute window only if they also had randomized a patient in the 0-90 minute window, a strategy not replicated in any subsequent study. An individual patient data pooled analysis of six major alteplase trials in 2004 included 2,775 patients and identified potential benefit extending out to 4.5h from onset²⁶³, a finding subsequently confirmed by the third European-Australasian Cooperative Stroke Study (ECASS-III) for the 3-4.5h time window¹²⁰. A further systematic review and meta-analysis of nine trials in 2012 by Wardlaw.et al also strengthened the benefit of IV alteplase²⁶⁴.

A large randomized, controlled trial, the third International Stroke Trial (IST-3)²⁶⁵ reported effect sizes consistent with previous trials, but inclusion of patients with very different age and severity in different time windows rendered interpretation of the trial difficult in isolation. Interestingly, elderly people (>80 yrs) seem to benefit as much as younger population. A meta-analysis of individual patient data, including IST-3 and 8 other RCTs of IV alteplase included 6,756 patients and concluded that alteplase given within 4.5 hours of onset significantly increases both survival free of dependence and excellent outcome (recovery with no or minimal symptoms) at 3 months, with no difference in mortality at final follow-up despite an increase in SICH, responsible for a slight excess of deaths within the first 7 days (fatal ICH risk 2.7% with alteplase compared to 0.4% among controls)²⁶¹. Overall, there was an absolute increase in disability-free survival of 10% for patients treated within 3h and of 5% for those treated between 3 and 4.5h.

1.13 Using imaging for treatment selection

Advanced imaging with MRI or CT using probabilistic perfusion thresholds allows assessment of the extent of viable (penumbral) and non-viable (core) tissue, and it has been hypothesised that this may allow individualised treatment decisions, including delayed intervention in individuals with favourable brain imaging features²⁶⁶. Five completed IV thrombolysis studies^{15,246,248,267-269} have used penumbral “mismatch” (i.e. the penumbra volume exceeds core volume by an arbitrarily defined ratio) to select patients, predominantly in extended time windows between 3 and 9 hours. A meta-analysis^{218,249} of these studies found that favourable imaging features at baseline were associated with increased recanalisation, reperfusion and attenuated infarct growth compared to unfavourable imaging features. However, functional outcomes were not better than control (placebo) groups, and treatment was associated with increased mortality and risk of ICH. Mechanical Retrieval and Recanalisation of Stroke Clots Using Embolectomy (MR RESCUE) study²⁶⁹, a randomised-controlled trial designed to examine whether MRI features predicted benefit from delayed Intra arterial thrombectomy, found no imaging - treatment effect interaction: outcomes were good in those with good scans, and poor in those with poor scans, but the intervention had no effect. In contrast, MRI profile and response to endovascular reperfusion in the non-randomised second Diffusion and Perfusion Imaging Evaluation for Understanding Stroke Evolution (DEFUSE-2) study²⁶⁸ found that patients with favourable “target mismatch” had better outcomes following intra-arterial treatment. The populations in these two studies had very different characteristics (e.g. median core volume in MR RESCUE was 60ml compared with 15ml in DEFUSE-2), indicating very different selection biases. Imaging parameters to define core and penumbra remain highly heterogeneous in published literature¹⁴⁷. Recent thrombectomy trials used target mismatch population after 5 hours for inclusion in their studies^{16,17,270,271}. Further Intra arterial thrombectomy studies with extended time window included target mismatch population^{272,273}. Better validated and platform-independent software tools^{274,275} are not yet in widespread use. RAPID software (iSchema View, Menlo Park, CA)²⁷⁶ has been used in recent trials testing IV alteplase between 4.5 -9 hrs including target mismatch patients^{250 277}.

Advanced imaging within 4.5h may offer stratification and improve safety by excluding stroke mimics²⁷⁸ and patients with high risk of ICH or poor outcome^{15,279}, and including patients with minor stroke or rapidly improving symptoms who exhibit high risk of deterioration based on imaging features²⁸⁰. Whether these hypothetical gains outweigh the detriment of additional delay in treatment delivery is being evaluated in a randomised controlled trial, the Penumbra and Recanalisation Acute Computed Tomography in Ischaemic Stroke Evaluation (PRACTISE) trial which will compare NCCT and multimodal CT (NCCT, CT perfusion and CTA)²⁸¹.

1.14 Intra arterial therapy (IAT)

Intra-arterial treatment (IAT) with thrombolytic drugs or mechanical devices offers an alternative treatment option to IV thrombolysis (IVT) in patients with contraindications. In addition, IAT as an adjunctive treatment to IVT is effective in large artery occlusions, which exhibit low rates of recanalisation after IVT and for basilar artery thrombosis. The earlier randomised trials have found no difference in outcomes in the IAT arms, whether as a direct comparator to IVT under 4.5h²⁸²; additional to IVT compared with IVT alone²⁸³; or with MRI-based imaging selection compared to best medical treatment, including IVT in the majority²⁸⁴.

Several trials were published in recent past which have all showed benefit of IAT as an adjunct to IVT compared to IVT alone in large artery occlusion^{16,17,270,271,285}. These trials were run efficiently with selective target population with proximal large vessel occlusion. Moreover, the stent retrievers were different to the earlier studies. An individual patient meta analysis showed that number needed to treat to have one additional patient to have reduced disability of at least 1 score on modified Rankin score at 90 days was 2.6¹³. These trials included only patients with modified Rankin score of 2 or less. Most studies used identification of salvageable tissue on imaging as an inclusion criteria (Extending the time for thrombolysis in Emergency Neurological Deficits- Intra-Arterial (EXTEND-IA), Randomized Trial of Revascularization with Solitaire FR Device versus Best Medical Therapy in the Treatment of Acute Stroke Due to Anterior Circulation Large Vessel Occlusion Presenting within Eight Hours of Symptom Onset (REVASCAT), Solitaire with intention for Thrombectomy as Primary

Endovascular Treatment (SWIFT-PRIME), Endovascular Treatment for small Core and Anterior Circulation Proximal Occlusion with Emphasis on Minimising Computed Tomography to Recanalisation Times (ESCAPE)) whereas Multi- Centre Randomised Clinical Trial of Endovascular treatment for Acute Ischemic Stroke in the Netherlands (MR CLEAN) did not. The trials varied in onset to endovascular treatment for a maximum from 6hrs-12 hrs. All the trials with extended time windows required a favourable profile of salvageable brain tissue for inclusion. Hence, thrombectomy based on CT/CTA alone, commencing procedure after 5 hours has no proven benefit. An NIHSS score of 6 or more was inclusion criteria for all these trials.

Diffusion-Weighted Imaging or Computerized Tomography Perfusion Assessment with Clinical Mismatch in the Triage of Wake Up and Late Presenting Strokes Undergoing Neuro-intervention (DAWN) trial in time window of 6-24 hrs after symptom onset showed in target mismatch group using automated RAPID software, thrombectomy has a strong treatment effect²⁷². The Endovascular Therapy Following Imaging Evaluation for Ischemic Stroke (DEFUSE-3) trial was stopped early due to positive results from DAWN study²⁷³.

1.15 Cerebral angiogram

The vessel status is not available in routine cerebral parenchymal imaging with CT or MRI. Hyper dense artery sign (HAS) on CT is highly specific and moderately sensitive for intracranial arterial obstruction by thrombus²⁸⁶. Stroke imaging protocol can include imaging of both extra cranial and intracranial vessels either using MRA or CTA. If proximal large arterial occlusion is found, intra arterial thrombectomy can be considered. Recent positive endovascular trials all selected patients with proximal anterior circulation occlusion^{17,270,271}. In minor or rapidly improving stroke a vessel occlusion or intra cranial stenosis may predict later deterioration²⁸⁰. CTA can be done only with a contrast injection using a bolus tracking method. MRA can be done without contrast (Time of flight (TOF) MRA) or with gadolinium contrast. Contrast enhanced (CE) MRA can show low flow state in stenotic areas whereas TOF may show complete occlusion²⁸⁷.

Contrast examination has high signal to noise ratio but both have low spatial resolution than CT angiogram.

1.16 Cerebral Collateral circulation

The collateral circulation refers to the vasculature that compensate cerebral blood flow when normal blood flow is impaired or restricted due to severe stenosis or occlusion of the principal supplying arteries²⁸⁸. Single phase CTA or multi-phase CTA gives complete collateral information. Disadvantage of conventional CTA is that it is single snap shot in time of contrast filled blood vessels. There is risk of misclassifying patients with good collaterals as poor if image acquisition is too early²⁸⁹. Multi-phase CTA generates time resolved cerebral angiograms of the brain vasculature from skull base to vertex²⁸⁹. Collaterals are recruited to protect ischemic tissue, and wide variations in clinical features and the extent of recovery can be partly attributed to the collateral network comprised of the circle of willis and leptomeningeal vessels^{288,290,291}. Several studies have demonstrated that in patients with good collaterals, clinical outcomes are better²⁹²⁻²⁹⁷. The extent of cerebral infarction is dependent on collateral vessels. Good collaterals are associated but not invariably with large penumbra and maintaining it by limiting core expansion²⁹⁷. Final Infarct volumes were smaller in patients with good collaterals²⁹⁶. Subjects with proximal vessel occlusion with diminished collaterals experienced increased risk of worsening and death²⁹⁵. If poor collaterals are demonstrated, risk of haemorrhage may be increased with thrombolysis treatment²⁹⁸. When revascularisation was achieved benefit was less observed in patients with poor collaterals.

A recent systematic review and meta analysis showed evidence of impact of pre treatment collateral circulation on the outcome of patients with IV thrombolysis²⁹⁹. A favourable role of good collateral circulation was demonstrated with favourable functional outcome, lower risk of symptomatic intra cerebral haemorrhage. Such findings may be attributable to lower NIHSS score and smaller infarct volume in patients with better collateral circulation. No significant correlation was found between collateral status and recanalisation

or reperfusion. Some authors reported that good collaterals have more protective role even in those who do not recanalise^{293,300}. Bang et al., showed patients with good collaterals achieved more benefit of endovascular therapy²⁴. In a systematic review and meta analysis to investigate the effect of collateral status on outcomes after endovascular therapies , pre treatment good collaterals status was associated with slightly better recanalisation, reperfusion rates³⁰¹; lower risk of symptomatic intra cerebral haemorrhage, more favourable functional outcomes and reduced risk of death³⁰².

Chapter 2 Study Population and Methods

2.1 Study population

Study population for this thesis work included a database of three different studies: Alteplase versus Tenecteplase in Stroke Thombolysis (ATTEST)³⁰³, Pathophysiology of acute post-stroke hyperglycemias in relation to brain perfusion and arterial patency (POSH, unpublished), the multicentre Acute Stroke Imaging Study (MASIS)³⁰⁴. Safety in Stroke Thrombolysis (SITS) study in chapter 8 included the SITS registry database from May 2003- March 2013.

*The multicentre Acute Stroke Imaging Study (MASIS)*³⁰⁴ (n=83): This study purpose was to investigate the role of multimodal Imaging in acute stroke. Patients under 6 hours of stroke symptoms onset were recruited and followed up to 3 months (Fig.2-1). Feasibility of imaging with CT and MRI at different time-points was examined as part of the MASIS study. In summary, acute stroke patients admitted to the three participating stroke centres (Aberdeen Royal Infirmary, Western General Hospital, Edinburgh and Institute of Neurosciences, Southern General Hospital, Glasgow) between August 2008 and March 2010 were prospectively screened for recruitment to MASIS, an observational study examining clinical, imaging and blood biomarkers of salvageable tissue and outcome after ischemic stroke.

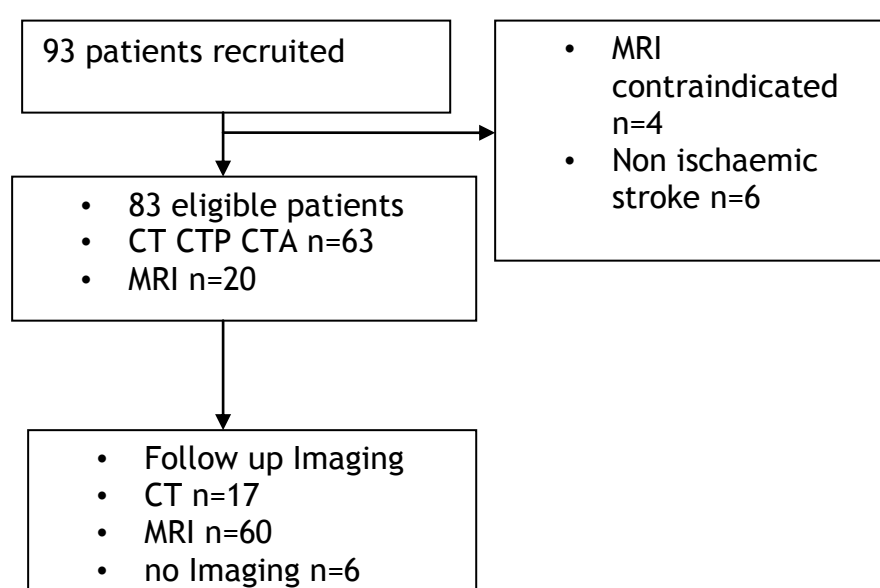


Figure 2-1 Flow chart of MASIS study subjects included in thesis

Pathophysiology of acute post-stroke hyperglycemias in relation to brain perfusion and arterial patency (POSH unpublished): Primary hypothesis was, whether there is difference in growth of irreversibly damaged tissue after stroke between patients in whom blood glucose is normal, in whom blood glucose is increased early (<6hrs), in whom blood glucose is normal early but increases later (>6hrs). Patients with stroke within 6 hrs were recruited in Southern General Hospital, Glasgow. They had CT, CTA, and CTP at admission and follow up CT at 24-48 hrs. Additionally in those with occlusion on admission CTA also had repeat CTA. Patients were followed to 30 days (Fig.2-2).

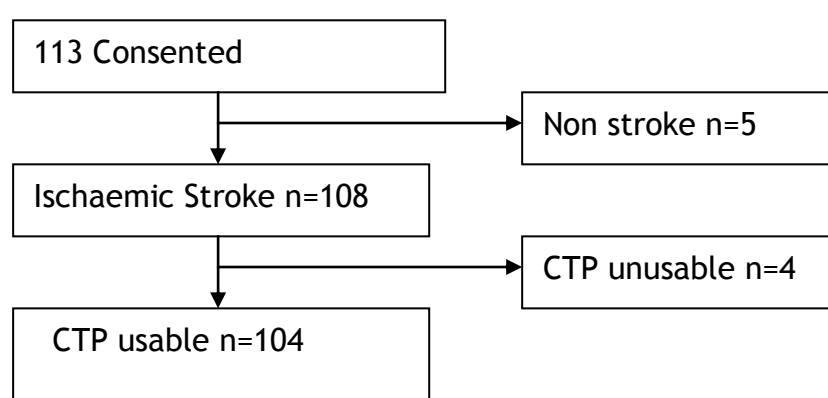


Figure 2-2 Flow chart of POSH study population included in thesis

*Alteplase versus Tenecteplase in Stroke Thrombolysis (ATTEST)*³⁰³: Pilot phase Prospective Randomised Open label Blinded End-point (PROBE) study compared markers of biological activity to inform the design of larger definitive trial comparing the efficacy and safety of Alteplase and Tenecteplase as thrombolytic agents in eligible patients with acute ischemic stroke. Patients eligible for thrombolysis under current standards are randomised to receive either Alteplase or Tenecteplase between January 2012 and September 2013. This was a single centre study carried out in Institute of Neurological sciences, Southern General Hospital, Glasgow. The primary outcome is amount of penumbral tissue salvaged between the two treatment arms. All patients underwent CT, CTA and CTP on admission and CT, CTA at 24hours. Patients were followed to 3 months (Fig.2-3).

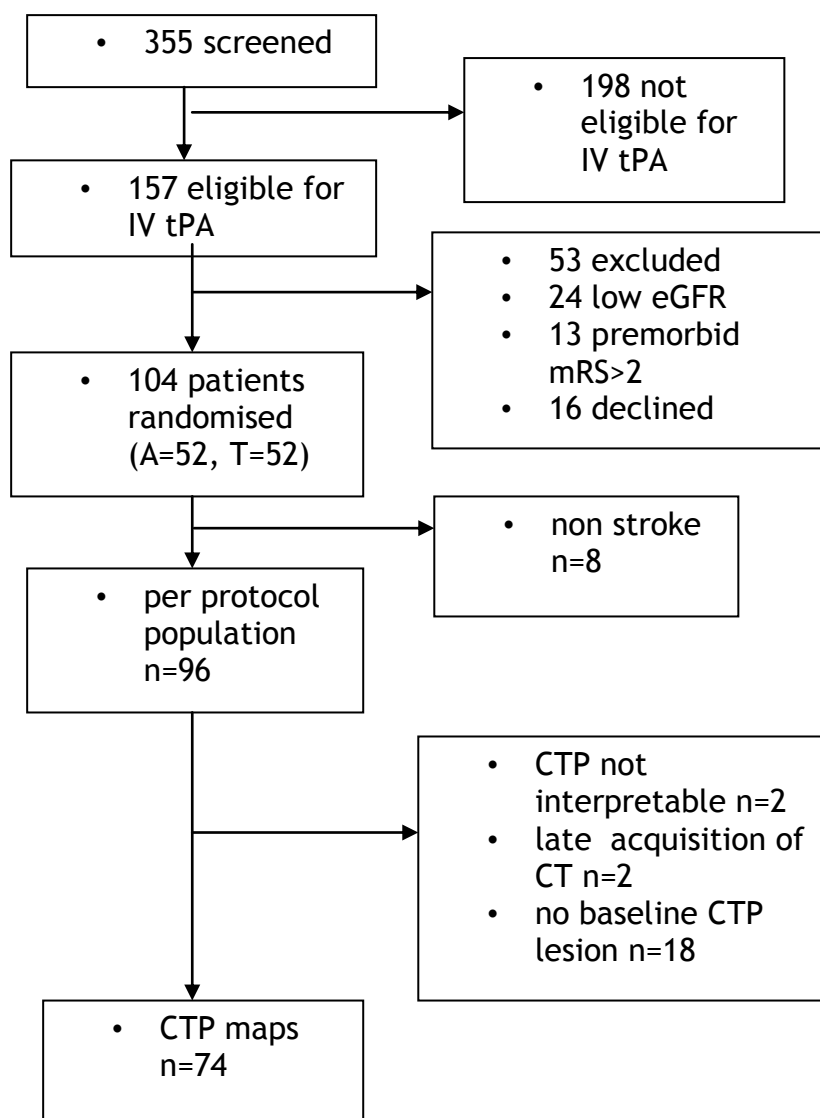


Figure 2-3 Flow chart of ATTEST study subjects

2.2 Imaging

2.2.1 Imaging acquisition

Imaging was performed on a Philips Brilliance 64 multi detector scanner. Whole brain NCCT was acquired first, (5 mm slice thickness FOV 218 x 218 mm, 120 kv, 171 mA or 0.9 mm slice thickness, FOV 250x250 mm, 120 kV, 404 mA) followed by CTP with 40 mm slab coverage from the basal ganglia (8x5 mm slices, FOV 25 cm, 80 kVp, 476 mA, 2 second cycle time, 30 cycles) using a 50 ml contrast bolus administered at 5 mls per second (350 Xenetix) via a large-gauge cannula. A CTA covering aortic arch to the top of the lateral ventricles (0.67 mm slice thickness,

120 kV, 475 mA) was acquired during the first arterial pass of contrast (Xenetix 350, 60 mls, followed by 30 mls of saline bolus, both given at 5 ml per second).

Follow up brain imaging consisted of whole brain non-contrast CT followed by intracranial CTA from base of skull to the top of vertex. Follow up CTA was only performed in patients with an arterial occlusion on initial CTA.

2.2.2 Imaging processing and analysis

Study imaging records were transferred from clinical scanners or radiology archives after removal of individual identifiers from the Digital Imaging and Communications in Medicine (DICOM) file and were identified with the study number. All imaging analysis was undertaken on separate secure computer workstations using a commercially available software package MiStar (Apollo Medical Imaging Technology, Melbourne, Australia <http://www.apollomit.com/products.htm>). Imaging studies were anonymised, and analysed independently by two research fellows (BC, XH) blinded to treatment allocation after the recruitment completion to minimise the odds of recognising scans with treatment allocation. The images are assigned randomly (non consecutive subjects) when performing the analysis. Inter-observer agreement was assessed for all parameters analysed. Volumetric analysis was carried out by each research fellow twice. The average of the four readings was taken as the final reading for analysis. Disagreements in categorical readings were resolved by the consensus of experienced neurologists or neuro-radiologists blinded to treatment allocation.

The inter-rater agreements were assessed initially in test set of scans and then evaluated in the full set of the scans. The test scan set (n=18) was randomly selected from our Imaging archive. The inter-rater agreements for continuous variables were assessed with an intra-class correlation coefficient (Tables 2.1 & 2.2) and categorical variables were examined with weighted kappa using stats direct.

Table 2-1 Test set inter-rater agreement in continuous variables

	Kappa	95% CI
Ischaemic core	0.87	(-9.95-23ml)

Penumbra volume	0.92	(20.8-11.3ml)
Co registered Infarct volume	0.8	(-31-73.4ml)
Total infarct volume	0.94	(-22.2-70.2ml)

Weighted kappa for arterial patency (n=20) was 0.46 (95% CI 0.2-0.7).

Table 2-2 Study scans Inter-rater agreement in continuous variables

	kappa	95% CI
Core volume	0.96	(16.2-19.9 ml)
Penumbra volume	0.91	(-30.2-30.1ml)
Co registered Infarct volume	0.91	(-57.3-26.4 ml)
Total infarct volume	0.91	(-92.9-47.3ml)

The weighted kappa for baseline occlusion site was 0.63 (95%CI 0.49-0.77); Arterial patency at 24-48 hrs kappa=0.68 (95% CI 0.48-0.89) with TIMI and kappa=0.7 (95%CI 0.5-0.89) with TICl. Brain swelling at 24-48 hrs -kappa= 0.5 (95%CI 0.36-0.65). Classification of ICH according to ECASS-III kappa= 0.75 (95%CI 0.6-0.91). Hyper dense vessel sign on baseline NCCT kappa=0.6 (95%CI 0.42-0.8). ASPECT score baseline NCCT kappa=0.41(95%CI 0.29-0.53) on follow-up CT kappa=0.69 (95%CI 0.57-0.81).

Given the low agreement in categorical variables, the discrepancies in baseline occlusion and recanalisation were resolved by referencing the reports of radiologist who were not aware of the treatment allocation. The ICH classification was adjudicated by experienced external readers from the University of Calgary (Dr Andrew Demchuk, Prof Michael Hill). Any remaining categorical parameter disagreements were settled by Prof Keith Muir.

The MiStar software package provides four parameters when processing CTP: cerebral blood flow (CBF), cerebral blood volume (CBV), mean transit time (MTT), and delay time (DT) (Fig. 2-4). In summary, deconvolution of tissue enhancement curves and arterial input function (AIF) selected from the contra-lesional anterior cerebral artery was performed using modified singular value decomposition (SVD) with compensation for the effects of arterial delay and dispersion. Venous Output function was manually selected from superior sagittal sinus. Motion correction was applied automatically using package provided options. A noise elimination technique “close clustering” of $<5\text{mm}^2$ was used to minimise the small artifactual pixels probably induced by noise³⁰⁵. After arterial input function (AIF) and Venous Output function (VOF) selection, a Hounsfield Unit filter was applied in order to mask CSF (15 HU) and bone (700 HU), leaving only brain parenchyma as far as possible (fig.2-5 &2-6). Voxels with CBV values $>90\text{ cm}^3/100\text{g}$ were then masked (fig.2-7), as arterial voxels mimic tissue areas of high perfusion and their exclusion improves the accuracy of CTP relative to PET¹⁵⁵.

A series of delay time values, DT_i ranging from 0 to T_{max} were applied and for each delay time value a modelled arterial transport function was convolved with the measured global AIF to produce the AIF_i which was used for SVD deconvolution of the tissue curve to produce an impulse residue function IRF_i with its maximum appearing T_{max}(i). DT was determined as the minimal DT_i value which produces T_{max} (i) =0. Cerebral Blood Flow (CBF) and Cerebral Blood Volume (CBV) were calculated from the peak height and area under tissue enhancement curves

respectively, and Mean Transit Time (MTT) = CBV/CBF (central volume theorem)¹⁶⁹.

Ischaemic core was defined as tissue with reduced CBF (relative CBF <40% of contra lesional hemisphere) and prolonged delay time (relative DT >2 sec); penumbra volume was defined as tissue with relative DT >2 sec but relative CBF \geq 40% of contra lateral¹⁴⁸.

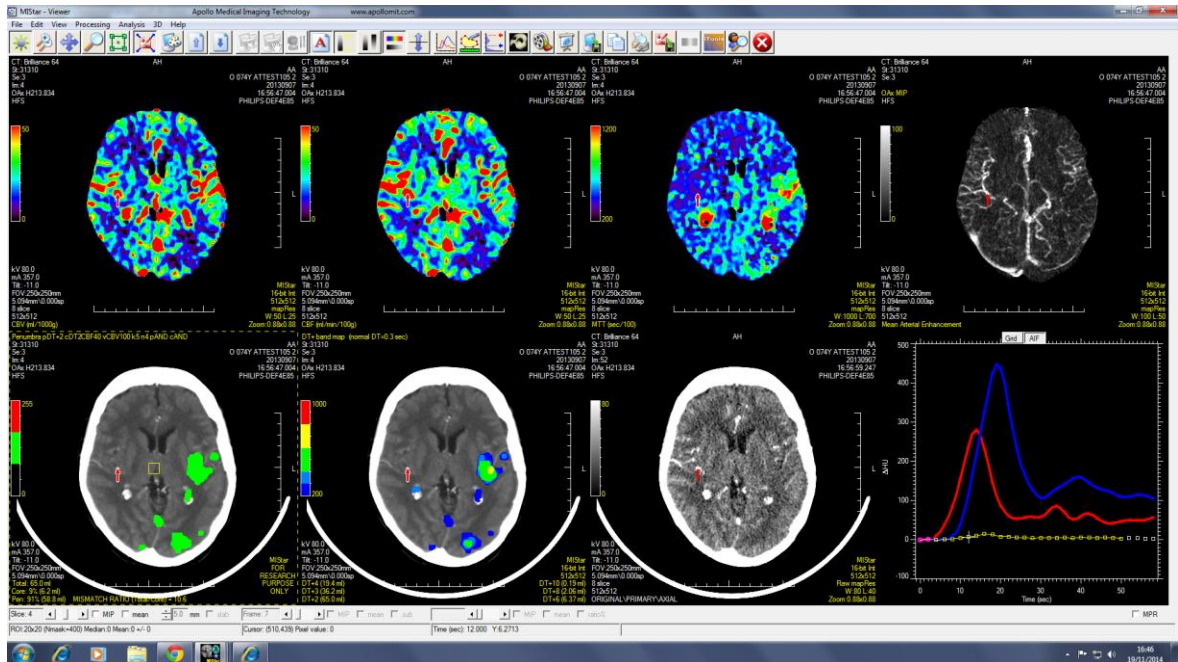


Figure 2-4 CTP maps

CTP maps generated with MIStar software (Top four panels: CBV, CBF, MTT, angiography; Lower four panels: penumbra map, DT, contrast CT, and time-attenuation curve for arterial input function (AIF, red), and venous output function (VOF, blue)

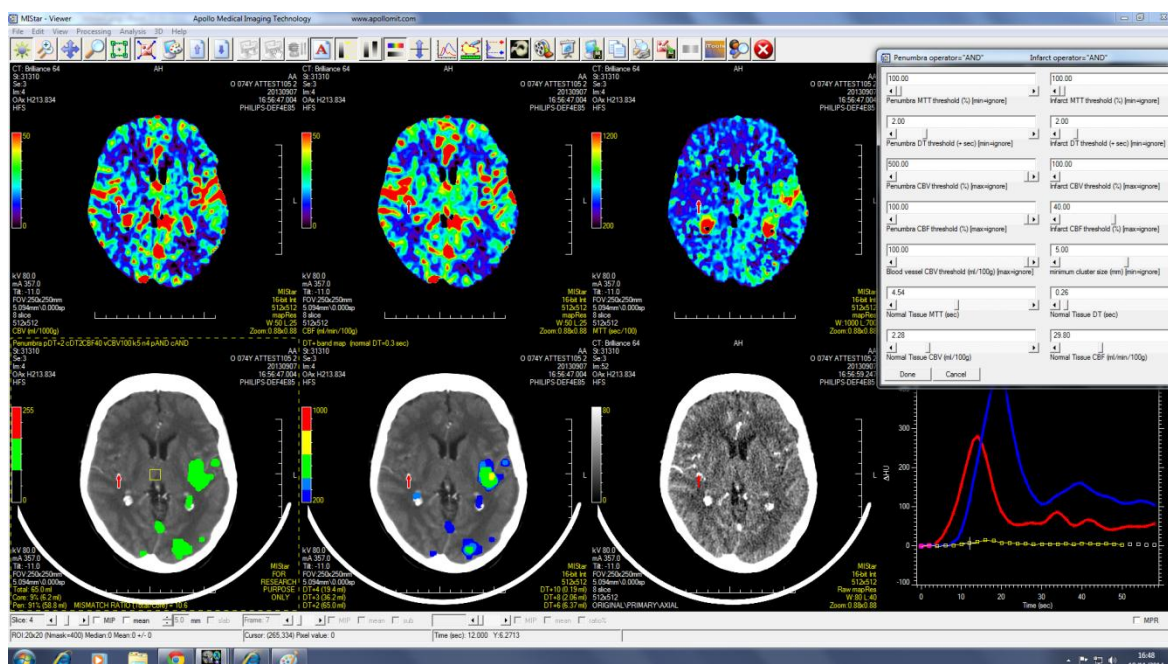


Figure 2-5 CTP maps thresholding

CT maps as in fig. 2-4 with insert showing selection of thresholds for core, penumbra

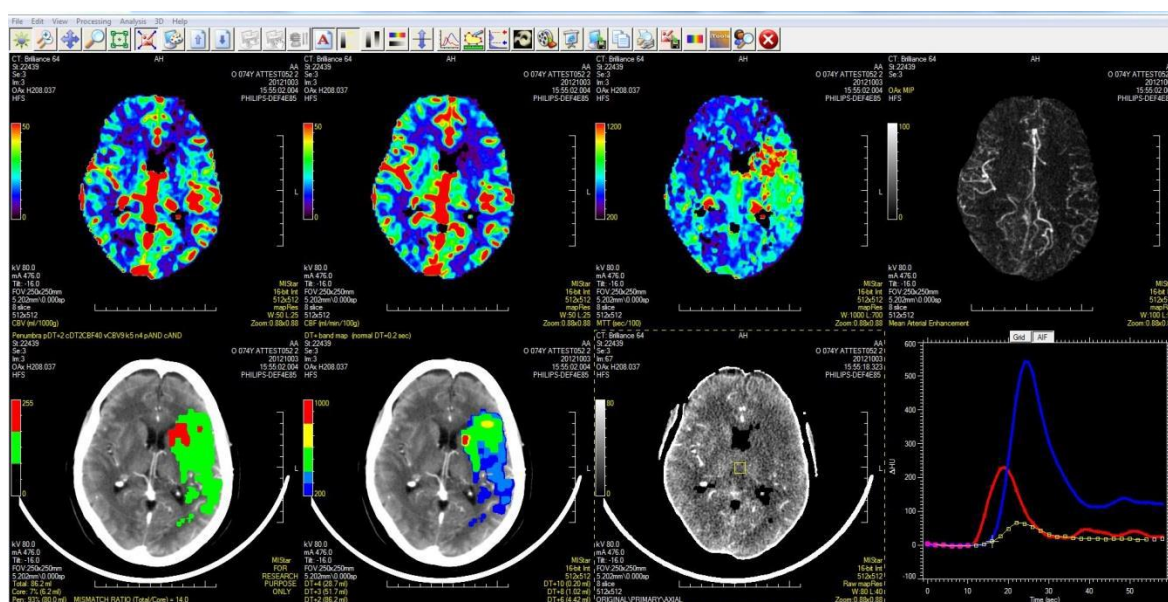


Figure 2-6 CTP maps with bone, CSF masking

CTP maps as in fig.2-6 after applying core, penumbra thresholds and masking CSF and bone (bottom panel second from right, bone is excluded)

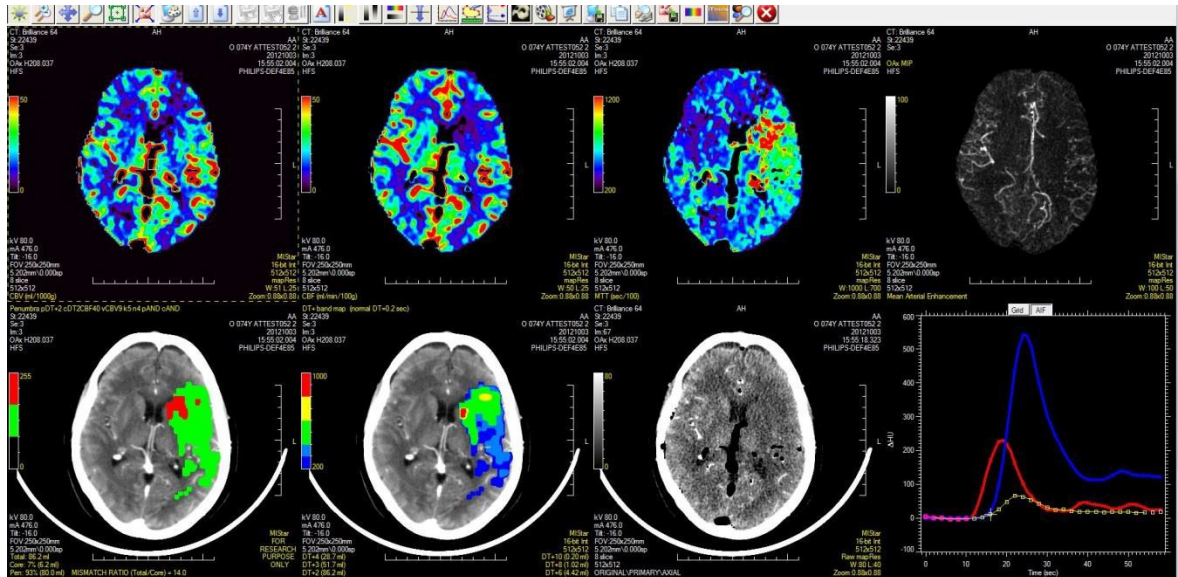


Figure 2-7 CTP maps with thresholding for CBV

CTP maps as in fig.2-6 after applying thresholds masking voxels with CBV value $>90\text{cm}^3/100\text{g}$

Because of the limited coverage of CTP, the co-registered infarct volume was calculated for penumbral salvage. Both follow up CT and CTP scans were loaded side by side into a fusion tool using MIStar (fig.2-8). A rigid body 3D transformation was used to register the follow up structural imaging to the perfusion scan. Structural CT sequences were reformatted manually and visually verified to match the orientation of the original CTP (fig.2-9). Reformatted structural CT slices resulting from co-registration were used to measure the final infarct volume with manually drawn ROIs using visual inspection (fig. 2-10 & 2-11). The combination of the co-registered infarct volume and the infarct volume beyond the co-registered slices produces the total infarct volume.



Figure 2-8 CTP, CT coregistration step 1

Left hand side maps as in fig.2-4, right hand side follow up NCCT images

To minimise the opportunity of including false positive pixels, ROIs drawn for final infarct volume measurement were transposed onto the corresponding CTP slice (Fig.2-13). Manual adjustment was applied when necessary in order to match to the same anatomical region. The penumbra volume that was infarcted was calculated from the ROI on the corresponding CTP slice. The following equations were used to determine relevant values:

- Infarct Growth = Co-registered infarct volume - Core volume
- Penumbra volume salvaged = penumbra volume - penumbra volume that infarcted;
- Percentage of penumbra salvaged = (penumbra salvage/penumbra volume) x100

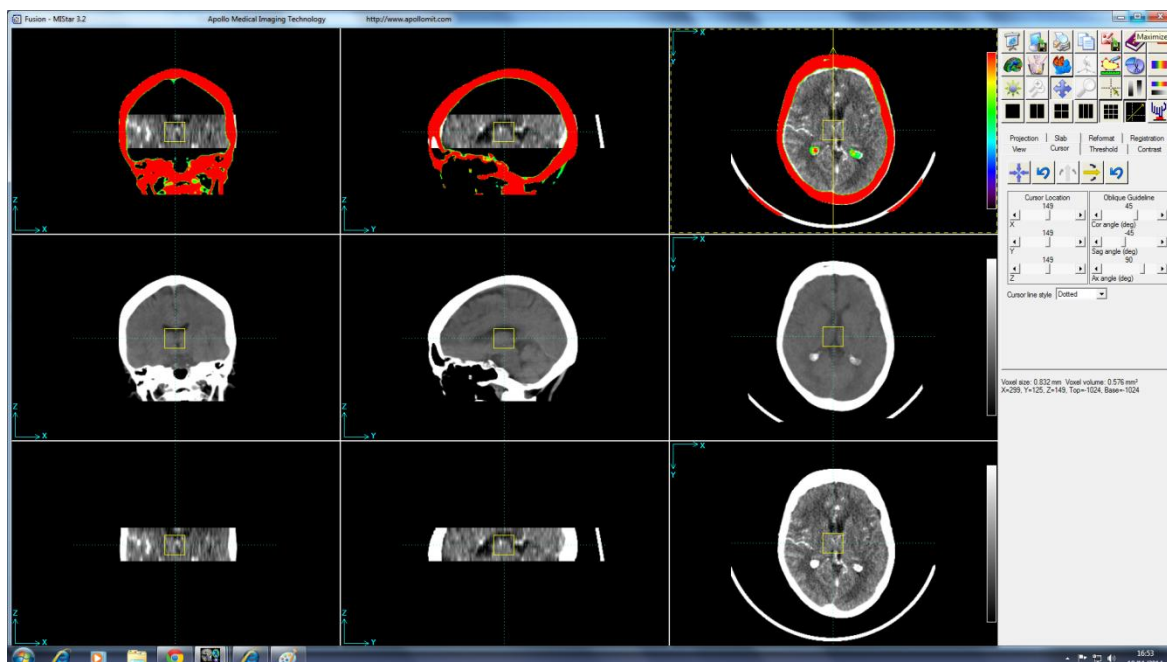


Figure 2-9 CTP, CT Coregistration- step 2

Top 3 panels: CT perfusion with superimposed (red) 24 hr CT following co-registration; middle three panels: 24 hr CT at the same anatomic level; lower three panels: CT perfusion at the same anatomic level

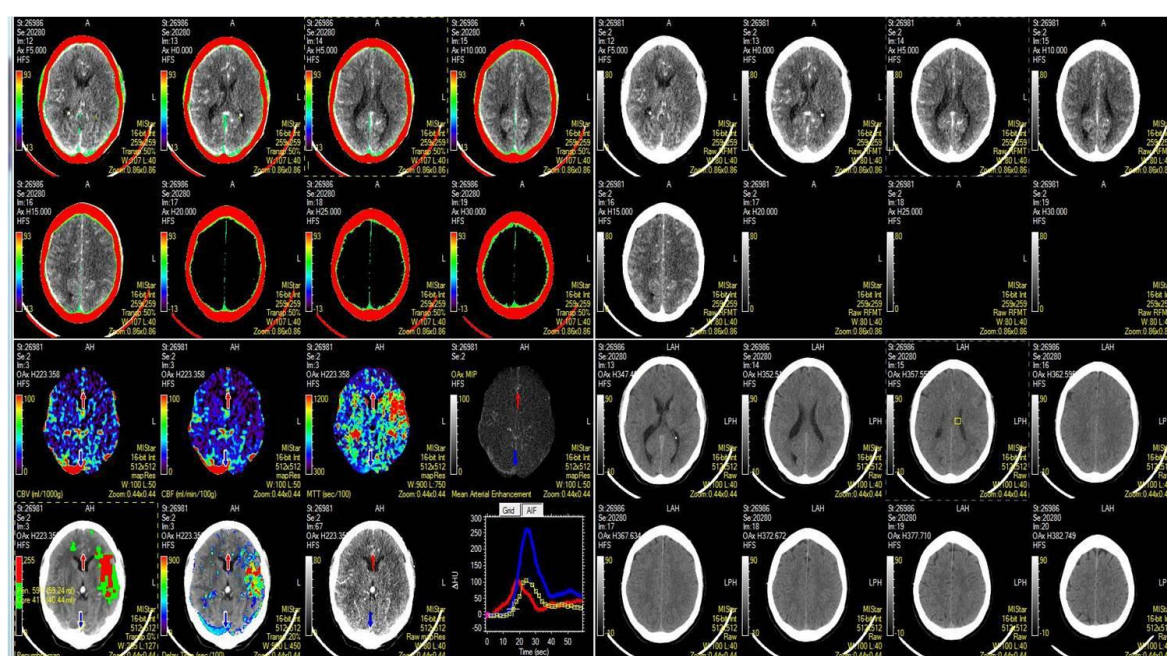


Figure 2-10 CTP, CT Coregistration- step 3

Reformatted 24 hours CT (with the red colour overlay – top left eight panels) presented in a same window as the original 24 hour CT (lower right eight panels) and baseline CTP (lower left eight panels; CT perfusion angiography (top right eight panels)

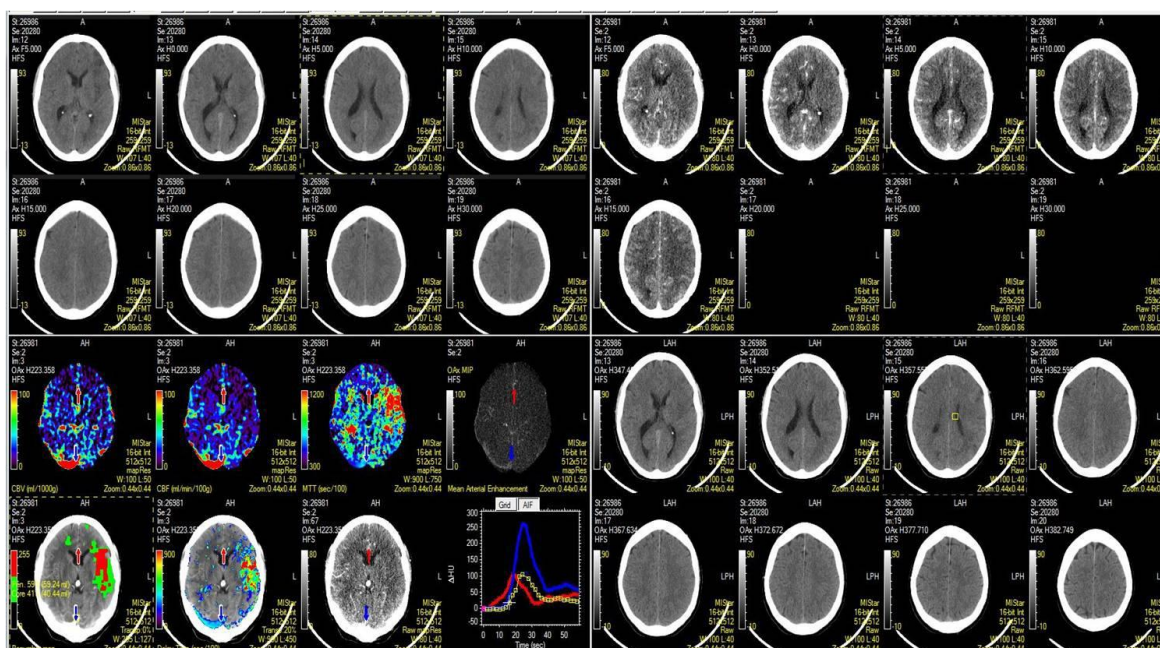


Figure 2-11 Reformatting of images after coregistration

Reformatted 24 hours CT (with the red colour overlay turned off – top left eight panels) presented in a same window as the original 24 hours CT (lower right eight panels) and baseline CTP (lower left eight panels). CT perfusion angiography (top right eight panels)

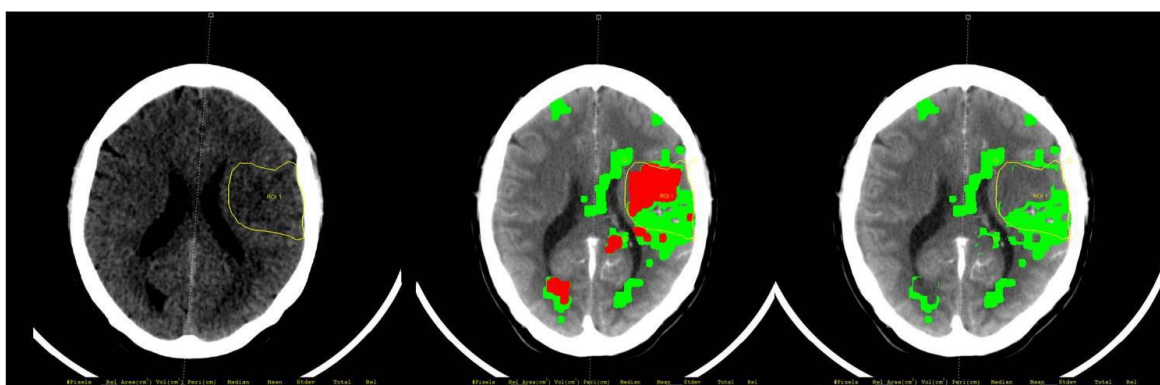


Figure 2-12 ROIs for core, penumbra

ROI of final infarct volume (Left) transposed to the penumbra/core (middle. Green- penumbra; red-core) map; by applying thresholds either core or penumbra can be chosen (right)

2.3 Collateral grading:

Patients with arterial occlusion in the Internal carotid artery (ICA) or proximal Middle cerebral artery (MCA) vessels had perfusion scans evaluated to determine the direction of blood flow distal to the vessel occlusion. 4-D angiographic appearances of the 4cm perfusion slab were displayed as a Maximum Intensity projection (MIP) image and evaluated in cine mode. The 4-D angiographic appearances permitted visualisation of arterial filling in normal and ischemic tissue beds in real time or at faster rates if needed adjusted by the operator. The

effect permitted the presence of contrast enhancement in distal portions of an arterial distribution to be seen prior to filling of the proximal portions and thereby confirming that flow in the relevant territory is truly collateral in nature. Without being able to confirm the retrograde direction of flow it would be impossible to say if CTA appearances were due to collateral filling and not simply due to delayed anterograde flow due to an incomplete arterial occlusion/stenosis. The use of perfusion data to confirm flow direction has been previously demonstrated using the same software packaging²⁹⁷. The effect is best appreciated when viewed in the cine mode, but can be appreciated using a series of screenshots taken at 2 second intervals as seen in figure below (fig.2-13).

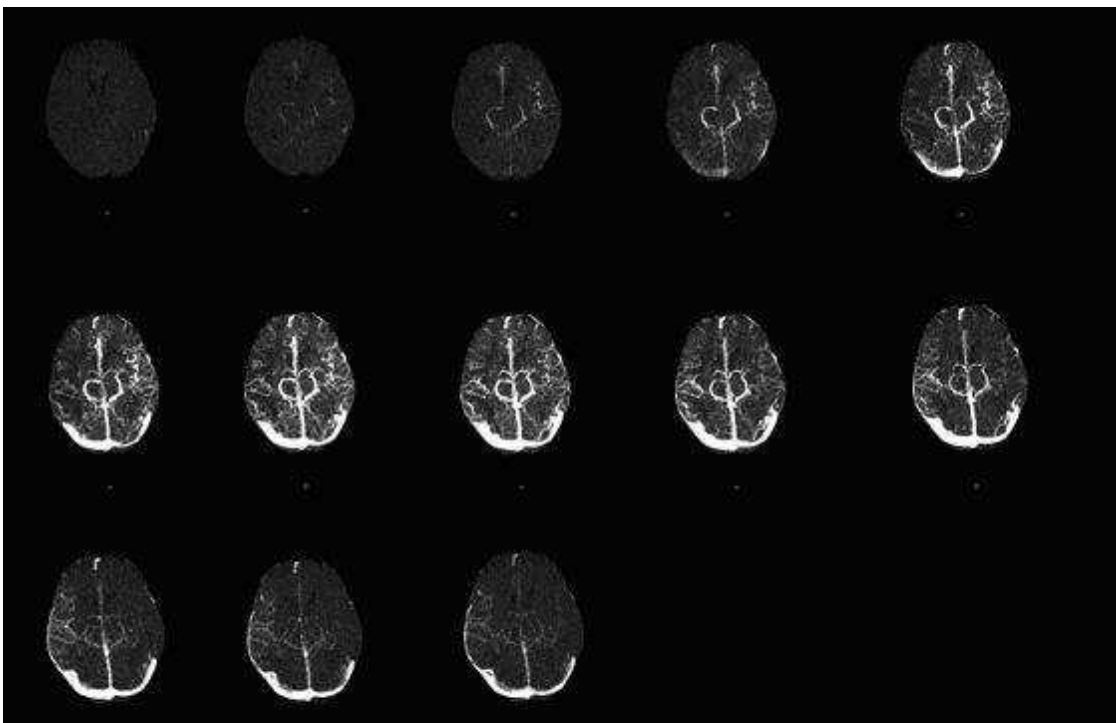


Figure 2-13 CTP angiography for collateral grading

4D CTP angiography demonstrating retrograde flow: Right MCA occlusion with perfusion scan MIP shown at 2 second intervals. The right MCA demonstrates delayed contrast filling, but the distal portion fills prior to proximal portion confirming that flow in ischemic area is retrograde and collateral in origin

If retrograde flow was seen on CT Perfusion, collaterals were graded on baseline CTA qualitatively²⁹⁷. We defined collaterals as good (angiographic flow distal to occlusion), moderate (angiographic flow to ischemic territory but not distal to occlusion), or poor (contrast opacification only in distal superficial branches). We used a modified Miteff's classification to incorporate terminal ICA, M1 and M2 occlusion, whereas the original classification excluded M2 occlusion²⁹⁷.

2.4 Recanalisation

Recanalisation was determined on follow up CT Angiogram at 24 hrs using a TIMI scale, a grading system adapted from cardiologists to describe recanalisation and reperfusion in revascularisation studies (Table 2-3). Recanalisation was defined as Thrombolysis in Myocardial Infarction (TIMI) grading 2- 3 in CTA^{306 307}.

Thrombolysis in cerebral infarction (TICI) score was designed for conventional angiography, and dynamic function is crucial to use it accurately³⁰⁸. Since conventional CTA provide a single phased image, the TICI scale is unlikely to describe recanalisation more accurately than TIMI scale. Since introduction of endovascular therapies Modified TICI scale was recommended³⁰⁷.

Table 2-3 TIMI scale

Grade	TIMI
0	No reperfusion
1	Penetration without reperfusion
2	Partial reperfusion
3	Complete reperfusion

2.5 Haemorrhage classification

On 24h NCCT, we classified ICH as per European Cooperative Acute Stroke Study II (ECASS II) criteria,²⁶² and SICH as any ICH with increase in NIHSS \geq 4 points²⁶².

Haemorrhagic transformation following ischemic stroke is classified into four types (Fig.2-14):

Haemorrhagic infarction 1 (HI 1) - small petechiae along the margins of the infarct

Haemorrhagic infarction 2 (HI 2) -confluent petechiae within the infarcted area but no space occupying effect;

Parenchymal haematoma 1 (PH 1) - Blood clots in \leq 30% of the infarcted area with space occupying effect;

Parenchymal haematoma 2 (PH 2) - Blood clots in >30% of the infarcted area with space occupying effect. Any PH1 or PH2 were considered significant haemorrhage.

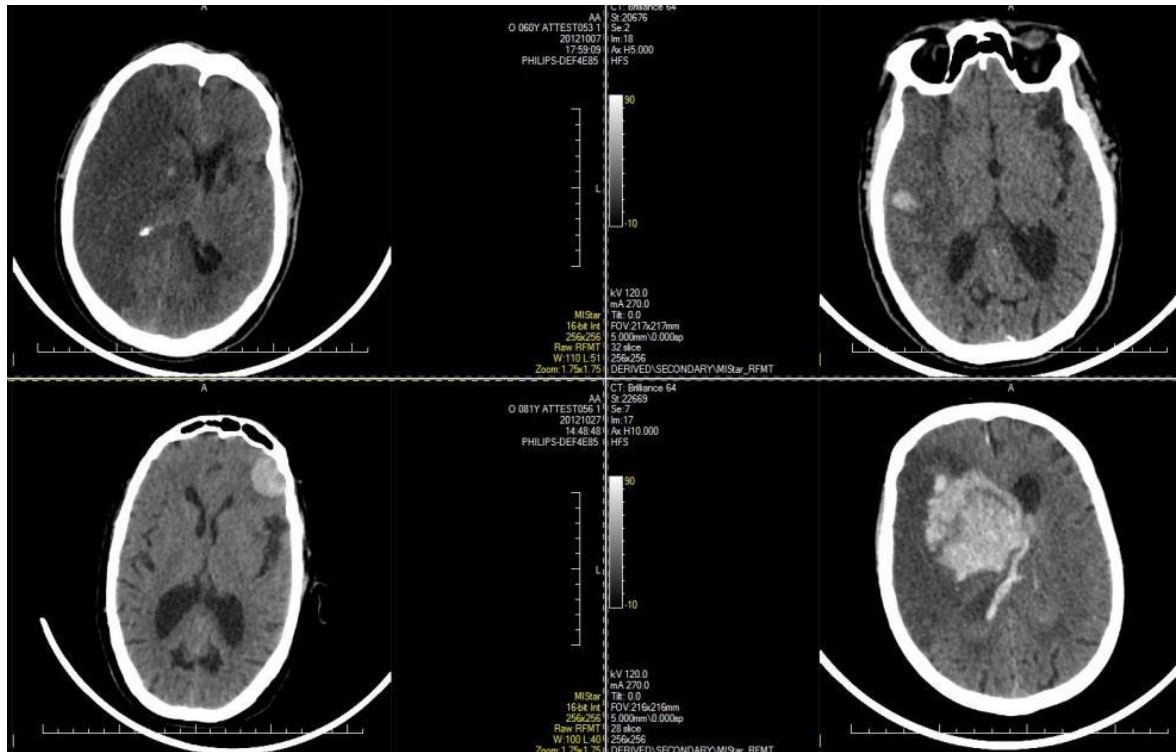


Figure 2-14 ECASS II classification of ICH





Examples from the ATTEST study imaging (from above left clockwise: HI1, HI2, PH1, PH2)

Safe Implementation of thrombolysis in stroke Monitoring (SITS-MOST) proposed that only PH type haemorrhage with deterioration in NIHSS \geq 4 is clinically significant³⁰⁹.

2.6 Oedema classification

Brain oedema classification was as adapted from IST-3 trial as no swelling (grade 0), effacement of lateral ventricle (grade 1), effacement of lateral plus third ventricles (grade 2), or midline shift (grade 3. Table 2-4)³¹⁰. In this thesis work, I used grades 2-3 as significant brain oedema.

Table 2-4 Brain swelling classification (adapted from IST-3 trial)

Brain swelling	
No Swelling (grade 0)	
Effacement of adjacent lateral ventricle (grade 1)	
Effacement of the lateral and the third ventricle (grade 2)	
Midline shift (grade 3)	

2.7 Modified Rankin Scale

The modified Rankin scale is an ordinal hierarchical grading from zero (no symptoms) to six (death) for measuring the degree of disability or dependence in daily activity (table 2-5). It is the most used functional outcome scale in stroke research studies. There is relatively lower inter-rater agreement compared with other scales³¹¹. Inter-observer reliability improved moderately with the structured mRS interview and video training system³¹².

Table 2-5 Modified Rankin scale

Scale	Description
0	No symptoms at all.
1	No significant disability despite symptoms; able to carry out all usual duties and activities.

2	Slight disability; unable to carry out all previous activities, but able to look after own affairs without assistance.
3	Moderate disability; requiring some help for more complex tasks (e.g. finances), but able to walk without assistance. Able to manage alone at home for at least 1 week.
4	Moderately severe disability; unable to walk without assistance and unable to attend to own bodily needs without assistance. Able to be left alone for at least a few hours during the day.
5	Severe disability; bedridden, incontinent and requiring constant nursing care and attention.
6	Dead.

Chapter 3 **Methods for Capillary Transit Time Heterogeneity (CTTH) work in Chapters 6, 7**

3.1 Introduction

Using a multimodal imaging database from 3 different single centre studies, we derived the maps for several perfusion parameters. The study population was detailed in chapter 2. The perfusion parameters derived included: Cerebral blood flow (CBF), Cerebral blood volume (CBV), Mean transit time (MTT), Delay time (DT), Tmax, Capillary transit time heterogeneity (CTTH) and Coefficient of variation (COV) maps using vascular (parametric) method. Scans were read by one research fellow (BC) experienced in perfusion imaging, blinded to the clinical information and functional outcomes. MATLAB platform (2014 version) was used for image analysis (PGUI perfusion analysis software: centre for functionally integrative neuroscience CFIN, Aarhus University Hospital, Norrebrogade, Denmark). First, all the anonymised scans digital imaging and communications in medicine (DICOM) data was decoded to tailor to transfer into the dedicated pipeline developed locally in Brain imaging lab, Aarhus University, Denmark. These images were converted to Neuroimaging Informatics Technology Initiative (NIFTI) files. Then, masks were drawn for Infarct, manually in 24h followup non-contrast CT (NCCT) scans. Broadly the steps involved in deriving CTP parameters are below:

- DICOM file Conversion to NIFTI
- Baseline detection of contrast bolus arrival (automated)
- Motion correction (automated): 2D approach was adapted
- Check Motion Correction (manual): some slices where motion artefact was detected, it was interpolated with the adjacent slice Concentration conversion (automated)

- Arterial Input function (AIF), venous output function (VOF) selection (Anterior cerebral artery (ACA) and sagittal sinus respectively were chosen manually)
- Check baseline of concentration curves (manual)
- Vessel removal for perfusion (PWI) Images (by applying threshold manually)
- Deconvolution (automated) : standard SVD (s SVD), circular SVD (o SVD), Vascular(parametric) methods
- Re-slice follow up NCCT to thicker (5mm) slices(automated)
- Automatic segmentation (Grey matter (GM), white matter (WM), Cerebrospinal fluid (CSF) space)
- Co registration (automated) of follow up NCCT to the acute NCCT at first followed by manual correction with acute CTP images. Co registration of CTP with follow-up NCCT was also done by automated method. By checking manually, whichever method co-registered best was used for the analysis.
- Cleanup (automated)
- Segmentation: Follow up NCCT mask for Infarct area (manual), TTP mask (ROI tool and manual adjustment if needed)

3.2 Detailed steps

Perfusion CT images were processed using MATLAB package (version 2014 Matlab, Math works, <https://de.mathworks.com/products/matlab.html>) to derive the CTP parameters. Motion correction of CTP images was carried out by a 2 dimensional approach by a special filter. Motion correction was checked for each subject, and, if required, Interpolation of slices was carried out in some (n=20), but restricting to not more than 3 non contiguous slices for each patient (Fig.3-

1). Interpolation of 3 slices, 2 slices in 4 subjects, one slice in 15 subjects was performed.

If interpolation is not possible due to excessive motion artefacts, they were excluded from the study (n=15).

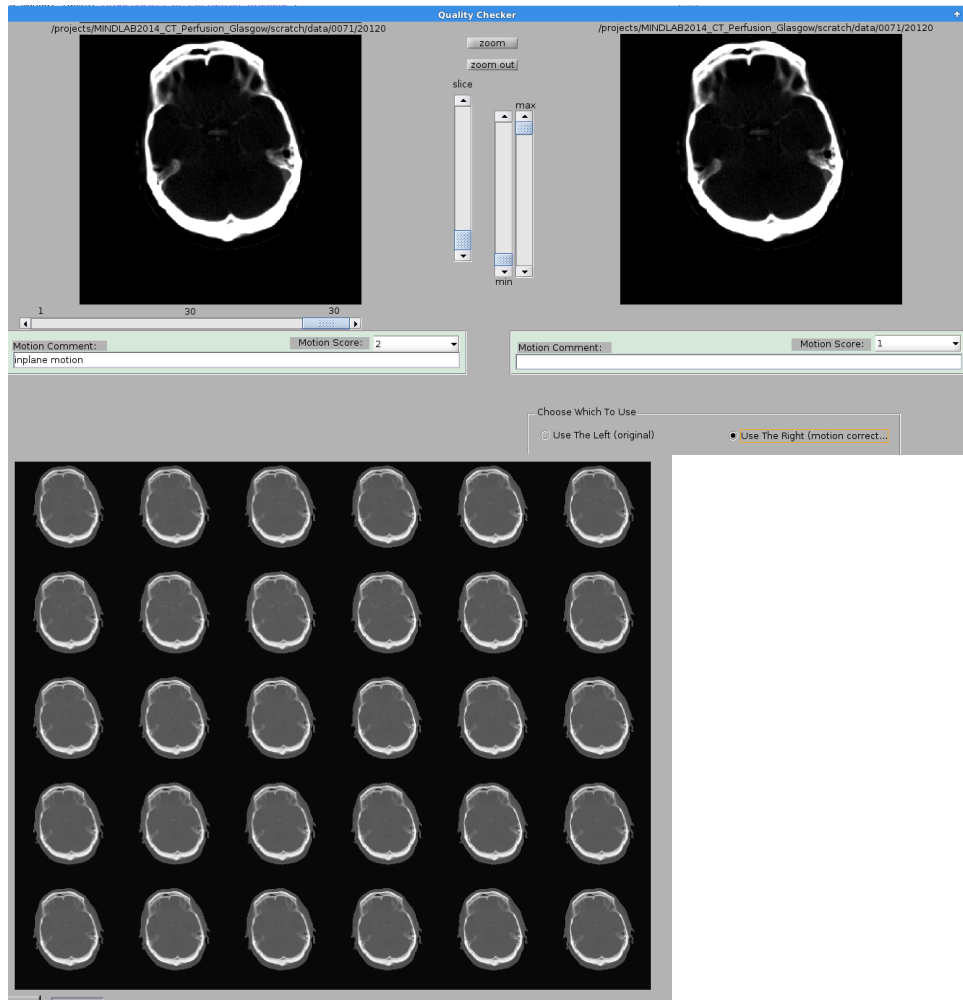


Figure 3-1 Motion correction of CTP images

Top: left before motion correction right: after motion correction. Bottom: serial images of CTP after motion correction

A delay corrected deconvolution steps (standard SVD, circular SVD, vascular model) are then applied to generate the parametric maps MTT, CBF, CBV, DT, Tmax . In addition, CTTH, COV, OEF_{max} maps were obtained only in vascular model. The deconvolution applies an arterial input and venous output function which were selected manually. I selected Anterior cerebral artery (ACA) and

vertical segment of Superior sagittal sinus respectively for Arterial Input function (AIF), Venous output function (VOF) with an ROI tool (Fig.3-2). Region of Interest (ROI) was chosen manually by reader (BC), software then identifies the reference voxels within these ROIs. This can be manually adjusted if needed (e.g. add more voxels, if required). An example of arterial, venous curves for a few subjects is shown in Fig. 3-3.

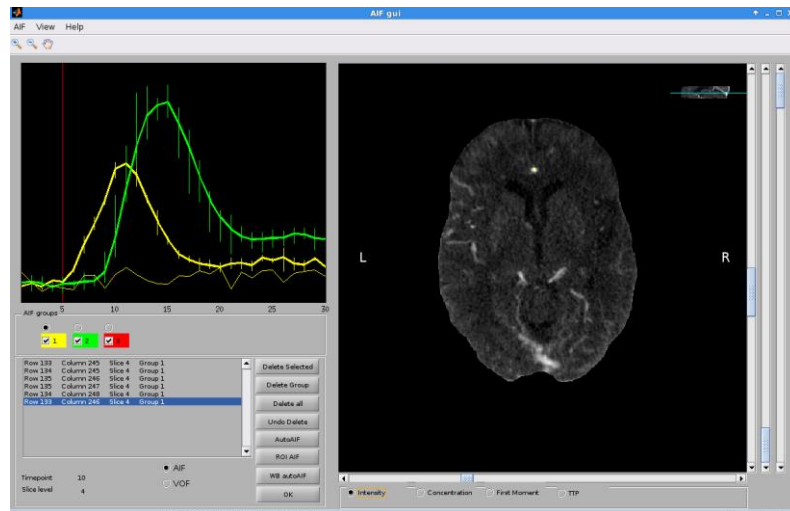


Figure 3-2 AIF, VOF selection

Left: curves (yellow-arterial, green-venous) after selection of voxels Right: ROIs placed on Anterior cerebral artery (ACA) and Sagittal sinus

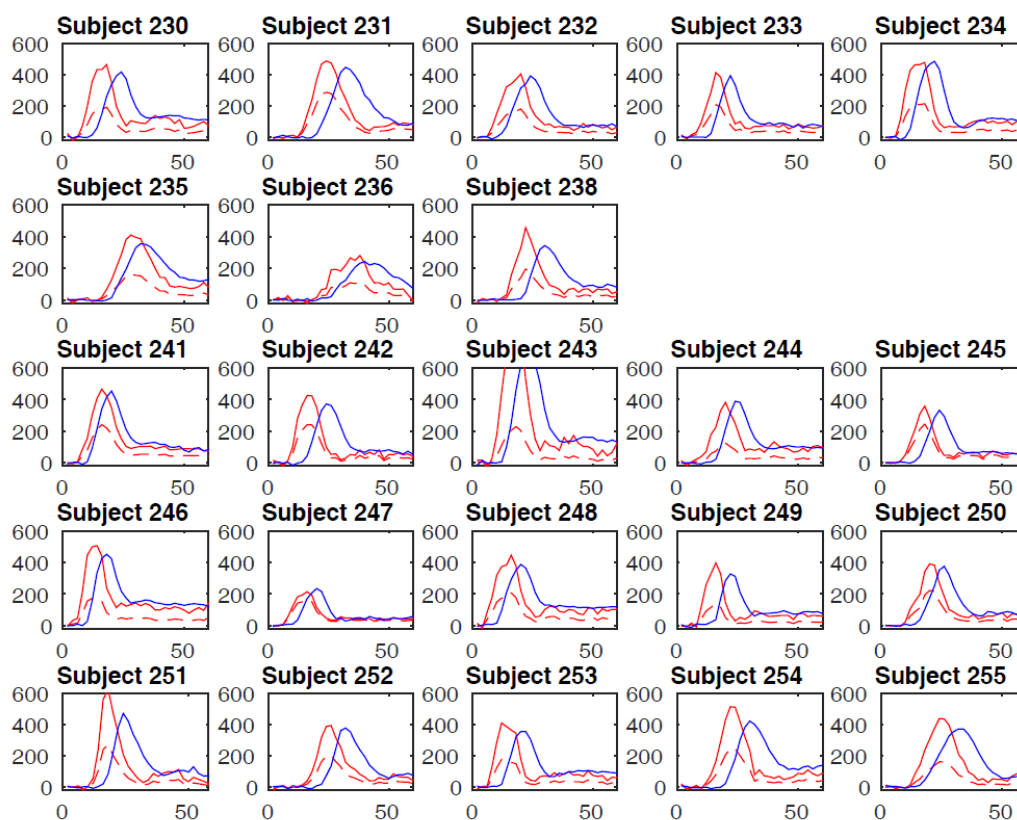


Figure 3-3 AIF and VOF curves

Arterial and venous curves in different subjects (Red curve is arterial and blue is venous).

The software applies curve fitting by least mean squares to obtain time concentration curves for each voxel (Fig.3-4). The baseline curves were carefully inspected for each subject to adjust the start volume and end volume of the baseline before the uptake of the arterial curve (Fig 3-4). I selected start volume (start of baseline) as 0 and end of baseline to be a minimum of 1. Some subjects (n=16) had no baseline (i.e. both start volume and end volume were 0 with take off from start of the baseline) and therefore deconvolution was not possible; baseline unenhanced signal variation was not available to compare with voxels with substantial signal increase.

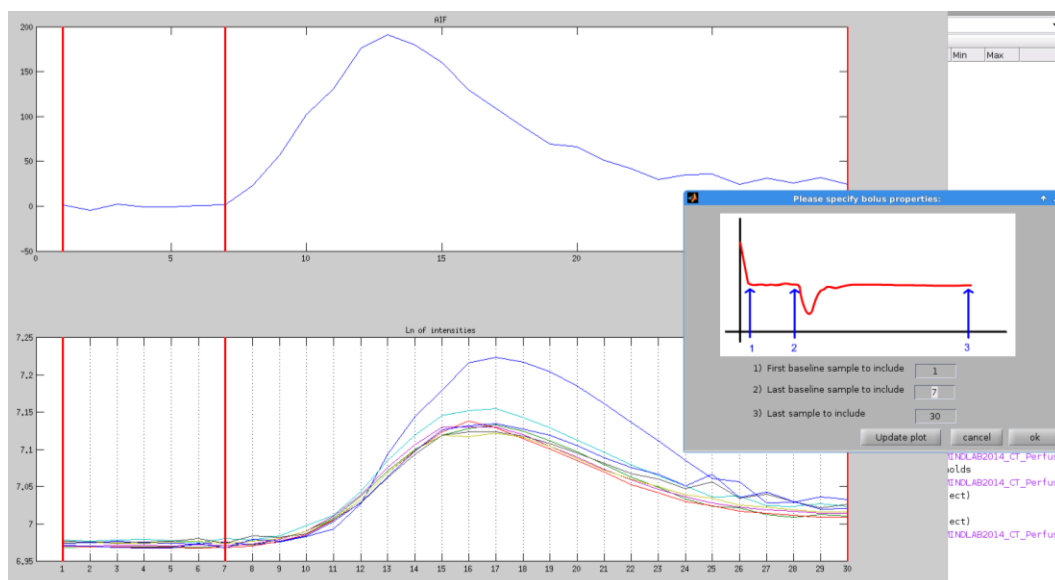


Figure 3-4 Concentration tissue curves

Bottom graph shows the curves for each voxel and top graph is the cumulative curve. Small insert shows manual selection points of start and end values for baseline.

I removed the peripheral vasculature by applying threshold for each subject individually (Fig.3-5). The distribution of threshold application for all the subjects is shown on histogram in the fig.3-6. An example of CTP images after vasculature removal is shown in Figure 3-7.

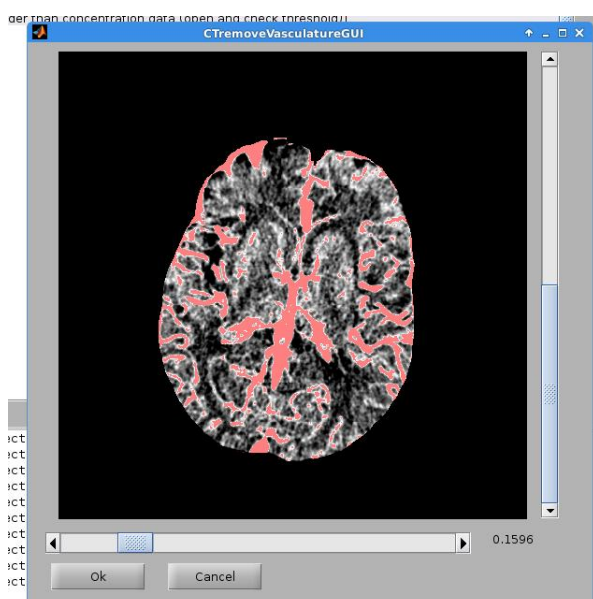


Figure 3-5 Vasculature removal from CTP

Pink colour is vasculature-manually threshold can be changed to obtain optimal vasculature removal.

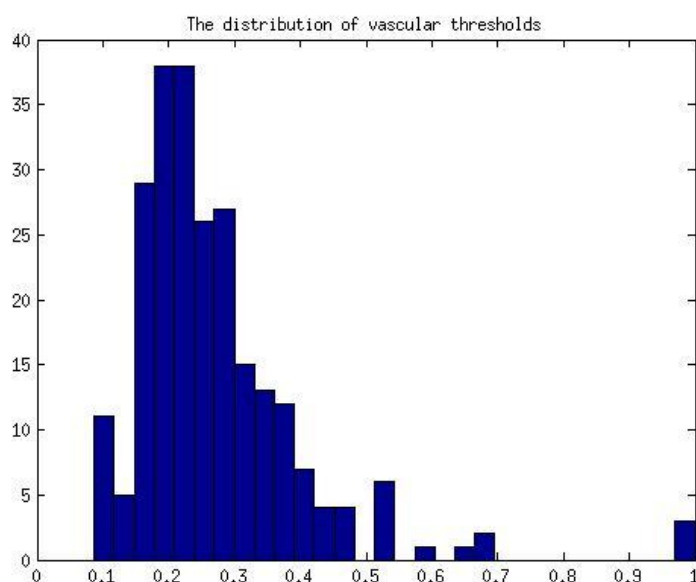


Figure 3-6 Histogram of distribution of vascular thresholds

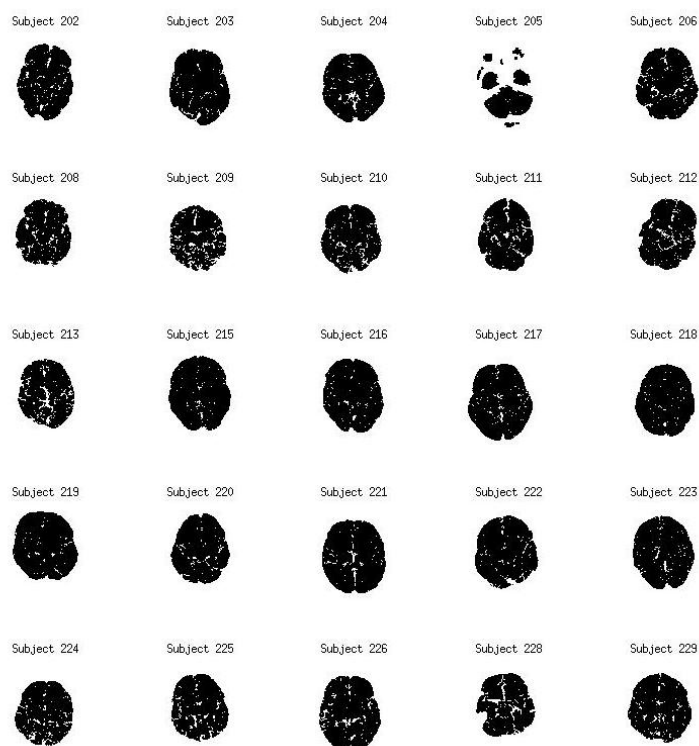


Figure 3-7 Examples of CTP images after vasculature removal

Separately, time to peaks (TTP) was outlined with ROI tool with manual adjustment if needed (Fig.3-8 &3-9). TTP maps are used to delineate the area of

hypoperfusion. From these outlined areas, other perfusion parameters were derived. CBV map is calculated from the area under the time enhancement curve for each voxel. Then central volume principle ($CBF=CBV/MTT$) is applied. Automatic segmentation of GM, WM, and CSF was also done.

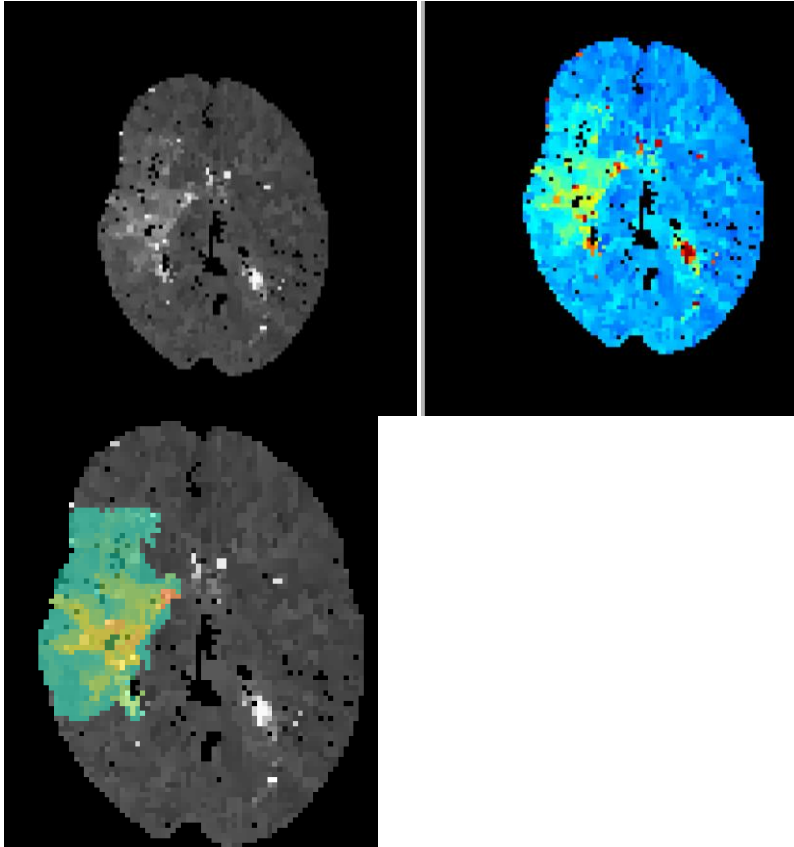


Figure 3-8 ROI drawing of TTP mask

First ROI tool is drawn around the abnormal TTP zone (Top left and right) with manual adjustment if necessary (Bottom)

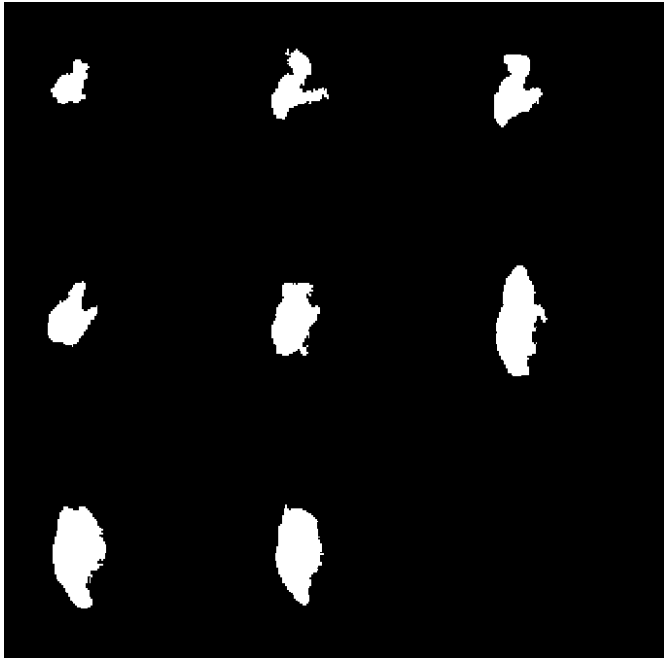


Figure 3-9 TTP masks after ROIs chosen in a subject

Segmentation of total infarct volume in non contrast CT at follow up (n=169) was done manually outlining the hypo attenuation area (Fig.3-10). Co-registration of acute NCCT to follow-up CT was conducted manually. Co-registration was assessed manually for satisfactory results. A few scans were not properly gantry corrected. If acute scans were not properly gantry corrected, I manually co registered the CTP with follow up CT (n=15). An automated co-registration of CTP with follow-up CT was also carried out (Fig.3-11). A few were excluded that were not able to be co registered (n=2). The best co-registration mode (manual or automated) was chosen visually inspecting all the subjects. Co-registration of CTP with Follow up MRI scans was not adequate so those with follow up MRI (n=11) were excluded from the study.

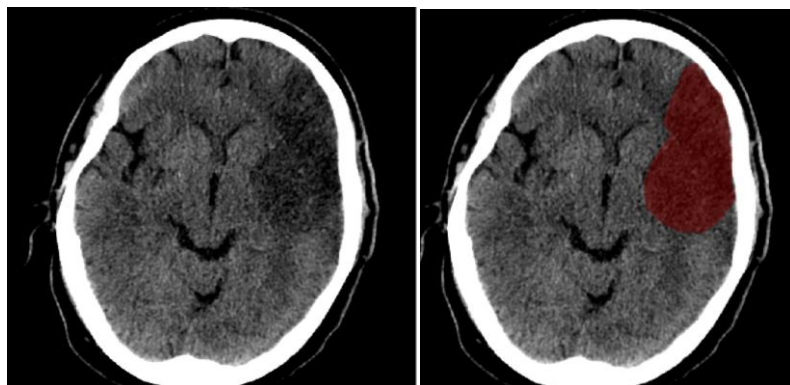


Figure 3-10 CT Infarction ROI

masks are drawn manually for Infarct area on follow up CT

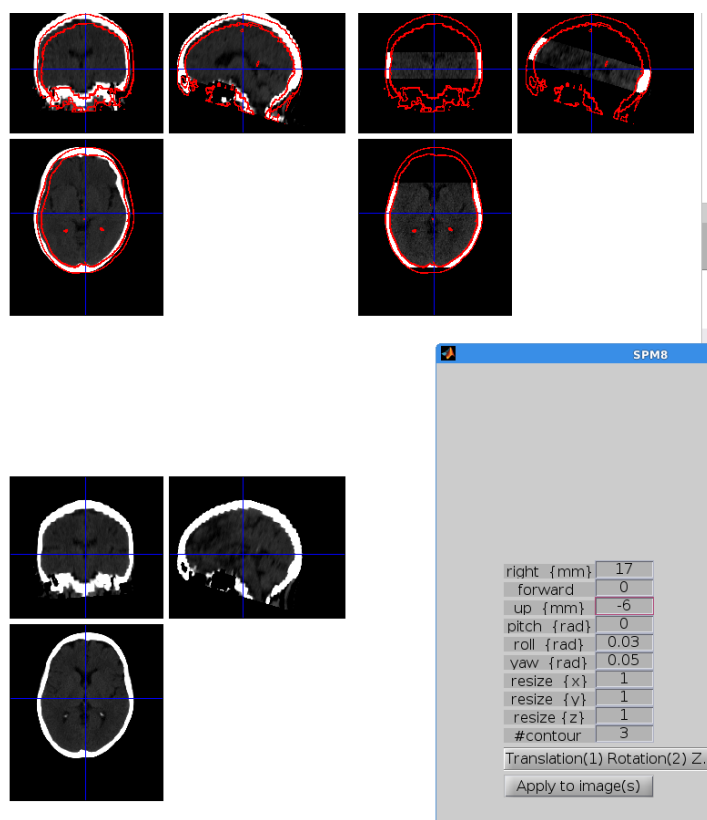


Figure 3-11 Coregistration of Follow up CT and acute CTP

Top left- follow up CT (in red) overlapped on acute CT. Bottom left- follow up CT. Top right- follow up CT (red) overlapping CTP image. Bottom right shows a dialogue box to change yaw, roll and pitch.

Selection of automated or manually co registered images was chosen for each individual based on the best registration method by visually inspecting for each subject. There are some examples in figures below. In the first example (fig.3-

12) there is good correlation of both methods, in second example (fig.3-13) the manual co registration is better than automated, in third (fig.3-14) automated is -better than manual)

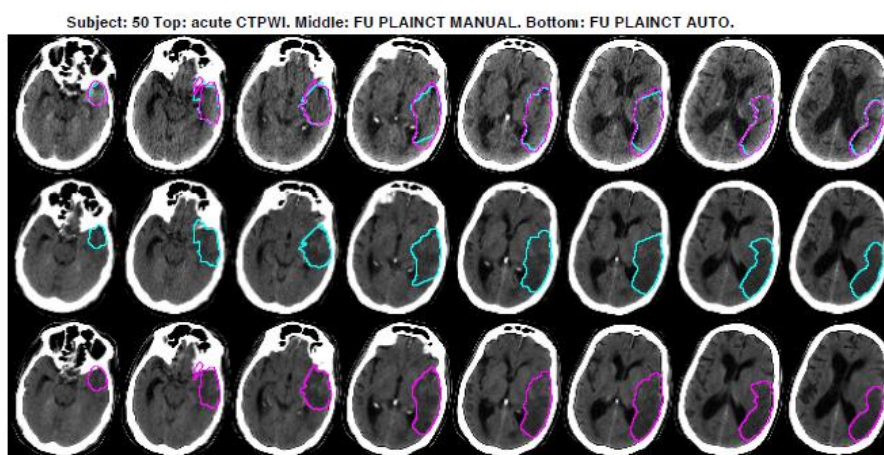


Figure 3-12 An Illustration of good coregistration of both manual and automated methods
 Top: acute CTP, middle:follow up NCCT manual, bottom-:follow up NCCT automated. Infarction masks are shown in pink, blue ROIs

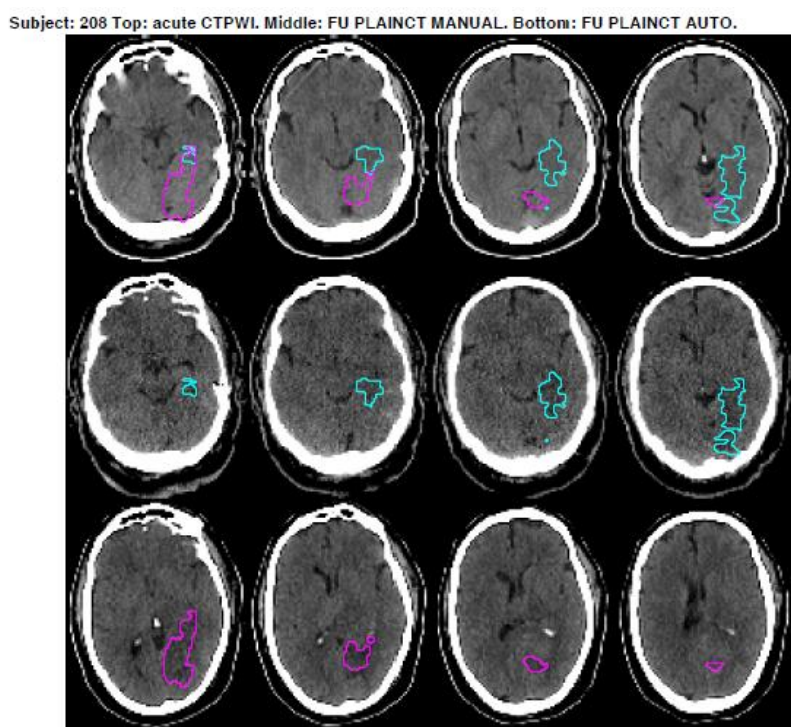


Figure 3-13 An Illustration of manual coregistration better than automated method
 Top: acute CTP Middle: follow up NCCT manual bottom: follow up NCCT automated. Infarction masks are shown in pink, blue ROIs

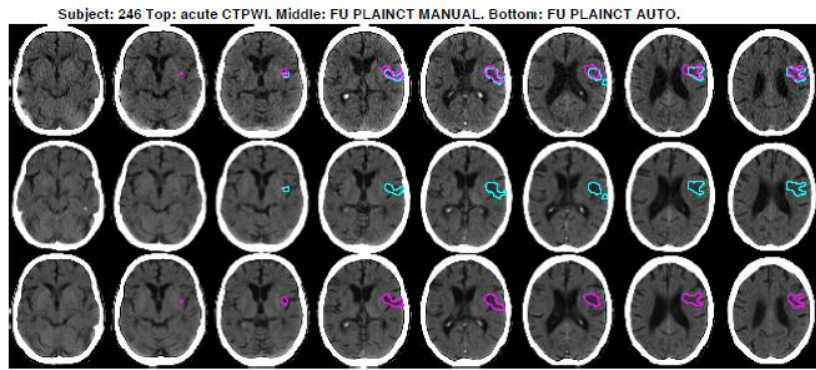


Figure 3-14 An Illustration of automated coregistration better than manual method

Top: acute CTP Middle: follow up NCCT manual bottom: follow up NCCT automated. Infarction masks are shown in pink, blue ROIs

Core, penumbra volumes are derived using Wintermark's method (Core=CBV $<2\text{ml}/100\text{g}/\text{min}$, Penumbra= relative MTT $>145\%$)¹⁴¹. Non bolus voxels where no contrast arrived during scan and values are undetermined (Fig 3-15) and non bolus voxels which are centred in CBV area (Fig 3-16), but also in White matter (WM) where signal to noise ratio (SNR) is low (Fig 3-17), are excluded from all the masks. This may have reduced CBV core mask significantly. Moreover, CBV mask may be scattered diffusely across the whole of brain. If so, I corrected by removing regions with CBV $<1\text{ml}$ (Fig 3-18).

MTT mask often included a non TTP area (Fig 3-19). Sometimes, the infarct (FI) is found to be outside the TTP area. To reduce this, we included MTT from TTP area plus Infarct area in follow up scan (FI) which is called "union mask". An example of Core, penumbra, final infarct masks is shown in Fig 3-20.

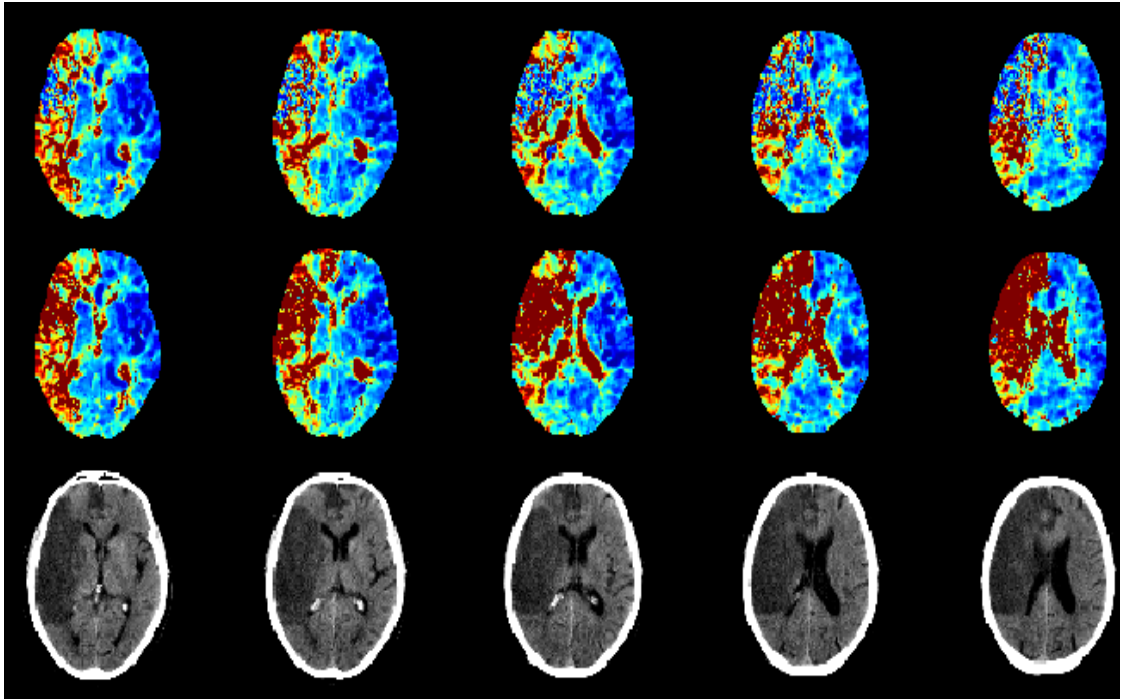


Figure 3-15 Non bolus voxels

Non-Bolus voxel regions shown on MTT maps. Top row-bolus arrival, middle row-MTT is set long to show non bolus areas in red colour, bottom row follow up NCCT with infarction

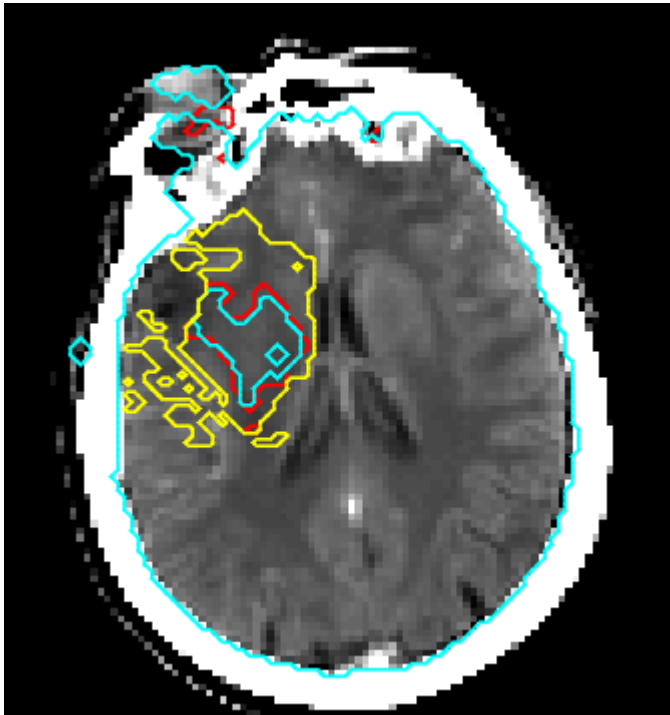


Figure 3-16 Non bolus mask

final Infarct (Yellow ROI). non-bolus area (Light blue ROI). CBV core (Red ROI)

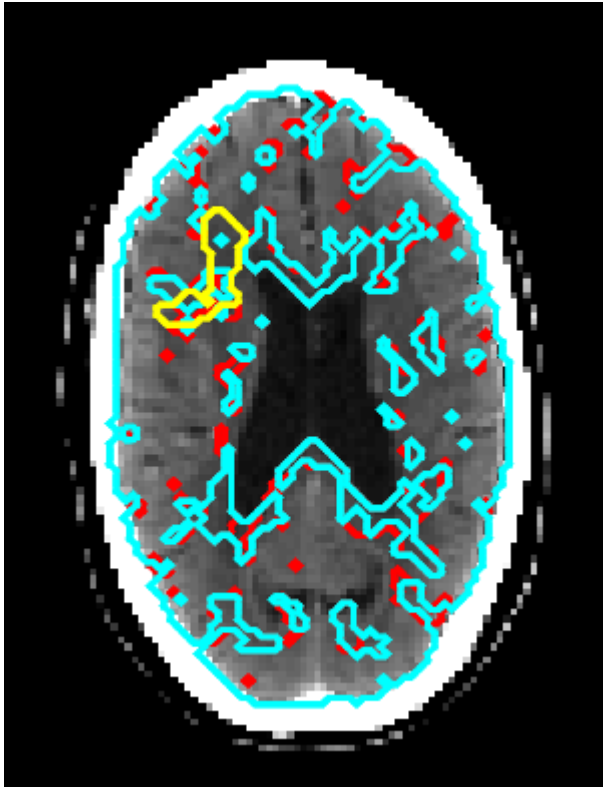


Figure 3-17 Non bolus voxels (light blue) in White matter

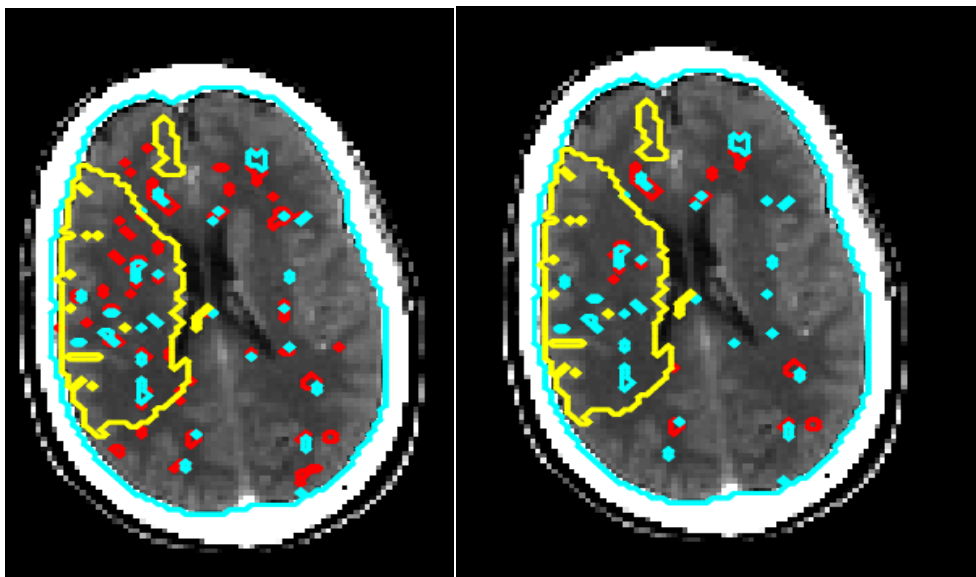


Figure 3-18 Scattered CBV voxels

CBV (red) scattered diffusely in white matter (blue). Left: Before excluding $CBV < 1\text{ml}$. Right: after removing $CBV < 1\text{ml}$ voxels.

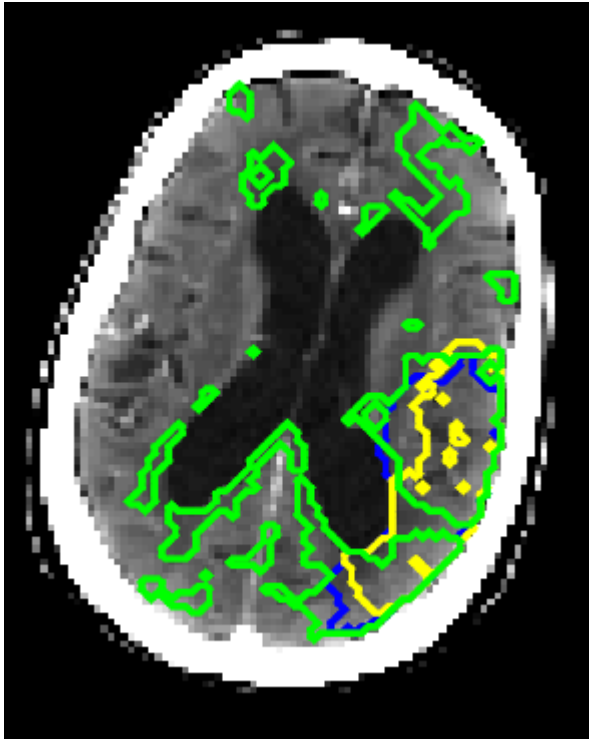


Figure 3-19 Final masks derived after the previous steps
 MTT (green), TTP (blue), Final Infarct (yellow)

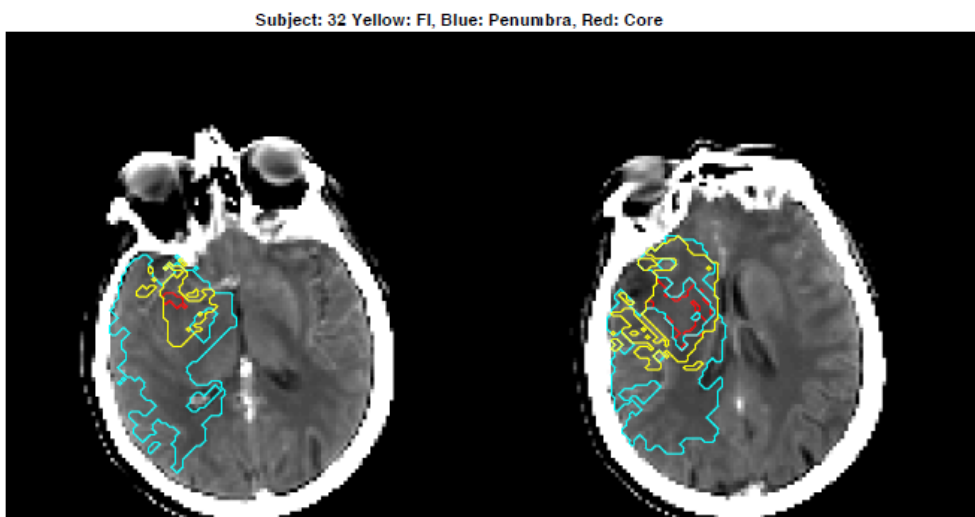


Figure 3-20 Final masks after fusion of MTT, FU Infarction
 Final Infarct (Yellow), core (red), penumbra (blue) masks

Example figures with different maps (standard SVD, Vascular model) derived are shown in fig 3-21 & 3-22.

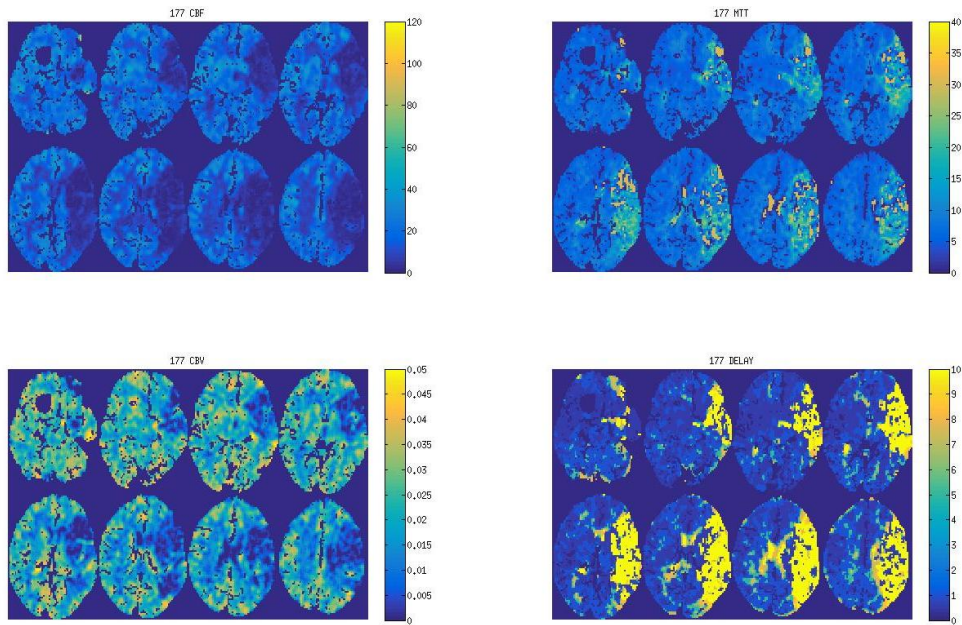


Figure 3-21 An example of standard SVD map

CBF, CBV, delay metric and MTT maps are shown in anti clockwise from top left.

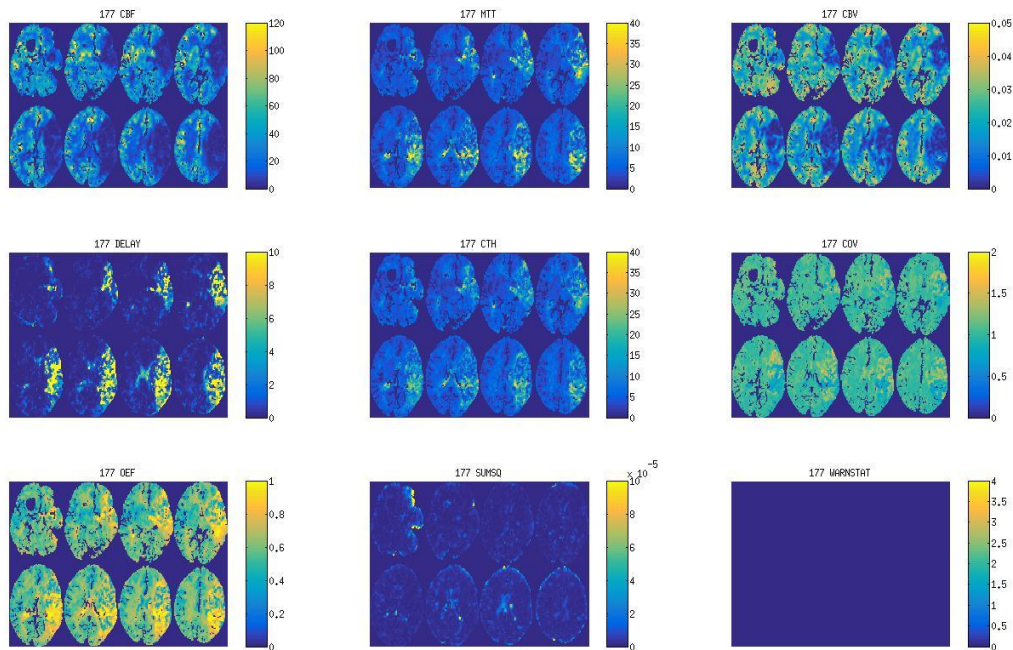


Figure 3-22 An example of vascular model map

Top row- CBF, MTT, CBV ; Middle row- DT, CTH, COV; Bottom row- OEF .

An example of CSF mask, mirror masks for Infarct, TTP masks is shown (fig. 3-23). A 3 dimensional approach is used for mirroring masks in NCCT, and 2 dimensional approaches were used for TTP masks.

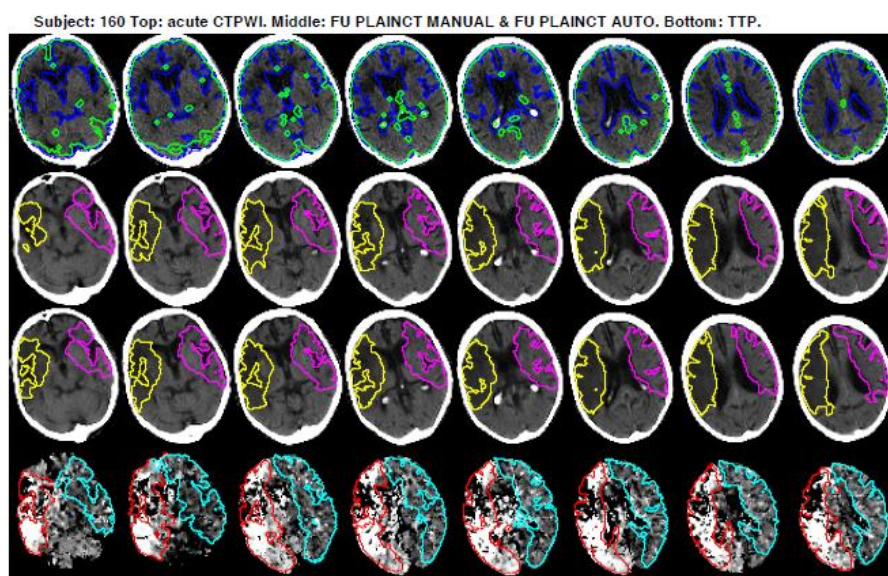


Figure 3-23 Mirroring of TTP, FU Infarct masks

Brain (green), CSF (blue), infarct (yellow) and mirrored infarct (pink) , TTP (red) and mirrored TTP in contra lateral brain (blue).

An example of Core, penumbra and final infarct masks drawn after the previous steps is shown in Fig 3-24.

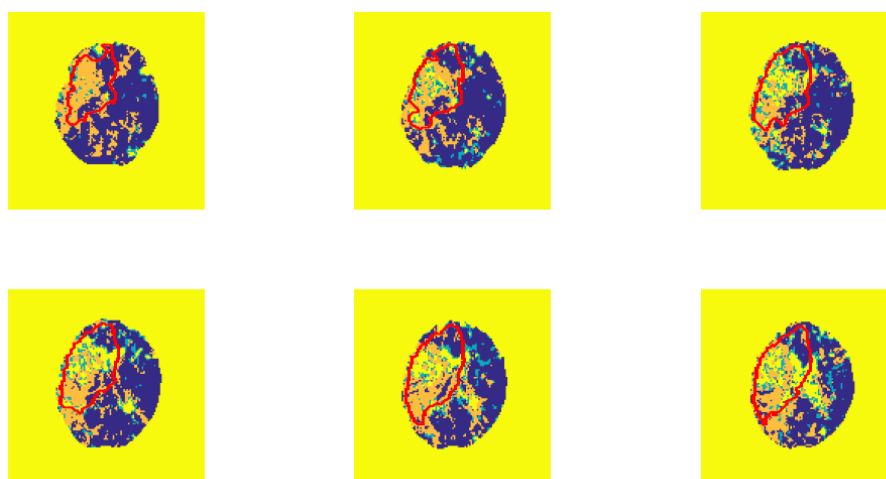


Figure 3-24 Core, penumbra and FU Infarction masks

Infarct (red ROI), penumbra (orange voxels), and core (blue voxels)

An example of non-core, non-penumbra infarction is shown in Fig 3-25.

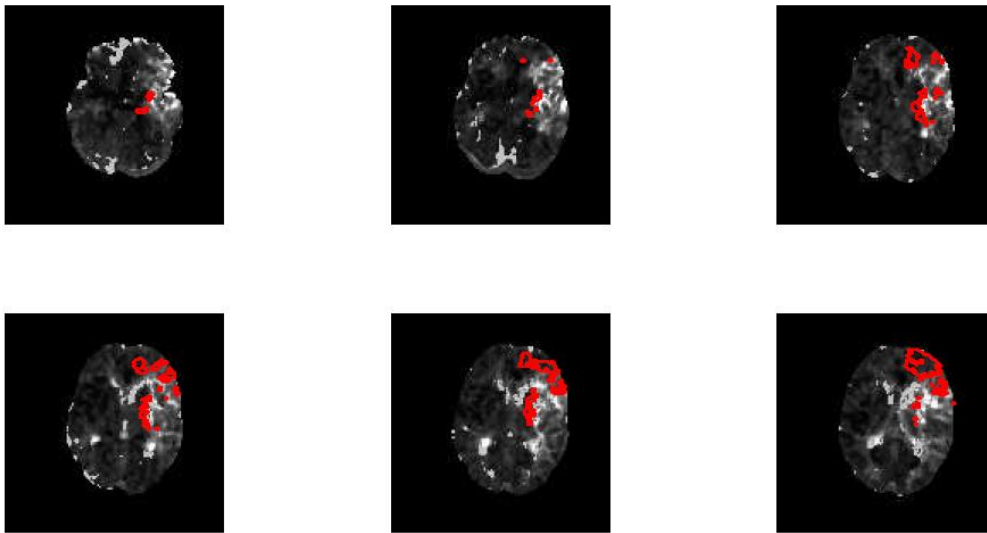


Figure 3-25 An example of non-core-non-penumbra Infarct mask.
Infarct masks shown in red ROIs on a grey scale MTT

Finally, we obtained an excel sheet with median, mean values of CBF, CBV, MTT, CTTH and COV of all voxels in different tissue zones as described above. The values are from all the voxels in core, penumbra, noncore, non penumbra infarct tissue, and normal contra lateral brain.

3.3 Study population of CTTH work

From the 3 studies detailed in chapter 2, a total of 299 subjects have were eligible (MASIS n=83; POSH n=113; ATTEST n=103). 34 subjects were excluded: of which, 16 had no perfusion imaging done, 12 had non stroke diagnosis, and 5 subjects had CTP done after thrombolysis. Incomplete CTP was done in one subject .Scans with Jog mode (n=7) were included as maps appeared satisfactory.

Out of remaining 265 subjects, 167 have core, penumbra maps available. 143 subjects have a follow-up imaging (CT (n=132) and MRI (n=11)), 24 have no follow up imaging. I excluded subjects with follow up MRI as the co registration was not satisfactory.132 subjects have a follow up CT and perfusion maps were

available in all of these except 1 subject. This constituted the final study population (fig.3-26).

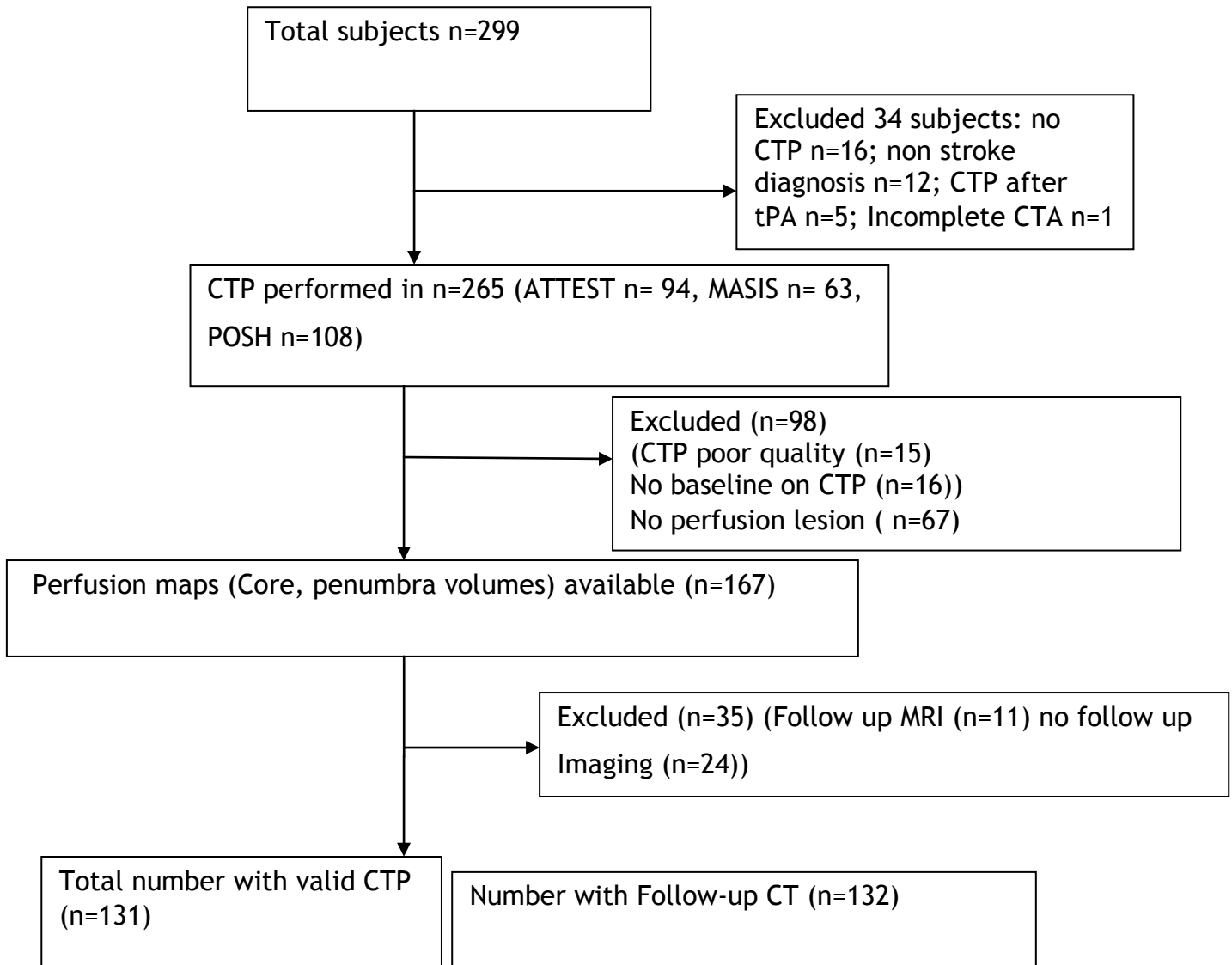


Figure 3-26 Flow chart of study population for CTTH work

Chapter 4 Does the Penumbra Shrink over Time? Penumbra volume and collaterals in the first 6 hours after acute ischemic stroke

4.1 Introduction

In animal focal ischaemia models, CBF thresholds for prediction of infarction differ over time; severe CBF reduction results in infarction within a short time, while it takes longer for less severe CBF reduction to result in infarction⁸⁴. Conventionally, core is believed to grow over time at the expense of penumbra, and is understood to be a consequence of the dynamic interaction of multiple factors including peri-infarct spreading depressions and adverse neurochemical events³¹³.

Consistent with animal data on penumbra decline, the probability of favourable clinical outcome declines rapidly with increasing onset-to-treatment in IV Thrombolysis^{261,314}, from onset-to-reperfusion time in endovascular reperfusion^{13,315}. “Collateral failure” and consequent penumbral loss as a function of duration of ischaemia is assumed to be a major explanatory factor for this time dependence³¹⁶.

Clinical imaging observations are, however, not uniformly consistent with this explanation. Several human studies show persistence of imaging features accepted as consistent with penumbra for much longer across modalities including PET^{113,115} MRI²¹⁵, MRI perfusion-diffusion mismatch^{244,317} almost periods of up to 48h. Penumbra with Xenon CT represented a constant proportion (one third) of hypoperfused territory while core volume was variable from individual to individual within 6 hours of MCA occlusion³¹⁸. In proximal arterial occlusion, good collaterals were associated with both favourable tissue and clinical outcomes, while time from onset was unrelated to either collateral grade or mismatch proportion²⁹⁷. In patients treated with endovascular therapy, the interaction of good collaterals and reperfusion, but not time from symptom onset to reperfusion, influenced penumbral tissue loss³¹⁹.

I investigated the relationship of penumbra volume, collateral status and their interaction with time within 6 hours of stroke onset. Our hypothesis was that penumbra would generally shrink in size with time, and good collateral score is associated with existence of larger penumbra at later time points.

4.2 Methods

4.2.1 Study Population

I selected data from subjects recruited at a single centre (Southern General Hospital, Glasgow) to one of three multimodal imaging studies during 2008-2013. Two studies were observational (one study investigating feasibility of complex imaging, the multicentre Acute Stroke Imaging Study (MASIS)³⁰⁴, one study investigating Pathophysiology of acute post-stroke hyperglycemias in relation to brain perfusion and arterial patency (POSH, unpublished),) and one was a trial phase II randomised trial comparing alteplase and tenecteplase in stroke thrombolysis (ATTEST)³⁰³. In the two observational studies, all ischemic stroke patients aged >18 years and presenting < 6 hours after onset were eligible. Exclusion criteria were contraindications to iodinated contrast (allergy or eGFR <30ml/min). Patients underwent NCCT, CT angiography (CTA) and CT perfusion at baseline (< 6hours) with follow-up CT and CTA (if occlusion was present on baseline imaging) approximately 24h later. Favourable outcome was defined as modified Rankin scale (mRS) 0-2 at final review (30 or 90 days, depending on individual study). Endovascular treatment was not used.

For this chapter, I selected subjects with a perfusion lesion and anterior territory arterial occlusion (ICA, M1, M2, or M3).

Using data from three studies in acute ischaemic stroke patients <6h after onset imaged with multimodal CT, I measured core and penumbra volumes, collateral status, and target mismatch (defined as core volume<50ml, perfusion lesion volume>15ml, mismatch ratio>1.8). Patients were grouped by onset to imaging time (<3, 3-4.5, 4.5-6h). I explored correlates of penumbra proportion by multivariable linear regression.

4.2.2 Imaging acquisition

All scans were performed on a Philips Brilliance 64 multi detector scanner. Whole brain NCCT was acquired first, (5 mm slice thickness FOV 218 x 218 mm, 120 kv, 171 mA or 0.9 mm slice thickness, FOV 250x250 mm, 120 kV, 404 mA) followed by CTP with 40 mm slab coverage from the basal ganglia (8x5 mm slices, FOV 25 cm, 80 kVp, 476 mA, 2 second cycle time, 30 cycles) using a 50 ml contrast bolus administered at 5 mls per second (350 Xenetix) via a large-gauge cannula. A CTA covering aortic arch to the top of the lateral ventricles (0.67 mm slice thickness, 120 kV, 475 mA) was acquired during the first arterial pass of contrast (Xenetix 350, 60 ml, followed by 30 ml of saline bolus, both given at 5 ml per second).

4.2.3 Imaging processing and analysis

Imaging studies were anonymised, and analysed independently by two research fellows (BC, XH) blinded to treatment allocation after the recruitment completion to minimise the odds of recognising scans with treatment allocation. CT perfusion was processed offline using MiStar (Apollo Medical Imaging Technology, Melbourne, Australia) commercial software. Deconvolution of tissue enhancement curves and arterial input function (AIF) selected from the anterior cerebral artery was performed using modified singular value decomposition (SVD) with compensation for the effects of arterial delay and dispersion. Delay time (DT) was determined by a delay corrected SVD deconvolution by applying a series of delay time (DT) values, with actual delay time being minimum DT value, which produces $T_{max}=0^{320}$. Cerebral Blood Flow (CBF) and Cerebral Blood Volume (CBV) were calculated from the peak height and area under tissue enhancement curves respectively, and Mean Transit Time (MTT) = CBV/CBF.

4.2.4 Penumbra definition

Ischaemic core was defined as tissue with reduced CBF (relative CBF <40% of contra lateral hemisphere) and prolonged delay time (relative DT >2 sec); penumbra volume was defined as tissue with relative DT >2 sec but relative CBF \geq 40% of contra lateral¹⁴⁸. I used Penumbra proportion ((penumbra volume/ total ischemic lesion volume) \times 100) throughout this paper.

4.2.5 Collateral scores

If retrograde flow was seen on CTP as detailed in chapter 2, collaterals were graded on CTA qualitatively²⁹⁷. I defined collaterals as good (angiographic flow distal to occlusion), moderate (angiographic flow to ischemic territory but not distal to occlusion), or poor (contrast opacification only in distal superficial branches). I used a modified Miteff's classification to incorporate terminal ICA, M1 and M2 occlusion, whereas the original classification excluded M2 occlusion²⁹⁷.

4.2.6 Target mismatch

Target mismatch was defined as a perfusion lesion >15 ml with core volume < 50 ml and mismatch between perfusion lesion and core >1.8 ³²¹. To account for the limited z axis (4cm) coverage of CTP, I reduced the 70ml threshold used by Endovascular Therapy for Ischemic stroke with perfusion-Imaging selection (EXTEND-IA)¹⁶ and MRI profile and response to endovascular reperfusion after stroke (DEFUSE-2)³²¹ trials proportionately, by dividing the mean of (Co-registered Infarct volume over 4cm/Total Infarct volume from whole brain NCCT) in the non-recanalised group. This figure was 0.715 (i.e. approximately 70% of total infarct is in the 4 cm slab covered by CTP). This was multiplied by 70ml, to yield an adjusted volume of 50ml to define target mismatch.

4.2.7 Statistical analysis

I compared the groups across 3 time epochs: <180 min, 180-270 min, and >270 min from stroke onset to CTP acquisition time. I used chi-square test or Fisher's test for categorical variables and Mann-Whitney tests for continuous variables. I conducted linear regression for the prediction of penumbra proportion. I used IBM SPSS Statistics 22 version for all the statistical analysis.

4.3 Results

From a total of 263 subjects, 180 had a visible perfusion lesion on perfusion imaging, 147 of whom had anterior territory occlusion (ICA=40, M1=60, M2= 39,

M3= 8); CTP was available in 144 subjects, who constituted the main analysis population. Collateral assessment was possible in 118 with retrograde flow on CTP-SI, who constituted the population analysed for relationship to collaterals (Fig.4-1). 28 patients with anterograde flow distally from occlusion were excluded from collateral grading as they would not represent true collateral circulation. In the main analysis group, the overall population had median age 74 years (IQR 63-81) and median NIHSS 15(10-20). On initial imaging, median ASPECT score was 7 (5-9), median core volume 23ml (IQR 11-48), and median penumbra volume 42 ml (IQR 25-65). Occlusion was present in the ICA (or tandem) in 39 (27%), MCA M1 segment in 59 (41%), M2 in 38 (26%), and M3 in 8 (5%). Baseline characteristics in the subgroup of 118 with assessable collateral status did not differ from the overall study population.

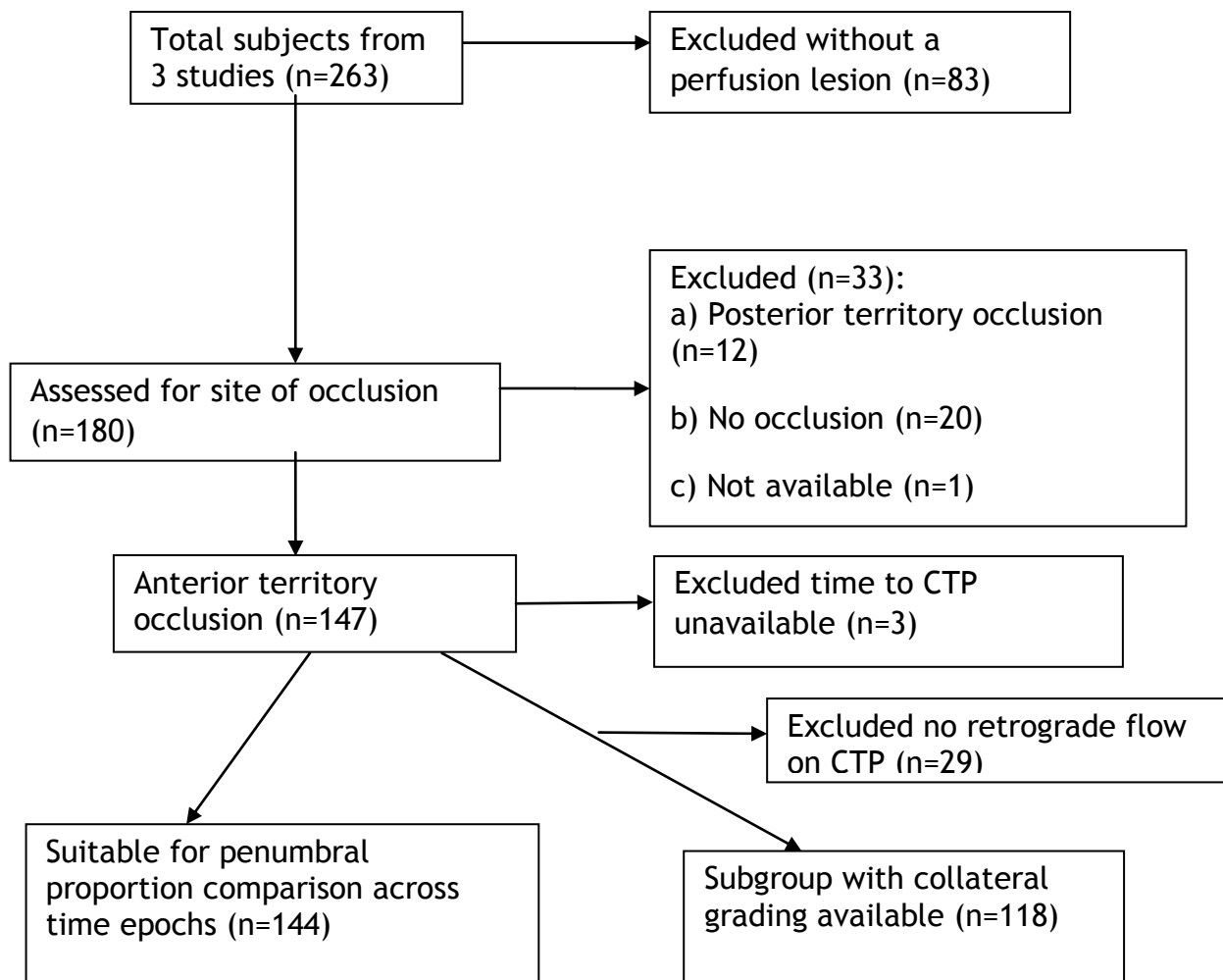


Figure 4-1 Study population CONSORT diagram

Baseline clinical and imaging characteristics across time epochs (<3, 3-4.5, >4.5 h) are detailed in Table 4-1. There were no significant differences in baseline characteristics. Across time epochs, neither proportions of penumbra (59%, 64%, 75% at <3, 3-4.5, >4.5h respectively, $p=0.4$; Figure 4-2), penumbra volumes (41(22-58), 46 (32-69), 40 (26-76) at <3, 3-4.5, >4.5 h respectively, $p=0.3$; Figure 4-2) nor poor collaterals (15/56 (27%), 14/47 (30%), 4/15 (27%) at <3, 3-4.5, >4.5h, $p=0.9$; Figure 4-2) differed significantly.

Table 4-1 Baseline characteristics of study population (n=144)

	Time to CT Perfusion (in minutes)			
	0-180 min(n=71)	181-270 min(n=58)	>270min(n=15)	p value
Female (n, %)	28 (39.4%)	32 (55%)	5 (33%)	0.1
Right side ischemia (n, %)	32(46%)	32 (55%)	7 (47%)	0.55
Age, years (median, IQR)	72(62-79)	76(70-81)	71(61-80)	0.053
NIHSS (median, IQR)	16(9-21)	14(10-19)	14.5(6.75-19)	0.34
ASPECT score (median, IQR)	7(5-9)	7(5-9)	6(5-7)	0.6
ASPECT score 0-4	11(15%)	11(19%)	1(7%)	0.1
ASPECT score 5-7	35(48%)	20(35%)	11(73%)	
ASPECT score 8-10	26(36%)	27(47%)	3(20%)	
Glucose (mmol/l)(median, IQR)	6.6(5.7-8.2)	6.8(5.6-8.2)	5.9(5.3-6.7)	0.3
Systolic Blood Pressure mmHg (median, IQR)	143(135-162)	149(137-171)	142(131-160)	0.5
Previous Stroke or TIA (n,%)	12/71(17%)	17/57(30%)	3/14(21.4%)	0.22
Atrial fibrillation (n, %)	29 (42%)	25 (47%)	3 (21%)	0.22

Diabetes	9 (13%)	6 (10%)	1(6.7%)	0.77
Hypertension (n, %)	43 (61%)	34 (58.6%)	8 (53%)	0.8
Hyperlipidemia (n, %)	36 (51%)	29 (50%)	9 (60%)	0.77
Site of vessel occlusion				
ICA/tandem occlusion (n, %)	19 (27%)	16 (27.6%)	4 (26/7%)	0.9
M1 (n, %) *	26 (36.6%)	26 (45%)	7 (47%)	
M2 (n, %) *	21 (29.6%)	14 (24%)	3 (20%)	
M3 (n, %)*	5 (7%)	2 (4%)	1 (6.7%)	
Core volume(ml)(Median, IQR)	26 (11.5-49.5)	23 (14-48)	15 (11-38)	0.7
Penumbra volume(ml)(Median, IQR)	41 (22.5-58)	46 (32-69)	40 (26-76)	0.3
Core proportion (%) †	41 (21-58)	36 (22-50)	25 (17-61)	0.4
Penumbra proportion (%)†	59 (41-79)	64 (50-78)	75 (39-82)	0.4
penumbra/core ratio (Median, IQR)	1.45(0.6-3.6)	1.8(1-3.6)	3(0.6-4.7)	0.3
Target mismatch (n, %)	39/70 (56%)	43/58 (74%)	10/15 (67%)	0.09
Good collaterals (n, %)	22/56 (39%)	17/47 (36%)	7/15 (47%)	0.9
Moderate collaterals (n, %)	19/56 (34%)	16/47 (34%)	4/15 (27%)	
Poor collaterals (n, %)	15/56 (27%)	14/47 (30%)	4/15 (27%)	

NIHSS: National Institute of Health Stroke Scale; ASPECTS: Alberta Stroke Program Early CT score; TIA: Transient Ischemic Attack; ICA: Internal Carotid artery; * Middle Cerebral Artery M1, M2, M3 segments; † proportion of core, penumbra in total perfusion volume.

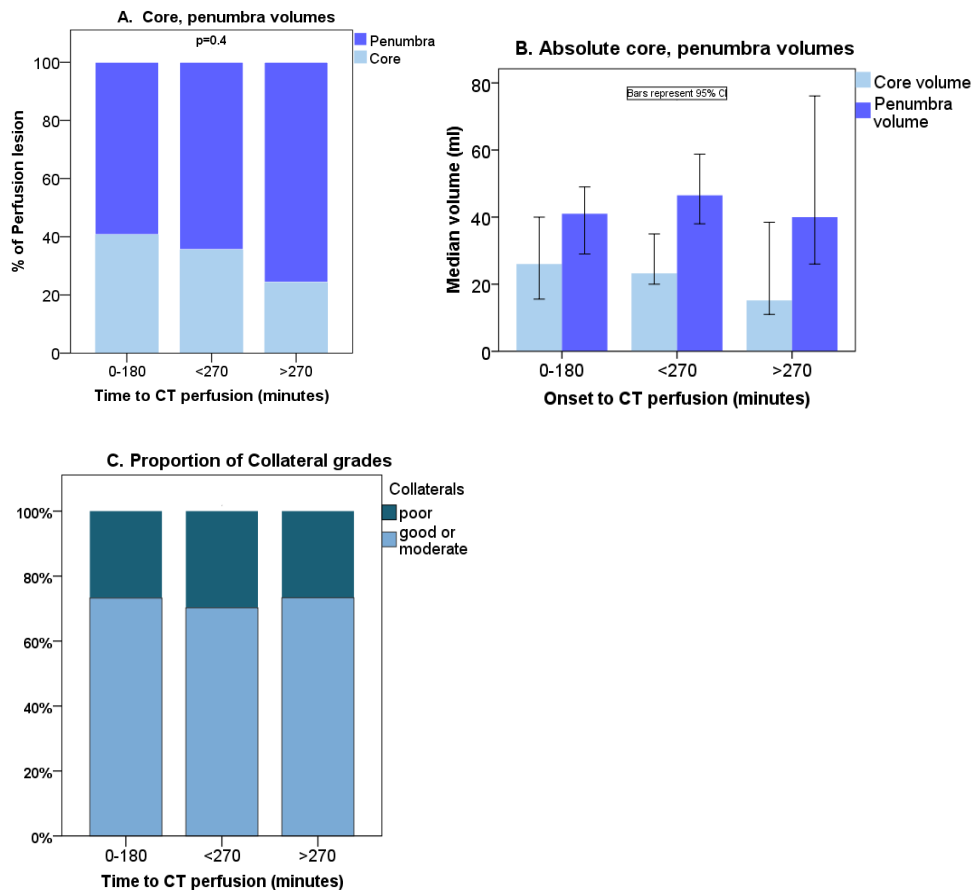


Figure 4-2 Core, penumbra volumes in relation to collaterals and time

Core, penumbra proportions and volumes (Panels A, B) and collateral proportion (Panel C) across time epochs.

Median penumbra proportion was 45% with poor collaterals versus 72% with good or moderate collaterals ($P < 0.001$); penumbra proportion was not clearly related to time to imaging ($R^2 = 0.003$, $p = 0.5$; Figure 3) but a trend for divergent effects by collateral status was seen (slight increase in penumbra over time with good or moderate collaterals versus reduced with poor, $R^2 = 0.03$ for both; $p = 0.08$; Figure 4-3).

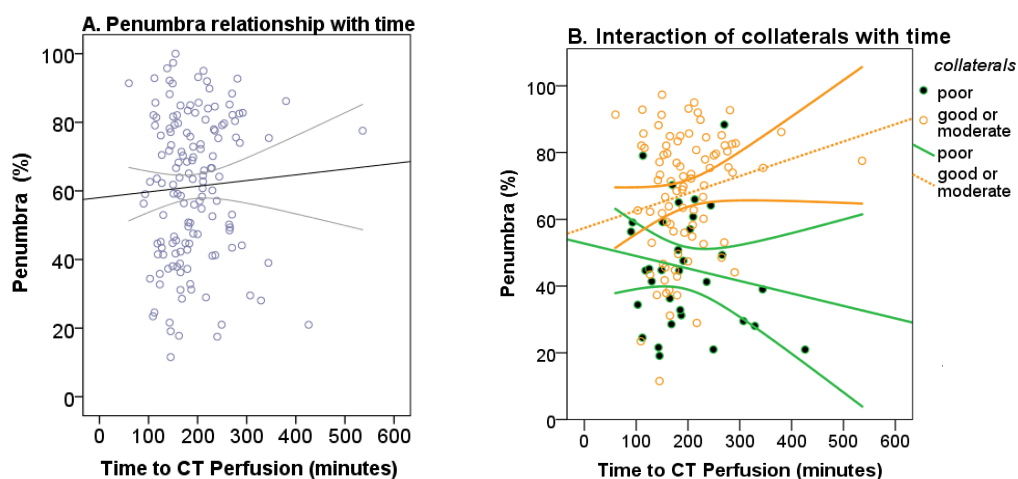


Figure 4-3 Penumbra volume in relation with collaterals and time

Penumbra relationship with time (Panel A), and, with interaction of collaterals and time (Panel B).

In univariate linear regression, potentially significant variables predicting proportion of penumbra ($p < 0.1$) were: large artery (ICA or M1) occlusion, good or moderate collaterals, time*good or moderate v poor collaterals, diabetes and NIHSS. Age, time to CTP, systolic blood pressure and blood glucose were not significant predictors of Penumbra proportion (Table 4-2).

Table 4-2 Univariate linear regression for predictors of penumbra proportion

variable	B coefficient (95% CI)	P value
ICA or M1 occlusion	-7(-14-0.4)	0.06
Time to CTP	0.2(-0.3-0.07)	0.5
(Good or moderate) versus poor collaterals	22(14-29)	<0.01
Time* ((good or moderate) v poor collaterals)	0.089 (-0.012-(0.2)	0.08
Diabetes	-11.37(-22-(-0.3)	0.043
NIHSS	-1.5(-1.9-(-1.05)	<0.01
Age	0.034(-0.28-0.34)	0.8
Blood glucose	-0.75(-0.18-0.37)	0.18
Systolic blood pressure	-0.089(-0.25-0.07)	0.2

In multivariable regression, NIHSS, good or moderate collaterals versus poor collaterals remained independently significant predictors of penumbra proportion (Table 4-3).

Table 4-3 Multivariate regression for predictors of penumbra proportion

Variable	B Coefficient (95% CI)	P value
NIHSS	-1.19-1.6-(-0.5)	<0.01
Good or moderate versus poor collaterals	16(8.7-24)	<0.001

I analysed a sub-group of ICA and M1 occlusion patients (n=100) to explore whether the lack of variability in penumbra proportion also holds true in a more homogeneous group. Penumbra proportion was not clearly related to time to imaging ($R^2=0.009$; $p=0.3$, fig. 4-4), but a trend for divergent effects by collateral status was again seen (slight increase in penumbra over time with good collaterals versus reduced with moderate or poor, $R^2=0.04$ for both; $p=0.09$, fig. 4-5).

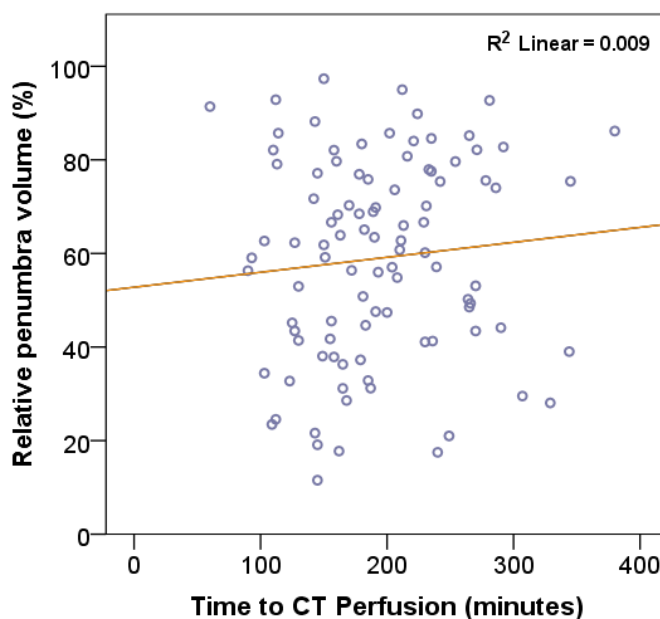


Figure 4-4 Penumbra in relation with time in proximal occlusion (ICA or M1) group

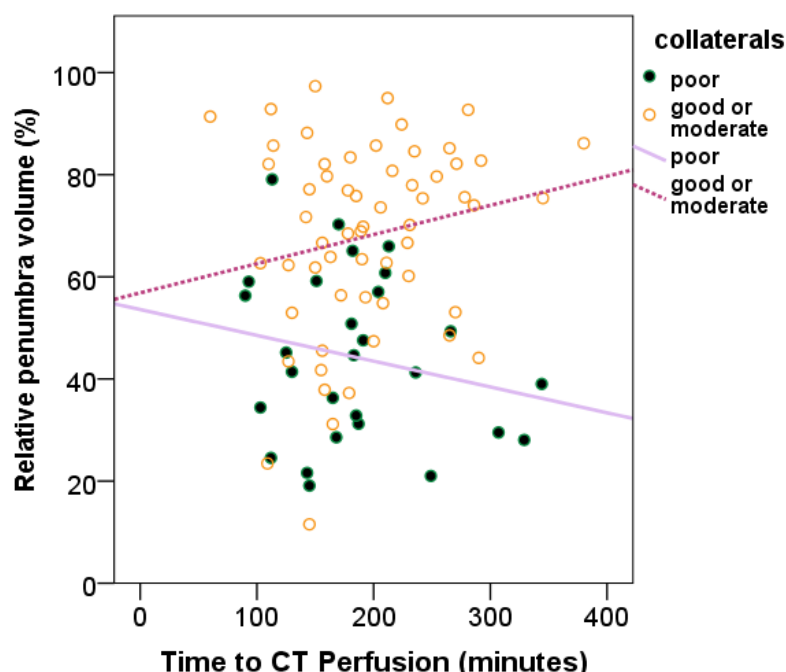


Figure 4-5 Collaterals and time relation with penumbra in proximal (ICA or M1) occlusion

4.4 Discussion

Our findings are consistent with previous reports showing persistence of an imaging-defined penumbra in humans, without apparent loss of volume that would explain the time-dependence of therapeutic benefit from reperfusion within the first 6h after stroke onset³¹⁸. This was the case regardless of whether penumbra was assessed by absolute volume, volume relative to core, the proportion of patients with “target mismatch”, or the presence of favourable collateral flow patterns. The sustained presence of penumbra on imaging in human studies contradicts the understanding from animal studies of the penumbra as a dynamic and time-dependent phenomenon, and the observed short effective time window for clinical benefit from reperfusion in unselected populations^{26,261,315}.

While penumbral imaging may enhance trial efficiency by identifying an optimised “responder” population³²², imaging-selection based trials target only a small proportion of patients (for example only 15% of intravenously thrombolysed patients were randomised in recent CT perfusion-based selection

for a randomised trial of endovascular bridging therapy¹⁶) and generalisation to draw conclusions regarding penumbral behaviour is not possible. The utility of reperfusion based on imaging-defined characteristics rather than time has notably not been demonstrated in several randomised, controlled trials of intravenous thrombolysis up to 9h after onset of stroke^{249,269,323}, in distinction to both observational studies of imaging-selected patients³²¹ and in recent trials of endovascular reperfusion^{270,271}. Whether this failure relates to difficulties in implementing complex imaging analysis in multiple centres, an intrinsic difference between thrombolysis and mechanical thrombectomy, or is simply an artefact of patient selection, is unknown.

Our main observation of interest was a potential divergent effect of penumbral proportion over time according to collateral status, with lower proportions of penumbra in later times being seen only among those with poor collateral flow. This observation challenges the concept of “collateral failure” as a general mechanism driving the loss of penumbral tissue over time, and instead suggests that the collateral status at initial presentation may define a group with a different natural history and much shorter time to intervene. These observations are consistent with previous studies. Bang and colleagues studied the interaction of collaterals and perfusion-diffusion mismatch (perfusion lesion defined as $T_{max} \geq 4$ s) and found that neither collateral grading, nor mismatch lesion volumes correlated with time³²⁴. Poor collaterals were independently correlated with larger infarct growth. Jung and colleagues, in 44 subjects with M1 or M2 occlusion undergoing endovascular therapy within 6 hours and resulting in at least partial reperfusion, showed that elapsed time accounted for only a minor proportion of penumbra tissue (defined as $T_{max} \geq 6$ s) loss in good collateral grades but a larger proportion in poor collateral grades³¹⁹.

These observations imply that perfusion imaging within the first 6 hours after onset is unnecessary if collateral flow is moderate or good - the proportion of penumbra is unlikely to vary significantly among these patients: among those with poor collaterals, however, additional tissue imaging to define whether target mismatch (or similar tissue definitions) are present may be necessary prior to reperfusion therapies.

A wide variety of methods for collateral assessment have been proposed,³²⁵ and only limited study of the consistency of these competing approaches has been undertaken. The approach used here, modified from that of Miteff,²⁹⁷ requires time-resolved vessel imaging, and may be closer to the multiphase CTA approach developed by Goyal and colleagues and deployed in the majority of patients recruited to the ESCAPE trial²⁷¹. Whether single-phase CTA would yield equivalent findings in clinical use is unclear, and in addition, all of these collateral assessment methods are confined to occlusions of the terminal ICA or proximal MCA. Validation using other methods of collateral assessment and in other vascular territories will be important.

Our conclusions are limited by the limited number of subjects, particularly after 4.5 hours from symptom onset, and the limited range of onset-to-imaging times that were covered in our dataset. To our knowledge, this is the first CT perfusion study assessing the association of penumbra volume with time and our patient cohort is larger than MRI based studies reported previously³¹⁹. We used validated thresholds^{320,326} for core and penumbra, but thresholds for CT perfusion are not uniform, and their derivation is based on limited numbers¹⁴⁷. In common with the majority of imaging studies, we have to infer the persistence of a presumed time-dependent imaging appearance from cross-sectional data rather than sequential imaging in each patient. Repeated imaging studies in the acute stroke population are logistically extremely difficult since patient care may be compromised, and in addition, radiation and contrast exposure limit the repeatability of CTP. Our CT scanner had restricted brain parenchyma coverage of 4 cm, requiring us to modify the definitions of “target mismatch” based on whole brain volumes in large detector CTP¹⁶ or MRI studies for this more restricted brain coverage, but the 50ml core volume criterion, while obtained by the ratio of 4cm coverage volume to whole brain volume, has not been validated independently.

In conclusion, we found no decrease in the proportion of CTP-defined penumbral perfusion within perfusion lesions, or the proportion of patients with target mismatch or favourable collateral patterns within the first 6 hours after stroke onset. A decline in proportion of penumbra with time was restricted to those

with poor collateral status. Given the strong effect of time on outcomes after reperfusion treatment, further investigations into the interaction between collaterals, penumbra and time is required

4.5 Conclusions

In a cross-sectional sample imaged within 6h, neither the proportions of penumbral tissue nor “target mismatch” varied by time from onset. A trend for reducing penumbra proportion only among those with poor collaterals may have pathophysiological and therapeutic importance.

Chapter 5 **Interaction of Recanalisation, Intracerebral Haemorrhage and Cerebral Oedema after Intravenous thrombolysis**

5.1 **Introduction**

Intravenous (IV) thrombolysis <4.5h after symptom onset significantly improves functional outcome, but carries increased risk of intra cerebral haemorrhage (ICH)^{10,120}. Reperfusion is proposed to be necessary both for ICH³²⁷ and vasogenic brain oedema⁴², the other major cause of early neurological deterioration after stroke.

Both the third International Stroke Trial (IST-3)³²⁸, and pooled analysis of IV alteplase trials²⁶¹, indicated slight excess of fatal symptomatic ICH (SICH) within 7 days of treatment (2.7% in IST-3). IST-3³²⁸ also reported a small excess risk of fatal brain swelling (1.5%) within 7 days, and the Alteplase Summary of Medicinal Product Characteristics(<https://www.medicines.org.uk/emc/medicine/308> section 4.4) states that “reperfusion of the ischemic area may induce cerebral oedema in the infarcted zone.” Vasogenic edema was associated with increased blood-brain barrier permeability after reperfusion in a rodent model^{329,330}, but complex interactions of severity and duration of ischemia, and timing of reperfusion confound this possible relationship³³¹. Space-occupying cerebral oedema is clinically associated with large artery occlusions that recanalise rarely with IV rtPA³³², and no excess risk of brain oedema was reported in previous trials^{10,262}.

Different types of haemorrhage may have different mechanisms and clinical implications: hemorrhagic infarction type 1 &2 (HI1 or HI2²⁶²) may be an epiphenomenon of reperfusion with no adverse clinical implications, while, in contrast, parenchymal hematomas type 1 &2 with independent mass effect (PH1 or PH2²⁶²) are linked with clinical worsening and may be related to blood-brain barrier breakdown after reperfusion³³³.

Imaging features may interact with treatment. The Diffusion and perfusion Imaging evaluation for understanding stroke evolution (DEFUSE)¹⁵ study and combined analysis of DEFUSE and the Echoplanar Imaging Thrombolysis Evaluation Trial (EPITHET) studies³³⁴ found increased risk of PH1 or PH2 ICH when reperfusion occurred in patients with “large core” (large volumes of severely hypoperfused tissue on MRI). Interaction of early reperfusion with other indices of severe ischemia (large DWI volumes³³⁵, very low cerebral blood volume (CBV) on perfusion imaging³³⁶ or poor collaterals⁶⁰) has been reported to be associated with SICH after IV thrombolysis. The extent of vasogenic oedema may also interact with ischemic core volume (>50% hypodensity on CT was associated clinically with malignant brain oedema³³⁷), and in an animal model reperfusion of large volumes of severely ischemic tissue (CBF <40%) led to malignant oedema²⁰⁶.

Previous studies have not investigated the relationship of imaging characteristics (e.g. ischemic core volume), reperfusion, and their interaction with brain oedema and ICH after IV thrombolysis. We hypothesised that recanalisation in presence of a large core (large ischemic area) would be associated with significant haemorrhage, and persistent occlusion is associated with significant brain oedema.

5.2 Methods

5.2.1 Study population

I collected data from subjects treated with IV rtPA <4.5 hours after onset recruited at a single centre to one of three multimodal imaging studies during 2008-2013. Two studies were observational (one study investigating feasibility of complex imaging, the multicentre Acute Stroke Imaging Study (MASIS)³⁰⁴, one study investigating Pathophysiology of acute post-stroke hyperglycemias in relation to brain perfusion and arterial patency (POSH, unpublished),) and one was a trial phase II randomised trial comparing alteplase and tenecteplase in

stroke thrombolysis (ATTEST)³⁰³. In the two observational studies, all ischemic stroke patients aged >18 years and presenting < 6 hours after onset were eligible. Exclusion criteria were contraindications to iodinated contrast (allergy or eGFR <30ml/min). Patients underwent CT, CT angiography (CTA) and CT perfusion at baseline with follow-up CT and CTA (if occlusion was present on baseline imaging) approximately 24h later. Favourable outcome was defined as modified Rankin scale (mRS) 0-2 at final review (30 or 90 days, depending on individual study). Endovascular treatment was not used.

5.2.2 Image acquisition

Scans were acquired on a Philips Brilliance 64 multi detector scanner. Whole brain NCCT (5 mm slice thickness FOV 218 x 218 mm, 120 kv, 171 mA or 0.9 mm slice thickness, FOV 250x250 mm, 120 kV, 404 mA) was followed by CTP with 40 mm slab coverage from the basal ganglia (8x5 mm slices, FOV 25 cm, 80 kVp, 476 mA, 2 second cycle time, 30 cycles) using a 50 ml contrast bolus administered at 5 mls per second (350 Xenetix) via a large-gauge cannula. CTA covering aortic arch to the top of the lateral ventricles (0.67 mm slice thickness, 120 kV, 475 mA) was acquired during the first arterial passage of contrast (Xenetix 350, 60 mls, followed by 30 mls of saline bolus, both given at 5 ml per second)

5.2.3 Image analysis

Anonymised imaging studies were analysed independently by two researchers (BC, XH). CTP was processed offline using MiStar (Apollo Medical Imaging Technology, Melbourne, Australia). Deconvolution of tissue enhancement curves and arterial input function (AIF) selected from the anterior cerebral artery was performed using modified singular value decomposition (SVD) with compensation for the effects of arterial delay and dispersion. Delay time (DT) was determined by a delay-corrected SVD deconvolution by applying a series of delay time (DT) values, with actual delay time being minimum DT value, which produces $T_{max=0}$ ³²⁰. DT and T_{max} are related but are not identical, and since DT is derived from a vascular transport model correcting for arterial delay and dispersion, thresholds are smaller than T_{max} ³⁰⁵. DT has demonstrated superior correlation with tissue at risk in recent studies³²⁶. Cerebral Blood Flow (CBF) and

Cerebral Blood Volume (CBV) were calculated from the peak height and area under tissue enhancement curves respectively, and Mean Transit Time (MTT) = CBV/CBF.

5.2.4 Core, penumbra definition

Ischemic core was defined as tissue with relative CBF <40% of contra lesional hemisphere and relative DT >2 sec; penumbra was defined as tissue with relative DT >2 sec but relative CBF \geq 40% of contra lateral brain¹⁴⁸. To account for limited z axis coverage of CTP, I reduced the 70ml threshold for large core used by EXTEND-IA¹⁴⁸ and DEFUSE-2³²¹ proportionately, by dividing the mean of (Co registered Infarct volume over 4cm/Total Infarct volume from whole brain NCCT) in the non-recanalised group: approximately 70% of the total infarct was covered by the CTP slab, therefore we considered large core to be >50ml. I evaluated baseline NCCT for ASPECT scores¹²⁷.

5.2.5 Collateral grading

Collaterals on baseline CTA were graded if retrograde flow was seen on CTP source images (CTP-SI),²⁹⁷ and defined as good (vessels reconstitute distal to the occlusion), moderate (vessels seen partially in ischemic territory), or poor (contrast opacification seen only in distal superficial branches). I modified Miteff's classification to incorporate M2 occlusion (the original classification excluded M2 occlusion)²⁹⁷.

5.2.6 Haemorrhage, oedema classification

On 24h NCCT, I classified ICH as per ECASS 2 criteria,²⁶² and SICH as any ICH with increase in NIHSS \geq 4 points²⁶². Any PH1 or PH2 were considered significant haemorrhage. Brain oedema was classified as per IST-3³¹⁰ as no swelling (0), effacement of lateral ventricle (1), effacement of lateral plus 3rd ventricles (2), or midline shift (3): we defined grades 2-3 as Significant Brain Oedema (SBE). Recanalisation was defined as Thrombolysis in Myocardial Infarction (TIMI) grading 2- 3 at 24 hour CTA^{306 307}.

As an exploratory analysis, early major neurological improvement (NIHSS 0 or 1, or improvement by \geq 8 points by 24h) was taken as a biomarker of early

reperfusion³³⁸, and outcomes were compared among three groups - i) no recanalisation ii) recanalisation but no early improvement (presumed late recanalisation) and iii) recanalisation and early improvement (presumed early recanalisation). Early neurological improvement independent of recanalisation status can predict 3m outcome³³⁹. Although recanalisation can be diagnosed with using early neurological improvement, there are a number of patients who have no recanalisation but ENI. This was proposed likely to be due to other biological factors such as collateral supply³⁴⁰.

I compared groups by recanalisation and ischemic core volume, using chi-squared tests or Fisher's exact tests for categorical variables, and Mann-Whitney tests for continuous variables. I evaluated the independent effect sizes of recanalisation, core volume and their interaction on imaging and clinical outcomes using logistic regression. I used IBM SPSS Statistics (version 22) for the statistical analysis.

5.3 Results

Of 263 subjects, 159 had anterior circulation stroke with vessel occlusion pre-treatment; we excluded 24 subjects presenting >4.5h after onset, and 12 in whom 24h CTA was not evaluable, leaving 123 subjects. Collateral grading was available in a subset of 106 subjects.

Median age was 74 years (IQR 62-80), median NIHSS 15 [IQR 9-20], and median symptom onset to treatment time 180min (IQR 151-210). Occlusion site was ICA or M1 in 84 (68%). Recanalisation on 24h CTA was seen in 80 (66%) (Tandem or proximal ICA 30%, M1 74%, M2 87% and M3 50% (Table 5-1)). Mean time interval from treatment to follow up imaging was 27.5 hrs (SD ±7). Detailed baseline characteristics are presented in Table.5-2. Tenecteplase was used in 31 patients and alteplase in 92.

Table 5-1 Recanalisation rates grouped by occlusion site in comparison with Interventional Management of Stroke (IMS-3) study

	Our study- Recanalisation (TIMI 2 or 3)*	IMS-3 rtPA treated group ³⁴¹

Tandem/ICA (n=30)	9/30 (30%)	56% proximal ICA 28% Tandem ICA
M1(n=54)	40/54 (74%)	80% -86%
M2(31)	27/31 (87%)	78%
M3(8)	4/8 (50%)	100% (M3 & M4)
*cumulative p value <0.01 IMS 3 Interventional Management of Stroke		

Table 5-2 Baseline characteristics of study population (n=123)

Variables	Recanalised (n=80)	Occluded (n=43)	P*
Age (median (IQR), years)	73 (63-81)	74 (62-79)	0.8
Male (n, %)	48 (60%)	21 (48.8%)	0.1
NIHSS baseline (median, IQR)	15(9-19)	14(9-20)	0.6
Onset to treatment time (median , IQR, min)	175(145-210)	190(165-206)	0.6
ASPECT score (median, IQR)	7(5-9)	7(5-9)	0.9
Occlusion Site:			<0.01
ICA/tandem (n, %) †	9 (11.3%)	21 (48.8%)	
M1 (n, %) †	40 (50%)	14 (32.6%)	
M2 (n, %) †	27 (33.8%)	4 (9.3%)	
M3 (n, %) †	4 (5%)	4 (9.3%)	
Cardio-embolic (n, %) ‡	34(47.9%)	16 (39%)	0.7
TACI (n, %) §	54 (67.5%)	30 (69.8%)	0.7
Atrial Fibrillation (n, %)	35 (47.9%)	14 (33.3%)	0.17

Diabetes (n, %)	8 (10%)	5 (11.6%)	0.7			
History of Stroke or Transient Ischemic attack (n, %)	14 (18%)	7 (16.3%)	1.0			
Hypertension (n, %)	45 (56.3%)	26 (62%)	0.5			
Smoker (n, %)	23 (28.8%)	14 (32.6%)	0.3			
On anti platelets (n, %)	42 (52.5%)	24 (55.8%)	0.8			
Imaging outcomes in relation to recanalisation within small or large core groups (n=122)¶						
	Core small(<50ml) (n=95)	Core large(>50ml) (n=27)	p			
ICA or M1 occlusion †	57(69%)	26(96%)	<0.001			
Poor (vs. good or moderate) collaterals	9/78(11.5%)	12/22(54.5%)	<0.01			
Poor outcome (mRS 3-6 at 30 or 90 days)	51(54%)	24(89%)	0.001			
	Recanal	Occluded	P	Recanalise	Occlud	P value

	ised (n=63)	(n=32)	value	d (n=16)	ed(n=1 1)	
Any ICH (n, %)	19 (30%)	4 (12%)	0.06	8 (50%)	4 (36%)	0.5
HI1 or HI2 (vs. no ICH, PH1, PH2)	14 (22%)	3 (9.4%)	0.16	7 (44%)	3 (27%)	0.4
Type of haemorr hage#						0.25
No ICH (n, %) #	44 (70%)	28 (87%)	0.35	8 (50%)	7 (63.6%)	
HI1 (n, %) #	5 (8%)	2 (6%)		3 (19%)	3 (27%)	
HI2 (n, %) #	9 (14%)	1 (3%)		4 (25%)	0 (0%)	
PH1 (n, %) #	1 (1.6%)	0 (0%)		0 (0%)	1 (9%)	

PH2 (n, %)	4 (6%)	1 (3%)		1 (6%)	0 (0%)	
Any oedema (n, %)	19 (31%)	15 (47%)	0.13	12 (75%)	8 (73%)	0.9
Oedema type**						0.38
No oedema (n, %)**	44 (70%)	17 (53%)	0.17	4 (25%)	3 (27%)	
Effacement of lateral ventricle (n, %)**	16 (25%)	13 (40%)		3 (19%)	4 (36%)	

Effacement of lateral and 3 rd ventricle (n, %)**	2 (3%)	0 (0%)		6 (37.5%)	1 (9%)	
Midline shift (n, %)**	1 (1.6%)	2 (6.3%)		3 (19%)	3 (27%)	
SICH (n, %) #	4 (6%)	1 (3%)	0.5	0	2 (18%)	0.07
Significant ICH (n, %)	5 (8%)	1 (3%)	0.36	1 (6%)	1 (9%)	0.8
SBE (n, %) ††	3 (5%)	2 (6%)	0.7	9 (56%)	4 (36%)	0.3
Poor outcome (mRS>2) (n, %)	20 (47%)	22 (69%)	0.04	13 (81%)	11 (100%)	0.13

* Chi-square test or Fisher test for categorical variables, Mann-whitney test for continuous variables

ASPECT score: Alberta stroke Early CT Score

† ICA-Internal Carotid artery, M1,M2,M3- branches of Middle cerebral artery

‡ Cardio embolic versus other aetiologies (large artery atherosclerosis, lacunar stroke, unknown cause)

§ Total anterior circulation Infarction(TACI) versus other stroke types

|| one subject out of total study population (n=123) did not have core size available

#Haemorrhage classification according to ECASS-2 criteria

** Brain oedema classification by IST-3 criteria

††SBE: Significant Brain Oedema

Most haemorrhages were HI1 or HI2 (28 (23%)) and there were few PH1 or PH2 (8 (6%)). There was a trend for recanalisation to be associated with any ICH (28 (35%) v 8 (18%); $p=0.06$), predominantly HI1/HI2 (22 (27.5%) v 6 (14%); $p=0.08$), while incidence of PH1/PH2 did not differ (6 (7.6%) v 2 (4.6%); $p=0.5$. Fig.5-1). Oedema of any grade was less frequent with 24h recanalisation, although not significantly (32 (40%) v 23 (53%); $p=0.15$) and significant brain oedema was not related to recanalisation (12 (15%) v 6 (12%); $p=0.8$. Fig.5-2).

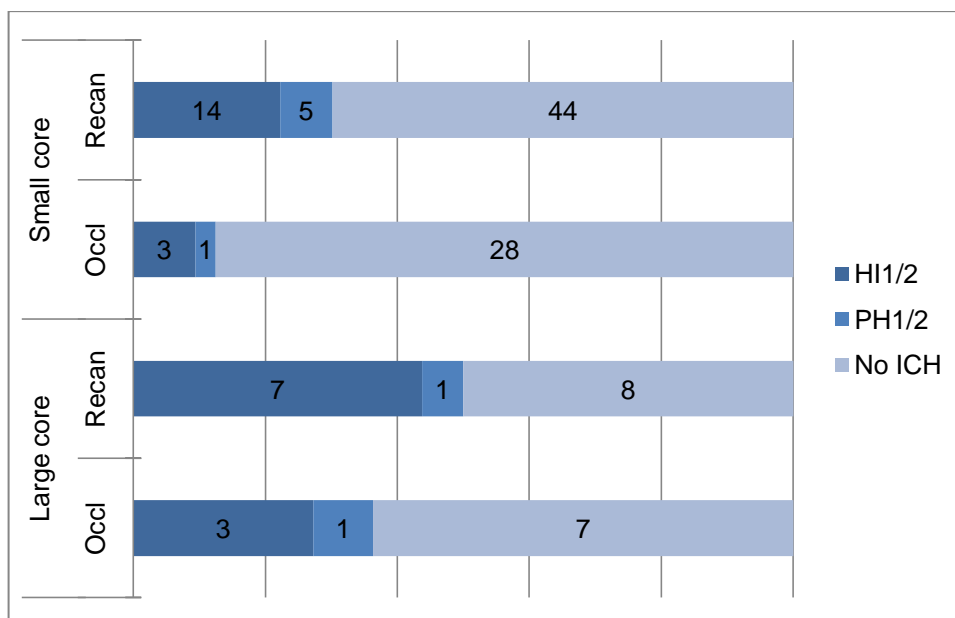


Figure 5-1 Types of haemorrhage in occluded vs. recanalised small or large core groups
 (HI1/2: Haemorrhagic Infarction type 1 or 2; PH1/2: Parenchymal haematoma type 1 or 2; No ICH: No Intra cerebral haemorrhage; Recan: Recanalised; Occl: Occluded)

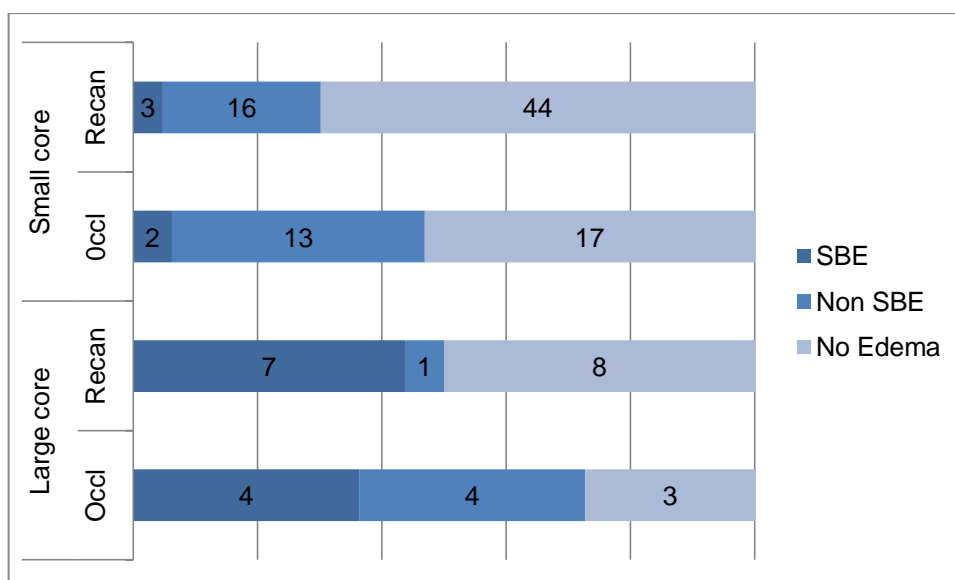


Figure 5-2 Types of oedema in occluded vs. recanalised small or large core groups
 (SBE: Significant Brain Oedema; Non-SBE: Non significant Brain Oedema; Recan: Recanalised; Occl: Occluded)

Neither significant oedema (12/92 alteplase-treated versus 6/31 tenecteplase-treated, OR 0.6, 95% CI 0.2-1.8; $p=0.4$), nor significant haemorrhage (8/92 alteplase-treated versus 0/31 tenecteplase-treated, $p=0.2$; odds ratio not calculable) was associated with thrombolytic agent.

After adjusting for 24h recanalisation, large core (>50ml) was associated with both haemorrhage and oedema, most notably with SBE, although no significant relationship with PH1/PH2 ICH or SICH was evident. Recanalisation was also associated with a trend towards any ICH, particularly HI1/2 ICH, but not to oedema (Table 5-3). Regression analysis did not identify significant interaction of large core and 24h recanalisation for any outcome (Table 5-3). Recanalisation was associated with significantly reduced odds of death or dependence (mRS 3-6) at day 30 or 90, while large core volume was associated with increased odds of these outcomes.

Table 5-3 Regression for association of large core and recanalisation, and their interaction for imaging and clinical outcomes

	Any ICH*	HI1 or HI2†	Significant ICH*	SICH‡	Any oedema	SBES	Good 90d mRS (0-2)
Large core (OR (95% CI); p)	4 (1.6-9.5); p=0.003	2.9 (1.13-7.8); p=0.03	1.2 (0.23-6.5); p=0.8	1.6 (0.3-8.5); p=0.6	5.4 (2-14); p<0.01	17.4 (5.3-57); p<0.01	0.15 (0.04-0.5); p=0.03
Recanalisation (OR (95% CI); p)	2.3 (0.97-5.5); p=0.06	2.5 (0.9-6.9); p=0.08	1.7 (0.33-8.8); p=0.5	0.8 (0.17-3.8); p=0.8	0.5 (0.27-1.18); p=0.13	1.45 (0.4-4.9); p=0.55	2.8 (1.2-6.8); p=0.02
Large core * Recanalisation	0.34 (0.05-	0.7 (0.09-6); p=0.8	0.25 (0.007-9);	p=1	1.7 (0.2-11);	3(0.2-34) p=0.37	p=0.99#

(OR (95%CI); p)	2.2); p=0.26		p=0.45		p=0.56		
<p>* ICH Intra cerebral haemorrhage, † Hemorrhagic infarction type 1 or 2, ‡ Symptomatic Intra cerebral haemorrhage, § Significant Brain Oedema, Since 0% of recanalised group in large core has SICH, the corresponding odds ratios cannot be calculated,# since 100% of occluded group in large core have poor 90dmRS, the corresponding odds ratios cannot be calculated.</p>							

Early neurological improvement occurred in 36 patients: 45 had recanalised by 24h but did not exhibit early major improvement, and 38 showed no recanalisation and no early improvement. Oedema and hemorrhagic outcomes were generally lower and day 90 mRS is better in the group with presumed early recanalisation, but did not differ significantly between the late recanalisers and those with no recanalisation (Table 5- 4). Different types haemorrhage and oedema in each of these groups is shown in bar chart (fig. 5-3 & 5-4). 90 day modified Rankin scales are shown on grotto bars comparing these groups in fig. 5-5.

Table 5-4 Comparison of early improvers vs. non-early improvers

	Early improvement (n=36)	No early improvement/Recanalised (n=45)	No early improvement/Non-recanalised (n=38)	P value §
Any ICH	5 (14%)	19 (42%)	9 (24%)	0.014
Significant ICH	1 (3%)	5 (11%)	2 (5%)	0.3
SICH*	0	3 (7%)	3 (8%)	0.25
Any oedema	7 (19%)	24 (53%)	21 (55%)	0.002
SBE	2 (5.6%)	10 (22%)	6 (16%)	0.11
Good 90d mRS	22 (63%)	12 (27%)	10 (26%)	0.001
ICH: Intra cerebral haemorrhage *SICH as per ECASS-2 criteria SBE: Significant brain oedema § chi-square values				

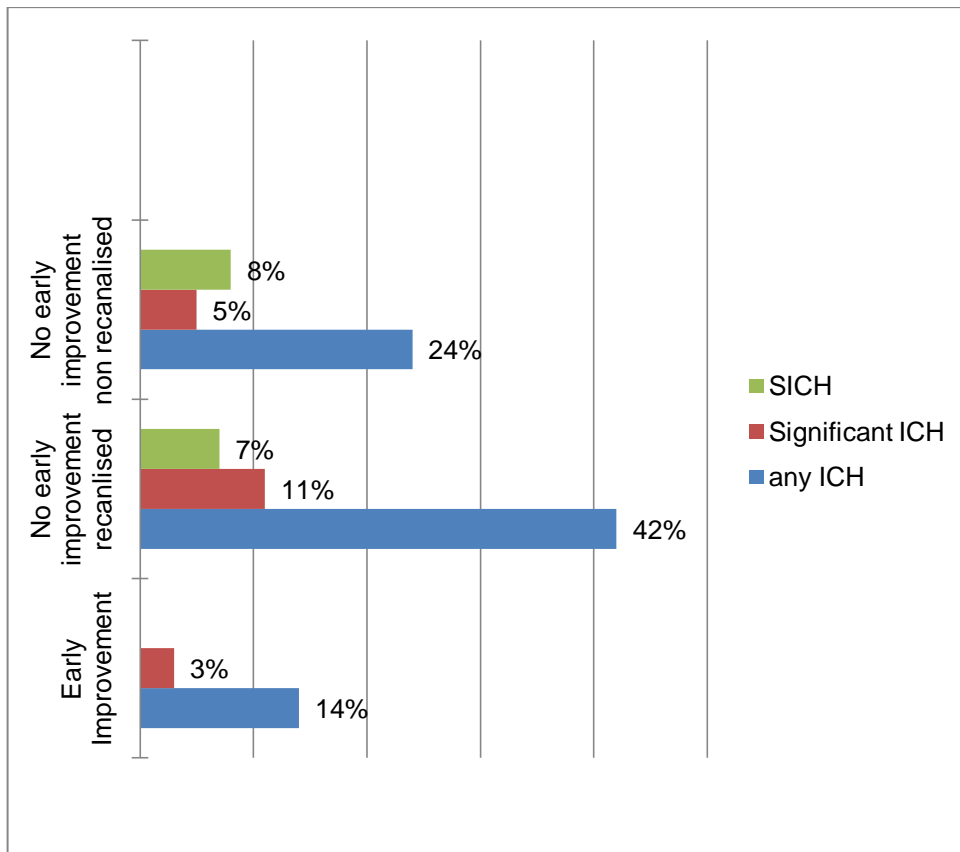


Figure 5-3 Type of haemorrhage in early improvers vs. non early improvers

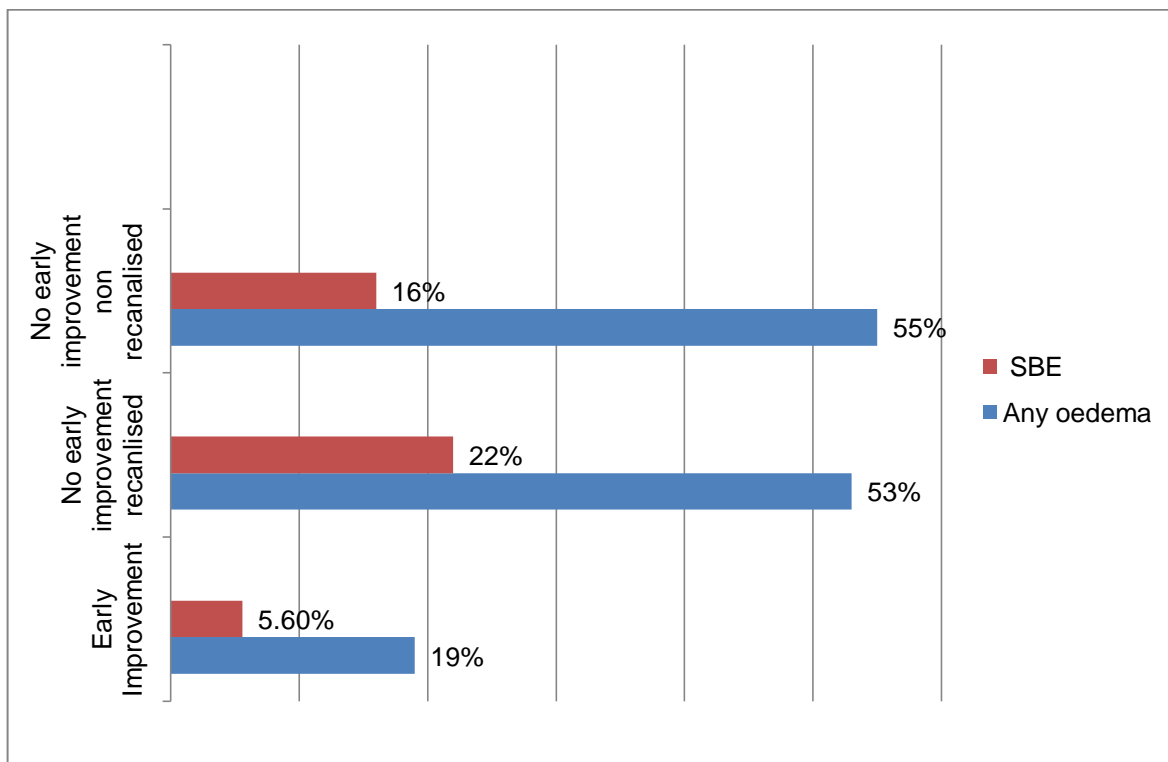


Figure 5-4 Types of oedema in early improvers vs. non early improvers

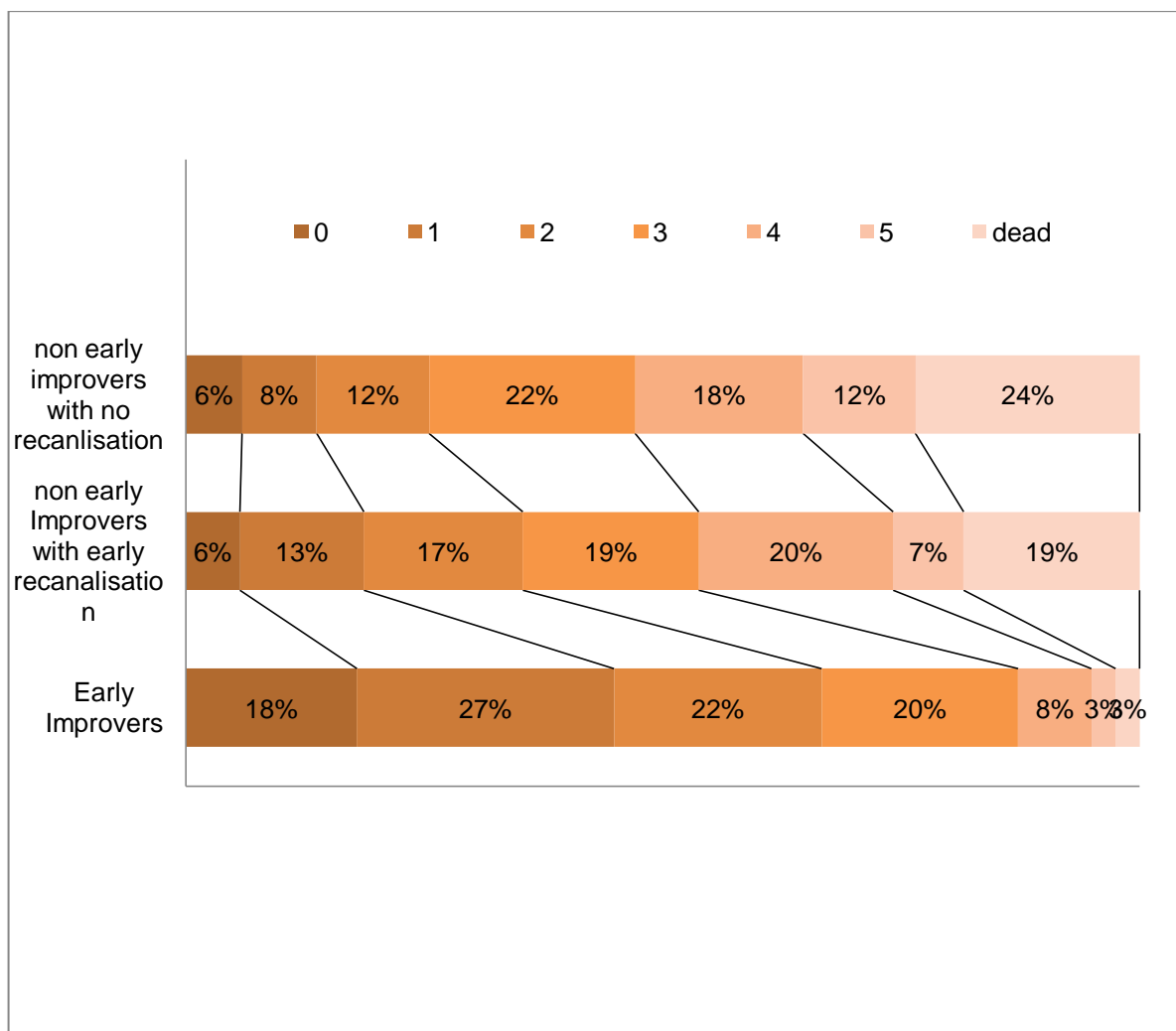


Figure 5-5 90 day modified Rankin scales in early improvers vs. non early improvers

5.4 Discussion

Recent focus on potential hazards of IV rtPA highlights limited data on the interaction of patient characteristics, especially ischaemic tissue volumes, reperfusion and the pathophysiology of haemorrhage and brain oedema. Few patients have been studied with detailed brain imaging³³⁴, only a proportion of whom have received thrombolytic therapy; animal models^{206,342} may not recapitulate the human situation, and other data derived from series of late endovascular intervention³⁴³.

Our cohort allowed the study of interactions between 24h recanalisation, perfusion characteristics and incidence of both ICH and early brain oedema. We found ICH incidence comparable to previous literature, for example ICH of all kinds seen in 34% (48% in ECASS-II²⁶²), and SICH in 5.7% (7.7% in a meta-analysis IV thrombolysis²⁶⁴). Incidence of early vasogenic brain oedema of any degree (45%) and SBE (6.8%) are comparable to reported figures for oedema³²⁹ and SBE (4% in IST-3)³²⁸ that used similar definitions, although other definitions yield variations in incidence³⁴⁴. Recanalisation rate (66%) in our study was identical to that reported in the IMS-3 rtPA treated group, as were recanalisation rates by occlusion site³⁴¹.

The major predictor of ICH and SBE in our study was the presence of a large “core”. This is consistent with a rodent study in which infarct volume, but not reperfusion, was associated with oedema³⁴⁵. Literature on reperfusion and post-ischemic oedema in non-human primates examined only early time points (< 6 hours) of unclear clinical relevance^{84,206,346}. Recanalisation in our study, in contrast, was associated only with a trend towards HI1/2 ICH. Neither recanalisation, large core nor their interaction was associated with clinically relevant PH1/2 ICH. DEFUSE¹⁵ reported potential interaction of large core and early reperfusion in provoking SICH, and defined the “malignant profile” based on MRI features similar to the CTP features in our study. Of 6 DEFUSE subjects with the “malignant profile,” 3 experienced (uniformly fatal) SICH. The combined EPITHET and DEFUSE studies³³⁴ included only 27 “malignant profile” patients, of whom 6/9 who reperfused developed PH1/2 ICH, compared to 2/18 without reperfusion. Despite similar patient numbers, we were unable to replicate this interaction. Since perfusion characteristics may better define ICH risk than diffusion-weighted MRI³⁴⁷, it seems unlikely that this is due to a difference between MRI and CT-based tissue viability assessment methods.

As an exploratory analysis, we assessed major early clinical improvement as a biomarker of early reperfusion. This group had significantly fewer ICH or oedema events and greater probability of favourable 90 day outcome. The incidence of significant ICH or oedema did not differ between those with presumed late recanalisation and those without recanalisation, but it is not possible to exclude a relationship between late recanalisation and adverse imaging outcomes.

Good clinical outcome was strongly associated with 24h recanalisation (OR 2.8 (1.2-6.8); $p=0.02$) and was less likely with large core (OR 0.15 (0.04-0.5); $p=0.03$), consistent with previous observations³⁴⁸, but there was no significant interaction between these variables in predicting good 90 day outcome. This is consistent with the known prognostic value of both variables^{348,349}, but also with the lack of interaction between endovascular treatment effect and CTP features.³⁵⁰

Our study has limitations. As a single centre, retrospective analysis, independent replication in other settings is desirable. The small number of clinically significant hemorrhagic and brain swelling outcomes inevitably lead to wide confidence intervals around the effect estimates, encompassing the possibility that recanalisation may be related to either significant oedema or ICH, and means that conclusions must be cautious: nonetheless, with a larger number of outcome events we were unable to replicate earlier reports of an association with ICH, as discussed above. No classification of brain oedema has been reported consistently in clinical studies, and different classification methods may yield different incidence. The timing of brain imaging for outcome assessment in our dataset (mean 27.5h after IV thrombolysis) is too early to detect maximal brain swelling, but while this might underestimate the severity of brain oedema, it seems unlikely to underestimate the incidence of significant brain oedema based on data that indicate that 95% of cases progressing to malignant MCA infarction were identifiable on 24h CT³⁴⁴. CTP analysis was based on validated thresholds, but standardisation is not yet agreed¹⁴⁷. Since we had access to angiographic outcome data only at approximately 24h, we could not discriminate early from late recanalisation, which may carry different risks of ICH,³⁵¹ although we undertook exploratory analyses using early clinical improvement as a biomarker for this. We used TIMI 2-3 (partial or complete recanalisation) since even partial restoration of flow might be expected to impact on adverse complications, whereas TIMI 3 would be more strongly related to favourable clinical outcomes, which was an endpoint of secondary interest in this study. The overall recanalisation rate at 24h in our study (66%) matches that reported by the IMS-3 (65%) based on a 24h CTA endpoint, with comparable individual occlusion site recanalisation rates³⁴¹, offering further reassurance about external validity.

Our findings indicate that 24h recanalisation itself is not significantly associated with early vasogenic oedema, or significant haemorrhage, questioning the widespread attribution of these outcomes to “reperfusion injury.” The association of large core with both significant oedema, and also poor outcome in spite of recanalisation, is consistent with recent clinical trial strategies that have sought to exclude such patients from reperfusion therapies. Observational data cannot define risk: benefit ratio, however, and it is important to bear in mind that excluding “large core” patients might represent an efficient clinical trial strategy, but that risk: benefit balance in this group remains to be determined: treatment in this group may still be associated with net benefit.

5.5 Conclusions

Among patients treated with IV rtPA, 24h recanalisation was not independently associated with significant early (24h) vasogenic oedema or significant haemorrhage, although incidence of HI/HI2 ICH was higher. Large ischemic core was associated with both significant brain oedema and poor outcome. There was no interaction of recanalisation and large core lesions for any imaging outcomes. Early major clinical improvement as a marker of probable early reperfusion was associated with lower incidence of both significant haemorrhage and oedema.

Chapter 6 **Explore Capillary transit time heterogeneity (CTTH) within different components of the tissue – core, penumbra, ‘non-core-non-penumbra’ infarct, normal brain**

6.1 Introduction

Capillary Transit time Heterogeneity (CTTH) values may reflect better on the micro-vascular flow regulation, providing a more accurate measure of tissue oxygenation (CMRO₂). The response to impaired capillary level tissue oxygen delivery (e.g. hyperaemia) is to modify inflow to capillary beds in order to homogenise transit time; therefore transit time heterogeneity may be an index of impaired capillary level oxygen delivery. Normal increase in CTTH theoretically could hamper an efficient oxygen extraction to the brain tissue.²³ Resting Brain has high heterogeneity of flow velocities²⁰⁰. This limits net oxygen extraction due to functional shunting. Normally neural activation gives rise to an increase in local brain tissue perfusion by recruiting previously non perfused capillaries³⁵². The capillary perfusion becomes homogenous^{200,353,354}. This is shown to counteract the inherent reduction in OEF as CBF increases^{23,355}, which is likely inherent property of passive microvasculature³⁵⁴. However, as brain diseases affect micro vascular regulation, a pathological non homogenous perfusion pattern arises. As a consequence of this transit times through capillaries vary more (existence of high flow and low flow capillaries) and leads to less oxygen availability for extraction²³. This abnormal capillary micro vascular regulation has been reported in diseases such as brain tumours, Alzheimer’s dementia, acute ischaemic stroke, small vessel disease^{184,185,355,356}. Preliminary results in humans show that both CBF and CTTH must be known to explain OEF in patients with Cerebrovascular disease³⁵⁵.

CBF, CBV, and a delay metric (T_{max}, MTT, TTP, DT) are used to predict brain tissue at risk in acute ischaemic stroke. Regional availability of oxygen in brain tissue (CMRO₂) is traditionally inferred from the magnitude of CBF and the concentration of oxygen in arterial blood. CBF is sensitive to regional levels of neuronal activity (i.e. neurovascular coupling³⁵⁷). The extent and duration of CBF reduction predicts the development of permanent infarction in acute stroke

²⁶. The microscopic distribution of the CBF is rarely considered. It has been proposed that heterogeneity of capillary transit times affects oxygen extraction efficiency^{23,185}. Therefore, cerebral blood flow, oxygen binding to haemoglobin, and capillary flow heterogeneity can influence oxygen delivery²³. Flow heterogeneity, along with CBF, can be derived from the slope of the deconvolved tissue curve¹⁷⁷. Extending the classic flow diffusion equation, capillary blood mean transit time (MTT) and capillary transit time heterogeneity (CTTH) combined determines the maximum OEF (OEF max) that can be achieved for a given tissue oxygen tension. The putative effects of increased CTTH were reported in stroke, traumatic brain injury, and dementia in a series of papers by Ostergaard et.al.^{184,358,359}. There is a need for robust estimation of CTTH, MTT, OEFmax to test the above hypotheses further. This will inform to what extent CBF or CTTH, or both contribute to tissue oxygen availability.

With reduced cerebral perfusion a mildly elevated CTTH and MTT leads to increased oxygen extraction in compliant normal vasculature. Coefficient of variation COV ($COV = CTTH/MTT$) remains unchanged. In micro vascular dysfunction (due to erythrocyte clogging), constriction of pericytes leads to severely increased CTTH. This leads to critical shunting of oxygenated blood in capillary bed with reduced CBF. Severe increased CTTH can make reperfusion futile if CTTH fails to normalise after recanalisation³⁵⁵. This is due to too fast transit times due to restoration and increase of CBF and hence reduced OEF. Severe increased CTTH is followed by decreased CTTH (homogenisation) as a result of stepwise capillary occlusions³⁶⁰. This represents “no-flow” phenomenon³⁶¹. Hypoperfused cerebral tissue with extreme flow homogenisation has been shown to correlate with final infarct^{21,187}. COV may predict infarction better than CTTH alone by removing inherent dependency of CTTH & MTT. A low COV predicted infarction if no recanalisation. Severe CTTH heterogenisation as well as homogenisation would entail high risk of infarction of hypoperfused brain tissue, where as mildly elevated CTTH represents tissue with low risk of infarction³⁶⁰.

We hypothesize that CTTH values significantly differ between the cerebral tissue compartments (core, penumbra, non-core-non-penumbra Infarct & normal brain) and hence CTTH can differentiate the tissue states better than conventional perfusion parameters (i.e. Cerebral Blood Flow (CBF), Cerebral Blood Volume

(CBV), Mean Transit Time (MTT)). This is of particular importance in the infarcted brain tissue that is neither in core nor in penumbra (non-core-non-penumbra Infarction).

The purpose of the study was to derive CTTH values and compare these values in different hypoperfused cerebral tissue compartments (core, penumbra, 'non-core-non-penumbra' tissue, contra lateral normal brain) in acute ischaemic stroke.

6.2 Methods

Using multimodal imaging from three studies from a single centre as described in previous chapters, I analysed multi parametric maps derived from acute CT perfusion (CTP). A novel parameter, CTTH was measured along with Cerebral Blood Flow (CBF), Cerebral Blood Volume (CBV), and Mean Transit Time (MTT) in a voxel wise method using a vascular (parametric) model (VM). A 24 hour follow up Non contrast CT (NCCT) was read for drawing final Infarction masks.

Core and penumbra were defined using Wintermark's method (Core=CBV <2ml/100g/min, Penumbra= relative MTT>145%). Scans were read by one Research fellow (BC) experienced in perfusion imaging, blinded to the clinical information and clinical outcomes. MATLAB 8.4 platform was used for image analysis. After detailed stepwise post processing as described in chapter 3, finally concentration time curve for each tissue voxel is derived.

A delay corrected deconvolution steps (standard SVD, circular SVD, vascular model) are then used to calculate the parametric maps (MTT, CBF, CBV, Tmax and TTP). Additionally, CTTH, Coefficient of variation (COV), OEF maps was obtained in vascular model. Coefficient of variation (COV) is a measure of the dissimilarity between the parametric capillary transit time heterogeneity (CTTH) and mean transit time (MTT) maps.

Time to peak map (TTP) was outlined with ROI tool with manual adjustment if needed for abnormal TTP. TTP maps were used to delineate the area of abnormal perfusion. From these outlined areas, the other parameters were

derived. Non bolus voxels where no contrast arrived were excluded from masks. CBV voxels were diffusely scattered, hence we corrected exuding voxels with $CBV < 1\text{ml}$ as explained in chapter 3. MTT mask often included a non TTP area. Sometimes, the infarction is found to be outside the TTP area. To reduce this, we included MTT from TTP area plus Infarct area in follow up scan (FI) which is called “union mask”.

CBV map is calculated from the area under the time enhancement curve for each voxel. Then Central volume theorem ($CBF = CBV / MTT$) is applied. Automatic segmentation of grey matter (GM), white matter (WM), Cerebrospinal Fluid (CSF) was done. The normal contra-lateral hemisphere was used to calculate relative (normalised) CBF, MTT. This was chosen as mirrored ROI of TTP map. ROIs from follow-up NCCT infarct volume, segmentation masks (GM, WM) and mirrored normal contra lateral side were placed on the parametric maps derived from all the methods. The individual voxel values were recorded on excel sheet. Mean and median values of all voxels for each parameter was produced after the initial steps as described above.

Mean ($\pm SD$), median ($\pm IQR$) values of different tissue level parameters (CTH, COV, CBF, CBV, and MTT) was compared using Kruskal- Wallis for comparing median values.

6.3 Results

Study population for the work on CTTH work was explained in chapter 3. Base line clinical characteristics of this group are shown in Table 6-1.

Table 6-1 Baseline characteristics of subjects included for final analysis (n=132)

Age (years)	Mean 70 (SD \pm 12) Median 73(IQR 18)
NIHSS	Mean 13 (SD \pm 7) Median 12 (IQR 10)
Systolic BP (mmHg)	Mean 146 (SD \pm 20) Median 144 (IQR 28)
Capillary blood glucose (mmol/l)	Mean 6.9 (SD \pm 2) Median 6.6 (IQR 2.2)
Hypercholesterolemia	65 (50%)
smoker	47 (36.4%)
Male gender	76 (59%)
Cardiac disease	29 (24%)
Atrial fibrillation	43 (34%)
Diabetes	15 (11.6%)
Hypertension	72 (56%)
Penumbra volume	Mean 54 ml(SD \pm 35.8) Median 53.9 ml (IQR 60)
Core volume	Mean 5.5 ml (SD \pm 6.8) Median 2.9ml (IQR 7)

An example of vascular model map (fig.6-1) and SVD map (fig.6-2) generated are shown.

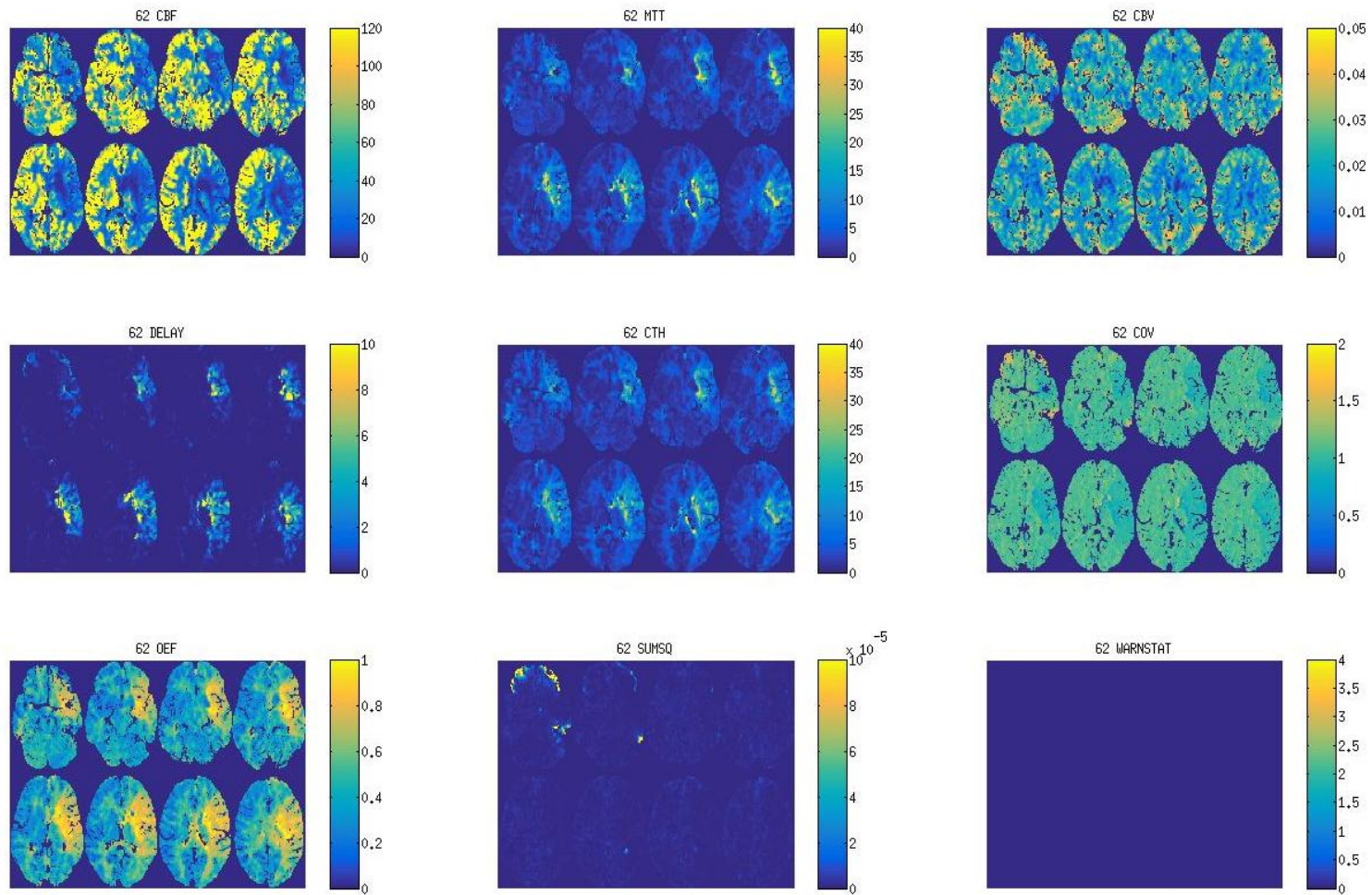


Figure 6-1 Example of maps derived in vascular model

Top row: left CBF, middle MTT, right CBV Middle row: left Delay time, middle CTH, right COV. Bottom row: Left OEF

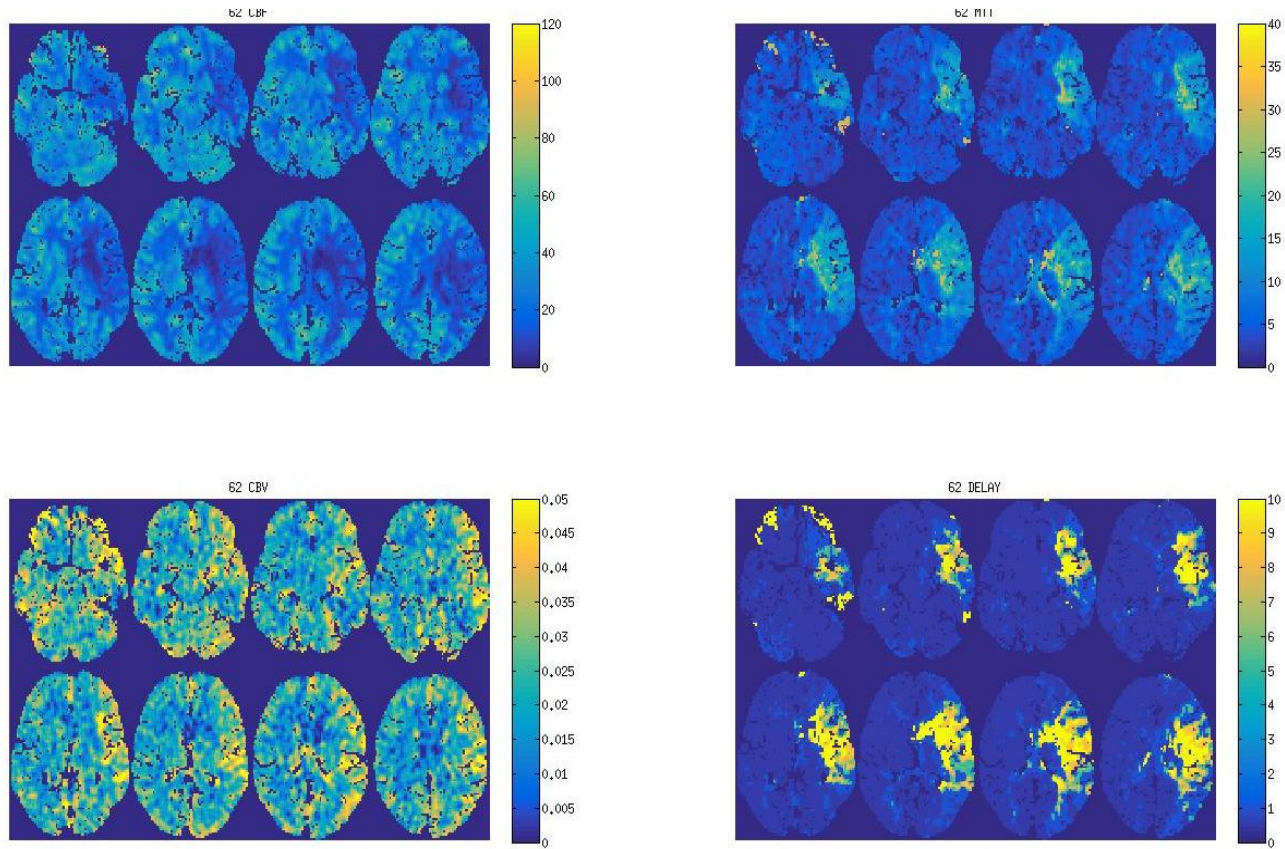


Figure 6-2 An example of SVD maps

CBF, MTT, Delay time and CBV maps are shown clockwise from top left side

An illustration of the ROIs showing infarct, a core and penumbra mask is shown in fig. 6-3.

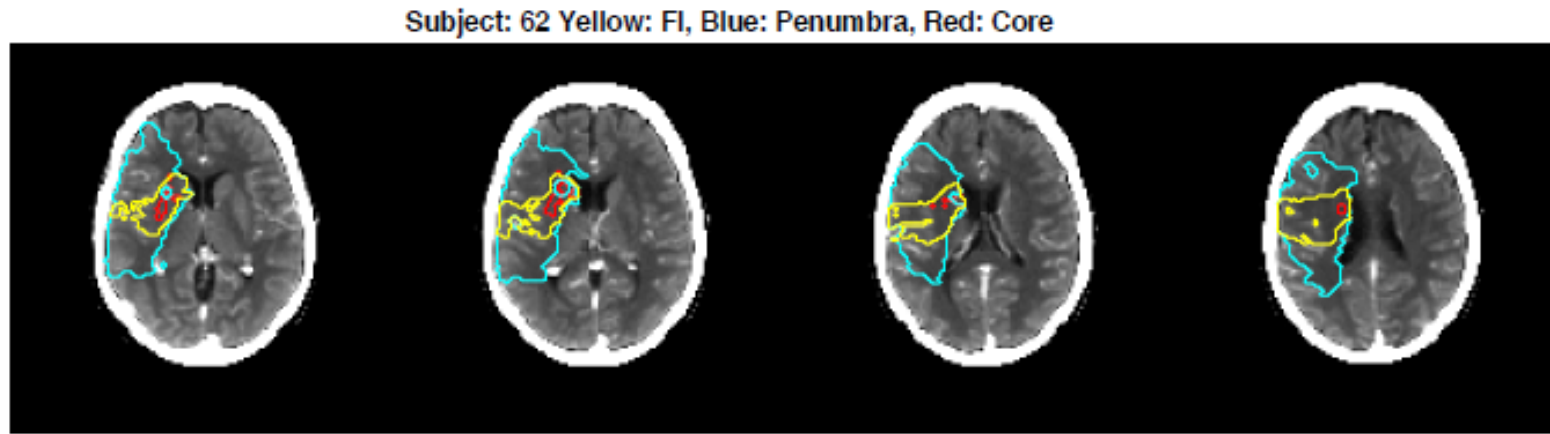


Figure 6-3 An example of ROIs for core, penumbra and FU Infarct (Infarct Yellow, Penumbra Blue, Core red).

In Table 6-2 the perfusion parameter values in different compartments (core, penumbra, and 'non-core-non-penumbra (NC/NP) infarction and normal brain) have been compared for significance.

Table 6-2 The perfusion parameters in different tissue zones (core, penumbra, 'non-core-non-penumbra' infarction and normal contralateral brain)

	Core mask (n=115)	Penumbra mask (n=130)	NC/NP Infarct mask (n=116)	Contra lateral Brain mask (n=132)	P (Parametric Repeated measures ANOVA)
Median MTT (seconds median, IQR)	9.6 (5.6)	10.9 (3.7)	4.7(1.74)	3.9 (1.1)	<0.01
Median CTTH (seconds median, IQR)	9.3 (4.7) (4.68)	10.8 (3)	5.1 (1.9)	4.2 (1.16)	<0.01
Median COV (seconds median, IQR)	0.98 (0.075) 0	0.97 (0.045))	1.05 (0.6)	1.05 (0.3)	<0.01
Median CBF (ml/100gm/min) (median, IQR)	6.8 (4.2)	14.4 (4.7)	31.3 (19)	34 (12)	<0.01
Median CBV (ml/100g/min)(median, IQR)	0.7 (0.2) 0.73)	2.3 (0.6)	2.6 (0.9)	2.39 (0.05)	<0.01

Between two group comparisons of median values of perfusion parameters using non parametric comparison (Friedman test) showed p values <0.001. I compared the values of each parameter between core, penumbra; between penumbra, NC/NP and between NC/NP, normal brain. Only Coefficient of Variation (COV) did not reach significance between NC/NP and normal brain (p=0.5). Box plots for comparing each parameter (CTTH, MTT, CBV and CBF) in these compartments is shown in fig.6-4, 6-5, 6-6 & 6-7.

Median of CTTH (median of voxels) value is 13.13 s in penumbra that Infarcted and 10.5 s in penumbra that rescued (non parametric p <0.001).

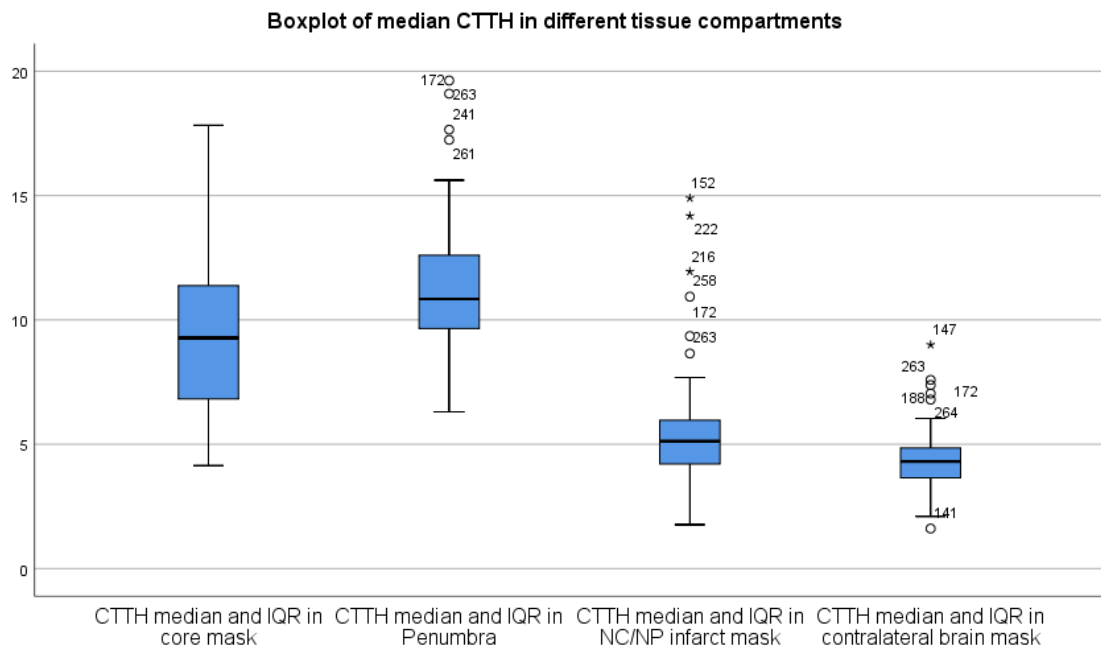


Figure 6-4 Box plot of median CTTH in different tissue zones
 NC/NP: non-core-non-penumbra. Y axis is CTTH time in seconds.

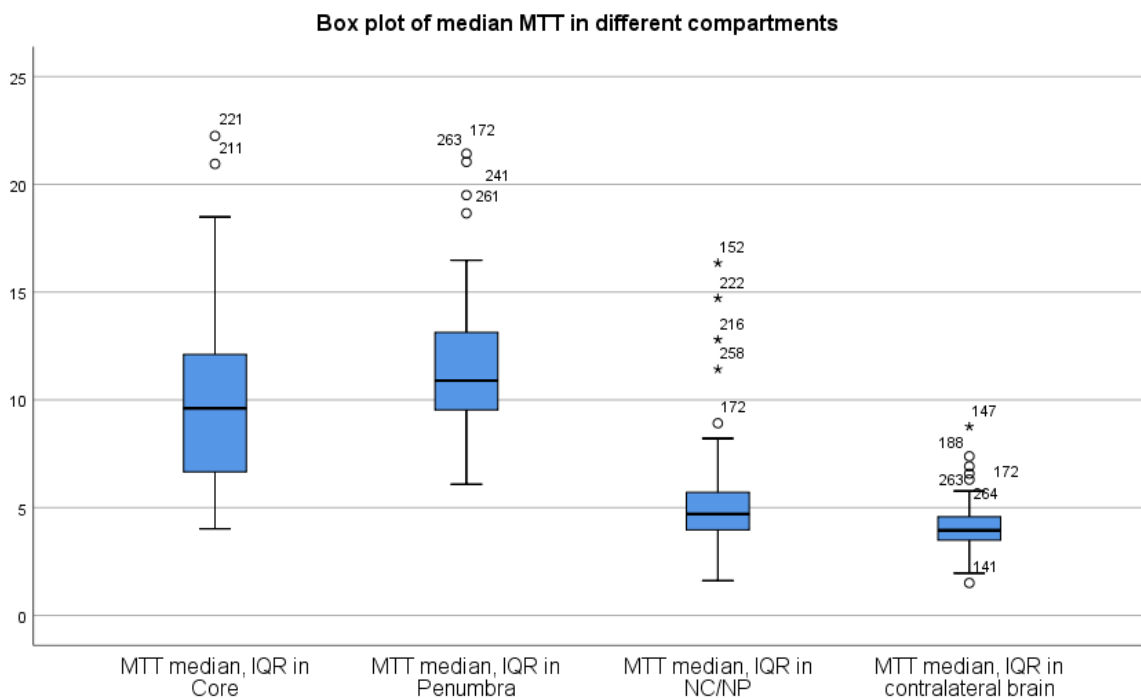


Figure 6-5 Box plot of median MTT in different tissue zones
 NC/NP: non-core-non-penumbra. Y axis is CTTH time in seconds.

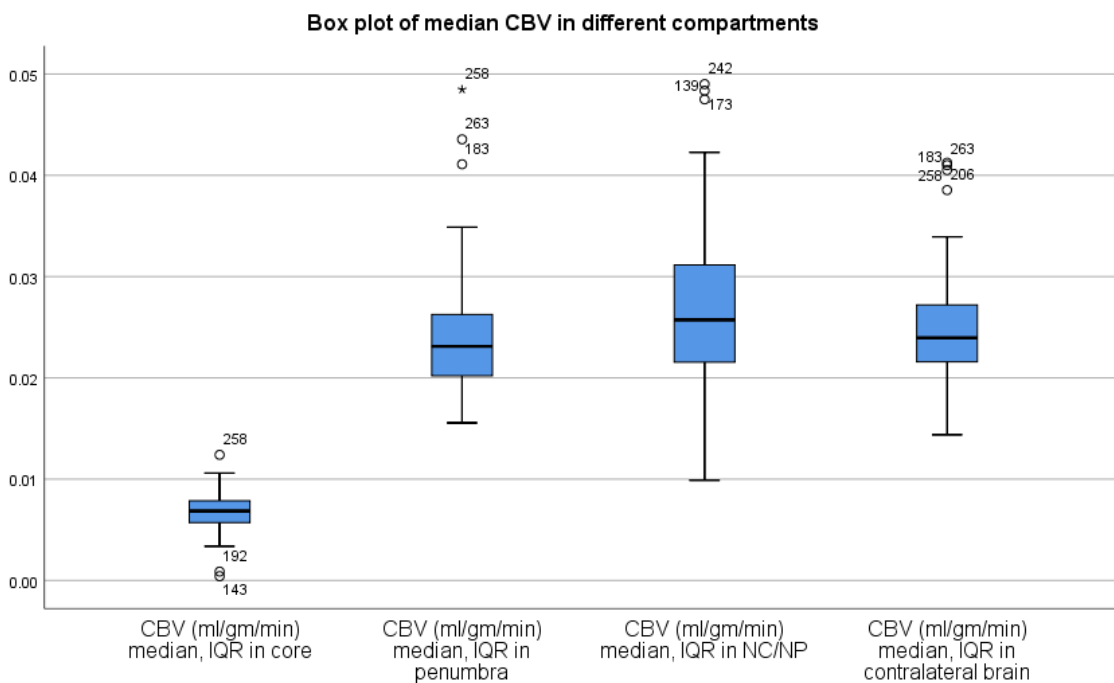


Figure 6-6 Box plot of median CBV in different tissue zones
 NC/NP: non-core-non-penumbra. Y axis is CTTH time in seconds.

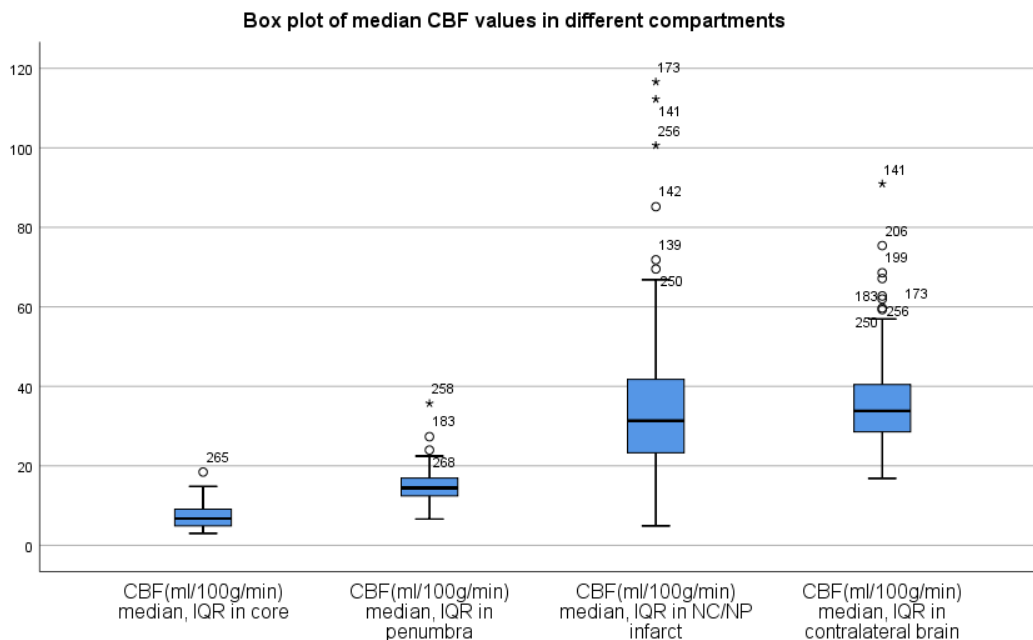


Figure 6-7 Box plot of median CBF in different tissue zones
 NC/NP: non-core-non-penumbra. Y axis is CTTH time in seconds.

6.4 Discussion

The delay metrics Tmax, MTT are affected by transit time heterogeneity properties³⁶². It is speculated that this shortcoming may have affected the predictive ability of existing transit time metrics^{223,363}. CTTH, COV might represent missing step towards distinguishing tissue with benign oligoemia from salvageable tissue. I have successfully processed the CTTH values from a large cohort of CT perfusion scans. CTTH values are significantly different in tissue compartments; however, from the results above, it is not clear that they discriminate core from penumbra. In our cohort CTTH and MTT are correlated. CTTH co varies with MTT as hypoperfusion contributes to elevated CTTH³⁶⁴. It may mean that CTTH is only giving the same qualitative information about perfusion as a prolonged MTT, whereas CBF, CBV values are clearly different in core and penumbra. Median CBF (median of voxels) is 6.8 ml/100g/min (IQR 4.2) in core and 14.4 ml/100g/min (IQR 4.7) in penumbra. Median CBV is 0.7 ml/100g/min (IQR 0.2) in core and 2.3 ml/100g/min (IQR 0.6) in penumbra. The inverse relationship between CBF and CTTH in our study is consistent with the theory that increased blood flow would homogenise capillary flow²⁰⁰. In a study of 23 healthy human controls using DCE-MRI, average CTTH of 0.93s (IQR 1.33s) was seen in putamen grey matter³⁶⁵. In subjects with carotid stenosis, there is marked difference in ipsilateral brain (CTH 4.2 s) and contra-lateral brain (CTTH 1.8s). CTTH values are much higher than healthy volunteers. In anaesthetised rats, resting brain CTTH was 1-1.3 s, while activation decreased it to 0.2-0.7 s³⁶⁶.

Accurate and reproducible estimation of CTTH in voxel-wise calculation is necessary. CTTH values are likely to be between 10-20 seconds in compliant, passive micro vasculature in penumbra³⁶⁴. Earlier human studies investigated the relationship of intra-voxel flow heterogeneity and tissue fate using perfusion weighted MRI^{21,187}. These studies did not quantify capillary heterogeneity but reported intra-voxel deviations of relative flow distribution compared to normal tissue. Similar to our results, Engedal et al, using perfusion weighted MRI, showed mean CTTH of 12 sec (SD +/-7.6), mean COV of 1.0 (SD +/- 0.2), CBF 21 (SD +/- 20) ml/100ml/min and MTT 13 sec (SD +/- 11) in the cerebral tissue

with prolonged MTT of > 5 sec (i.e. hypoperfused tissue). The subjects in their study included: all patients who presented within 6h of symptom onset with acute, non-lacunar, ischaemic stroke with a NIHSS score ≥ 4 (European multi centre database); all Ischaemic stroke patients eligible for IV thrombolysis (regional database). A low COV (i.e. extreme homogenisation) was strongly associated with Infarction in absence of recanalisation at 24hrs. COV may predict infarction better than CTTH alone by removing inherent dependency of CTTH & MTT and therefore expected to remain constant during changes in perfusion pressure. Mildly elevated CTTH positively predicted functional outcomes³⁶⁰. CTTH values in our cohort are slightly higher, they all had stroke with varying vascular risk factors. Hence CTTH values are higher with large variance (COV).

Increased volumes of mildly elevated CTTH (10-20 sec) positively predicted favourable clinical outcome in acute ischemic stroke with a LVO³⁶⁴. However, there is no correlation between mildly elevated CTTH and final infarct volume.

I have not looked at individual patients with carotid occlusion and how it influences CTTH. We do not have information on different brain tissues (deep grey matter, white matter, grey matter).

Our study has limitations with small cohort of patients with only ischaemic stroke (i.e. not homogenous population). The study subject cohorts were different in three non randomised studies leading to heterogeneous population. There is no external validation for the methodology in deriving the novel parameters (CTTH, COV). Approximation of flow patterns to the flexible two-parameter gamma function is widely used in micro vascular research. Nevertheless, this approximation might not be appropriate in disease conditions such as ischaemia. No experimental studies directly compared CTTH with OEF measured by PET. We have used perfusion thresholds as per Wintermark's criteria. The core, penumbra measurements may not be replicable with other criteria using different perfusion parameters and thresholds. Other valuable exercise would have been to have derived thresholds for CTTH along with other parameters in core, penumbra tissues (with core meaning the hypoperfused tissue correlating with final infarction if recanalised, penumbra meaning hypoperfused tissue correlating with final infarction if non recanalised).

6.5 Conclusions

I successfully derived new perfusion parameters CTTH, COV using the vascular model. Although CTTH values did not differ significantly in tissue zones (core, penumbra), this needs to be tested in large number of subjects with further validation work.

Chapter 7 What are the clinical characteristics of subjects with 'non-core-non-penumbra' infarction?

7.1 Introduction

Infarction of acutely silent tissue (non-core-non-penumbra) was previously described in literature³⁶⁷. This was shown to negatively impact clinical outcome. In the classic core/penumbra model, both the core and the penumbra contribute to the clinical deficit and together constitute the symptomatic tissue. Imaging studies have shown that combined volumes of core and penumbra correlate better with acute clinical scores, and that salvage of penumbral tissue is associated with improvement in clinical scores³⁶⁸. So called 'Oligaemia' is found surrounding hypoperfused tissue which is assumed to be clinically silent and not at risk of infarction. Bang et al, reported occurrence of new DWI lesions after 1 week in >50% of anterior circulation strokes predominantly involving areas initially affected by only mild hypoperfusion³⁶⁹. Infarction of silent tissue is plausible in circumstances such as cerebral blood flow in oligoemia falls below penumbral and then infarction threshold³⁶⁷. This can happen for example in hypotension when cerebrovascular autoregulation is negatively affected in leptomeningeal collaterals. Embolisation of clot into distal branch of occluded artery could contribute to infarction of acutely silent, contiguous brain tissue. Delayed tissue damage from inflammation was also proposed as contributory for infarction of acutely silent tissue³⁷⁰. In unexplained early neurological deterioration (<24 hrs after stroke onset) subjects an infarct growth beyond the initial penumbra was shown to be larger than matched controls with no early neurological deterioration³⁷¹. Cerebral pericytes which regulate capillary diameter during functional activation are susceptible in conditions such as age, hypertension and diabetes³⁵⁹. Even if blood flow to a given region of brain is adequate to the oxygen needs, a mal distribution of flow (Capillary flow heterogeneity, CTTH) can lead to variations in oxygen extraction.

We hypothesised that pre-stroke co morbidities may reflect a propensity for extension of infarction beyond the defined compartments (core, penumbra). We

further hypothesised that extension of infarction may reflect capillary dysfunction that would be evident in abnormal CTTH.

Using the similar subjects and methods as detailed in chapter 7, I investigated the subjects with ‘non-core,-non -penumbral’ infarction to evaluate any differences in clinical characteristics such as vascular risk factors.

7.2 Methods

I used the same dataset and methods as in chapter 7. Wintermark’s validated thresholds (Core=CBV <2ml/100g/min, Penumbra= relative MTT>145%) for core, penumbra were applied. Most subjects were found have an infarction outside the core and penumbra tissue (hence we called non- core-non-penumbra infarct). The median volume of NC/NP infarction on follow-up CT was 2.3 ml, hence we decided to use this value as cut off. We defined a threshold of >2.3ml as significant non-core-non-penumbra (NC/NP) Infarct brain volume.

I compared the groups (non-core-non-penumbra infarction >2.3 vs. \leq 2.3ml) for a demographic data, clinical scores, and map-derived volumes using appropriate categorical or numerical statistical test for comparison. I called the group with non-core-non-penumbra infarct volume >2.3 as ‘non-core-non-penumbra Infarction’ groups in discussion.

7.3 Results

Median time of symptom onset to CTP imaging was 188 min (IQR 83). Mean time was 198 min (SD +/-69). The volumes of total penumbra, salvaged penumbra, non-core-non-penumbra infarction and Infarction on CT slices co-registered to CTP space; proportions of salvaged penumbra, non-core-non-penumbra infarction (with infarction volume in CT slices co registered to CTP space) and non-core-non-penumbra (with total penumbra volume) are shown in Table 7-1. Clinical, Imaging characteristics of the subjects with NC/NP \leq 2.3ml vs. >2.3 ml is shown in Table 7-2.

Table 7-1 Volumes of Salvaged Penumbra, Infarction and 'non-core-non-penumbra' infarction

Penumbra volume median(IQR)	Infarction in CTP co registered CT slices median(IQR)	Salvaged penumbra median(IQR)	Salvaged penumbra/total penumbra (%)	Non-core-non-penumbra-infarction/Infarction in CTP co-registered CT slices (%)	NC/NP median (IQR)	NCNP/penumbra (%)
54 ml (23-84)	9.9 ml (0-39)	33.7 ml (12-56)	73 (30-92)	20 (9-40)	2.33 ml (0.7-8.5)	6 (1-21)

Table 7-2 Clinical, Imaging characteristics of the subjects with NC/NP \leq 2.3 ml vs. $>$ 2.3 ml

	NC/NP FI \leq 2.3ml (N=64)	NC/NP FI $>$ 2.3ml (N=65)	P value (mann- whitney)
Female n/N (%)	28/64 (44%)	25/65 (38%)	0.6
Smoker n/N (%)	20/64 (31%)	27/65 (41%)	0.3
Hypertension n/N (%)	34/64 (53%)	38/65 (58%)	0.6
Diabetes n/N (%)	5/64 (8%)	10/65 (15%)	0.3
Atrial fibrillation n/N (%)	19/63 (30%)	23/60 (38%)	0.35
Cardiac Disease n/N (%)	14/ 59 (24%)	15/62 (24%)	1
Capillary blood glucose (mmol/l) median (range)	6.5 (5.7-7.6)	6.8 (5.6-8.1)	0.4
Systolic BP (mean \pm -SD)	147 (21)	147 (20)	0.9
Age median(years, range)	73 (63-80)	72 (61-79)	0.26
NIHSS median (range)	9 (6-15)	16 (10-19)	$<$ 0.01
OTT* (minutes, mean \pm -SD)	181 (46)	183 (49)	0.8
Median CTTH (seconds)	4.1 (3.6-4.9)	4.3 (3.8-4.8)	0.5
Core volume median (ml, IQR)	2.1 (4.7)	6.1 (8.7)	$<$ 0.001
Penumbra volume median (ml, IQR)	38.7 (65)	62 (52)	0.011
Follow up infarct median volume in CT co registered to CTP space (ml, IQR)	9.9 (16.8)	57.6 (45.8)	$<$ 0.001
NC/NP infarct median volume (ml, IQR)	0.7 (1.4)	8.2 (14.5)	$<$.0001
OTT Onset to treatment time; NIHSS National Institute of Health stroke Scale ; CTTH Capillary transit time heterogeneity			

Out of the total subjects with recanalisation status available (n=100), 55 subjects have recanalised (i.e. achieved TIMI grade 2 or 3). Box plot of median CTTH values are shown in fig.8-2 comparing median CTTH in penumbra which has infarcted (13.2 s, IQR 4) and penumbra that is rescued (10.35 s, IQR 1.7) in only recanalised subjects.

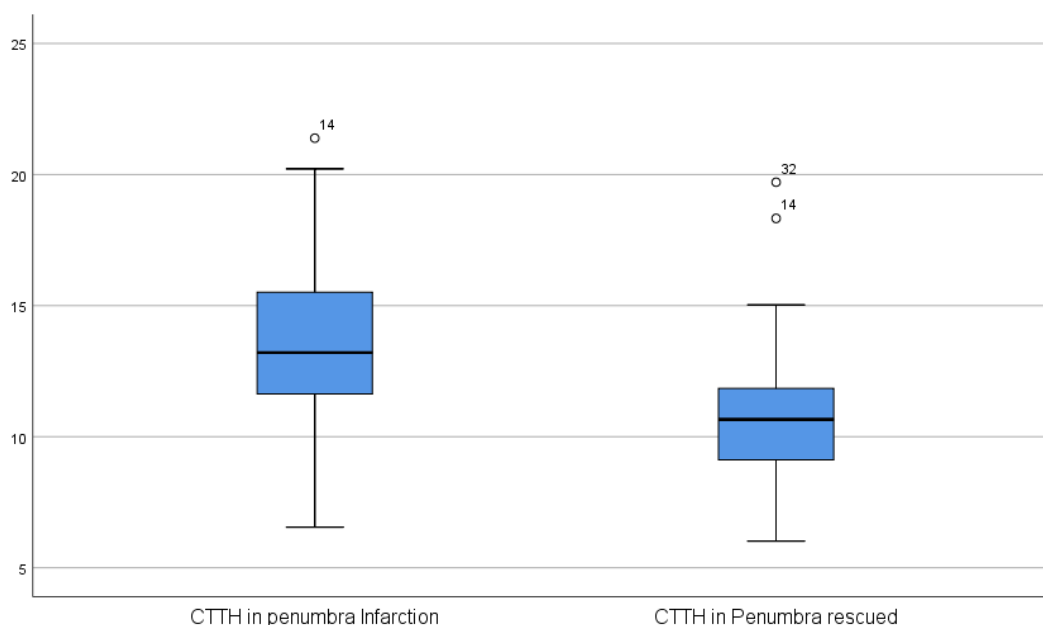


Figure 7-1 Box plot of median CTTH values in penumbra infarcted vs. rescued in recanalised subjects. (Y axis represents CTTH (sec)).

7.4 Discussion

'Non-core-Non-penumbra' infarction group has larger hypoperfused area (penumbra volume 62ml vs. 39ml, (p=0.001)) leading to larger final infarction volume (57 ml vs. 9.9ml). This could be due to infarction of oligoemic tissue surrounding the penumbra. The accurate separation of benign oligoemia with penumbra is a challenge²⁶⁰. The use of blood flow threshold levels to define salvageability of brain tissue and to predict infarct growth is affected conceptually by collateral supply, peri-infarct depolarisations and dynamic nature of penumbra. These same factors could lead to growth of penumbra into regions of oligoemia³⁶⁷.

Perfusion thresholds can be time dependent to differentiate the tissue zones, with for example even smaller reductions in CBF can lead to infarction at later time from stroke onset³⁷². The proportion of “noncore non penumbra infarction” constituting the infarction in CTP slices is on average 20% in our study, whereas in a study of anterior circulation Ischemic stroke non-core-non-penumbra infarction constituted 11%²⁶⁰. In their study, substantial volume (arbitrarily considered >1ml) was seen in 7/34 (21%; up to 8ml) of patients, representing on average 11% (up to 83%) of final Infarction volume in the 2 slices of CTP²⁶⁰. In our study, median volume of non-core-non-penumbra infarction was 2.3ml (up to 8.5ml, similar to Alawneh et al²⁶⁰ group).

Clinical characteristics did not differ in between those with NC/NP volume >2.3 ml or <2.3 ml, presumably due to inherent bias in distinguishing with median volume. In Alawneh et al study CT perfusion protocol consisted of 2 contiguous 10mm slices (20mm thickness), where as in our study CT perfusion slice was 40mm thickness. In their study, 1ml of acutely silent but Infarcted tissue volume was arbitrarily considered significant. Our median volume for arbitrarily dividing significant to non significant infarction of “non core non penumbra tissue” is similar to their group after correcting for the limited brain coverage. Higher NIHSS and larger penumbra volumes were seen in the group with NC/NP volume >2.3 ml.

Median penumbra volume saved in our cohort was 33.7 ml (average 77% of penumbra is rescued). Alawneh et al study in 34 CTP subjects with mean Onset to imaging time of 136 min, showed salvaged penumbra median volume of 59ml (85% penumbra rescued)²⁶⁰.

The lack of clear association of non-core-non-penumbra infarction with CTTH might simply reflect smaller number of subjects. It is potentially difficult to reliably measure CTTH in such small volumes. Median CTTH value is relatively higher in the penumbra tissue that has infarcted in comparison to the penumbra that is rescued after recanalisation. This may suggest the theory that higher CTTH value despite reperfusion leads to Infarction³⁵⁵. Sudden increase in CBF after reperfusion in capillaries with too fast flow would lead to low OEFmax.

Our study has limitations. The CT perfusion images has limited brain coverage and hence cannot be certain if the volumes for infarction and tissue parameters correlate to a whole brain imaging. Since all subjects had non-core-non-penumbra infarction, we arbitrarily divided into two groups using median volume (2.3 ml) as cut off, but this has bias in understanding the difference between those with larger infarction in this region to those with small infarction. The CTTH values for the NC/NP tissue region itself is not derived but the overall CTTH value for the subjects with or without NC/NP infarction is derived. This does not give true information on CTTH variability in the region of interest as such. Our study has limitations with small cohort of patients with only ischaemic stroke (i.e. not homogenous population). The study subject cohorts were different in three non randomised studies leading to heterogeneous population. There is no external validation for the methodology in deriving the novel parameters (CTTH, COV). Approximation of flow patterns to the flexible two-parameter gamma function is widely used micro vascular research. Nevertheless, this approximation might not be appropriate in disease conditions such as ischaemia. No experimental studies directly compared CTTH with OEF measured by PET. The core, penumbra values are derived with Wintermark's thresholds. The thresholds may not replicable with other perfusion parameters and thresholds.

7.5 Conclusions

I did not identify any significant difference of CTTH values in subjects with non-core-non-penumbra infarction tissue; however this is very novel method and needs further work with validation. An analysis in larger group of subjects would be helpful in better understanding of the role of CTTH in “non-core-non-penumbra” infarction. This parameter can potentially be a key factor in determining tissue fate; perhaps this is the missing link for inadequate prediction with current transit time metrics.

Chapter 8 **Is secondary transfer for stroke thrombolysis optimal? - Comparing outcomes between two hospitals with different model of care and with the rest of UK**

8.1 **Introduction**

Intravenous thrombolysis in ischemic stroke is beneficial if given within 4.5 hours of symptom onset^{373, 120}, with benefits being highly time-dependent²⁶¹. Despite being recognised as recommended treatment supported by the highest level of evidence in national and international guidelines for more than a decade, IV thrombolysis is not universally available at all hospitals where stroke patients are admitted. Consequently, patients with acute stroke may be transferred to a stroke centre in order to be treated. The outcomes of patients accessing a primary stroke centre directly have not been compared to those transferred secondarily from a referring hospital.

Bias from the source of patient referral was reported, with more patients aged >80 were referred from primary care, whereas, those referred from Emergency departments were <80 years³⁷⁴. Factors including older age, high blood glucose, stroke severity, pre-stroke disability, and blood pressure are significant prognostic factors^{375,376}, and several of these (notably age and severity of stroke) interact with time to presentation²⁶¹. Longer time from symptom onset to treatment is associated with poorer outcomes based on clinical trials^{263,377}.

Registry based studies show heterogeneity in patient outcomes based on regional differences or socioeconomic status^{378,379}. Risk adjusted inpatient mortality was higher among patients from lower income areas³⁸⁰. The inverse relationship of socio-economic status and stroke outcomes was reported in a secondary analysis of a study investigating quality of stroke services in Scottish hospitals³⁸¹. Patients from deprived regions are more likely to be dependent or death at 6 months compared to affluent regions. Analysis from the Safe Implementation of Thrombolysis in Stroke (SITS) register identified different treatment biases in UK and non-UK SITS countries³⁸²: UK SITS-MOST patients had more severe stroke (median NIHSS 14.5 vs. 12), accounting for differences in outcome (48% of UK

patients achieved independence (modified Rankin Score 0-2) compared to 55% of non-UK). Provision of all relevant processes of care reduces medical complications after stroke³⁸³. A prospective cohort English study has shown that patients admitted to higher levels of organisation are more likely to receive high quality care and reduced mortality³⁸⁴. Implementation of centralised stroke services has trade off between improved, focussed stroke care with longer travel times and potentially delays in stroke treatments. Centralisation of stroke services has shown improved length of stay, improved time to scan and in some improved mortality^{385,386}.

Glasgow city population has been recognised to have poor health status compared to rest of the UK (“Glasgow effect” https://en.wikipedia.org/wiki/Glasgow_effect). The model of stroke care can influence patient outcomes. In Glasgow, Southern General Hospital (SGH) has transfer from peripheral hospital model, whereas, Western Infirmary Glasgow (WIG) has local thrombolysis only model. We sought to explore the potential impact of different referral systems for IV thrombolysis by exploring SITS registry data for two different hospitals in the same city; and to compare outcomes in these hospitals against those seen in the rest of the UK.

Our hypothesis was that SGH taking referrals from poorer part of Glasgow, and wider geographical catchment will have poorer outcomes compared to a local hospital in Glasgow. We also believe that peripheral hospital referrals contribute to poorer outcomes. In addition, we were also interested to compare the outcomes in direct admissions with secondary transfers SGH.

8.2 Methods

I undertook a retrospective, observational study comparing outcomes in different geographical regions using SITS registry data. The Safe Implementation of Thrombolysis in Stroke (SITS) registry was established as part of the conditional European licence for alteplase in order to confirm clinical trial findings in routine practice³⁸⁷. The SITS platform is an internet -based interactive stroke registry, which serves as a tool for structured data entry and is an instrument for centres to compare their own treatment results with

national and global performance. SITS is an ongoing, prospective, academic-driven, multinational register for centres using thrombolysis for the treatment of acute ischemic stroke. After increased time window to 4.5 hrs since publication of ECASS III¹²⁰, there was a concern that increased time window would lead to delays and potentially increased haemorrhage and mortality with treatment delays. SITS registry was aimed to assess the implementation of prolonged time window for thrombolysis, to investigate whether the increased time window has resulted in prolongation of admission-to-treatment time, and to evaluate treatment safety and functional outcome in a large patient cohort.

I analysed data from the SITS registry for all thrombolysed stroke patients from May 2003 to March 2013. I collected separate data for two hospitals within Glasgow (Southern General Hospital SGH, Western Infirmary Glasgow WIG) and for the rest of the UK (excluding these two hospitals). SGH provide IV thrombolysis service to secondary transfers from a wide geographical area in South of Glasgow with a population catchment of over 500,000 population and admitting patients from over 6 district general hospitals. Victoria Infirmary (VIC) is a closely linked hospital to SGH and therefore transfers from this hospital or direct admissions to SGH are considered primary SGH admissions and remaining admissions as peripheral referrals (or secondary SGH admissions) for the analysis. WIG has catchment of 225,000 population of own and other referrals from north of Glasgow hospitals. Since year 2015 the Stroke service has been redesigned in Glasgow. VIC, WGI hospital services have moved to SGH.

Outcomes:

The 90 day modified Rankin score (mRS) was analysed as a dichotomised variable, defining good outcome as mRS 0-2. We analysed death at 90 days, the incidence of SITS Monitoring Study (SITS-MOST)-defined symptomatic intra-cerebral haemorrhage (Parenchymal haematoma type 2 (PH2) or remote Parenchymal haematoma type 2 (PHR2) with deterioration in NIHSS of ≥ 4 or death)³⁸⁸ and clinically relevant significant haemorrhage (Parenchymal Haematoma type 1 or 2 or Remote Parenchymal Haematoma type 1 or 2).

Statistical analysis:

Sample size calculation was not performed as this study was a non randomised comparison of groups. Unadjusted comparisons between SGH, peripheral referrals to SGH, WIG, and rest of the UK (r UK) were done using Kruskal-Wallis test for numerical variables and chi-square or Fisher's tests for categorical variables, as appropriate. Data were analysed without and with adjustment for baseline prognostic factors, and onset to treatment time (OTT) was specifically tested. We carried out univariate and multivariate logistic regression for the outcomes with hospital site as an explanatory variable and adjustment for other variables. The variables entered in regression models are detailed in table below. Variables with p value <0.1 on univariate regression were entered into multivariate logistic regression. Onset to treatment time (OTT) was forced in if not already significant in univariate regression. The variables included in the regression models were: Age, pre-stroke modified Rankin score (0-1 vs. 2-5), Onset to treatment time, Baseline NIHSS, systolic BP, Capillary blood glucose (mmol/l), Weight (kg), Oxford stroke type (TACI v other), female gender, Hypertension, Hyper lipidemia, Smoking, Diabetes, Atrial Fibrillation, congestive heart failure, Previous stroke, Stroke aetiology(Embolic v other) and hospital locations.

As adjustment for baseline prognostic variables does not necessarily capture all relevant factors, I additionally undertook propensity score matching³⁸⁹ (comparison of SGH, rUK groups) using nearest neighbourhood method with R statistics. The variables used for matching between UK and SGH were: Age, NIHSS, Diastolic BP, Capillary blood Glucose (mmol/l), Hypertension, Diabetes, Hyper lipidemia, Smoking, Atrial fibrillation, Previous Stroke, Congestive Heart failure, Pre stroke modified Rankin score (0-1 vs. 2-5), Antiplatelet use, Stroke type (Embolic v Other), Oxford stroke classification(TACI v Other). As there are a large number of covariates, conventional matching would have been difficult and would have resulted in dropping a large number of cases. Propensity score matching summarize many covariates into a single score.

I used SPSS 21 for descriptive, binary logistic regression analysis for the main outcomes in both before matching (SGH, peripheral transfers, WIG and r UK) and after matching (SGH, peripheral transfers, r UK cohorts). I also then measured the risk of death within 90 days between sites by log rank test and Cox's proportional hazards regression method.

8.3 Results:

Out of 11120 patients who received IV thrombolysis, 7504 had 90 day modified Rankin score available (fig.8-1). Baseline characteristics of study population are illustrated in Table8-1.

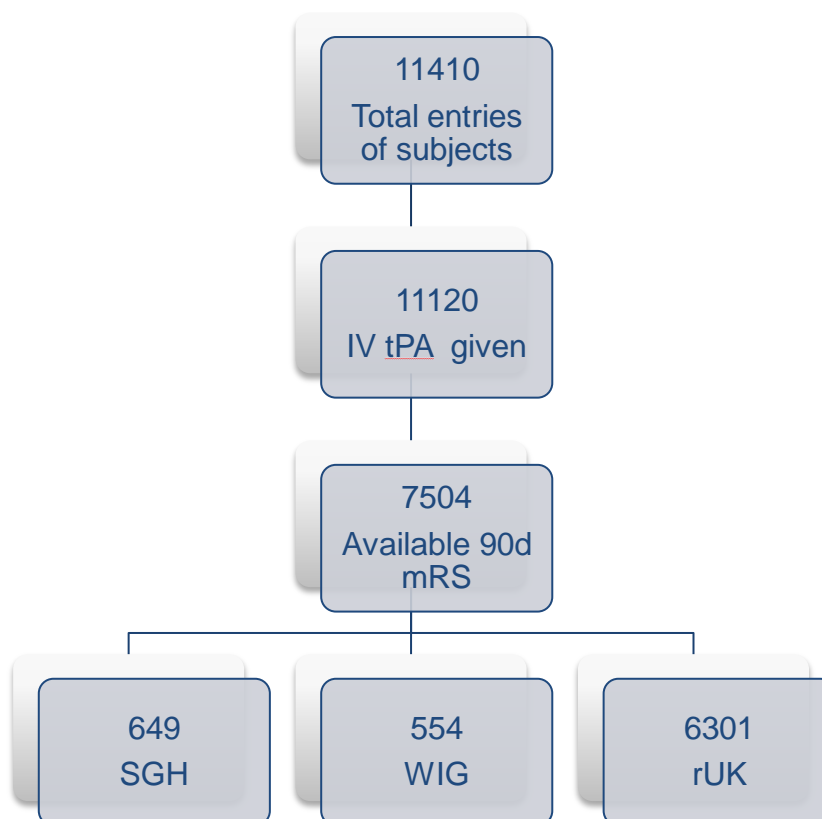


Figure 8-1 Study population CONSORT diagram
(SGH- Southern General Hospital, WIG-Western Infirmary Glasgow, r UK- rest of the UK)

Table 8-1 Baseline characteristics of study population

	SGH (n=307)	Peripheral referrals (n=342)	WIG (n=554)	rUK (n=6301)	P value
Median age (IQR), years	72 (61-79)	70 (62-78)	71.5(61-79)	72(62-79)	0.4
Female gender (%, n)	48% (145/302)	46% (15/338)	48% (264/554)	45% (2824)	0.4
Median NIHSS (IQR)	14 (7-20)	15 (9-20)	11(6-18)	13(8-19)	<0.01
Pre stroke mRS (0-1) (%, n)	80%(236/293)	89%(294/329)	83.4%(462/554)	87.4% (5207/5957)	0.001
mRS0	66.9% (196/293)	72.9% (240/329)	65.7% (364/554)	72.9% (4343/5957)	<0.001
mRS 1	10.2% (40/293)	16.4% (54/329)	17.7% (98/554)	14.5% (864/5957)	
mRS 2	10.2% (30/293)	9.1% (30/329)	10.5% (58/554)	8% (478/5957)	
mRS3	9.2%	1.5% (5/329)	6.1% (34/554)	4.3%	

	(27/293)			(258/5957)	
mRS 4	0	0	0	0	
mRS5	0	0	0	0.2% (14/5957)	
Hypertension (% , n)	60%, (180/299)	62% (207/333)	61.9%, (341/551)	57.7%, (3527/6108)	0.1
Diabetes (%, n)	14% (41/300)	12% (41/336)	13% (72/553)	14% (867/6194)	0.7
Hyper lipidemia (%, n)	19% (58/299)	23% (77/336)	38% (209/549)	35% (2031/5765)	<0.01
Smoker (% , n)	28% (84/297)	25% (84/331)	30.5% (167/548)	20% (1151/5799)	<0.01
Atrial Fibrillation (% , n)	35% (104/308)	26% (86/335)	30.6% (169/552)	24% (1455/6069)	<0.01
Congestive Heart failure (%, n)	3.3% (10/300)	5% (17/336)	7.8% (43/552)	5% (306/6085)	0.018
Previous stroke (% , n)	20% (60/299)	14.6% (49/336)	18% (98/540)	12.2% (756/6183)	<0.01
On	54%	44% (148/335)	52.4% (290/553)	40.3% (2502/6216)	<0.01

antiplatelet (%, n)	(163/300)				
On anti hypertensives (%, n)	51% (152/299)	49% (165/336)	60.2% (333/553)	48% (2943/6115)	<0.01
Median capillary blood glucose(IQR), mmol/l	6.4 (5.5- 7.6)	6.3 (5.6-7.6)	6.1 (5.3-7.3)	6.4 (5.6-7.8)	<0.01
Median Systolic blood pressure(IQR), mmHg	149 (135- 163)	149 (131-164)	141 (126-159)	149 (133-163)	<0.01
Median Diastolic blood pressure (IQR),mmHg	77 (67-85)	75 (65-86)	77 (69-86)	80 (70-90)	<0.01
TACI (%, n)¶	56% (166/296)	60% (198/333)	41% (226/5520)	47.6% (2909/6114)	<0.01
PACI (%, n)¶	35% (103/296)	28% (93)	36.8% (203)	36.7% (2246)	
POCI (%, n)¶	1.4% (4)	1.2% (4)	1.3% (7)	0.3% (20)	

LACI 9%, n)¶	8% (23)	11.4% (38)	21% (116)	15.4% (939)	
Large vessel atherosclerosis (% , n)*	34.5% (99/287)	33% (107/326)	53%(272/513)	44.6% (2453/5500)	<0.01
Cardioembolic (% , n)*	52% (150)	50% (162)	33.9% (174)	27.4% (1506)	
Lacunar (% , n)*	4% (14)	3% (9)	9%(46)	10.8% (594)	
Unknown/Uncertain (% , n)*	10% (29)	13% (43)	4% (21)	17.2% (947)	
Onset to Door Time(IQR),min	70 (50-96)	97 (64-139)	120 (90-150)	150 (120-165)	<0.01
Onset to Treatment Time(IQR),min	145 (115-175)	173 (145-195)	170 (145-190)	180 (160-205)	<0.01
Door To Imaging time(IQR),min	33 (20-50)	28 (15-49)	15 (9-27)	15 (8-22)	<0.01
Door To Treatment time (IQR),min	68 (50-94)	66.5 (47-95)	40 (25-55)	60 (47-95)	<0.01

¶ Oxford stroke classification (TACI-Total anterior circulation Infarct; PACI-Partial anterior circulation Infarct; LACI-Lacunar Infarction; POCI-Posterior circulation Infarct)

*Stroke aetiological classification using TOAST criteria

Unadjusted important clinical outcomes (Haemorrhage, functional outcome at 90 days and death) are illustrated in Table.8-2. 90 day modified Rankin score distribution is shown in grotto bars in Fig. 8-2.

Table 8-2 Un-adjusted improtant clinical outcomes in different hospital groups

	SGH (n=307)	Peripher al referrals (n=342)	WIG (n=554)	UK (n=6301)	P value
SITS-MOST SICH haemorrha ge (n, %)	2/260 (0.8%)	4/269 (1.4%)	12/539 (2.2%)	77/5784 (1.3%)	0.3
Significant haemorrha ge (PH1 or PH2 or PHR1 or PHR2) (n, %)	27/293 (9%)	29/327 (9%)	54/542 (10%)	456/601 7 (7.6%)	0.18
Death (n/N, %)	66/302 (22%)	90/338 (26%)	90/554 (16%)	1227/63 01 (19.5%)	0.001
unfavourab le 90day mRS (2-6) (n, %)	240/302 (80%)	266/338 (80%)	371/554 (67%)	3936/63 01 (62.5%)	<0.01
Poor 90 day mRS (3-6) (n, %)	179/302 (59%)	219/338 (65%)	264/554 (48%)	2928/63 01 (46%)	<0.01
SITS-MOST Safety in Stroke Thrombolysis Monitoring study, SICH- Symptomatic Intra cerebral Haemorrhage PH1, PH2 - Parenchymal haemorrhage type 1, type 2 respectively, PHR1, PHR2- Remote Parenchymal haemorrhage type 1 & 2 respectively					

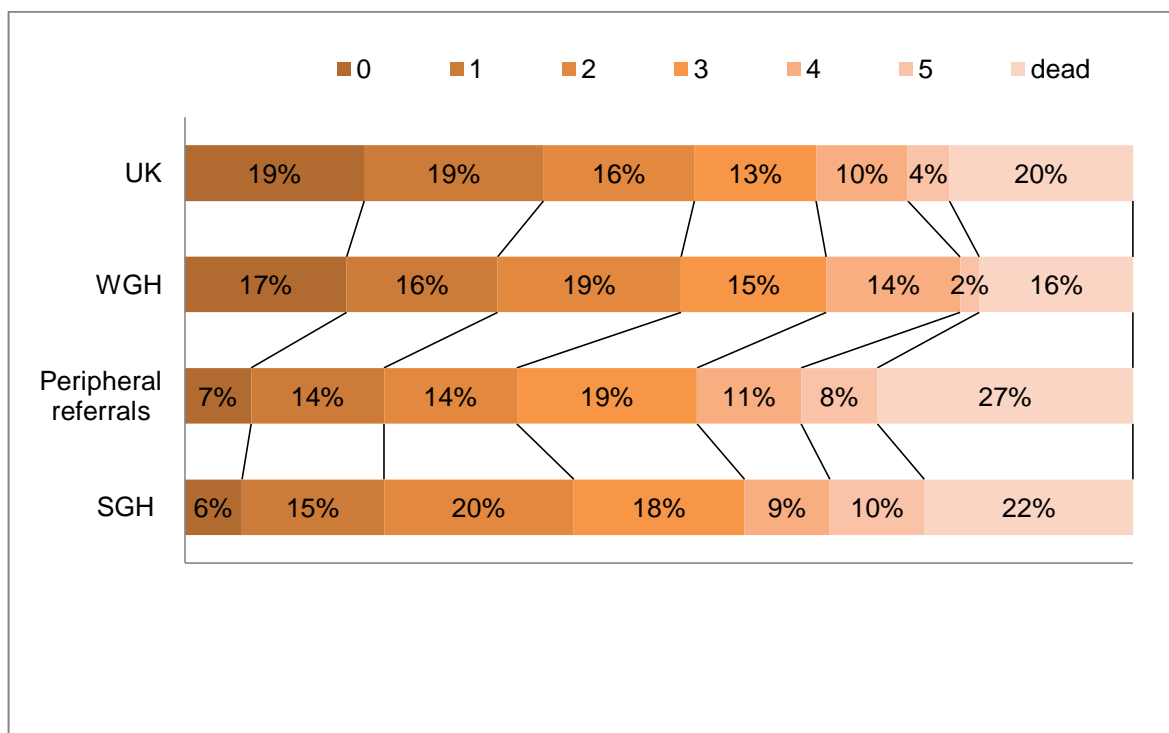


Figure 8-2 90 day modified Rankin scales in different hospitals
mRS is classified into 0,1,2,3,4,5 and 6 (death).

8.3.1 Regression analysis

Univariate regression and multivariate regression analyses for the poor 90 day outcome (modified Rankin score 3-6) are illustrated in Table 8-3 and 8-4 respectively.

Table 8-3 Univariate regression for poor 90 day modified Rankin score (mRS3-6) in all study population

Variables	OR(95%CI)	P value
Age (years)	1.04(1.03-1.04)	<0.01
Onset to Treatment Time(OTT, min)	0.99(0.99-1.003)	0.2
Pre stroke mRS 0-1	0.26(0.22-0.3)	<0.01
NIHSS	1.18(1.17-1.19)	<0.01
Systolic Blood pressure(mmHg)	1(0.99-1.003)	0.63

Capillary blood Glucose (mmol/l)	1.1(1.08-1.12)	<0.01
Weight(kg)	0.99(0.98-0.99)	<0.01
Female gender	1.28(1.17-1.4)	<0.01
Hypertension	1.27(1.15-1.4)	<0.01
Diabetes	1.4(1.23-1.6)	<0.01
Hyper lipidemia	0.97(0.8-1.07)	0.5
Smoking	0.78(0.7-0.8)	<0.01
Atrial fibrillation	1.67(1.5-1.8)	<0.01
Congestive Heart failure	1.8(1.5-2.2)	<0.01
Previous stroke	1.24(1.08-1.4)	<0.01
TACI vs. Other (Oxford classification)§	3.3(3 -3.7)	<0.01
Embolic vs. other stroke types ¶	1.36(1.2-1.5)	<0.01
r UK (reference)		
SGH	1.7(1.3-2.12)	<0.01
Peripheral referrals	2.12 (1.7-2.6)	<0.01
WIG	1.05 (0.88-1.25)	0.6
§ Oxford stroke classification ¶ TOAST classification		

Table 8-4 Multivariate regression for poor 90 day modified Rankin score (mRS3-6)

Variables	OR (95%CI)	P value
Age	1.03(1.023-1.32)	<0.01
NIHSS	1.18(1.17-1.2)	<0.01
Capillary blood glucose (mmol/l)	1.07(1.05 -1.1)	<0.01

Pre-Stroke mRS 0-1	0.3(0.25-0.36)	<0.01
Onset to treatment time (min, forced)	1.002(1.001-1.003)	<0.01
<i>rUK (reference)</i>		
SGH	1.7 (1.26-2.3)	<0.01
Peripheral referrals	2.22 (1.7-2.9)	<0.01
WIG	1.3 (1.06-1.6)	0.014

In multivariate regression analysis, adjusted (for all variables with $p < 0.1$) poor 90 day outcome (mRS >2) remained significantly higher in SGH (OR 1.7 (1.26-2.3); $p < 0.01$), peripheral referrals (OR 2.22 (1.7-2.9); $p < 0.01$) and WIG (OR 1.3 (1.06-1.6), $P = 0.014$) compared to rUK. Increasing age, higher baseline NIHSS, pre-stroke mRS score 0-1, higher capillary blood glucose, longer onset to treatment time independently predicted the poor outcome (see table 6-4).

Univariate regression for death at 90 days is shown in Table 8-5. Multivariate regression for death at day 90 is shown in Table 8-6.

Table 8-5 Univariate regression for death at 90 days in all study population

	OR(95%CI)	P value
Age (years)	1.06(1.05-1.07)	<0.01
Onset to Treatment Time(OTT, min)	0.999(0.998-1.001)	0.3
Pre stroke mRS 0-1	0.336(0.3-0.4)	<0.01
NIHSS	1.14(1.13-1.15)	<0.01
Systolic BP (mmHg)	1.002(1-1.005)	<0.06
Capillary blood Glucose (mmol/l)	1.11(1.08-1.13)	<0.01
Weight (Kg)	0.986(0.98-0.99)	<0.01
Female gender	1.09(0.97-1.22)	0.14
Hypertension	1.25(1.1-1.4)	<0.01

Diabetes	1.46(1.25-1.7)	<0.01
Hyper lipidemia	0.99(0.87-1.12)	0.88
smoking	0.6(0.52-0.72)	<0.01
Atrial fibrillation	1.9(1.68-2.16)	<0.01
Congestive Heart failure	2.1(1.67-2.6)	<0.01
Previous stroke	1.24(1.06-1.46)	<0.01
TACI vs. Other (Oxford classification)§	2.7(2.4-3.1)	<0.01
Embolic vs. other stroke types ¶	1.5(1.3 -1.7)	<0.01
rUK (reference)		
SGH plus VIC	1.15 (0.8-1.5)	0.3
Peripheral referrals	1.5 (1.17-1.9)	0.001
WIG	0.8 (0.6-1)	0.065
§Oxford classification ¶TOAST classification		

Table 8-6 Multivariate regression for death at 90days

Variables	OR(95%CI)	P Value
Age (years)	1.05(1.04-1.06)	<0.01
NIHSS	1.14(1.12-1.15)	<0.01
Capillary Blood glucose (mmol/l)	1.09(1.06-1.12)	<0.01
Pre-Stroke mRS 0-1	0.54(0.45-0.65)	<0.01
Hypertension	0.8(0.7-0.9)	<0.05
Onset to treatment time (min; forced)	1.002(1.000-1.004)	0.03
r UK (reference)		
SGH plus VIC	1.06 (0.76-1.5)	0.7
Peripheral referrals	1.46 (1.08-1.98)	0.013
WIG	0.92 (0.7-1.2)	0.56

In multivariate regression (Table 8-6), adjusted Death was only significantly higher in, peripheral referrals (1.46 (1.08-1.98), $p=0.013$) but not SGH direct admissions (Odds ratio 1.06, 95%CI, 0.76-1.5, $p=0.7$), WIG (0.92 (0.7-1.2); $p=0.56$) compared to rUK. Higher Age, higher NIHSS, higher capillary blood Glucose, and longer onset to treatment time were positively associated, and pre stroke mRS (0-1), Hypertension negatively with death in multivariate regression (Table 8-6).

8.3.2 Survival analysis

Death occurred in 61 patients in SGH, 88 patients in Peripheral referrals, 86 patients in WIG, and 1169 patients in rUK. No day of death was available in 68 patients who were “imputed” to death at day “90”. The Log-rank test and Cox proportional hazards regression for death at day 90 comparing SGH, peripheral referrals, rUK, WIG are shown below (Fig.8-3, 8-4 & Table.8-7).

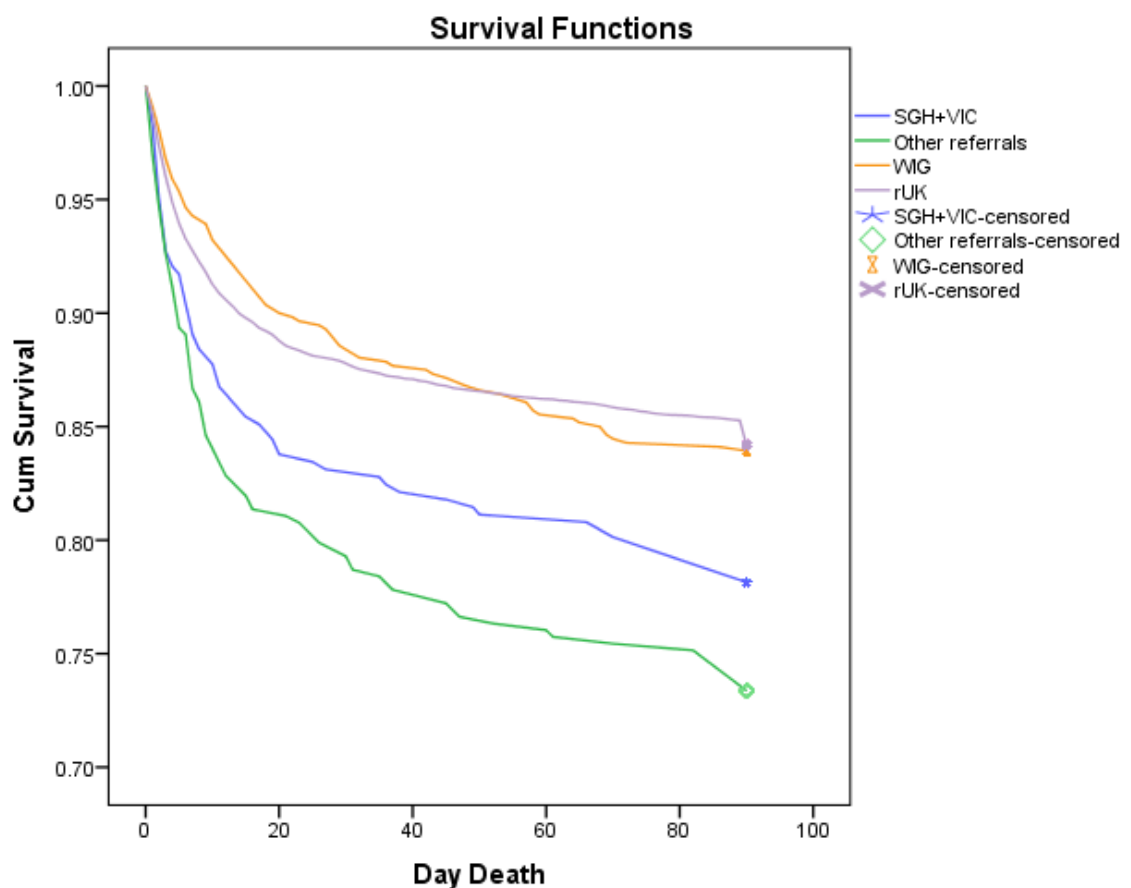


Figure 8-3 Log rank test comparing hospitals (Log-Rank $p<0.01$)

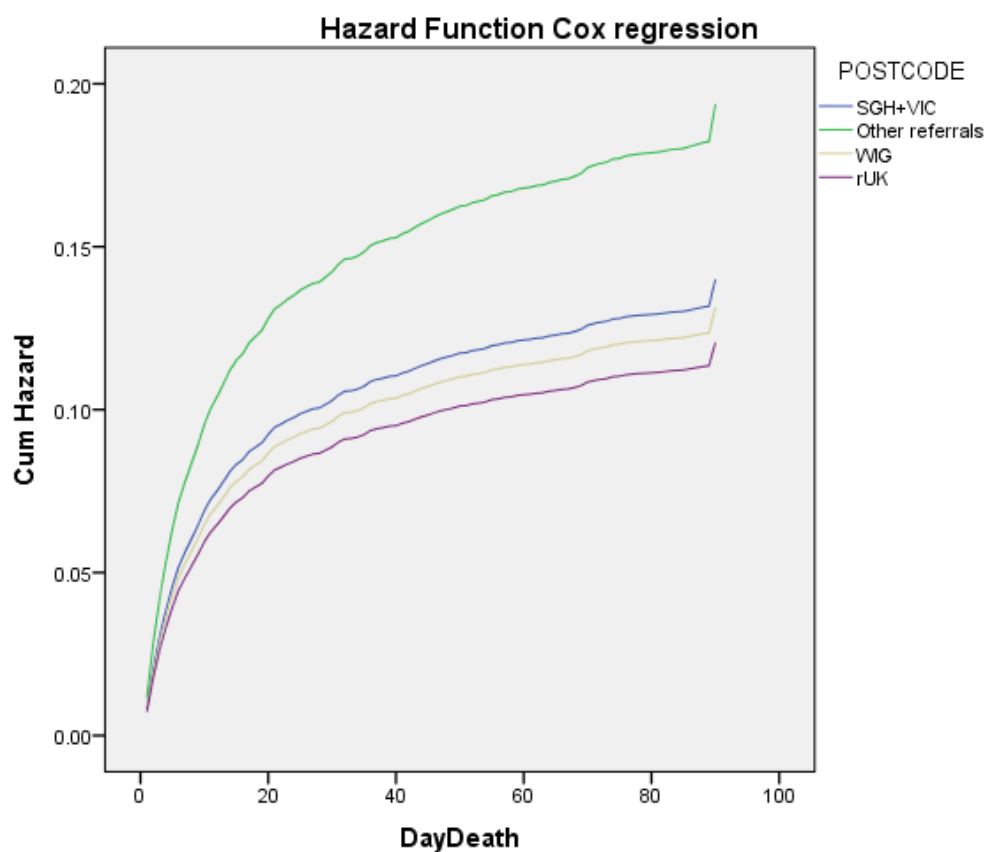


Figure 8-4 Cox's proportion Hazard function

Table 8-7 Cox's regression analysis for death at 90 days

Variable	Hazard Ratio (95% CI)	P value
Age	1.039 (1.034-1.045)	<.001
NIHSS	1.1 (1.1-1.12)	<0.01
Pre stroke mRS (0-1)	0.68 (0.6-0.79)	<0.01
Capillary blood glucose (mmol/l)	1.07 (1.05-1.09)	<0.01
rUK (reference)		
SGH	1.16 (0.9-1.5)	0.26
Peripheral referrals	1.6 (1.3-2)	<0.001
WIG	1.09 (0.9-1.36)	0.45

In addition, the causes of death in different sites are illustrated in figure 8- 5.

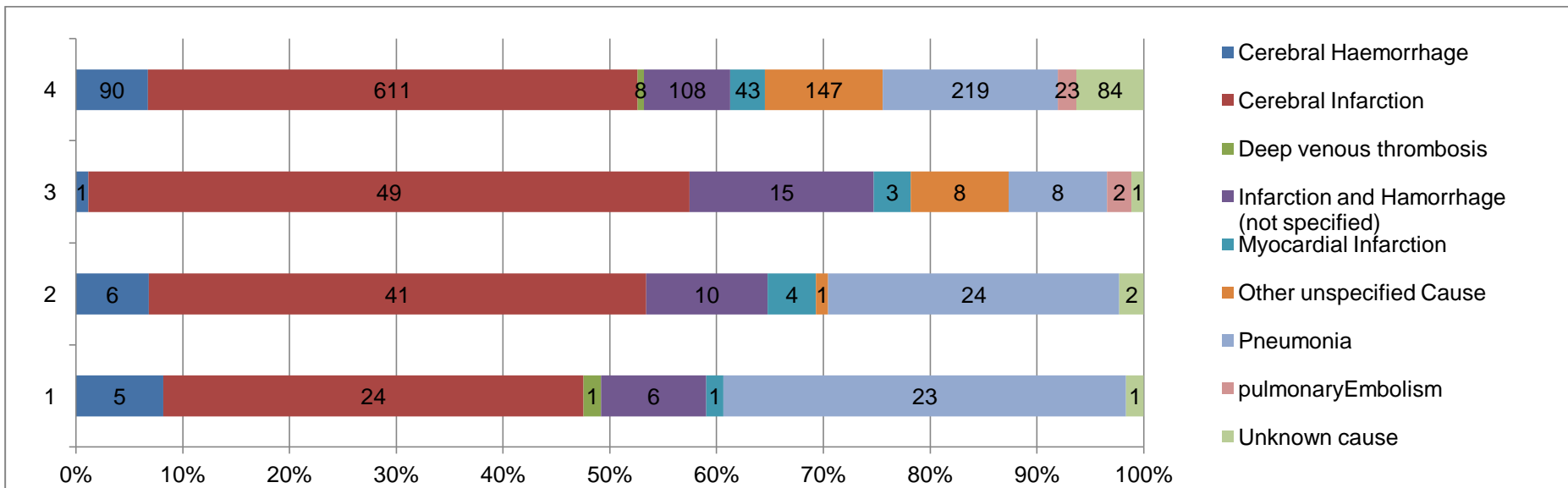


Figure 8-5 Causes of death in the hospitals
 (1= SGH 2= Peripheral referrals to SGH 3=WIG 4=UK)

8.3.3 Propensity score matching of SGH with UK subjects

565 subjects were matched between SGH and rUK. Distribution of propensity score matching is shown in fig. 8-6 & 8-7. The variables used for matching has been described in the methods section. Univariate and multivariate regression analysis for poor outcome and death at 90 days are shown in Tables 6-8 to 6-11. Post matching, SGH has significantly increased poorer outcome (OR 1.6 (1.1-2.3); $p=0.013$), death (OR 1.8 (1.15-2.7); $p=0.008$), than rUK; peripheral referrals also have higher poorer outcome (OR 2.1 (1.4-3); $p<0.01$), death (OR 2.1 (1.4-3); $p=0.01$) than rUK.

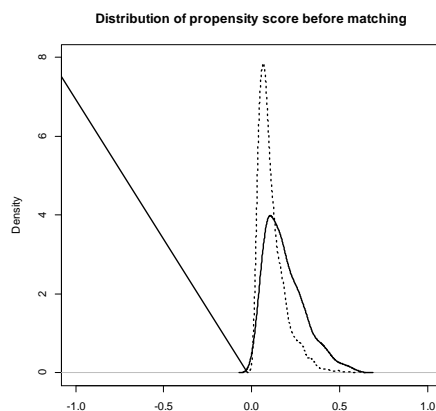


Figure 8-6 Propensity score distribution before matching (—SGH, ----- UK)

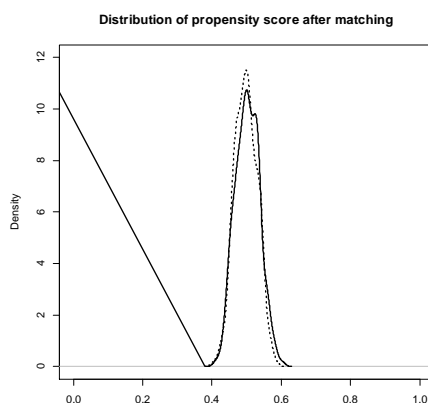


Figure 8-7 Propensity score distribution after matching (—SGH, ----- UK)

Table 8-8 Univariate regression for poor outcome at 90 days (mRS>2) in SGH, UK post matched groups

Variables	OR(95%CI)	P value
Age (years)	1.04(1.03-1.05)	<0.01
Onset to treatment time (IQR, min)	1.003(1.0-1.006)	0.04
Pre-Stroke mRS0-1	0.23(0.14-0.365)	<0.01
NIHSS	1.17(1.15-1.2)	<0.01
Systolic Blood pressure (mmHg)	1.001(0.99-1.007)	0.64
Capillary blood Glucose (mmol/l)	1.13(1.06-1.2)	<0.01
Weight (kg)	0.986(0.978-0.994)	<0.01
Female gender	1.5(1.2-1.9)	0.001
Hypertension	1.3(1.006-1.6)	0.04
Diabetes	2(1.4-3)	<0.01
Hyper lipidemia	1.06(0.79-1.4)	0.7
Smoking	0.7(0.5-0.9)	0.01
Atrial Fibrillation	1.28(0.99-1.676)	0.06
Congestive Heart Failure	1.05(0.5-2.06)	0.9
Previous stroke	1.78(1.26-2.5)	0.001

TACI v other stroke types (Oxford classification)	3.34(2.6-4.3)	<0.01
Embolic v other stroke types	1.3(1.01-1.63)	0.036
rUK (reference)		
SGH	1.37 (1.02-1.85)	0.03
Peripheral referrals	1.76 (1.32-2.36)	<0.01

Table 8-9 Multivariate regression for poor outcomes at 90 days (mRS>2) in SGH, UK post matched group

Variables	OR(95%CI)	P Value
Age (years)	1.03(1.02-1.04)	<0.01
NIHSS	1.18(1.15-1.2)	<0.01
Capillary blood Glucose (mmol/l)	1.1(1.02-1.2)	0.01
Onset to treatment time (min)	1.004 (1.001-1.008)	0.023
Pre-Stroke mRS (0-1)	2.65 (1.58-4.44)	<0.01
Previous Stroke	1.52 (1.006-2.28)	0.047
rUK (reference)		
SGH	1.6 (1.1-2.3)	0.013
Peripheral referrals	2.1(1.46-3)	<0.01

Table 8-10 Univariate regression for death at 90 days in SGH, UK post matched groups

Variables	OR(95%CI)	P value
Age (years)	1.07(1.05-1.08)	<0.01
Onset to treatment time (min)	1.002(0.99-1.006)	0.2
Pre stroke mRS 0-1	0.34(0.3-0.6)	<0.01
NIHSS	1.13(1.1-1.16)	<0.01
Systolic Blood pressure (mmHg)	1.008(0.99-1.013)	0.08
Capillary blood Glucose (mmol/l)	1.14(1.076-1.25)	<0.01
Weight (kg)	0.98(0.97-0.99)	<0.01
Female gender	0.9(0.67-1.25)	0.4
Hypertension	1.4(1.03-1.9)	<0.05
Diabetes	1.72(1.16-2.5)	<0.01
Hyperlipidemia	1.07(0.75-1.5)	0.7
Smoking	0.57(0.39-0.8)	<0.01
Atrial Fibrillation	1.74(1.27-2.36)	<0.01
Congestive Heart Failure	1.46(0.67-3.2)	0.34
Previous stroke	1.05(0.7-1.5)	0.78

TACI v other stroke types (Oxford classification)	2.5(1.8-3.5)	<0.01
Embolic v other stroke types	1.4(1.02-1.86)	<0.05
rUK (reference)		
SGH	1.7 (1.15-2.5)	0.007
Peripheral referrals	2.1 (1.5-3)	<0.01

Table 8-11 Multivariate regression for death at 90 days in SGH, UK post matched groups

Variables	OR(95%CI)	P Value
Age	1.05(1.03-1.07)	<0.01
NIHSS	1.13(1.09-1.16)	<0.01
Capillary blood Glucose (mmol/l)	1.11(1.04-1.9)	0.002
Onset to treatment time (min)	1..006 (1.002-1.01)	0.008
r UK (reference)		
SGH	1.8 (1.16-2.7)	0.008
Peripheral referrals	2.1 (1.38-3.2)	0.001

8.4 Discussion

Different systems have been evaluated to increase access to IV thrombolysis, including “telemedicine” (TEMPIS³⁹⁰), “scan in a van”³²⁵, “helicopter transfer”³⁹¹. Differences in patient outcomes after IV thrombolysis according to system of care have been less investigated. The issues raised by transfer of patients between healthcare facilities with different access to treatments have been highlighted by endovascular thrombolysis, where an interplay of transfer times and in-hospital efficiency (expressed as door to needle time for IV thrombolysis) dictates the boundaries that determine appropriate care pathways (direct

transfer to an endovascular centre - the “mother ship” paradigm - or initial local thrombolysis initiation and subsequent transfer - the “drip and ship” paradigm).

The risk factors and service characteristics differed in many important respects across groups. Within the Glasgow services, differences in patient characteristics likely reflect different population health states in the areas served by different hospitals, although they likely also reflect different physician behaviour, access to complex imaging, and other organisational features (note lesser severity at WIG, different risk factor profiles etc). The secondary transfer cases include referral bias and patient selection by the tertiary hospital in addition to transfer delay.

Is there a “Glasgow Effect”?

The Glasgow population shows a higher prevalence of several adverse prognostic markers, high prevalence of co-morbidities, and greater degree of pre-stroke dependence.

The “Glasgow effect” (https://en.wikipedia.org/wiki/Glasgow_effect) describes an unexpectedly poor health and life expectancy of the population of Glasgow compared to the rest of the UK, that cannot be explained by poverty alone^{392,393}. Although socio-economic status, cultural factors and other health related risk factors all undoubtedly contribute this phenomenon, it remains elusive as to why these health inequalities exist. In multivariable analysis, independent predictors of poor outcome - increasing age, higher baseline NIHSS, higher pre-stroke modified Rankin scale, higher capillary blood glucose, and longer onset to treatment time - were the same as found by other studies^{375,394}. West of Scotland stroke thrombolysis patients from all three groups, however, had significantly poorer outcomes compared to the rest of the UK independent of other factors. Mortality, excluding the secondary transfer cases, did not differ significantly from the rest of the UK in either conventional or propensity-matched analyses. It is possible that the poorer outcome, defined as day 90 mRS score of 0-2, reflects general co-morbidities of the west of Scotland population that are not adequately detected by the conventional vascular risk factor profile and demographics available from this dataset. Data on frailty, co-morbidities and social deprivation were not available, but are likely highly relevant to

functional outcomes (e.g. Charlson co-morbidity index³⁹⁵). The pre-stroke estimated mRS was also significantly worse among west of Scotland patients (mRS \geq 2 was seen in 20% of SGH, 17% WGI compared to 13% in the rest of the UK. Modified Rankin score of 3 was found in 9.2% in SGH, 6.4% in WGI and 4.3% in UK).

Is secondary transfer of patients associated with poorer outcome?

Secondary transfer patients differed by good pre-morbid mRS and longer onset to treatment time, but even after adjusting for other predictors, functional outcomes were poorer among those transferred from outside Glasgow and mortality was higher, in both multivariable and propensity-matched analyses. The poorer outcome among these patients cannot be clearly explained from the available data. Causes and timing of death exhibit no clear pattern, the majority of deaths in all groups resulting from initial cerebral effects of stroke. Repatriation to the parent hospital was determined by patient status and was not dictated by administrative policies. Almost all parent hospitals had dedicated stroke units throughout the study period.

Our study has several limitations. We compared disproportionate subject numbers using non-randomised subjects in a registry database. I did not calculate sample size as this was a non-randomised comparison. Propensity score matching was carried to adjust for large covariates but this method can have bias. Nevertheless, the results are similar with or without propensity score matching suggesting validity. Registry database can have limitations with entry errors and missing information. We have missing information and particularly missing 90d modified Rankin score. There are several imaging parameters that can influence the outcomes (e.g. ASPECTS score), which we do not have information for adjusting. Although other factors were adjusted this may still be inadequate in terms of baseline population characteristics. Comparing the outcomes between direct stroke admissions to DGH referrals can be done perhaps in different way to what I have done in this thesis. All DGH referrals to both the Glasgow hospitals can be compared to the direct admissions to both hospitals in non randomised way. However, we proposed to explore the geographical factors (larger catchment in SGH) and also socio-economic factors (poorer populations in SGH catchment), hence used the comparison between

hospitals, and compared only direct admissions with DGH referrals to SGH only. In Univariate logistic regression there are many parameters tested for the clinical outcomes. All the parameters that were significant in univariate regression were chosen for multivariate regression. The issue with this method is, too many variables can cancel each other's effect for a smaller sample size (over fitting model) and the results could be confounded.

8.5 Conclusions

Poorer 90 day outcomes after thrombolysis occurred frequently at a hospital that accepted secondary transfer patients compared to a hospital in the same city that did not routinely take such patients. Adjusted mortality was significantly higher in peripheral referrals versus direct SGH admissions, WIG compared to rest of UK. These poorer outcomes were accounted for by the secondary transfer patients.

Chapter 9 : Summary of chapters: Exploration of Perfusion Imaging; Applicability of Capillary transit time heterogeneity (CTTH) in perfusion Imaging; Stroke outcomes in different Care settings

9.1 Introduction

Stroke outcomes are heterogeneous and several predictive factors have been shown to influence, some of which are related to patient factors and some are to tissue Imaging. Majority of thesis chapters explored imaging related factors relevant to tissue outcomes in Ischaemic stroke, and to complement this I have also conducted a clinical outcome comparison between two hospitals and to rest of the UK using SITS stroke database. Here, I have summarised the Imaging chapters and clinical outcomes chapter and how they complement each other in the sections below.

9.2 Imaging factors

CT Perfusion can provide cerebral blood flow values and with the severity of CBF reduction, the brain tissue outcome can be predicted. A severely reduced CBF would lead to tissue infarction. The animal models have consistently shown that increasing time from a large vessel occlusion, the size of irreversibly damaged brain tissue increases in size. This was shown to be due to infarction of the penumbra spreading from the core, if there is no restoration of blood flow. The lepto-meningeal collateral failure was also thought to contribute to this expansion of irreversibly ischaemic tissue³¹³. The intra venous thrombolysis clinical studies in humans also showed that benefit from treatment drops with increasing time reaching to no benefit after 4.5 hours²⁶¹. These trials used only plain CT imaging for patient selection. The heterogeneous Imaging factors (such as location of vessel occlusion, lepto-meningeal collateral status, core, penumbra volumes) were not included in these human trials. However, several human advanced imaging studies showed that penumbra can persist in significant proportion in some patients up to longer time delays than 4.5 hours. This is shown to be useful in patient selection for later time window thrombolysis trials such as EXTEND and thrombectomy trials such as DEFUSE 3^{251,273}. Failure of

collateral flow is associated with infarct growth is observed in recent thrombectomy trials³¹⁶.

In this thesis, I have explored whether the penumbra volume reduces with increasing time and particularly tested if good vs. poor collaterals can influence this. Within 6 hours of symptom onset, the penumbra volume did not change significantly with increasing time under 6 hours across a cross section of patients. However, a divergent effect with trend for penumbra volume decreasing with increasing time in patients with poor collaterals was seen. Similar to our findings, Miteff et al showed that good collaterals are associated with large penumbra by limiting expansion of core²⁹⁷. Good collaterals are shown to be associated with favourable clinical outcomes in earlier clinical studies^{292,396}. Due to this overwhelming evidence, subjects with poor collateral status or large “core” were excluded from a landmark thrombectomy trial²⁷¹. Fast progressors (Subjects with fast Infarct growth) have poor collaterals and hence greater need for speedy and earlier intervention in comparison to slow progressors (Subjects with slow Infarct growth) who have good collaterals³⁹⁷.

The Imaging outcomes after ischemic stroke also influence patient outcomes. Haemorrhage and oedema after ischemic stroke have negative influence in patient outcomes. The stroke complications haemorrhage and cerebral oedema can be predicted from patient and baseline imaging factors. In this thesis, I investigated perfusion imaging factors (e.g. core volume), recanalisation status and how they interact in relation to haemorrhage and oedema outcomes. Plain CT can help in excluding stroke mimics and can show early ischaemic signs. Measuring the extent of early ischemic signs with ASPECT score can be valuable in predicting the extent of Ischemia and risk of malignant oedema and haemorrhage^{398,399}. However, plain CT does not give information on perfusion status, collaterals and of course on recanalisation. Previous studies showed increased risk of symptomatic haemorrhage if reperfusion occurred in a large ischaemic area (i.e. large core)³³⁴. However, interaction of recanalisation and core tissue in both oedema and haemorrhage outcomes after IV thrombolysis was not previously studied. We hypothesised that recanalisation of a large ischaemic core would cause significant haemorrhage and non-recanalisation would lead to significant oedema. In my study, a large core volume was associated with any haemorrhage and significant brain oedema, and recanalisation with any

haemorrhage. However, interaction of core size, recanalisation was not associated with haemorrhage or oedema. Oedema, haemorrhage was less seen in early improvers (recanalised) compared to no improvers (late recanalised) or no improvers (non-recanalised).

Although several CT perfusion parameters have been validated, there is no standardisation of what parameters and what thresholds best define the brain tissue into core, penumbra. Moreover, micro vascular capillary heterogeneity is not incorporated and homogeneity is assumed in the standard perfusion models. Capillary transit time heterogeneity (CTTH) was hypothesised and in this thesis using CT perfusion images, CTTH was at first derived through a complex model; once successful, CTTH was then explored in studying two main Imaging aspects; does CTTH differ significantly in core, penumbra and non-core-non-penumbra tissue (i.e. Does CTTH vary significantly in penumbra and non-core-non-penumbra infarction); does the subjects with non-core-non-penumbra tissue infarction have different risk factors and patient demographics; whether CTTH values vary significantly in this group. This information would complement other patient outcome factors in previous chapters. Although the CTTH work did not provide any definitive answers, we were successful in deriving the Capillary level parameter in CT perfusion complementing MR perfusion capillary level work and paving the way for larger studies using CT perfusion images.

9.3 Stroke care model and/ or Organisational factors:

The literature on stroke patient outcomes comparison in different stroke care models is limited. Hyper-acute stroke Units covering a larger geographical area could lead to treatment delays and also lead to bias in treating even most severe strokes if transferred from smaller centres. Transferred patients contributed to higher risk of poorer outcomes in hospital registry study⁴⁰⁰. Also, patient demographics such as socio-economic status which is not captured routinely could contribute to patient outcomes. Repatriation of patients from one hospital to other hospital may compromise continuity of care and lead to poor functional outcomes. In this thesis, stroke outcomes were compared between two hospitals in Glasgow (with a different geographical catchment and socio-economic status) and with the rest of the UK. Referrals from small hospitals to Southern General hospital had poorer outcomes and increased mortality

compared to the direct admissions. This was not fully explained by the onset to treatment time. This may be due to other factors as mentioned above, such as socio-economic status, lack of continuity of care as these patients were more likely to be repatriated soon after acute stroke.

Imaging selection can potentially assist decision making in patients requiring inter hospital transfer. If perfusion parameters identify poor collateral and large core, then reperfusion has to happen very quickly to be beneficial and reduce risk of ICH. Transfer of such patients beyond a time threshold could potentially be avoided and local delivery of thrombolytic therapy may be the best option available. Conversely, slow progressor with good collateral patients could be selected for transfer and endovascular treatment. Imaging triage could be a mechanism for improving the quality of regional stroke networks to minimise futile inter hospital transfer.

In conclusion, in this thesis, I have explored Ischaemic Stroke outcomes encompassing advanced imaging and stroke care models.

Bibliography

1. Murray CJ, Lopez AD. Alternative projections of mortality and disability by cause 1990-2020: Global Burden of Disease Study. *Lancet*. 05/24 1997;349(9064):1498-1504.
2. Kelly-Hayes M, Beiser A, Kase CS, Scaramucci A, D'Agostino RB, Wolf PA. The influence of gender and age on disability following ischemic stroke: the Framingham study. *Journal of stroke and cerebrovascular diseases : the official journal of National Stroke Association*. / 2003;12(3):119-126.
3. Rothwell PM, Coull AJ, Giles MF, et al. Change in stroke incidence, mortality, case-fatality, severity, and risk factors in Oxfordshire, UK from 1981 to 2004 (Oxford Vascular Study). *Lancet*. 06/12 2004;363(9425):1925-1933.
4. Di Carlo A. Human and economic burden of stroke. *Age Ageing*. Jan 2009;38(1):4-5.
5. *National Heart, Lung and Blood Institute: Incidence and Prevalence: 2006 Chart Book on Cardiovascular and Lung Diseases*. Bethesda MD2006.
6. Palomeras Soler E, Fossas Felip P, Casado Ruiz V, Cano Orgaz A, Sanz Cartagena P, Muriana Batiste D. The Mataro Stroke Registry: a 10-year registry in a community hospital. *Neurologia*. Jun 2015;30(5):283-289.
7. Adams HP, Jr., Bendixen BH, Kappelle LJ, et al. Classification of subtype of acute ischemic stroke. Definitions for use in a multicenter clinical trial. TOAST. Trial of Org 10172 in Acute Stroke Treatment. *Stroke; a journal of cerebral circulation*. Jan 1993;24(1):35-41.
8. Grau AJ, Weimar C, Buggle F, et al. Risk factors, outcome, and treatment in subtypes of ischemic stroke: the German stroke data bank. *Stroke; a journal of cerebral circulation*. Nov 2001;32(11):2559-2566.
9. Ay H, Furie KL, Singhal A, Smith WS, Sorensen AG, Koroshetz WJ. An evidence-based causative classification system for acute ischemic stroke. *Annals of neurology*. Nov 2005;58(5):688-697.
10. Tissue plasminogen activator for acute ischemic stroke. The National Institute of Neurological Disorders and Stroke rt-PA Stroke Study Group. *The New England journal of medicine*. Dec 14 1995;333(24):1581-1587.
11. Hacke W, Kaste M, Bluhmki E, et al. Thrombolysis with alteplase 3 to 4.5 hours after acute ischemic stroke. *N Engl J Med*. Sep 25 2008;359(13):1317-1329.
12. Rodrigues FB, Neves JB, Caldeira D, Ferro JM, Ferreira JJ, Costa J. Endovascular treatment versus medical care alone for ischaemic stroke: systematic review and meta-analysis. *Bmj*. Apr 18 2016;353:i1754.
13. Goyal M, Menon BK, van Zwam WH, et al. Endovascular thrombectomy after large-vessel ischaemic stroke: a meta-analysis of individual patient data from five randomised trials. *Lancet*. Apr 23 2016;387(10029):1723-1731.
14. Inter collegiate Stroke Working Party. National Clinical Guidelines For Stroke. Royal College of Physicians.; 2016.
[https://www.strokeaudit.org/SupportFiles/Documents/Guidelines/2016-National-Clinical-Guideline-for-Stroke-5t-\(1\).aspx](https://www.strokeaudit.org/SupportFiles/Documents/Guidelines/2016-National-Clinical-Guideline-for-Stroke-5t-(1).aspx).
15. Albers GW, Thijs VN, Wechsler L, et al. Magnetic Resonance Imaging Profiles Predict Clinical Response to Early Reperfusion: The Diffusion and

- Perfusion Imaging Evaluation for Understanding Stroke Evolution (DEFUSE) Study. *Ann.Neurol.* 2006 2006;60(5):508-517.
16. Campbell BC, Mitchell PJ, Kleinig TJ, et al. Endovascular therapy for ischemic stroke with perfusion-imaging selection. *The New England journal of medicine.* Mar 12 2015;372(11):1009-1018.
 17. Saver JL, Goyal M, Bonafe A, et al. Stent-retriever thrombectomy after intravenous t-PA vs. t-PA alone in stroke. *The New England journal of medicine.* Jun 11 2015;372(24):2285-2295.
 18. Bekkers SC, Yazdani SK, Virmani R, Waltenberger J. Microvascular obstruction: underlying pathophysiology and clinical diagnosis. *Journal of the American College of Cardiology.* Apr 20 2010;55(16):1649-1660.
 19. del Zoppo GJ, Schmid-Schonbein GW, Mori E, Copeland BR, Chang CM. Polymorphonuclear leukocytes occlude capillaries following middle cerebral artery occlusion and reperfusion in baboons. *Stroke; a journal of cerebral circulation.* Oct 1991;22(10):1276-1283.
 20. Soares BP, Tong E, Hom J, et al. Reperfusion is a more accurate predictor of follow-up infarct volume than recanalization: a proof of concept using CT in acute ischemic stroke patients. *Stroke; a journal of cerebral circulation.* Jan 2010;41(1):e34-40.
 21. Ostergaard L, Sorensen AG, Chesler DA, et al. Combined diffusion-weighted and perfusion-weighted flow heterogeneity magnetic resonance imaging in acute stroke. *Stroke; a journal of cerebral circulation.* May 2000;31(5):1097-1103.
 22. del Zoppo GJ, Mabuchi T. Cerebral microvessel responses to focal ischemia. *Journal of cerebral blood flow and metabolism : official journal of the International Society of Cerebral Blood Flow and Metabolism.* Aug 2003;23(8):879-894.
 23. Jespersen SN, Ostergaard L. The roles of cerebral blood flow, capillary transit time heterogeneity, and oxygen tension in brain oxygenation and metabolism. *Journal of cerebral blood flow and metabolism : official journal of the International Society of Cerebral Blood Flow and Metabolism.* Feb 2012;32(2):264-277.
 24. Bang OY, Saver JL, Kim SJ, et al. Collateral Flow Predicts Response To Endovascular Therapy For Acute Ischemic Stroke. *Stroke; a journal of cerebral circulation.* Mar 2011;42(3):E95-E95.
 25. Shi Y, Wardlaw JM. Update on cerebral small vessel disease: a dynamic whole-brain disease. *Stroke and vascular neurology.* Sep 2016;1(3):83-92.
 26. Astrup J, Siesjo BK, Symon L. Thresholds in cerebral ischemia - the ischemic penumbra. *Stroke; a journal of cerebral circulation.* Nov-Dec 1981;12(6):723-725.
 27. Pakkenberg B, Gundersen HJ. Neocortical neuron number in humans: effect of sex and age. *J Comp Neurol.* Jul 28 1997;384(2):312-320.
 28. Clarke DD SL. Circulation and energy metabolism of the brain. In: Siegel G AB, Albers RW, SFisher S, ed. *Basic Neurochemistry: Molecular, Cellular, and Medical Aspects.* 6 ed. Philadelphia: Lippincott-Raven; 1999:637-669.
 29. Astrup J, Symon L, Branston NM, Lassen NA. Cortical evoked potential and extracellular K⁺ and H⁺ at critical levels of brain ischemia. *Stroke; a journal of cerebral circulation.* Jan-Feb 1977;8(1):51-57.
 30. Choi DW. Excitotoxic cell death. *Journal of neurobiology.* Nov 1992;23(9):1261-1276.
 31. Siesjo B. Calcium, excitotoxins, and brain damage. *News Physiol Sci.* 1990(5):120-125.

32. Bhardwaj A, Northington FJ, Ichord RN, Hanley DF, Traystman RJ, Koehler RC. Characterization of ionotropic glutamate receptor-mediated nitric oxide production in vivo in rats. *Stroke; a journal of cerebral circulation*. Apr 1997;28(4):850-856; discussion 856-857.
33. Lipton P. Ischemic cell death in brain neurons. *Physiological reviews*. Oct 1999;79(4):1431-1568.
34. Allen CL, Bayraktutan U. Oxidative stress and its role in the pathogenesis of ischaemic stroke. *International journal of stroke : official journal of the International Stroke Society*. Dec 2009;4(6):461-470.
35. Wang Q, Tang XN, Yenari MA. The inflammatory response in stroke. *J Neuroimmunol*. Mar 2007;184(1-2):53-68.
36. Love S. Apoptosis and brain ischaemia. *Prog Neuropsychopharmacol Biol Psychiatry*. Apr 2003;27(2):267-282.
37. Hossmann KA. Periinfarct depolarizations. *Cerebrovascular and brain metabolism reviews*. Fall 1996;8(3):195-208.
38. Dohmen C, Sakowitz OW, Fabricius M, et al. Spreading depolarizations occur in human ischemic stroke with high incidence. *Annals of neurology*. Jun 2008;63(6):720-728.
39. Grubb RL, Jr., Raichle ME, Phelps ME, Ratcheson RA. Effects of increased intracranial pressure on cerebral blood volume, blood flow, and oxygen utilization in monkeys. *Journal of neurosurgery*. Oct 1975;43(4):385-398.
40. Powers WJ. Cerebral hemodynamics in ischemic cerebrovascular disease. *Ann Neurol*. 1991;29(3):231-240.
41. Sette G, Baron JC, Mazoyer B, Levasseur M, Pappata S, Crouzel C. Local brain haemodynamics and oxygen metabolism in cerebrovascular disease. Positron emission tomography. *Brain : a journal of neurology*. Aug 1989;112 (Pt 4):931-951.
42. Simard JM, Kent TA, Chen MK, Tarasov KV, Gerzanich V. Brain oedema in focal ischaemia: molecular pathophysiology and theoretical implications. *Lancet Neurol*. Mar 2007;6(3):258-268.
43. Hossmann KA HW. Textbook of Stroke Medicine. In: Brainin M HD, ed. *Textbook of Stroke Medicine*. Vol 1. NewYork: Cambridge University Press; 2010:19.
44. Mori K, Miyazaki M, Iwase H, Maeda M. Temporal profile of changes in brain tissue extracellular space and extracellular ion (Na⁺), K⁺) concentrations after cerebral ischemia and the effects of mild cerebral hypothermia. *Journal of neurotrauma*. Oct 2002;19(10):1261-1270.
45. Hoehn-Berlage M, Miyazawa T, Kloiber O, Hossmann KA. 31P NMR spectroscopic investigation of brain resuscitation: global reversible ischemia of rat brain. *Minerva anesthesiologica*. Oct 1994;60(10):493-496.
46. Betz AL, Iannotti F, Hoff JT. Brain edema: a classification based on blood-brain barrier integrity. *Cerebrovascular and brain metabolism reviews*. Summer 1989;1(2):133-154.
47. Yang Y, Rosenberg GA. Blood-brain barrier breakdown in acute and chronic cerebrovascular disease. *Stroke; a journal of cerebral circulation*. Nov 2011;42(11):3323-3328.
48. Tanaka M, Ishihara Y, Mizuno S, et al. Progression of vasogenic edema induced by activated microglia under permanent middle cerebral artery occlusion. *Biochemical and biophysical research communications*. Feb 5 2018;496(2):582-587.
49. Simard JM, Chen M, Tarasov KV, et al. Newly expressed SUR1-regulated NC(Ca-ATP) channel mediates cerebral edema after ischemic stroke. *Nature medicine*. Apr 2006;12(4):433-440.

50. Simard JM, Tsybalyuk N, Tsybalyuk O, Ivanova S, Yurovsky V, Gerzanich V. Glibenclamide is superior to decompressive craniectomy in a rat model of malignant stroke. *Stroke; a journal of cerebral circulation*. Mar 2010;41(3):531-537.
51. Sheth KN, Kimberly WT, Elm JJ, et al. Exploratory analysis of glyburide as a novel therapy for preventing brain swelling. *Neurocritical care*. Aug 2014;21(1):43-51.
52. Khatri R, McKinney AM, Swenson B, Janardhan V. Blood-brain barrier, reperfusion injury, and hemorrhagic transformation in acute ischemic stroke. *Neurology*. Sep 25 2012;79(13 Suppl 1):S52-57.
53. Wang X, Tsuji K, Lee SR, et al. Mechanisms of hemorrhagic transformation after tissue plasminogen activator reperfusion therapy for ischemic stroke. *Stroke; a journal of cerebral circulation*. Nov 2004;35(11 Suppl 1):2726-2730.
54. Sussman ES, Connolly ES, Jr. Hemorrhagic transformation: a review of the rate of hemorrhage in the major clinical trials of acute ischemic stroke. *Frontiers in neurology*. 2013;4:69.
55. Jaillard A, Cornu C, Durieux A, et al. Hemorrhagic transformation in acute ischemic stroke. The MAST-E study. MAST-E Group. *Stroke; a journal of cerebral circulation*. Jul 1999;30(7):1326-1332.
56. Kidwell CS, Saver JL, Carneado J, et al. Predictors of hemorrhagic transformation in patients receiving intra-arterial thrombolysis. *Stroke; a journal of cerebral circulation*. Mar 2002;33(3):717-724.
57. Tan S, Wang D, Liu M, Zhang S, Wu B, Liu B. Frequency and predictors of spontaneous hemorrhagic transformation in ischemic stroke and its association with prognosis. *Journal of neurology*. May 2014;261(5):905-912.
58. Nogueira RG, Gupta R, Jovin TG, et al. Predictors and clinical relevance of hemorrhagic transformation after endovascular therapy for anterior circulation large vessel occlusion strokes: a multicenter retrospective analysis of 1122 patients. *Journal of neurointerventional surgery*. Jan 2015;7(1):16-21.
59. Paciaroni M, Agnelli G, Corea F, et al. Early hemorrhagic transformation of brain infarction: rate, predictive factors, and influence on clinical outcome: results of a prospective multicenter study. *Stroke; a journal of cerebral circulation*. Aug 2008;39(8):2249-2256.
60. Bang OY, Saver JL, Kim SJ, et al. Collateral Flow Averts Hemorrhagic Transformation After Endovascular Therapy for Acute Ischemic Stroke. *Stroke; a journal of cerebral circulation*. Aug 2011;42(8):2235-U2329.
61. Pulsinelli WA, Brierley JB. A new model of bilateral hemispheric ischemia in the unanesthetized rat. *Stroke; a journal of cerebral circulation*. May-Jun 1979;10(3):267-272.
62. Garcia JH. Experimental ischemic stroke: a review. *Stroke; a journal of cerebral circulation*. Jan-Feb 1984;15(1):5-14.
63. Hossmann KA. Animal Models of Cerebral Ischemia. 1. Review of Literature. *Cerebrovascular diseases*. 1991;1(suppl 1)(Suppl. 1):2-15.
64. Garcia JH, Liu KF, Ho KL. Neuronal necrosis after middle cerebral artery occlusion in Wistar rats progresses at different time intervals in the caudoputamen and the cortex. *Stroke; a journal of cerebral circulation*. Apr 1995;26(4):636-642; discussion 643.
65. Hudgins WR, Garcia JH. Transorbital approach to the middle cerebral artery of the squirrel monkey: a technique for experimental cerebral

- infarction applicable to ultrastructural studies. *Stroke; a journal of cerebral circulation*. Mar-Apr 1970;1(2):107-111.
66. Hossmann KA, Schuier FJ. Experimental brain infarcts in cats. I. Pathophysiological observations. *Stroke; a journal of cerebral circulation*. Nov-Dec 1980;11(6):583-592.
 67. Tamura A, Graham DI, McCulloch J, Teasdale GM. Focal cerebral ischaemia in the rat: 1. Description of technique and early neuropathological consequences following middle cerebral artery occlusion. *Journal of cerebral blood flow and metabolism : official journal of the International Society of Cerebral Blood Flow and Metabolism*. 1981;1(1):53-60.
 68. Koizumi J YY, Nakazawa T, Oeneda G. Experimental studies of ischemic brain edema. A new experimental model of cerebral embolism in rats in which recirculation can be introduced in the ischemic area. *Jpn J Stroke*. 1986;8:1-8.
 69. Back T, Hoehn-Berlage M, Kohno K, Hossmann KA. Diffusion nuclear magnetic resonance imaging in experimental stroke. Correlation with cerebral metabolites. *Stroke; a journal of cerebral circulation*. Feb 1994;25(2):494-500.
 70. Kogure K, Alonso OF. A pictorial representation of endogenous brain ATP by a bioluminescent method. *Brain research*. Oct 13 1978;154(2):273-284.
 71. Paschen W, Niebuhr I, Hossmann KA. A bioluminescence method for the demonstration of regional glucose distribution in brain slices. *Journal of neurochemistry*. Feb 1981;36(2):513-517.
 72. Paschen W. Regional quantitative determination of lactate in brain sections. A bioluminescent approach. *Journal of cerebral blood flow and metabolism : official journal of the International Society of Cerebral Blood Flow and Metabolism*. Dec 1985;5(4):609-612.
 73. Hossmann KA MG. *Multimodal Mapping of the ischemic Penumbra in Animal Models*. Newyork: Mercel Dekker; 2007.
 74. Welsh FA, Marcy VR, Sims RE. NADH fluorescence and regional energy metabolites during focal ischemia and reperfusion of rat brain. *Journal of cerebral blood flow and metabolism : official journal of the International Society of Cerebral Blood Flow and Metabolism*. May 1991;11(3):459-465.
 75. Hata R, Maeda K, Hermann D, Mies G, Hossmann KA. Dynamics of regional brain metabolism and gene expression after middle cerebral artery occlusion in mice. *Journal of cerebral blood flow and metabolism : official journal of the International Society of Cerebral Blood Flow and Metabolism*. Feb 2000;20(2):306-315.
 76. Marchal G, Benali K, Iglesias S, Viader F, Derlon JM, Baron JC. Voxel-based mapping of irreversible ischaemic damage with PET in acute stroke. *Brain*. 1999;122 (Pt 12):2387-2400.
 77. Heiss WD, Kracht L, Grond M, et al. Early [(11)C]Flumazenil/H(2)O positron emission tomography predicts irreversible ischemic cortical damage in stroke patients receiving acute thrombolytic therapy. *Stroke*. 2000;31(2):366-369.
 78. Kuge Y, Yokota C, Tagaya M, et al. Serial changes in cerebral blood flow and flow-metabolism uncoupling in primates with acute thromboembolic stroke. *Journal of cerebral blood flow and metabolism : official journal of the International Society of Cerebral Blood Flow and Metabolism*. Mar 2001;21(3):202-210.

79. Marchal G, Benali K, Iglesias S, Viader F, Derlon JM, Baron JC. Voxel-based mapping of irreversible ischaemic damage with PET in acute stroke. *Brain : a journal of neurology*. Dec 1999;122 (Pt 12):2387-2400.
80. Symon L, Branston NM, Strong AJ, Hope TD. The concepts of thresholds of ischaemia in relation to brain structure and function. *Journal of clinical pathology. Supplement*. 1977;11:149-154.
81. Symon L, Pasztor E, Branston NM. The distribution and density of reduced cerebral blood flow following acute middle cerebral artery occlusion: an experimental study by the technique of hydrogen clearance in baboons. *Stroke*. 1974;5(3):355-364.
82. Hossmann KA. Viability thresholds and the penumbra of focal ischemia. *Ann Neurol*. Oct 1994;36(4):557-565.
83. Muir KW, Buchan A, von Kummer R, Rother J, Baron JC. Imaging of acute stroke. *Lancet Neurol*. Sep 2006;5(9):755-768.
84. Jones TH, Morawetz RB, Crowell RM, et al. Thresholds of focal cerebral ischemia in awake monkeys. *J Neurosurg*. Jun 1981;54(6):773-782.
85. Baron JC. Mapping the ischaemic penumbra with PET: a new approach. *Brain : a journal of neurology*. Jan 2001;124(Pt 1):2-4.
86. Lassen NA, Fieschi C, Lenzi GL. Ischemic Penumbra and Neuronal Death - Comments on the Therapeutic Window in Acute Stroke with Particular Reference to Thrombolytic Therapy. *Cerebrovascular diseases*. 1991;1:32-&.
87. Symon L, Lassen NA, Astrup J, Branston NM. Thresholds of ischaemia in brain cortex. *Advances in experimental medicine and biology*. Jul 4-7 1977;94:775-782.
88. Baron JC. Mapping the ischaemic penumbra with PET: implications for acute stroke treatment. *Cerebrovascular diseases*. Jul-Aug 1999;9(4):193-201.
89. Mies G, Ishimaru S, Xie Y, Seo K, Hossmann KA. Ischemic thresholds of cerebral protein synthesis and energy state following middle cerebral artery occlusion in rat. *Journal of cerebral blood flow and metabolism : official journal of the International Society of Cerebral Blood Flow and Metabolism*. Sep 1991;11(5):753-761.
90. Paschen W, Mies G, Hossmann KA. Threshold relationship between cerebral blood flow, glucose utilization, and energy metabolites during development of stroke in gerbils. *Experimental neurology*. Sep 1992;117(3):325-333.
91. Allen KL, Busza AL, Proctor E, et al. Controllable graded cerebral ischaemia in the gerbil: studies of cerebral blood flow and energy metabolism by hydrogen clearance and ³¹P NMR spectroscopy. *NMR in biomedicine*. May-Jun 1993;6(3):181-186.
92. Naritomi H, Sasaki M, Kanashiro M, Kitani M, Sawada T. Flow thresholds for cerebral energy disturbance and Na⁺ pump failure as studied by in vivo ³¹P and ²³Na nuclear magnetic resonance spectroscopy. *Journal of cerebral blood flow and metabolism : official journal of the International Society of Cerebral Blood Flow and Metabolism*. Feb 1988;8(1):16-23.
93. Branston NM, Strong AJ, Symon L. Extracellular potassium activity, evoked potential and tissue blood flow. Relationships during progressive ischaemia in baboon cerebral cortex. *Journal of the neurological sciences*. Jul 1977;32(3):305-321.
94. Morawetz RB, Crowell RH, DeGirolami U, Marcoux FW, Jones TH, Halsey JH. Regional cerebral blood flow thresholds during cerebral ischemia. *Federation proceedings*. Oct 1979;38(11):2493-2494.

95. Astrup J S, Branston NM, Lassen NA Thresholds of cerebral ischemia. In: schmiedek P GO, Spetzler RF, ed. *Microsurgery for stroke*. Berlin: Springer-verlag; 1976:16-21.
96. Heiss WD, Hayakawa T, Waltz AG. Cortical neuronal function during ischemia. Effects of occlusion of one middle cerebral artery on single-unit activity in cats. *Arch Neurol*. Dec 1976;33(12):813-820.
97. Branston NM, Symon L, Crockard HA, Pasztor E. Relationship between the cortical evoked potential and local cortical blood flow following acute middle cerebral artery occlusion in the baboon. *Experimental neurology*. Nov 1974;45(2):195-208.
98. Morawetz RB, DeGirolami U, Ojemann RG, Marcoux FW, Crowell RM. Cerebral blood flow determined by hydrogen clearance during middle cerebral artery occlusion in unanesthetized monkeys. *Stroke; a journal of cerebral circulation*. Mar-Apr 1978;9(2):143-149.
99. Heiss WD, Graf R, Wienhard K, et al. Dynamic penumbra demonstrated by sequential multitracer PET after middle cerebral artery occlusion in cats. *Journal of cerebral blood flow and metabolism : official journal of the International Society of Cerebral Blood Flow and Metabolism*. Nov 1994;14(6):892-902.
100. Heiss WD, Graf R. The ischemic penumbra. *Current opinion in neurology*. Feb 1994;7(1):11-19.
101. Heiss WD, Rosner G. Functional recovery of cortical neurons as related to degree and duration of ischemia. *Annals of neurology*. Sep 1983;14(3):294-301.
102. Heiss WD. The ischemic penumbra: correlates in imaging and implications for treatment of ischemic stroke. The Johann Jacob Wepfer award 2011. *Cerebrovascular diseases*. 2011;32(4):307-320.
103. Denny-Brown D, Meyer JS. The cerebral collateral circulation. II. Production of cerebral infarction by ischemic anoxia and its reversibility in early stages. *Neurology*. Aug 1957;7(8):567-579.
104. Kaplan B, Brint S, Tanabe J, Jacewicz M, Wang XJ, Pulsinelli W. Temporal thresholds for neocortical infarction in rats subjected to reversible focal cerebral ischemia. *Stroke; a journal of cerebral circulation*. Aug 1991;22(8):1032-1039.
105. Mies G, Iijima T, Hossmann KA. Correlation between peri-infarct DC shifts and ischaemic neuronal damage in rat. *Neuroreport*. Jun 1993;4(6):709-711.
106. Pappata S, Fiorelli M, Rommel T, et al. PET study of changes in local brain hemodynamics and oxygen metabolism after unilateral middle cerebral artery occlusion in baboons. *Journal of cerebral blood flow and metabolism : official journal of the International Society of Cerebral Blood Flow and Metabolism*. May 1993;13(3):416-424.
107. Touzani O, Young AR, Derlon JM, et al. Sequential studies of severely hypometabolic tissue volumes after permanent middle cerebral artery occlusion. A positron emission tomographic investigation in anesthetized baboons. *Stroke; a journal of cerebral circulation*. Nov 1995;26(11):2112-2119.
108. Young AR, Sette G, Touzani O, et al. Relationships between high oxygen extraction fraction in the acute stage and final infarction in reversible middle cerebral artery occlusion: an investigation in anesthetized baboons with positron emission tomography. *Journal of cerebral blood flow and metabolism : official journal of the International Society of Cerebral Blood Flow and Metabolism*. Nov 1996;16(6):1176-1188.

109. Touzani O, Young AR, Derlon JM, Baron JC, MacKenzie ET. Progressive impairment of brain oxidative metabolism reversed by reperfusion following middle cerebral artery occlusion in anaesthetized baboons. *Brain research*. Aug 29 1997;767(1):17-25.
110. Young AR, Touzani O, Derlon JM, Sette G, MacKenzie ET, Baron JC. Early reperfusion in the anesthetized baboon reduces brain damage following middle cerebral artery occlusion: a quantitative analysis of infarction volume. *Stroke*. Mar 1997;28(3):632-637; discussion 637-638.
111. Perel P, Roberts I, Sena E, et al. Comparison of treatment effects between animal experiments and clinical trials: systematic review. *Bmj*. Jan 27 2007;334(7586):197.
112. Baron JC, Frackowiak RS, Herholz K, et al. Use of PET methods for measurement of cerebral energy metabolism and hemodynamics in cerebrovascular disease. *Journal of cerebral blood flow and metabolism : official journal of the International Society of Cerebral Blood Flow and Metabolism*. Dec 1989;9(6):723-742.
113. Furlan M, Marchal G, Viader F, Derlon JM, Baron JC. Spontaneous neurological recovery after stroke and the fate of the ischemic penumbra. *Annals of neurology*. Aug 1996;40(2):216-226.
114. Heiss WD, Huber M, Fink GR, et al. Progressive derangement of periinfarct viable tissue in ischemic stroke. *Journal of cerebral blood flow and metabolism : official journal of the International Society of Cerebral Blood Flow and Metabolism*. Mar 1992;12(2):193-203.
115. Marchal G, Beaudouin V, Rioux P, et al. Prolonged persistence of substantial volumes of potentially viable brain tissue after stroke: a correlative PET-CT study with voxel-based data analysis. *Stroke; a journal of cerebral circulation*. Apr 1996;27(4):599-606.
116. Read SJ, Hirano T, Abbott DF, et al. The fate of hypoxic tissue on 18F-fluoromisonidazole positron emission tomography after ischemic stroke. *Annals of neurology*. 2000;48(2):228-235.
117. Markus R, Reutens DC, Kazui S, et al. Hypoxic tissue in ischaemic stroke: persistence and clinical consequences of spontaneous survival. *Brain : a journal of neurology*. Jun 2004;127(Pt 6):1427-1436.
118. Demchuk AM, Hill MD, Barber PA, Silver B, Patel SC, Levine SR. Importance of early ischemic computed tomography changes using ASPECTS in NINDS rtPA Stroke Study. *Stroke; a journal of cerebral circulation*. Oct 2005;36(10):2110-2115.
119. Tanne D, Kasner SE, Demchuk AM, et al. Markers of increased risk of intracerebral hemorrhage after intravenous recombinant tissue plasminogen activator therapy for acute ischemic stroke in clinical practice: the Multicenter rt-PA Stroke Survey. *Circulation*. Apr 09 2002;105(14):1679-1685.
120. Hacke W, Kaste M, Bluhmki E, et al. Thrombolysis with alteplase 3 to 4.5 hours after acute ischemic stroke. *The New England journal of medicine*. 09/25 2008;359(13):1317-1329.
121. Dzialowski I, Weber J, Doerfler A, Forsting M, von Kummer R. Brain tissue water uptake after middle cerebral artery occlusion assessed with CT. *Journal of neuroimaging : official journal of the American Society of Neuroimaging*. Jan 2004;14(1):42-48.
122. Marks MP. CT in ischemic stroke. *Neuroimaging clinics of North America*. Aug 1998;8(3):515-523.

123. Na DG, Kim EY, Ryoo JW, et al. CT sign of brain swelling without concomitant parenchymal hypoattenuation: comparison with diffusion- and perfusion-weighted MR imaging. *Radiology*. Jun 2005;235(3):992-948.
124. Butcher KS, Lee SB, Parsons MW, et al. Differential prognosis of isolated cortical swelling and hypoattenuation on CT in acute stroke. *Stroke; a journal of cerebral circulation*. Mar 2007;38(3):941-947.
125. Parsons MW, Pepper EM, Bateman GA, Wang Y, Levi CR. Identification of the penumbra and infarct core on hyperacute noncontrast and perfusion CT. *Neurology*. Mar 6 2007;68(10):730-736.
126. Mullins ME, Schaefer PW, Sorensen AG, et al. CT and conventional and diffusion-weighted MR imaging in acute stroke: study in 691 patients at presentation to the emergency department. *Radiology*. Aug 2002;224(2):353-360.
127. Barber PA, Demchuk AM, Zhang J, Buchan AM. Validity and reliability of a quantitative computed tomography score in predicting outcome of hyperacute stroke before thrombolytic therapy. ASPECTS Study Group. Alberta Stroke Programme Early CT Score. *Lancet*. May 13 2000;355(9216):1670-1674.
128. Sorensen AG, Buonanno FS, Gonzalez RG, et al. Hyperacute stroke: evaluation with combined multisection diffusion-weighted and hemodynamically weighted echo-planar MR imaging. *Radiology*. May 1996;199(2):391-401.
129. Gonzalez RG, Schaefer PW, Buonanno FS, et al. Diffusion-weighted MR imaging: diagnostic accuracy in patients imaged within 6 hours of stroke symptom onset. *Radiology*. Jan 1999;210(1):155-162.
130. Tomura N, Uemura K, Inugami A, Fujita H, Higano S, Shishido F. Early CT finding in cerebral infarction: obscuration of the lentiform nucleus. *Radiology*. Aug 1988;168(2):463-467.
131. Hacke W, Kaste M, Fieschi C, et al. Intravenous thrombolysis with recombinant tissue plasminogen activator for acute hemispheric stroke. The European Cooperative Acute Stroke Study (ECASS). *Jama*. Oct 4 1995;274(13):1017-1025.
132. von Kummer R, Allen KL, Holle R, et al. Acute stroke: usefulness of early CT findings before thrombolytic therapy. *Radiology*. Nov 1997;205(2):327-333.
133. Wardlaw JM, Dorman PJ, Lewis SC, Sandercock PA. Can stroke physicians and neuroradiologists identify signs of early cerebral infarction on CT? *Journal of neurology, neurosurgery, and psychiatry*. Nov 1999;67(5):651-653.
134. von Kummer R, Holle R, Gizyska U, et al. Interobserver agreement in assessing early CT signs of middle cerebral artery infarction. *AJNR. American journal of neuroradiology*. Oct 1996;17(9):1743-1748.
135. Adams HP, Jr., Adams RJ, Brott T, et al. Guidelines for the early management of patients with ischemic stroke: A scientific statement from the Stroke Council of the American Stroke Association. *Stroke; a journal of cerebral circulation*. Apr 2003;34(4):1056-1083.
136. Lansberg MG, Albers GW, Beaulieu C, Marks MP. Comparison of diffusion-weighted MRI and CT in acute stroke. *Neurology*. Apr 25 2000;54(8):1557-1561.
137. Barber PA, Darby DG, Desmond PM, et al. Identification of major ischemic change. Diffusion-weighted imaging versus computed tomography. *Stroke; a journal of cerebral circulation*. Oct 1999;30(10):2059-2065.

138. Jaillard A, Hommel M, Baird AE, et al. Significance of early CT signs in acute stroke. A CT scan-diffusion MRI study. *Cerebrovascular diseases*. 2002;13(1):47-56.
139. Dirnagl U, Iadecola C, Moskowitz MA. Pathobiology of ischaemic stroke: an integrated view. *Trends in neurosciences*. Sep 1999;22(9):391-397.
140. Parsons MW. Perfusion CT: is it clinically useful? *International journal of stroke : official journal of the International Stroke Society*. Feb 2008;3(1):41-50.
141. Wintermark M, Flanders AE, Velthuis B, et al. Perfusion-CT assessment of infarct core and penumbra: receiver operating characteristic curve analysis in 130 patients suspected of acute hemispheric stroke. *Stroke; a journal of cerebral circulation*. Apr 2006;37(4):979-985.
142. Baird AE, Benfield A, Schlaug G, et al. Enlargement of human cerebral ischemic lesion volumes measured by diffusion-weighted magnetic resonance imaging. *Ann Neurol*. May 1997;41(5):581-589.
143. Nagakane Y, Christensen S, Brekenfeld C, et al. EPITHET: Positive Result After Reanalysis Using Baseline Diffusion-Weighted Imaging/Perfusion-Weighted Imaging Co-Registration. *Stroke; a journal of cerebral circulation*. Jan 2011;42(1):59-64.
144. Marks MP, Olivot JM, Kemp S, et al. Patients with acute stroke treated with intravenous tPA 3-6 hours after stroke onset: correlations between MR angiography findings and perfusion- and diffusion-weighted imaging in the DEFUSE study. *Radiology*. Nov 2008;249(2):614-623.
145. Parsons MW, Christensen S, McElduff P, et al. Pretreatment diffusion- and perfusion-MR lesion volumes have a crucial influence on clinical response to stroke thrombolysis. *Journal of cerebral blood flow and metabolism : official journal of the International Society of Cerebral Blood Flow and Metabolism*. Jun 2010;30(6):1214-1225.
146. Kucinski T, Naumann D, Knab R, et al. Tissue at risk is overestimated in perfusion-weighted imaging: MR imaging in acute stroke patients without vessel recanalization. *AJNR. American journal of neuroradiology*. Apr 2005;26(4):815-819.
147. Dani AK, Thomas RGR, Chappell FM, et al. Computed tomography and magnetic resonance perfusion imaging in ischemic stroke: Definitions and thresholds. *Annals of neurology*. 2011 2011;70(3):384-401.
148. Bivard A, Spratt N, Levi C, Parsons M. Perfusion computer tomography: imaging and clinical validation in acute ischaemic stroke. *Brain : a journal of neurology*. Nov 2011;134(Pt 11):3408-3416.
149. Axel L. Cerebral perfusion CT techniques. *Radiology*. Dec 2004;233(3):935; author reply 935.
150. Fiebach JB, Schellinger PD, Jansen O, et al. CT and diffusion-weighted MR imaging in randomized order: diffusion-weighted imaging results in higher accuracy and lower interrater variability in the diagnosis of hyperacute ischemic stroke. *Stroke; a journal of cerebral circulation*. Sep 2002;33(9):2206-2210.
151. Parsons MW, Pepper EM, Chan V, et al. Perfusion computed tomography: Prediction of final infarct extent and stroke outcome. *Annals of neurology*. November 2005;58(5):672-679.
152. Rother J, Jonetz-Mentzel L, Fiala A, et al. Hemodynamic assessment of acute stroke using dynamic single-slice computed tomographic perfusion imaging. *Arch Neurol*. Aug 2000;57(8):1161-1166.
153. Wintermark M, Fischbein NJ, Smith WS, Ko NU, Quist M, Dillon WP. Accuracy of dynamic perfusion CT with deconvolution in detecting acute

- hemispheric stroke. *AJNR. American journal of neuroradiology*. Jan 2005;26(1):104-112.
154. Muir KW, Halbert HM, Baird TA, McCormick M, Teasdale E. Visual evaluation of perfusion computed tomography in acute stroke accurately estimates infarct volume and tissue viability. *Journal of Neurology, Neurosurgery and Psychiatry*. March 2006;77(3):334-339.
 155. Kudo K, Terae S, Katoh C, et al. Quantitative cerebral blood flow measurement with dynamic perfusion CT using the vascular-pixel elimination method: comparison with H₂(15)O positron emission tomography. *AJNR. American journal of neuroradiology*. Mar 2003;24(3):419-426.
 156. Wintermark M, Thiran JP, Maeder P, Schnyder P, Meuli R. Simultaneous measurement of regional cerebral blood flow by perfusion CT and stable xenon CT: a validation study. *AJNR. American journal of neuroradiology*. May 2001;22(5):905-914.
 157. Murphy BD, Fox AJ, Lee DH, et al. White matter thresholds for ischemic penumbra and infarct core in patients with acute stroke: CT perfusion study. *Radiology*. Jun 2008;247(3):818-825.
 158. Kamalian S, Kamalian S, Maas MB, et al. CT cerebral blood flow maps optimally correlate with admission diffusion-weighted imaging in acute stroke but thresholds vary by postprocessing platform. *Stroke; a journal of cerebral circulation*. Jul 2011;42(7):1923-1928.
 159. Axel L. Cerebral blood flow determination by rapid-sequence computed tomography: theoretical analysis. *Radiology*. Dec 1980;137(3):679-686.
 160. Miles KA. Measurement of tissue perfusion by dynamic computed tomography. *The British journal of radiology*. May 1991;64(761):409-412.
 161. Konstas AA, Goldmakher GV, Lee TY, Lev MH. Theoretic basis and technical implementations of CT perfusion in acute ischemic stroke, part 1: Theoretic basis. *AJNR. American journal of neuroradiology*. Apr 2009;30(4):662-668.
 162. Mullani NA, Gould KL. First-pass measurements of regional blood flow with external detectors. *Journal of nuclear medicine : official publication, Society of Nuclear Medicine*. Jul 1983;24(7):577-581.
 163. Konstas AA, Goldmakher GV, Lee TY, Lev MH. Theoretic basis and technical implementations of CT perfusion in acute ischemic stroke, part 2: technical implementations. *AJNR. American journal of neuroradiology*. May 2009;30(5):885-892.
 164. Wintermark M, Maeder P, Thiran JP, Schnyder P, Meuli R. Quantitative assessment of regional cerebral blood flows by perfusion CT studies at low injection rates: a critical review of the underlying theoretical models. *European radiology*. 2001;11(7):1220-1230.
 165. TY L. Scientific basis and validation. In: Miles KA EJ, Konig M, ed. *Multidetector Computed Tomography in Cerebrovascular Disease*. Abingdon, UK: Informa Health Care; 2007:13-27.
 166. Ostergaard L, Weisskoff RM, Chesler DA, Gyldensted C, Rosen BR. High resolution measurement of cerebral blood flow using intravascular tracer bolus passages. Part I: Mathematical approach and statistical analysis. *Magnetic resonance in medicine*. Nov 1996;36(5):715-725.
 167. Calamante F, Gadian DG, Connelly A. Delay and dispersion effects in dynamic susceptibility contrast MRI: simulations using singular value decomposition. *Magnetic resonance in medicine*. Sep 2000;44(3):466-473.

168. Eastwood JD, Lev MH, Azhari T, et al. CT perfusion scanning with deconvolution analysis: pilot study in patients with acute middle cerebral artery stroke. *Radiology*. Jan 2002;222(1):227-236.
169. Meier P, Zierler KL. On the theory of the indicator-dilution method for measurement of blood flow and volume. *J Appl Physiol*. Jun 1954;6(12):731-744.
170. Ostergaard L. Principles of cerebral perfusion imaging by bolus tracking. *Journal of magnetic resonance imaging : JMRI*. Dec 2005;22(6):710-717.
171. Ostergaard L, Sorensen AG, Kwong KK, Weisskoff RM, Gyldensted C, Rosen BR. High resolution measurement of cerebral blood flow using intravascular tracer bolus passages. Part II: Experimental comparison and preliminary results. *Magnetic resonance in medicine*. Nov 1996;36(5):726-736.
172. Lee T BM. Implementing deconvolution analysis for perfusion CT. In: Miles KA EJ, Konig M, ed. *Multidetector Computed Tomography in Cerebrovascular disease*. Abingdon, UK: Informa Healthcare; 2007:29-45.
173. Wu O, Ostergaard L, Weisskoff RM, Benner T, Rosen BR, Sorensen AG. Tracer arrival timing-insensitive technique for estimating flow in MR perfusion-weighted imaging using singular value decomposition with a block-circulant deconvolution matrix. *Magnetic resonance in medicine*. Jul 2003;50(1):164-174.
174. Nabavi DG, Cenic A, Henderson S, Gelb AW, Lee TY. Perfusion mapping using computed tomography allows accurate prediction of cerebral infarction in experimental brain ischemia. *Stroke; a journal of cerebral circulation*. Jan 2001;32(1):175-183.
175. Calamante F, Gadian DG, Connelly A. Quantification of perfusion using bolus tracking magnetic resonance imaging in stroke: assumptions, limitations, and potential implications for clinical use. *Stroke; a journal of cerebral circulation*. Apr 2002;33(4):1146-1151.
176. Schaefer PW, Mui K, Kamalian S, Nogueira RG, Gonzalez RG, Lev MH. Avoiding "pseudo-reversibility" of CT-CBV infarct core lesions in acute stroke patients after thrombolytic therapy: the need for algorithmically "delay-corrected" CT perfusion map postprocessing software. *Stroke; a journal of cerebral circulation*. Aug 2009;40(8):2875-2878.
177. Ostergaard L, Chesler DA, Weisskoff RM, Sorensen AG, Rosen BR. Modeling cerebral blood flow and flow heterogeneity from magnetic resonance residue data. *Journal of cerebral blood flow and metabolism : official journal of the International Society of Cerebral Blood Flow and Metabolism*. Jun 1999;19(6):690-699.
178. Mouridsen K, Friston K, Hjort N, Gyldensted L, Ostergaard L, Kiebel S. Bayesian estimation of cerebral perfusion using a physiological model of microvasculature. *NeuroImage*. Nov 1 2006;33(2):570-579.
179. Andersen IK, Szymkowiak A, Rasmussen CE, et al. Perfusion quantification using Gaussian process deconvolution. *Magnetic resonance in medicine*. Aug 2002;48(2):351-361.
180. Mehndiratta A, MacIntosh BJ, Crane DE, Payne SJ, Chappell MA. A control point interpolation method for the non-parametric quantification of cerebral haemodynamics from dynamic susceptibility contrast MRI. *NeuroImage*. Jan 1 2013;64:560-570.
181. Calamante F, Gadian DG, Connelly A. Quantification of bolus-tracking MRI: Improved characterization of the tissue residue function using Tikhonov regularization. *Magnetic resonance in medicine*. Dec 2003;50(6):1237-1247.

182. Kroll K, Wilke N, Jerosch-Herold M, et al. Modeling regional myocardial flows from residue functions of an intravascular indicator. *The American journal of physiology*. Oct 1996;271(4 Pt 2):H1643-1655.
183. Friston KJ, Penny W. Posterior probability maps and SPMs. *NeuroImage*. Jul 2003;19(3):1240-1249.
184. Ostergaard L, Aamand R, Gutierrez-Jimenez E, et al. The capillary dysfunction hypothesis of Alzheimer's disease. *Neurobiology of aging*. Apr 2013;34(4):1018-1031.
185. Ostergaard L, Jespersen SN, Mouridsen K, et al. The role of the cerebral capillaries in acute ischemic stroke: the extended penumbra model. *Journal of cerebral blood flow and metabolism : official journal of the International Society of Cerebral Blood Flow and Metabolism*. May 2013;33(5):635-648.
186. Ostergaard L, Kristiansen SB, Angleys H, et al. The role of capillary transit time heterogeneity in myocardial oxygenation and ischemic heart disease. *Basic research in cardiology*. May 2014;109(3):409.
187. Perkio J, Soinne L, Ostergaard L, et al. Abnormal intravoxel cerebral blood flow heterogeneity in human ischemic stroke determined by dynamic susceptibility contrast magnetic resonance imaging. *Stroke; a journal of cerebral circulation*. Jan 2005;36(1):44-49.
188. Rosengarten B, Huwendiek O, Kaps M. Neurovascular coupling and cerebral autoregulation can be described in terms of a control system. *Ultrasound in medicine & biology*. Feb 2001;27(2):189-193.
189. Moskowitz MA, Lo EH, Iadecola C. The science of stroke: mechanisms in search of treatments. *Neuron*. Jul 29 2010;67(2):181-198.
190. Dawson VL, Dawson TM. Nitric oxide neurotoxicity. *Journal of chemical neuroanatomy*. Jun 1996;10(3-4):179-190.
191. Pacher P, Beckman JS, Liaudet L. Nitric oxide and peroxynitrite in health and disease. *Physiological reviews*. Jan 2007;87(1):315-424.
192. Iadecola C, Davisson RL. Hypertension and cerebrovascular dysfunction. *Cell metabolism*. Jun 2008;7(6):476-484.
193. Gursoy-Ozdemir Y, Yemisci M, Dalkara T. Microvascular protection is essential for successful neuroprotection in stroke. *Journal of neurochemistry*. Nov 2012;123 Suppl 2:2-11.
194. Ohkuma H, Suzuki S, Kudo K, Islam S, Kikkawa T. Cortical blood flow during cerebral vasospasm after aneurysmal subarachnoid hemorrhage: three-dimensional N-isopropyl-p-[(123)I]iodoamphetamine single photon emission CT findings. *AJNR. American journal of neuroradiology*. Mar 2003;24(3):444-450.
195. Tomita Y, Tomita M, Schiszler I, et al. Moment analysis of microflow histogram in focal ischemic lesion to evaluate microvascular derangement after small pial arterial occlusion in rats. *Journal of cerebral blood flow and metabolism : official journal of the International Society of Cerebral Blood Flow and Metabolism*. Jun 2002;22(6):663-669.
196. Donnan GA. *The Ischaemic penumbra: pathophysiology, imaging and therapy*. Vol 93. NewYork: Informa Healthcare; 2007.
197. Renkin EM. B. W. Zweifach Award lecture. Regulation of the microcirculation. *Microvascular research*. Nov 1985;30(3):251-263.
198. Mazzoni MC, Schmid-Schonbein GW. Mechanisms and consequences of cell activation in the microcirculation. *Cardiovascular research*. Oct 1996;32(4):709-719.
199. Lipowsky HH, Gao L, Lescanic A. Shedding of the endothelial glycocalyx in arterioles, capillaries, and venules and its effect on capillary

- hemodynamics during inflammation. *American journal of physiology. Heart and circulatory physiology*. Dec 2011;301(6):H2235-2245.
200. Stefanovic B, Hutchinson E, Yakovleva V, et al. Functional reactivity of cerebral capillaries. *Journal of cerebral blood flow and metabolism : official journal of the International Society of Cerebral Blood Flow and Metabolism*. May 2008;28(5):961-972.
 201. Hossmann KA, Sakaki S, Zimmerman V. Cation activities in reversible ischemia of the cat brain. *Stroke; a journal of cerebral circulation*. Jan-Feb 1977;8(1):77-81.
 202. Moseley ME, Kucharczyk J, Mintorovitch J, et al. Diffusion-weighted MR imaging of acute stroke: correlation with T2-weighted and magnetic susceptibility-enhanced MR imaging in cats. *AJNR. American journal of neuroradiology*. 5/1990 1990;11(3):423-429.
 203. Warach S, Chien D, Li W, Ronthal M, Edelman RR. Fast magnetic resonance diffusion-weighted imaging of acute human stroke. *Neurology*. 9/1992 1992;42(9):1717-1723.
 204. Hjort N, Christensen S, Solling C, et al. Ischemic injury detected by diffusion imaging 11 minutes after stroke. *Annals of neurology*. 9/2005 2005;58(3):462-465.
 205. Schuier FJ, Hossmann KA. Experimental brain infarcts in cats. II. Ischemic brain edema. *Stroke; a journal of cerebral circulation*. 11/1980 1980;11(6):593-601.
 206. Bell BA, Symon L, Branston NM. CBF and time thresholds for the formation of ischemic cerebral edema, and effect of reperfusion in baboons. *J Neurosurg*. 1/1985 1985;62(1):31-41.
 207. Noguchi K, Ogawa T, Inugami A, et al. MRI of acute cerebral infarction: a comparison of FLAIR and T2-weighted fast spin-echo imaging. *Neuroradiology*. 6/1997 1997;39(6):406-410.
 208. Thomalla G, Rossbach P, Rosenkranz M, et al. Negative fluid-attenuated inversion recovery imaging identifies acute ischemic stroke at 3 hours or less. *Annals of neurology*. 6/2009 2009;65(6):724-732.
 209. Ebinger M, Galinovic I, Rozanski M, Brunecker P, Endres M, Fiebich JB. Fluid-attenuated inversion recovery evolution within 12 hours from stroke onset: a reliable tissue clock? *Stroke; a journal of cerebral circulation*. 2/2010 2010;41(2):250-255.
 210. Thomalla G, Cheng B, Ebinger M, et al. DWI-FLAIR mismatch for the identification of patients with acute ischaemic stroke within 4.5 h of symptom onset (PRE-FLAIR): a multicentre observational study. *Lancet Neurol*. Nov 2011;10(11):978-986.
 211. Thomalla G, Simonsen CZ, Boutitie F, et al. MRI-Guided Thrombolysis for Stroke with Unknown Time of Onset. *The New England journal of medicine*. Aug 16 2018;379(7):611-622.
 212. Moseley ME, Kucharczyk J, Mintorovitch J, et al. Diffusion-weighted MR imaging of acute stroke: correlation with T2-weighted and magnetic susceptibility-enhanced MR imaging in cats. *AJNR. American journal of neuroradiology*. May 1990;11(3):423-429.
 213. Beaulieu C, De Crespigny A, Tong DC, Moseley ME, Albers GW, Marks MP. Longitudinal magnetic resonance imaging study of perfusion and diffusion in stroke: Evolution of lesion volume and correlation with clinical outcome. *Annals of neurology*. 1999;46(4):568-578.
 214. Barber PA, Davis SM, Darby DG, et al. Absent middle cerebral artery flow predicts the presence and evolution of the ischemic penumbra. *Neurology*. Apr 12 1999;52(6):1125-1132.

215. Schlaug G, Benfield A, Baird AE, et al. The ischemic penumbra: operationally defined by diffusion and perfusion MRI. *Neurology*. Oct 22 1999;53(7):1528-1537.
216. Karonen JO, Vanninen RL, Liu Y, et al. Combined diffusion and perfusion MRI with correlation to single-photon emission CT in acute ischemic stroke. Ischemic penumbra predicts infarct growth. *Stroke; a journal of cerebral circulation*. Aug 1999;30(8):1583-1590.
217. Neumann-Haefelin T, Wittsack HJ, Wenserski F, et al. Diffusion- and perfusion-weighted MRI. The DWI/PWI mismatch region in acute stroke. *Stroke; a journal of cerebral circulation*. Aug 1999;30(8):1591-1597.
218. Ogata T, Christensen S, Nagakane Y, et al. The Effects of Alteplase 3 to 6 Hours After Stroke in the EPITHET-DEFUSE Combined Dataset Post Hoc Case-Control Study. *Stroke; a journal of cerebral circulation*. Jan 2013;44(1):87-93.
219. Kidwell CS, Alger JR, Saver JL. Beyond mismatch: evolving paradigms in imaging the ischemic penumbra with multimodal magnetic resonance imaging. *Stroke; a journal of cerebral circulation*. Nov 2003;34(11):2729-2735.
220. Warach S, Gaa J, Siewert B, Wielopolski P, Edelman RR. Acute human stroke studied by whole brain echo planar diffusion-weighted magnetic resonance imaging. *Annals of neurology*. Feb 1995;37(2):231-241.
221. Baird AE, Warach S. Magnetic resonance imaging of acute stroke. *Journal of cerebral blood flow and metabolism : official journal of the International Society of Cerebral Blood Flow and Metabolism*. Jun 1998;18(6):583-609.
222. Kidwell CS, Saver JL, Mattiello J, et al. Thrombolytic reversal of acute human cerebral ischemic injury shown by diffusion/perfusion magnetic resonance imaging. *Annals of neurology*. Apr 2000;47(4):462-469.
223. Sobesky J, Zaro Weber O, Lehnhardt FG, et al. Does the mismatch match the penumbra? Magnetic resonance imaging and positron emission tomography in early ischemic stroke. *Stroke; a journal of cerebral circulation*. May 2005;36(5):980-985.
224. Heiss WD, Sobesky J, Hesselmann V. Identifying thresholds for penumbra and irreversible tissue damage. *Stroke; a journal of cerebral circulation*. Nov 2004;35(11 Suppl 1):2671-2674.
225. Sobesky J, Zaro Weber O, Lehnhardt FG, et al. Which time-to-peak threshold best identifies penumbral flow? A comparison of perfusion-weighted magnetic resonance imaging and positron emission tomography in acute ischemic stroke. *Stroke; a journal of cerebral circulation*. Dec 2004;35(12):2843-2847.
226. Guadagno JV, Warburton EA, Aigbirhio FI, et al. Does the acute diffusion-weighted imaging lesion represent penumbra as well as core? A combined quantitative PET/MRI voxel-based study. *Journal of cerebral blood flow and metabolism : official journal of the International Society of Cerebral Blood Flow and Metabolism*. Nov 2004;24(11):1249-1254.
227. Yamada K, Wu O, Gonzalez RG, et al. Magnetic resonance perfusion-weighted imaging of acute cerebral infarction: effect of the calculation methods and underlying vasculopathy. *Stroke; a journal of cerebral circulation*. Jan 2002;33(1):87-94.
228. Calamante F, Christensen S, Desmond PM, Ostergaard L, Davis SM, Connelly A. The physiological significance of the time-to-maximum (Tmax) parameter in perfusion MRI. *Stroke; a journal of cerebral circulation*. Jun 2010;41(6):1169-1174.

229. Butcher KS, Parsons M, MacGregor L, et al. Refining the perfusion-diffusion mismatch hypothesis. *Stroke; a journal of cerebral circulation*. Jun 2005;36(6):1153-1159.
230. Olivot JM, Mlynash M, Thijs VN, et al. Relationships between cerebral perfusion and reversibility of acute diffusion lesions in DEFUSE: insights from RADAR. *Stroke; a journal of cerebral circulation*. May 2009;40(5):1692-1697.
231. Schellinger PD, Fiebach JB, Jansen O, et al. Stroke magnetic resonance imaging within 6 hours after onset of hyperacute cerebral ischemia. *Annals of neurology*. Apr 2001;49(4):460-469.
232. Grandin CB, Duprez TP, Smith AM, et al. Which MR-derived perfusion parameters are the best predictors of infarct growth in hyperacute stroke? Comparative study between relative and quantitative measurements. *Radiology*. May 2002;223(2):361-370.
233. Liu Y, Karonen JO, Vanninen RL, et al. Cerebral hemodynamics in human acute ischemic stroke: a study with diffusion- and perfusion-weighted magnetic resonance imaging and SPECT. *Journal of cerebral blood flow and metabolism : official journal of the International Society of Cerebral Blood Flow and Metabolism*. Jun 2000;20(6):910-920.
234. Olivot JM, Mlynash M, Thijs VN, et al. Optimal Tmax threshold for predicting penumbral tissue in acute stroke. *Stroke; a journal of cerebral circulation*. Feb 2009;40(2):469-475.
235. Zaro-Weber O, Moeller-Hartmann W, Heiss WD, Sobesky J. MRI perfusion maps in acute stroke validated with 15O-water positron emission tomography. *Stroke; a journal of cerebral circulation*. Mar 2010;41(3):443-449.
236. Ebinger M, Brunecker P, Jungehulsing GJ, et al. Reliable perfusion maps in stroke MRI using arterial input functions derived from distal middle cerebral artery branches. *Stroke; a journal of cerebral circulation*. Jan 2010;41(1):95-101.
237. Thijs VN, Somford DM, Bammer R, Robberecht W, Moseley ME, Albers GW. Influence of arterial input function on hypoperfusion volumes measured with perfusion-weighted imaging. *Stroke; a journal of cerebral circulation*. Jan 2004;35(1):94-98.
238. Takasawa M, Jones PS, Guadagno JV, et al. How reliable is perfusion MR in acute stroke? Validation and determination of the penumbra threshold against quantitative PET. *Stroke; a journal of cerebral circulation*. Mar 2008;39(3):870-877.
239. Kane I, Sandercock P, Wardlaw J. Magnetic resonance perfusion diffusion mismatch and thrombolysis in acute ischaemic stroke: a systematic review of the evidence to date. *Journal of neurology, neurosurgery, and psychiatry*. May 2007;78(5):485-491.
240. Bristow MS, Simon JE, Brown RA, et al. MR perfusion and diffusion in acute ischemic stroke: human gray and white matter have different thresholds for infarction. *Journal of cerebral blood flow and metabolism : official journal of the International Society of Cerebral Blood Flow and Metabolism*. Oct 2005;25(10):1280-1287.
241. Wu O, Christensen S, Hjort N, et al. Characterizing physiological heterogeneity of infarction risk in acute human ischaemic stroke using MRI. *Brain : a journal of neurology*. Sep 2006;129(Pt 9):2384-2393.
242. Galinovic I, Brunecker P, Ostwaldt AC, Soemmer C, Hotter B, Fiebach JB. Fully automated postprocessing carries a risk of substantial

- overestimation of perfusion deficits in acute stroke magnetic resonance imaging. *Cerebrovascular diseases*. 2011;31(4):408-413.
243. Rordorf G, Koroshetz WJ, Copen WA, et al. Regional ischemia and ischemic injury in patients with acute middle cerebral artery stroke as defined by early diffusion-weighted and perfusion-weighted MRI. *Stroke; a journal of cerebral circulation*. May 1998;29(5):939-943.
 244. Staroselskaya IA, Chaves C, Silver B, et al. Relationship between magnetic resonance arterial patency and perfusion-diffusion mismatch in acute ischemic stroke and its potential clinical use. *Arch Neurol*. Jul 2001;58(7):1069-1074.
 245. Kane I, Carpenter T, Chappell F, et al. Comparison of 10 different magnetic resonance perfusion imaging processing methods in acute ischemic stroke: effect on lesion size, proportion of patients with diffusion/perfusion mismatch, clinical scores, and radiologic outcomes. *Stroke; a journal of cerebral circulation*. Dec 2007;38(12):3158-3164.
 246. Davis SM, Donnan DA, Parsons MW, et al. Effects of alteplase beyond 3 h after stroke in the Echoplanar Imaging Thrombolytic Evaluation Trial (EPITHET): a placebo-controlled randomised trial. *Lancet Neurol*. 2008 2008;7:299-309.
 247. Kakuda W, Lansberg MG, Thijs VN, et al. Optimal definition for PWI/DWI mismatch in acute ischemic stroke patients. *Journal of cerebral blood flow and metabolism : official journal of the International Society of Cerebral Blood Flow and Metabolism*. May 2008;28(5):887-891.
 248. Hacke W, Furlan A, Al-Rawi Y, et al. Intravenous desmoteplase in patients with acute ischaemic stroke selected by MRI perfusion.dif fusion weighted imaging or perfusion CT (DIAS-2): a prospective, randomised, double-blind, placebo-controlled study. *Lancet Neurol*. 2009 2009;8:141-150.
 249. Mishra NK, Albers GW, Davis SM, et al. Mismatch-based delayed thrombolysis: a meta-analysis. *Stroke; a journal of cerebral circulation*. Jan 2010;41(1):e25-33.
 250. Ringleb P, Bendszus M, Bluhmki E, et al. Extending the time window for intravenous thrombolysis in acute ischemic stroke using magnetic resonance imaging-based patient selection. *International journal of stroke : official journal of the International Stroke Society*. Jul 2019;14(5):483-490.
 251. Ma H, Campbell BCV, Parsons MW, et al. Thrombolysis Guided by Perfusion Imaging up to 9 Hours after Onset of Stroke. *The New England journal of medicine*. May 9 2019;380(19):1795-1803.
 252. Campbell BCV, Ma H, Ringleb PA, et al. Extending thrombolysis to 4.5-9 h and wake-up stroke using perfusion imaging: a systematic review and meta-analysis of individual patient data. *Lancet*. Jul 13 2019;394(10193):139-147.
 253. Kucinski T, Vaterlein O, Glauche V, et al. Correlation of apparent diffusion coefficient and computed tomography density in acute ischemic stroke. *Stroke; a journal of cerebral circulation*. 7/2002 2002;33(7):1786-1791.
 254. Lansberg MG, Albers GW, Beaulieu C, Marks MP. Comparison of diffusion-weighted MRI and CT in acute stroke. *Neurology*. 4/25/2000 2000;54(8):1557-1561.
 255. Chalela JA, Kidwell CS, Nentwich LM, et al. Magnetic resonance imaging and computed tomography in emergency assessment of patients with suspected acute stroke: a prospective comparison. *Lancet*. Jan 27 2007;369(9558):293-298.

256. Fiebach JB, Schellinger PD, Jansen O, et al. CT and diffusion-weighted MR imaging in randomized order: diffusion-weighted imaging results in higher accuracy and lower interrater variability in the diagnosis of hyperacute ischemic stroke. *Stroke; a journal of cerebral circulation*. 9/2002 2002;33(9):2206-2210.
257. Mohr JP, Biller J, Hilal SK, et al. Magnetic resonance versus computed tomographic imaging in acute stroke. *Stroke; a journal of cerebral circulation*. 5/1995 1995;26(5):807-812.
258. Wintermark M, Meuli R, Browaeys P, et al. Comparison of CT perfusion and angiography and MRI in selecting stroke patients for acute treatment. *Neurology*. Feb 27 2007;68(9):694-697.
259. Wintermark M, Reichhart M, Cuisenaire O, et al. Comparison of admission perfusion computed tomography and qualitative diffusion- and perfusion-weighted magnetic resonance imaging in acute stroke patients. *Stroke; a journal of cerebral circulation*. Aug 2002;33(8):2025-2031.
260. Alawneh JA, Jones PS, Mikkelsen IK, et al. Infarction of 'non-core-non-penumbra' tissue after stroke: multivariate modelling of clinical impact. *Brain : a journal of neurology*. Jun 2011;134(Pt 6):1765-1776.
261. Emberson J, Lees KR, Lyden P, et al. Effect of treatment delay, age, and stroke severity on the effects of intravenous thrombolysis with alteplase for acute ischaemic stroke: a meta-analysis of individual patient data from randomised trials. *Lancet*. Nov 29 2014;384(9958):1929-1935.
262. Hacke W, Kaste M, Fieschi C, et al. Randomised double-blind placebo-controlled trial of thrombolytic therapy with intravenous alteplase in acute ischaemic stroke (ECASS II). Second European-Australasian Acute Stroke Study Investigators. *Lancet*. Oct 17 1998;352(9136):1245-1251.
263. Hacke W, Donnan G, Fieschi C, et al. Association of outcome with early stroke treatment: pooled analysis of ATLANTIS, ECASS, and NINDS rt-PA stroke trials. *Lancet*. Mar 6 2004;363(9411):768-774.
264. Wardlaw JM, Murray V, Berge E, et al. Recombinant tissue plasminogen activator for acute ischaemic stroke: an updated systematic review and meta-analysis. *Lancet*. Jun 23 2012;379(9834):2364-2372.
265. Sandercock P, Wardlaw JM, Lindley RI, et al. The benefits and harms of intravenous thrombolysis with recombinant tissue plasminogen activator within 6 h of acute ischaemic stroke (the third international stroke trial [IST-3]): a randomised controlled trial. *Lancet*. Jun 23 2012;379(9834):2352-2363.
266. Donnan GA, Baron J, Ma H, Davis SM. Penumbra selection of patients for trials of acute stroke therapy. *Lancet Neurol*. 2009 2009;8:261-269.
267. Parsons MW, Spratt N, Bivard A, et al. A randomised trial of tenecteplase versus alteplase for acute ischaemic stroke. *N.Engl.J.Med*. 2012 2012;366:1099-1107.
268. Lansberg MG, Straka M, Kemp S, et al. MRI profile and response to endovascular reperfusion after stroke (DEFUSE 2): a prospective cohort study. *Lancet Neurol*. 2012 2012;11:860-867.
269. Kidwell C, Jahan R, Gornbein J, et al. A Trial of Imaging Selection and Endovascular Treatment for Ischemic Stroke. *New England Journal of Medicine*. 2013 2013;368:914-923.
270. Jovin TG, Chamorro A, Cobo E, et al. Thrombectomy within 8 Hours after Symptom Onset in Ischemic Stroke. *The New England journal of medicine*. Apr 17 2015.

271. Goyal M, Demchuk AM, Menon BK, et al. Randomized assessment of rapid endovascular treatment of ischemic stroke. *The New England journal of medicine*. Mar 12 2015;372(11):1019-1030.
272. Nogueira RG, Jadhav AP, Haussen DC, et al. Thrombectomy 6 to 24 Hours after Stroke with a Mismatch between Deficit and Infarct. *The New England journal of medicine*. Jan 4 2018;378(1):11-21.
273. Albers GW, Marks MP, Kemp S, et al. Thrombectomy for Stroke at 6 to 16 Hours with Selection by Perfusion Imaging. *The New England journal of medicine*. Feb 22 2018;378(8):708-718.
274. Lansberg MG, Lee J, Christensen S, et al. RAPID automated patient selection for reperfusion therapy: a pooled analysis of the Echoplanar Imaging Thrombolytic Evaluation Trial (EPITHET) and the Diffusion and Perfusion Imaging Evaluation for Understanding Stroke Evolution (DEFUSE) Study. *Stroke; a journal of cerebral circulation*. Jun 2011;42(6):1608-1614.
275. Inoue M, Mlynash M, Straka M, et al. Patients With the Malignant Profile Within 3 Hours of Symptom Onset Have Very Poor Outcomes After Intravenous Tissue-Type Plasminogen Activator Therapy. *Stroke; a journal of cerebral circulation*. Sep 2012;43(9):2494-2496.
276. Cereda CW, Christensen S, Campbell BCV, et al. A benchmarking tool to evaluate computer tomography perfusion infarct core predictions against a DWI standard. *Journal of cerebral blood flow and metabolism : official journal of the International Society of Cerebral Blood Flow and Metabolism*. Oct 2016;36(10):1780-1789.
277. Ma H, Campbell BCV, Churilov L. Thrombolysis up to 9 Hours after Onset of Stroke. Reply. *The New England journal of medicine*. Aug 1 2019;381(5):488-489.
278. Hopyan J, Ciarallo A, Dowlatshahi D, et al. Certainty of stroke diagnosis: Incremental benefit with CT perfusion over noncontrast CT and CT angiography. *Radiology*. 2010 2010;255(1):142-153.
279. Campbell BCV, Christensen S, Butcher KS, et al. Regional Very Low Cerebral Blood Volume Predicts Hemorrhagic Transformation Better Than Diffusion-Weighted Imaging Volume and Thresholded Apparent Diffusion Coefficient in Acute Ischemic Stroke. *Stroke; a journal of cerebral circulation*. 2010 2010;41:82-88.
280. Coutts SB, O'Reilly C, Hill MD, et al. Computed tomography and computed tomography angiography findings predict functional impairment in patients with minor stroke and transient ischaemic attack. *Int j. stroke*. Dec 2009;4(6):448-453.
281. El-Tawil S, Wardlaw J, Ford I, et al. Penumbra and re-canalization acute computed tomography in ischemic stroke evaluation: PRACTISE study protocol. *International journal of stroke : official journal of the International Stroke Society*. Aug 2017;12(6):671-678.
282. Ciccone A, Valvassori L, Ponzio M, et al. Intra-arterial or intravenous thrombolysis for acute ischemic stroke? The SYNTHESIS pilot trial. *Journal of neurointerventional surgery*. Mar 2010;2(1):74-79.
283. Broderick JP, Palesch YY, Demchuk AM, et al. Endovascular therapy after intravenous t-PA versus t-PA alone for stroke. *The New England journal of medicine*. Mar 7 2013;368(10):893-903.
284. Kidwell CS, Jahan R, Gornbein J, et al. A trial of imaging selection and endovascular treatment for ischemic stroke. *The New England journal of medicine*. Mar 7 2013;368(10):914-923.

285. Berkhemer OA, Fransen PS, Beumer D, et al. A randomized trial of intraarterial treatment for acute ischemic stroke. *The New England journal of medicine*. Jan 1 2015;372(1):11-20.
286. Mair G, Boyd EV, Chappell FM, et al. Sensitivity and specificity of the hyperdense artery sign for arterial obstruction in acute ischemic stroke. *Stroke; a journal of cerebral circulation*. Jan 2015;46(1):102-107.
287. Sohn CH, Sevick RJ, Frayne R. Contrast-enhanced MR angiography of the intracranial circulation. *Magnetic resonance imaging clinics of North America*. Nov 2003;11(4):599-614.
288. Liebeskind DS. Collateral circulation. *Stroke; a journal of cerebral circulation*. Sep 2003;34(9):2279-2284.
289. Menon BK, d'Esterre CD, Qazi EM, et al. Multiphase CT Angiography: A New Tool for the Imaging Triage of Patients with Acute Ischemic Stroke. *Radiology*. May 2015;275(2):510-520.
290. Liebeskind DS. Neuroprotection from the collateral perspective. *IDrugs : the investigational drugs journal*. Mar 2005;8(3):222-228.
291. Liebeskind DS. Understanding blood flow: the other side of an acute arterial occlusion. *International journal of stroke : official journal of the International Stroke Society*. May 2007;2(2):118-120.
292. Menon BK, Smith EE, Modi J, et al. Regional leptomeningeal score on CT angiography predicts clinical and imaging outcomes in patients with acute anterior circulation occlusions. *AJNR. American journal of neuroradiology*. Oct 2011;32(9):1640-1645.
293. Lima FO, Furie KL, Silva GS, et al. The pattern of leptomeningeal collaterals on CT angiography is a strong predictor of long-term functional outcome in stroke patients with large vessel intracranial occlusion. *Stroke; a journal of cerebral circulation*. Oct 2010;41(10):2316-2322.
294. Souza LC, Yoo AJ, Chaudhry ZA, et al. Malignant CTA collateral profile is highly specific for large admission DWI infarct core and poor outcome in acute stroke. *AJNR. American journal of neuroradiology*. Aug 2012;33(7):1331-1336.
295. Maas MB, Lev MH, Ay H, et al. Collateral vessels on CT angiography predict outcome in acute ischemic stroke. *Stroke; a journal of cerebral circulation*. Sep 2009;40(9):3001-3005.
296. Tan IY, Demchuk AM, Hopyan J, et al. CT angiography clot burden score and collateral score: correlation with clinical and radiologic outcomes in acute middle cerebral artery infarct. *AJNR. American journal of neuroradiology*. Mar 2009;30(3):525-531.
297. Miteff F, Levi CR, Bateman GA, Spratt N, McElduff P, Parsons MW. The independent predictive utility of computed tomography angiographic collateral status in acute ischaemic stroke. *Brain : a journal of neurology*. Aug 2009;132(Pt 8):2231-2238.
298. Schwamm LH, Rosenthal ES, Swap CJ, et al. Hypoattenuation on CT angiographic source images predicts risk of intracerebral hemorrhage and outcome after intra-arterial reperfusion therapy. *AJNR. American journal of neuroradiology*. Aug 2005;26(7):1798-1803.
299. Leng X, Lan L, Liu L, Leung TW, Wong KS. Good collateral circulation predicts favorable outcomes in intravenous thrombolysis: a systematic review and meta-analysis. *European journal of neurology : the official journal of the European Federation of Neurological Societies*. Dec 2016;23(12):1738-1749.
300. Rosenthal ES, Schwamm LH, Roccatagliata L, et al. Role of recanalization in acute stroke outcome: rationale for a CT angiogram-based "benefit of

- recanalization" model. *AJNR. American journal of neuroradiology*. Sep 2008;29(8):1471-1475.
301. Leng X, Fang H, Leung TW, et al. Impact of Collateral Status on Successful Revascularization in Endovascular Treatment: A Systematic Review and Meta-Analysis. *Cerebrovascular diseases*. 2016;41(1-2):27-34.
 302. Leng X, Fang H, Leung TW, et al. Impact of collaterals on the efficacy and safety of endovascular treatment in acute ischaemic stroke: a systematic review and meta-analysis. *Journal of neurology, neurosurgery, and psychiatry*. May 2016;87(5):537-544.
 303. Huang X, Cheripelli BK, Lloyd SM, et al. Alteplase versus tenecteplase for thrombolysis after ischaemic stroke (ATTEST): a phase 2, randomised, open-label, blinded endpoint study. *Lancet Neurol*. Apr 2015;14(4):368-376.
 304. Wardlaw JM, Muir KW, Macleod MJ, et al. Clinical relevance and practical implications of trials of perfusion and angiographic imaging in patients with acute ischaemic stroke: a multicentre cohort imaging study. *Journal of neurology, neurosurgery, and psychiatry*. Sep 2013;84(9):1001-1007.
 305. Bivard A, McElduff P, Spratt N, Levi C, Parsons M. Defining the extent of irreversible brain ischemia using perfusion computed tomography. *Cerebrovascular diseases*. 2011;31(3):238-245.
 306. The Thrombolysis in Myocardial Infarction (TIMI) trial. Phase I findings. TIMI Study Group. *The New England journal of medicine*. Apr 4 1985;312(14):932-936.
 307. Zaidat OO, Yoo AJ, Khatri P, et al. Recommendations on angiographic revascularization grading standards for acute ischemic stroke: a consensus statement. *Stroke; a journal of cerebral circulation*. Sep 2013;44(9):2650-2663.
 308. Higashida RT, Furlan AJ, Roberts H, et al. Trial design and reporting standards for intra-arterial cerebral thrombolysis for acute ischemic stroke. *Stroke; a journal of cerebral circulation*. Aug 2003;34(8):e109-137.
 309. Wahlgren N, Ahmed N, Davalos A. Thrombolysis with alteplase for acute ischaemic stroke in the Safe Implementation of Thrombolysis in Stroke-Monitoring Study (SITS-MOST): an observational study (vol 369, pg 275, 2007). *Lancet*. Mar 10 2007;369(9564):826-826.
 310. Wardlaw JM, Sellar R. A simple practical classification of cerebral infarcts on CT and its interobserver reliability. *AJNR. American journal of neuroradiology*. Nov 1994;15(10):1933-1939.
 311. Wilson JT, Hareendran A, Grant M, et al. Improving the assessment of outcomes in stroke: use of a structured interview to assign grades on the modified Rankin Scale. *Stroke; a journal of cerebral circulation*. Sep 2002;33(9):2243-2246.
 312. Quinn TJ, Dawson J, Walters MR, Lees KR. Exploring the reliability of the modified rankin scale. *Stroke; a journal of cerebral circulation*. Mar 2009;40(3):762-766.
 313. Hossmann KA. Pathophysiology and therapy of experimental stroke. *Cellular and molecular neurobiology*. Oct-Nov 2006;26(7-8):1057-1083.
 314. Lees KR, Bluhmki E, von Kummer R, et al. Time to treatment with intravenous alteplase and outcome in stroke: an updated pooled analysis of ECASS, ATLANTIS, NINDS, and EPITHET trials. *Lancet*. May 15 2010;375(9727):1695-1703.
 315. Khatri P, Yeatts SD, Mazighi M, et al. Time to angiographic reperfusion and clinical outcome after acute ischaemic stroke: an analysis of data

- from the Interventional Management of Stroke (IMS III) phase 3 trial. *Lancet Neurol.* Jun 2014;13(6):567-574.
316. Campbell BC, Christensen S, Tress BM, et al. Failure of collateral blood flow is associated with infarct growth in ischemic stroke. *Journal of cerebral blood flow and metabolism : official journal of the International Society of Cerebral Blood Flow and Metabolism.* Aug 2013;33(8):1168-1172.
 317. Darby DG, Barber PA, Gerraty RP, et al. Pathophysiological topography of acute ischemia by combined diffusion-weighted and perfusion MRI. *Stroke; a journal of cerebral circulation.* Oct 1999;30(10):2043-2052.
 318. Jovin TG, Yonas H, Gebel JM, et al. The cortical ischemic core and not the consistently present penumbra is a determinant of clinical outcome in acute middle cerebral artery occlusion. *Stroke; a journal of cerebral circulation.* Oct 2003;34(10):2426-2433.
 319. Jung S, Gilgen M, Slotboom J, et al. Factors that determine penumbral tissue loss in acute ischaemic stroke. *Brain : a journal of neurology.* Dec 2013;136(Pt 12):3554-3560.
 320. Bivard A, Levi C, Spratt N, Parsons M. Perfusion CT in acute stroke: a comprehensive analysis of infarct and penumbra. *Radiology.* May 2013;267(2):543-550.
 321. Lansberg MG, Straka M, Kemp S, et al. MRI profile and response to endovascular reperfusion after stroke (DEFUSE 2): a prospective cohort study. *Lancet Neurol.* Oct 2012;11(10):860-867.
 322. Muir KW. Heterogeneity of stroke pathophysiology and neuroprotective clinical trial design. *Stroke; a journal of cerebral circulation.* Jun 2002;33(6):1545-1550.
 323. Albers GW, von Kummer R, Truelsen T, et al. Safety and efficacy of desmoteplase given 3-9 h after ischaemic stroke in patients with occlusion or high-grade stenosis in major cerebral arteries (DIAS-3): a double-blind, randomised, placebo-controlled phase 3 trial. *Lancet Neurol.* Apr 30 2015.
 324. Bang OY, Saver JL, Buck BH, et al. Impact of collateral flow on tissue fate in acute ischaemic stroke. *Journal of neurology, neurosurgery, and psychiatry.* Jun 2008;79(6):625-629.
 325. Ebinger M, Winter B, Wendt M, et al. Effect of the use of ambulance-based thrombolysis on time to thrombolysis in acute ischemic stroke: a randomized clinical trial. *Jama.* Apr 23-30 2014;311(16):1622-1631.
 326. McVerry F, Dani KA, MacDougall NJ, MacLeod MJ, Wardlaw J, Muir KW. Derivation and Evaluation of Thresholds for Core and Tissue at Risk of Infarction Using CT Perfusion. *Journal of neuroimaging : official journal of the American Society of Neuroimaging.* Nov 2014;24(6):562-568.
 327. Wang X, Lo EH. Triggers and mediators of hemorrhagic transformation in cerebral ischemia. *Molecular neurobiology.* Dec 2003;28(3):229-244.
 328. Sandercock PAG, Wardlaw JM, Lindley RI, Cohen G, Grp IC. The third international stroke trial (IST-3) of intravenous rt-PA: effect of age and time on treatment effect among 3035 patients randomised. *Int j. stroke.* Dec 2012;7:6-6.
 329. Sage JI, Van Uitert RL, Duffy TE. Early changes in blood brain barrier permeability to small molecules after transient cerebral ischemia. *Stroke; a journal of cerebral circulation.* Jan-Feb 1984;15(1):46-50.
 330. Yang GY, Betz AL. Reperfusion-induced injury to the blood-brain barrier after middle cerebral artery occlusion in rats. *Stroke; a journal of cerebral circulation.* Aug 1994;25(8):1658-1664; discussion 1664-1655.

331. Schaller B, Graf R. Cerebral ischemia and reperfusion: the pathophysiologic concept as a basis for clinical therapy. *Journal of cerebral blood flow and metabolism : official journal of the International Society of Cerebral Blood Flow and Metabolism*. Apr 2004;24(4):351-371.
332. Hacke W, Schwab S, Horn M, Spranger M, De Georgia M, von Kummer R. 'Malignant' middle cerebral artery territory infarction: clinical course and prognostic signs. *Archives of Neurology*. 1996;53(4):309-315.
333. Thomalla G, Sobesky J, Kohrmann M, et al. Two tales: hemorrhagic transformation but not parenchymal hemorrhage after thrombolysis is related to severity and duration of ischemia: MRI study of acute stroke patients treated with intravenous tissue plasminogen activator within 6 hours. *Stroke; a journal of cerebral circulation*. Feb 2007;38(2):313-318.
334. Mlynash M, Lansberg MG, De Silva DA, et al. Refining the definition of the malignant profile: insights from the DEFUSE-EPITHET pooled data set. *Stroke; a journal of cerebral circulation*. May 2011;42(5):1270-1275.
335. Lansberg MG, Thijs VN, Bammer R, et al. Risk factors of symptomatic intracerebral hemorrhage after tPA therapy for acute stroke. *Stroke; a journal of cerebral circulation*. Aug 2007;38(8):2275-2278.
336. Hermitte L, Cho TH, Ozenne B, et al. Very low cerebral blood volume predicts parenchymal hematoma in acute ischemic stroke. *Stroke; a journal of cerebral circulation*. Aug 2013;44(8):2318-2320.
337. Kasner SE, Demchuk AM, Berrouschot J, et al. Predictors of fatal brain edema in massive hemispheric ischemic stroke. *Stroke; a journal of cerebral circulation*. Sep 2001;32(9):2117-2123.
338. Brown DL, Johnston KC, Wagner DP, Haley EC, Jr. Predicting major neurological improvement with intravenous recombinant tissue plasminogen activator treatment of stroke. *Stroke; a journal of cerebral circulation*. Jan 2004;35(1):147-150.
339. Kharitonova T, Mikulik R, Roine RO, et al. Association of early National Institutes of Health Stroke Scale improvement with vessel recanalization and functional outcome after intravenous thrombolysis in ischemic stroke. *Stroke; a journal of cerebral circulation*. Jun 2011;42(6):1638-1643.
340. Kucinski T, Koch C, Eckert B, et al. Collateral circulation is an independent radiological predictor of outcome after thrombolysis in acute ischaemic stroke. *Neuroradiology*. Jan 2003;45(1):11-18.
341. Demchuk AM, Goyal M, Yeatts SD, et al. Recanalization and clinical outcome of occlusion sites at baseline CT angiography in the Interventional Management of Stroke III trial. *Radiology*. Oct 2014;273(1):202-210.
342. Burggraf D, Martens HK, Dichgans M, Hamann GF. rt-PA causes a dose-dependent increase in the extravasation of cellular and non-cellular blood elements after focal cerebral ischemia. *Brain research*. Aug 20 2007;1164:55-62.
343. Kim JH, Bang OY, Liebeskind DS, et al. Impact of baseline tissue status (diffusion-weighted imaging lesion) versus perfusion status (severity of hypoperfusion) on hemorrhagic transformation. *Stroke; a journal of cerebral circulation*. Mar 2010;41(3):e135-142.
344. Strbian D, Meretoja A, Putaala J, Kaste M, Tatlisumak T, Helsinki Stroke Thrombolysis Registry G. Cerebral edema in acute ischemic stroke patients treated with intravenous thrombolysis. *International journal of stroke : official journal of the International Stroke Society*. Oct 2013;8(7):529-534.

345. Slivka A, Murphy E, Horrocks L. Cerebral edema after temporary and permanent middle cerebral artery occlusion in the rat. *Stroke; a journal of cerebral circulation*. Jun 1995;26(6):1061-1065; discussion 1065-1066.
346. Garcia JH, Kamijyo Y. Cerebral infarction. Evolution of histopathological changes after occlusion of a middle cerebral artery in primates. *Journal of neuropathology and experimental neurology*. Jul 1974;33(3):408-421.
347. Campbell BC, Christensen S, Butcher KS, et al. Regional very low cerebral blood volume predicts hemorrhagic transformation better than diffusion-weighted imaging volume and thresholded apparent diffusion coefficient in acute ischemic stroke. *Stroke; a journal of cerebral circulation*. Jan 2010;41(1):82-88.
348. Gasparotti R, Grassi M, Mardighian D, et al. Perfusion CT in patients with acute ischemic stroke treated with intra-arterial thrombolysis: Predictive value of infarct core size on clinical outcome. *American Journal of Neuroradiology*. April 2009;30(4):722-727.
349. Rha JH, Saver JL. The impact of recanalization on ischemic stroke outcome - A meta-analysis. *Stroke; a journal of cerebral circulation*. Mar 2007;38(3):967-973.
350. Borst J, Berkhemer OA, Roos YB, et al. Value of Computed Tomographic Perfusion-Based Patient Selection for Intra-Arterial Acute Ischemic Stroke Treatment. *Stroke; a journal of cerebral circulation*. Dec 2015;46(12):3375-3382.
351. Molina CA, Montaner J, Abilleira S, et al. Timing of spontaneous recanalization and risk of hemorrhagic transformation in acute cardioembolic stroke. *Stroke; a journal of cerebral circulation*. May 2001;32(5):1079-1084.
352. Krogh A. The supply of oxygen to the tissues and the regulation of the capillary circulation. *The Journal of physiology*. May 20 1919;52(6):457-474.
353. Kuschinsky W, Paulson OB. Capillary circulation in the brain. *Cerebrovascular and brain metabolism reviews*. Fall 1992;4(3):261-286.
354. Rasmussen PM, Jespersen SN, Ostergaard L. The effects of transit time heterogeneity on brain oxygenation during rest and functional activation. *Journal of cerebral blood flow and metabolism : official journal of the International Society of Cerebral Blood Flow and Metabolism*. Mar 2015;35(3):432-442.
355. Angleys H, Ostergaard L, Jespersen SN. The effects of capillary transit time heterogeneity (CTH) on brain oxygenation. *Journal of cerebral blood flow and metabolism : official journal of the International Society of Cerebral Blood Flow and Metabolism*. May 2015;35(5):806-817.
356. Schabel MC. A unified impulse response model for DCE-MRI. *Magnetic resonance in medicine*. Nov 2012;68(5):1632-1646.
357. Roy CS, Sherrington CS. On the Regulation of the Blood-supply of the Brain. *The Journal of physiology*. Jan 1890;11(1-2):85-158 117.
358. Ostergaard L, Engedal TS, Aamand R, et al. Capillary transit time heterogeneity and flow-metabolism coupling after traumatic brain injury. *Journal of cerebral blood flow and metabolism : official journal of the International Society of Cerebral Blood Flow and Metabolism*. Oct 2014;34(10):1585-1598.
359. Ostergaard L, Engedal TS, Moreton F, et al. Cerebral small vessel disease: Capillary pathways to stroke and cognitive decline. *Journal of cerebral blood flow and metabolism : official journal of the International Society of Cerebral Blood Flow and Metabolism*. Feb 2016;36(2):302-325.

360. Engedal TS, Hjort N, Hougaard KD, et al. Transit time homogenization in ischemic stroke - A novel biomarker of penumbral microvascular failure? *Journal of cerebral blood flow and metabolism : official journal of the International Society of Cerebral Blood Flow and Metabolism*. Nov 2018;38(11):2006-2020.
361. Hudetz AG, Feher G, Kampine JP. Heterogeneous autoregulation of cerebrocortical capillary flow: evidence for functional thoroughfare channels? *Microvascular research*. Jan 1996;51(1):131-136.
362. Mouridsen K, Hansen MB, Ostergaard L, Jespersen SN. Reliable estimation of capillary transit time distributions using DSC-MRI. *Journal of cerebral blood flow and metabolism : official journal of the International Society of Cerebral Blood Flow and Metabolism*. Sep 2014;34(9):1511-1521.
363. Rivers CS, Wardlaw JM, Armitage PA, et al. Do acute diffusion- and perfusion-weighted MRI lesions identify final infarct volume in ischemic stroke? *Stroke; a journal of cerebral circulation*. Jan 2006;37(1):98-104.
364. Potreck A, Loebel S, Pfaff J, et al. Increased volumes of mildly elevated capillary transit time heterogeneity positively predict favorable outcome and negatively predict intracranial hemorrhage in acute ischemic stroke with large vessel occlusion. *European radiology*. Jul 2019;29(7):3523-3532.
365. Larsson HBW, Vestergaard MB, Lindberg U, Iversen HK, Cramer SP. Brain capillary transit time heterogeneity in healthy volunteers measured by dynamic contrast-enhanced T1-weighted perfusion MRI. *Journal of magnetic resonance imaging : JMRI*. Jun 2017;45(6):1809-1820.
366. Schulte ML, Wood JD, Hudetz AG. Cortical electrical stimulation alters erythrocyte perfusion pattern in the cerebral capillary network of the rat. *Brain research*. Feb 14 2003;963(1-2):81-92.
367. Alawneh JA, Moustafa RR, Baron JC. Hemodynamic factors and perfusion abnormalities in early neurological deterioration. *Stroke; a journal of cerebral circulation*. Jun 2009;40(6):e443-450.
368. Baird AE, Lovblad KO, Dashe JF, et al. Clinical correlations of diffusion and perfusion lesion volumes in acute ischemic stroke. *Cerebrovascular diseases*. Nov-Dec 2000;10(6):441-448.
369. Bang OY, Kim GM, Chung CS, et al. Differential pathophysiological mechanisms of stroke evolution between new lesions and lesion growth: perfusion-weighted imaging study. *Cerebrovascular diseases*. 2010;29(4):328-335.
370. Hughes JL, Beech JS, Jones PS, Wang D, Menon DK, Baron JC. Mapping selective neuronal loss and microglial activation in the salvaged neocortical penumbra in the rat. *NeuroImage*. Jan 1 2010;49(1):19-31.
371. Tisserand M, Seners P, Turc G, et al. Mechanisms of unexplained neurological deterioration after intravenous thrombolysis. *Stroke; a journal of cerebral circulation*. Dec 2014;45(12):3527-3534.
372. Back T. Pathophysiology of the ischemic penumbra--revision of a concept. *Cellular and molecular neurobiology*. Dec 1998;18(6):621-638.
373. Marler JR, Brott T, Broderick J, et al. Tissue-Plasminogen Activator for Acute Ischemic Stroke. *New England Journal of Medicine*. 1995 1995;333(24):1581-1587.
374. McCormick MT, Muir KW. Referral bias may underestimate number of very elderly patients eligible for rtPA. *Stroke; a journal of cerebral circulation*. Apr 2006;37(4):942-943; author reply 943.
375. Konig IR, Ziegler A, Bluhmki E, et al. Predicting long-term outcome after acute ischemic stroke: a simple index works in patients from controlled

- clinical trials. *Stroke; a journal of cerebral circulation*. Jun 2008;39(6):1821-1826.
376. Weimar C, Konig IR, Kraywinkel K, Ziegler A, Diener HC, German Stroke Study C. Age and National Institutes of Health Stroke Scale Score within 6 hours after onset are accurate predictors of outcome after cerebral ischemia: development and external validation of prognostic models. *Stroke; a journal of cerebral circulation*. Jan 2004;35(1):158-162.
 377. Marler JR, Tilley BC, Lu M, et al. Early stroke treatment associated with better outcome: the NINDS rt-PA stroke study. *Neurology*. Dec 12 2000;55(11):1649-1655.
 378. Bogosavljevic V, Bodenat M, Beslac-Bumbasirevic L, et al. Intravenous thrombolysis for acute cerebral ischemia in Belgrade, Serbia: comparison with Lille, France. *European neurology*. 2011;66(1):30-36.
 379. Hanchate AD, Schwamm LH, Huang W, Hylek EM. Comparison of ischemic stroke outcomes and patient and hospital characteristics by race/ethnicity and socioeconomic status. *Stroke*. Feb 2013;44(2):469-476.
 380. Hanchate AD, Schwamm LH, Huang W, Hylek EM. Comparison of ischemic stroke outcomes and patient and hospital characteristics by race/ethnicity and socioeconomic status. *Stroke; a journal of cerebral circulation*. 2/2013 2013;44(2):469-476.
 381. Weir NU, Gunkel A, McDowall M, Dennis MS. Study of the relationship between social deprivation and outcome after stroke. *Stroke; a journal of cerebral circulation*. Apr 2005;36(4):815-819.
 382. Lees KR, Ford GA, Muir KW, et al. Thrombolytic therapy for acute stroke in the United Kingdom: experience from the safe implementation of thrombolysis in stroke (SITS) register. *QJM : monthly journal of the Association of Physicians*. Nov 2008;101(11):863-869.
 383. Ingeman A, Andersen G, Hundborg HH, Svendsen ML, Johnsen SP. Processes of care and medical complications in patients with stroke. *Stroke; a journal of cerebral circulation*. Jan 2011;42(1):167-172.
 384. Bray BD, Ayis S, Campbell J, et al. Associations between the organisation of stroke services, process of care, and mortality in England: prospective cohort study. *Bmj*. May 10 2013;346:f2827.
 385. Elameer M, Price C, Flynn D, Rodgers H. The impact of acute stroke service centralisation: a time series evaluation. *Future healthcare journal*. Oct 2018;5(3):181-187.
 386. Fulop NJ, Ramsay AI, Perry C, et al. Explaining outcomes in major system change: a qualitative study of implementing centralised acute stroke services in two large metropolitan regions in England. *Implementation science : IS*. Jun 3 2016;11(1):80.
 387. Kaste M, Thomassen L, Grond M, et al. Thrombolysis for acute ischemic stroke: a consensus statement of the 3rd Karolinska Stroke Update, October 30-31, 2000. *Stroke; a journal of cerebral circulation*. Nov 2001;32(11):2717-2718.
 388. Wahlgren N, Ahmed N, Davalos A, et al. Thrombolysis with alteplase for acute ischaemic stroke in the Safe implementation of Thrombolysis in Stroke-Monitoring Study (SITS-MOST): an observational study. *Lancet*. Jan-Feb 2007;369(9558):275-282.
 389. ROSENBAUM PR, RUBIN DB. The central role of the propensity score in observational studies for causal effects. *Biometrika*. 1983;70(1):41-55.
 390. Audebert HJ, Schultes K, Tietz V, et al. Long-term effects of specialized stroke care with telemedicine support in community hospitals on behalf of

- the Telemedical Project for Integrative Stroke Care (TEMPiS). *Stroke; a journal of cerebral circulation*. Mar 2009;40(3):902-908.
391. Reiner-Deitemyer V, Teuschl Y, Matz K, et al. Helicopter transport of stroke patients and its influence on thrombolysis rates: data from the Austrian Stroke Unit Registry. *Stroke; a journal of cerebral circulation*. May 2011;42(5):1295-1300.
 392. Reid M. Behind the "Glasgow effect". *Bulletin of the World Health Organization*. Oct 1 2011;89(10):706-707.
 393. Cowley J, Kiely J, Collins D. Unravelling the Glasgow effect: The relationship between accumulative bio- psychosocial stress, stress reactivity and Scotland's health problems. *Preventive medicine reports*. Dec 2016;4:370-375.
 394. Wahlgren N, Ahmed N, Eriksson N, et al. Multivariable analysis of outcome predictors and adjustment of main outcome results to baseline data profile in randomized controlled trials: Safe Implementation of Thrombolysis in Stroke-MOnitoring STudy (SITS-MOST). *Stroke; a journal of cerebral circulation*. 2008;39:3316-3322.
 395. Jimenez Caballero PE, Lopez Espuela F, Portilla Cuenca JC, Ramirez Moreno JM, Pedrera Zamorano JD, Casado Naranjo I. Charlson comorbidity index in ischemic stroke and intracerebral hemorrhage as predictor of mortality and functional outcome after 6 months. *Journal of stroke and cerebrovascular diseases : the official journal of National Stroke Association*. Oct 2013;22(7):e214-218.
 396. Bang OY, Saver JL, Kim SJ, et al. Collateral Flow Predicts Response to Endovascular Therapy for Acute Ischemic Stroke. *Stroke; a journal of cerebral circulation*. Mar 2011;42(3):693-699.
 397. Albers GW. Late Window Paradox. *Stroke; a journal of cerebral circulation*. Mar 2018;49(3):768-771.
 398. Kim H, Jin ST, Kim YW, Kim SR, Park IS, Jo KW. Predictors of malignant brain edema in middle cerebral artery infarction observed on CT angiography. *Journal of clinical neuroscience : official journal of the Neurosurgical Society of Australasia*. Mar 2015;22(3):554-560.
 399. Singer OC, Kurre W, Humpich MC, et al. Risk assessment of symptomatic intracerebral hemorrhage after thrombolysis using DWI-ASPECTS. *Stroke; a journal of cerebral circulation*. Aug 2009;40(8):2743-2748.
 400. Nickles AV, Roberts S, Shell E, et al. Characteristics and Outcomes of Stroke Patients Transferred to Hospitals Participating in the Michigan Coverdell Acute Stroke Registry. *Circulation. Cardiovascular quality and outcomes*. May 2016;9(3):265-274.

Index